



**$\gamma$ -synuclein, a novel player in the  
control of body lipid metabolism**

Steven J Millership

Submitted for the award of Doctor of  
Philosophy, January 2012



## **Abstract**

Synucleins are a family of homologous, predominantly neuronal proteins known for their involvement in neurodegeneration. In neurons  $\alpha$ -synuclein promotes the assembly of soluble-NSF-attachment receptor (SNARE) complexes required for fusion of synaptic vesicles with the plasma membrane during neurotransmitter release.  $\gamma$ -synuclein is highly expressed in human white adipose tissue (WAT) and this expression is increased in obesity. Here we show that  $\gamma$ -synuclein is nutritionally regulated in murine adipocytes and that  $\gamma$ -synuclein deficiency protects mice from high fat diet (HFD)-induced obesity and associated metabolic complications. When compared to HFD-fed wild type mice, HFD-fed  $\gamma$ -synuclein deficient mice display increased lipolysis, lipid oxidation and energy expenditure, and reduced adipocyte hypertrophy.  $\gamma$ -synuclein null adipocytes express more ATGL, a key lipolytic enzyme, and contain fewer SNARE complexes of a type involved in lipid droplet fusion. Thus,  $\gamma$ -synuclein may co-ordinately affect both lipid droplet formation and lipid hydrolysis. We also find that  $\gamma$ -synuclein deficiency causes alterations in lipid classes and fatty acid patterns in the adult murine brain. Together our data suggest that  $\gamma$ -synuclein is a novel regulator of lipid handling in both CNS neurons and adipocytes, with this adipocyte function becoming particularly important in conditions of nutrient excess.

‘We are unanimous in our belief that obesity is a hazard to health and a detriment to well being. It is common enough to constitute one of the most important public health problems of our time.’

*J.C. Waterlow, 1976*

**DECLARATION**

This work has not previously been accepted in substance for any degree and is not concurrently submitted in candidature for any degree.

Signed ..... (candidate)      Date .....

**STATEMENT 1**

This thesis is being submitted in partial fulfillment of the requirements for the degree of .....(insert MCh, MD, MPhil, PhD etc, as appropriate)

Signed ..... (candidate)      Date .....

**STATEMENT 2**

This thesis is the result of my own independent work/investigation, except where otherwise stated.

Other sources are acknowledged by explicit references.

Signed ..... (candidate)      Date .....

**STATEMENT 3**

I hereby give consent for my thesis, if accepted, to be available for photocopying and for inter-library loan, and for the title and summary to be made available to outside organisations.

Signed ..... (candidate)      Date .....

## **Acknowledgements**

Without the help and support of the people around me, all of this work would not have been possible. From Cardiff University I would like to thank Dr Irina Guschina for help with lipid analysis, as well as Dr Ricardo Brambilla for his efforts during lentivirus work. I also acknowledge the work put in by Stephen Paisey and Pavel Tokarchuk of the Experimental MRI Centre, and advice from Mr Derek Scarborough in the histology unit. I would like to thank of all the animal technicians in our Transgenic Animal Facility here in Cardiff. I am also grateful for the assistance from Dr Pieter Oort and Dr Sean Adams in California concerning ELISA studies, and Dr Peter Voshol and Dr Justin Rochford in Cambridge University for their help with metabolic analysis. A special mention is for Dr Natalia Ninkina, who has provided the bulk of my scientific training over the past few years, and also a large number of conversations involving helpful advice and entertaining anecdotes. I have been extremely lucky to have Dr Rosalind John as a mentor during my PhD, she has provided advice and support on more times than I can recall.

All of the people on the 4<sup>th</sup> and 5<sup>th</sup> floor of the Life Sciences building here in Cardiff have provided a combination of much needed advice, materials and alcoholic beverages that have made the last few years such an enjoyable part of my life. I can't help but feel that the long days spent in the lab have always been a choice rather than a chore. These people are Mathew Van De Pette, Dr Simon Tunster, Dr Owen Peters, Natalie Connor-Robson, Luke Bradshaw and quite often, our adopted lab member, Dr Tatyana Shelkovnikova. All of the people around me have been a pleasure to work with and deserve special credit for putting up with me during my constant talking and the throwing of our lab mascots, the toy mice (!).

Finally I want to thank the three most important people in all of this, both of my parents and my supervisor, Prof. Vladimir Buchman. My parents have got me through a number of difficult times in the past, and without them I would not be the person I am today. On top of this, Prof. Buchman has been like a second father to me throughout my PhD, putting faith in me as an undergraduate and pushing me to achieve what I didn't feel I could. I will be lucky to have another mentor or boss during my career that gives even half of what Prof. Buchman has offered.

## Contents

<b>1. Introduction</b>	<b>1</b>
1.1. Obesity	2
1.2. Adipose tissue	3
<i>1.2.1. BAT</i>	3
<i>1.2.2. WAT</i>	3
1.3. Adipogenesis: adipocyte hypertrophy and hyperplasia	5
1.4. NEFA storage and release in the white adipocyte	6
<i>1.4.1. NEFA storage</i>	6
<i>1.4.2. NEFA release and the major lipolytic pathways</i>	9
<i>1.4.2.1. Perilipins and the PAT family</i>	
<i>1.4.2.2. Hormone sensitive lipase (HSL)</i>	
<i>1.4.2.3. Adipose triglyceride lipase (ATGL)</i>	
<i>1.4.2.4. Final stages of TAG hydrolysis</i>	
<i>1.4.2.5. aP2/fatty-acid binding protein 4 (FABP-4)</i>	
<i>1.4.3. Other pro-lipolytic molecules involved in the regulation of lipolysis</i>	12
<i>1.4.3.1. Natriuretic peptides</i>	
<i>1.4.3.2. Tumour necrosis factor-<math>\alpha</math></i>	
<i>1.4.4. Anti-lipolytic pathways</i>	14
<i>1.4.5. Blunted catecholamine-stimulated lipolysis in obesity</i>	15
1.5. Adipocyte secretion of ‘adipokines’	16

1.5.1. <i>Leptin</i>	16
1.5.2. <i>Adiponectin</i>	17
1.6. Theories on how obesity leads to insulin resistance	19
1.6.1. <i>'WAT expansion' hypothesis and downstream lipotoxicity</i>	19
1.6.2. <i>NEFA impairment of skeletal muscle insulin signaling</i>	20
1.6.3. <i>A less beneficial array of adipokine secretion     from larger adipocytes</i>	21
1.7. Synucleins	23
1.7.1. <i><math>\alpha</math>-synuclein</i>	23
1.7.1.1. <i><math>\alpha</math>-synuclein gene and protein structure</i>	
1.7.1.2. <i>Proposed function for <math>\alpha</math>-synuclein</i>	
1.7.1.3. <i><math>\alpha</math>-synuclein and neurodegeneration</i>	
1.7.2. <i><math>\beta</math>-synuclein</i>	27
1.7.2.1 <i><math>\beta</math>-synuclein gene and protein structure</i>	
1.7.2.2. <i><math>\beta</math>-synuclein and neurodegeneration</i>	
1.7.2.3. <i>Modelling loss of <math>\beta</math>-synuclein in vivo</i>	
1.7.3. <i><math>\gamma</math>-synuclein</i>	28
1.7.3.1. <i><math>\gamma</math>-synuclein gene and protein structure</i>	
1.7.3.2. <i><math>\gamma</math>-synuclein expression and function</i>	
1.7.3.3. <i><math>\gamma</math>-synuclein and cancer</i>	
1.7.3.4. <i><math>\gamma</math>-synuclein and neurodegeneration</i>	
1.7.3.5. <i>Modelling loss of <math>\gamma</math>-synuclein in vivo</i>	

1.7.4. Synucleins and lipids	32
1.7.4.1. Lipid interaction and multimerisation of synucleins	
1.7.4.2. Effects of synucleins on lipid metabolism in the brain	
1.7.5. Expression of $\gamma$ -synuclein in white adipose tissue	
1.8. Aims	39
<b>2. Experimental Procedures</b>	<b>40</b>
2.1. Solutions	41
2.2. Animals	45
2.2.1. $\gamma$ -synuclein null mutant mice	
2.2.2. Genotyping by conventional PCR	
2.2.3. Husbandry & Diets	
2.2.4. Tissue Collection	
2.3. Magnetic resonance imaging (MRI) analysis	47
2.4. Whole-body metabolic analysis	48
2.5. Glucose- / Insulin Tolerance Testing	48
2.6. Lentiviral expression of $\gamma$ -synuclein	49
2.6.1. DNA fragment amplification	
2.6.2. Purification of insert DNA, and ligation, transformation and plasmid analysis	
2.6.3. Lentiviral production	
2.6.4. Lentiviral transduction of cells <i>in vivo</i> and <i>in vitro</i>	
2.7. Blood chemistry	51

2.8. Isolation of cell populations from WAT	51
2.9. Adipocyte lipolysis	52
2.10. Semi Quantitative Western blotting	52
<i>2.10.1. Protein extraction</i>	
<i>2.10.2. Total protein quantification</i>	
<i>2.10.3. SDS-PAGE &amp; protein transfer</i>	
<i>2.10.4. Antibodies and detection</i>	
2.11. RNA expression analysis	56
<i>2.11.1. RNA extraction and cDNA synthesis</i>	
<i>2.11.2. Quantitative PCR</i>	
2.12. Co-immunoprecipitation	59
2.13. Histological techniques	60
<i>2.13.1. Haematoxylin &amp; Eosin (H&amp;E) staining</i>	
<i>2.13.2. Immunohistochemistry</i>	
<i>2.13.3. Adipocyte size measurement</i>	
<i>2.13.3.1. Using Image J</i>	
<i>2.13.3.2. According to Ashwell et al. (1976)</i>	
2.14. Lipid analysis	62
<i>2.14.1. Lipid extraction and separation</i>	
<i>2.14.2. Gas chromatography</i>	
2.15. <i>In vitro</i> experiments	63
<i>2.15.1. Cell culture</i>	
<i>2.15.1.1. Mouse embryonic fibroblasts</i>	

2.15.1.2. <i>Stable cell lines</i>	
2.15.2. <i>ERK activation assay</i>	
2.15.3. <i>Immunocytochemistry</i>	
2.16. Statistical analysis	67
<b>3. WAT expression of <math>\gamma</math>-synuclein</b>	<b>68</b>
3.1. Overview	69
3.2.1. Results: Cell-specificity and subcellular localisation of $\gamma$ -synuclein in murine WAT	69
3.2.2. Results: Nutritional regulation of $\gamma$ -synuclein in murine WAT	73
3.3. Summary of results and discussion	76
<b>4. Effect of <math>\gamma</math>-synuclein deficiency in a mouse model of HFD-induced obesity</b>	<b>77</b>
4.1. Overview	78
4.2.1. Results: $\gamma$ -synuclein <sup>-/-</sup> mice are resistant to diet-induced obesity	78
4.2.2. Results: Loss of $\gamma$ -synuclein rescues mice from HFD-induced hyperinsulinaemia and hepatosteatosis	90
4.2.3. Results: Increased whole-body lipid utilisation and energy expenditure in $\gamma$ -synuclein <sup>-/-</sup> mice	95
4.3. Summary of results and discussion	99

<b>5. <math>\gamma</math>-synuclein and lipid metabolism in <i>in vivo</i> and <i>in vitro</i> fat cells</b>	<b>102</b>
5.1. Overview	103
5.2.1. Results: Increased adipocyte lipolysis in $\gamma$ -synuclein <sup>-/-</sup> mice	103
5.2.2. Results: The expression of proteins involved in lipid metabolism is not altered in WAT of $\gamma$ -synuclein <sup>-/-</sup> mice	106
5.2.3. Results: $\gamma$ -synuclein mRNA expression is not altered during differentiation of 3T3-L1 cells, nor is there any detectable level of $\gamma$ -synuclein proteins from these cells	113
5.2.4. Results: $\gamma$ -synuclein mRNA expression is downregulated by isobutylmethylxanthine (IBMX) in certain cell lines in culture	115
5.3. Summary of results and discussion	117
<b>6. Effect of <math>\gamma</math>-synuclein deficiency on SNARE complex formation in white adipocytes</b>	<b>121</b>
6.1. Overview	122
6.2. Results: $\gamma$ -synuclein promotes assembly of SNARE complexes in WAT	122
6.3. Summary of results and discussion	126
<b>7. Lipid classes and fatty acid patterns in brains of <math>\gamma</math>-synuclein<sup>-/-</sup> mice</b>	<b>127</b>
7.1. Overview	128
7.2.1. Results: Increased oleic acid levels in plasma of $\gamma$ -synuclein <sup>-/-</sup> mice	128
7.2.2. Results: Increased proportion of phosphatidylserine in midbrain polar lipids of $\gamma$ -synuclein <sup>-/-</sup> mice	130
7.2.3. Results: Alterations in fatty acid patterns of phosphatidylserine	133

and ethanolamine phospholipids in cortex of $\gamma$ -synuclein <sup>-/-</sup> mice	
7.2.4. Results: Alterations in fatty acid patterns in various other major polar lipids in cortex and midbrain of $\gamma$ -synuclein <sup>-/-</sup> mice	136
7.3. Summary of results and discussion	142
<b>8. Final Discussion</b>	<b>145</b>
8.1. A possible role for $\gamma$ -synuclein in white adipose tissue	146
8.2. A possible role for $\gamma$ -synuclein in brain lipid homeostasis	150
8.3. Final comments	151
<b>Bibliography</b>	<b>152</b>
<b>Appendix</b>	<b>185</b>

## List of figures & tables

<b>Fig. 1.1.</b> Overview of lipogenesis	8
<b>Fig. 1.2.</b> Lipolytic machinery of the adipocyte	13
<b>Table 1.1.</b> Summary of the major effects of key adipokines secreted from WAT	18
<b>Fig. 1.3.</b> Overview of some key functional domains of the synuclein family	25
<b>Fig. 1.4.</b> Northern blot analysis of $\gamma$ -synuclein mRNA in mouse tissues	36
<b>Fig. 1.5.</b> Quantitative RT-PCR analysis of $\gamma$ -synuclein mRNA in neuronal and adipose tissues of adult wild type mice	37
<b>Fig. 1.6.</b> Analysis of $\gamma$ -synuclein expression in various mouse tissues using Western blotting	38
<b>Table 2.1.</b> Antibodies used in Western blotting experiments	55
<b>Table 2.2.</b> Summary of primer sequences used in qPCR experiments	58
<b>Fig. 3.1.</b> Cell-specific expression of $\gamma$ -synuclein in murine WAT	70
<b>Fig. 3.2.</b> Subcellular localization of $\gamma$ -synuclein in WAT and MEF adipocytes	72
<b>Fig. 3.3.</b> WAT expression of $\gamma$ -synuclein in response to changes in nutritional status in mice	74
<b>Fig. 4.1.</b> Raw weights of wild type and $\gamma$ -synuclein <sup>-/-</sup> mice fed LFD or HFD	80
<b>Fig. 4.2.</b> Quantification of body fat volume by MRI	81
<b>Fig. 4.3.</b> WAT mass to body mass ratios	82
<b>Fig. 4.4.</b> Calorific intake and faecal lipid content	84

<b>Fig. 4.5.</b> Adipocyte size quantification in epididymal and subcutaneous WAT	85
<b>Fig. 4.6.</b> Size of adipocytes from $\gamma$ -synuclein <sup>-/-</sup> mice with local re-expression of $\gamma$ -synuclein by lentivirus delivery	86
<b>Fig. 4.7.</b> PCR analysis of the $\gamma$ -synuclein mRNA transcript using cDNA from WAT and MEFs	88
<b>Fig. 4.8.</b> Adipocyte differentiation of mouse embryonic fibroblasts (MEFs) in culture	89
<b>Fig. 4.9.</b> Effect of $\gamma$ -synuclein deficiency on lipid accumulation outside WAT	90
<b>Table 4.1.</b> Analysis of various metabolic markers in plasma and glucose/insulin tolerance testing	93
<b>Fig. 4.10.</b> Plasma levels of leptin and insulin	94
<b>Fig. 4.11.</b> Whole-body metabolic analysis	96
<b>Fig. 4.12.</b> Substrate utilization during CLAMS analysis	97
<b>Fig. 4.13.</b> Physical activity during CLAMS analysis	98
<b>Fig. 5.1.</b> Lipolysis and NEFA levels in epididymal WAT	105
<b>Fig. 5.2.</b> mRNA expression analysis of genes known to affect fat storage	108
<b>Fig. 5.3.</b> Quantitative RT-PCR analysis of mRNA encoding proteins involved in lipid metabolism in WAT, BAT and liver	109
<b>Fig. 5.4.</b> Protein expression analysis of genes known to affect fat storage	110
<b>Fig. 5.5.</b> Expression analysis of proteins involved in nutrient sensing and cell growth	111

<b>Fig. 5.6.</b> Dynamics of ERK phosphorylation following lentivirus-mediated overexpression of $\gamma$ -synuclein	112
<b>Fig. 5.7.</b> $\gamma$ -synuclein mRNA and protein expression during differentiation of 3T3-L1 cells	114
<b>Fig. 5.8.</b> Effect of IBMX on $\gamma$ -synuclein mRNA expression in various cell types in culture	116
<b>Fig. 6.1.</b> Quantification of SNARE complexes in WAT	124
<b>Fig. 6.2.</b> Analysis of SNARE protein expression in WAT	125
<b>Table 7.1.</b> Fatty acid composition in the plasma of wild type and $\gamma$ -synuclein <sup>-/-</sup> mice	129
<b>Table 7.2.</b> Fatty acid composition of the total polar lipid fraction from cortex or midbrain of wild type and $\gamma$ -synuclein <sup>-/-</sup> mice	131
<b>Fig. 7.1.</b> Midbrain and cortex polar lipid composition from wild type and $\gamma$ -synuclein <sup>-/-</sup> mice	132
<b>Fig. 7.2.</b> Fatty acid composition of phosphatidylserine from midbrain or cortex in wild type and $\gamma$ -synuclein <sup>-/-</sup> mice	134
<b>Fig. 7.3.</b> Fatty acid and dimethylacetal composition of ethanolamine phospholipids from midbrain and cortex of wild type and $\gamma$ -synuclein <sup>-/-</sup> mice	135
<b>Table 7.3.</b> Fatty acid composition in individual polar lipid classes from cortex or midbrain of wild type and $\gamma$ -synuclein <sup>-/-</sup> mice	138
<b>Fig. 8.1.</b> A proposed model for the role of $\gamma$ -synuclein in white adipocytes in times of energy surplus	149

## Abbreviations

<i>3-KAT</i>	<i>3-ketoacyl-CoA thiolase B</i>
<i>ACC-1</i>	<i>acetyl-CoA carboxylase</i>
<i>AD</i>	<i>Alzheimer's disease</i>
<i>AMPK</i>	<i>AMP-dependent protein kinase</i>
<i>aP2</i>	<i>adipocyte protein 2</i>
<i>ARA</i>	<i>arachidonic acid</i>
<i>ATGL</i>	<i>adipose triglyceride lipase</i>
<i>BAT</i>	<i>brown adipose tissue</i>
<i>BMI</i>	<i>body mass index</i>
<i>BCSG1</i>	<i>breast cancer-specific gene 1</i>
<i>C/EBP</i>	<i>CCAAT-enhancer binding protein</i>
<i>Cer</i>	<i>cerebroside</i>
<i>CerPCho</i>	<i>sphingomyelin</i>
<i>CGI-58</i>	<i>comparative gene identification 58</i>
<i>CHO</i>	<i>carbohydrate</i>
<i>CLAMS</i>	<i>comprehensive lab animal monitoring system</i>
<i>CNS</i>	<i>central nervous system</i>
<i>CSL</i>	<i>catecholamine-stimulated lipolysis</i>
<i>DAG</i>	<i>diacylglycerol</i>
<i>DHA</i>	<i>docosahexaenoic acid</i>
<i>DMSO</i>	<i>dimethyl sulfoxide</i>

<i>ED</i>	<i>epididymal</i>
<i>ERK</i>	<i>extracellular signal-related kinase</i>
<i>GAPDH</i>	<i>glyceraldehyde 3-phosphate dehydrogenase</i>
<i>GFP</i>	<i>green fluorescent protein</i>
<i>GTT</i>	<i>glucose tolerance test</i>
<i>HFD</i>	<i>high fat diet</i>
<i>HSL</i>	<i>hormone sensitive lipase</i>
<i>IBMX</i>	<i>Isobutylmethylxanthine</i>
<i>IGF-1</i>	<i>insulin-like growth factor 1</i>
<i>IL-6</i>	<i>interleukin 6</i>
<i>ITT</i>	<i>insulin tolerance test</i>
<i>LD</i>	<i>lipid droplet</i>
<i>LFD</i>	<i>low fat diet</i>
<i>LPL</i>	<i>lipoprotein lipase</i>
<i>MEF</i>	<i>mouse embryonic fibroblast</i>
<i>MGL</i>	<i>monoglyceride lipase</i>
<i>MRI</i>	<i>magnetic resonance imaging</i>
<i>NAC</i>	<i>non-amyloid beta component peptide</i>
<i>NEFA</i>	<i>non-esterified fatty acid</i>
<i>PD</i>	<i>Parkinson's disease</i>
<i>PKA</i>	<i>protein kinase A</i>
<i>PKG</i>	<i>protein kinase G</i>
<i>PNS</i>	<i>peripheral nervous system</i>

<i>PPAR</i>	<i>peroxisome proliferator-activated receptors</i>
<i>PtdCho</i>	<i>phosphatidylcholine</i>
<i>PtdEtn</i>	<i>phosphatidylethanolamine</i>
<i>Ptd2Gro</i>	<i>cardiolipin</i>
<i>PtdIns</i>	<i>phosphatidylinositol</i>
<i>PtdSer</i>	<i>phosphatidylserine</i>
<i>PUFA</i>	<i>polyunsaturated fatty acid</i>
<i>RER</i>	<i>respiratory exchange ratio</i>
<i>SC</i>	<i>subcutaneous</i>
<i>SNAP</i>	<i>synaptosomal-associated protein</i>
<i>SNARE</i>	<i>soluble N-ethylmaleimide-sensitive factor attachment protein receptor</i>
<i>SREBP</i>	<i>sterol regulatory element-binding protein</i>
<i>ST</i>	<i>sulfatide</i>
<i>TAG</i>	<i>triacylglycerol</i>
<i>TLC</i>	<i>thin-layer chromatography</i>
<i>TZD</i>	<i>thiazolidinediones</i>
<i>TNF-<math>\alpha</math></i>	<i>tumour necrosis factor-<math>\alpha</math></i>
<i>T2DM</i>	<i>type II diabetes mellitus</i>
<i>UCP-1</i>	<i>uncoupling protein 1</i>
<i>UTR</i>	<i>untranslated region</i>
<i>VAMP</i>	<i>vesicle-associated membrane protein</i>
<i>WAT</i>	<i>white adipose tissue</i>

## **Chapter 1 - Introduction**

## **1. Introduction**

The misbalance in body metabolism manifested in conditions like obesity is an important risk factor for the development of many common debilitating disorders, including type II diabetes mellitus (T2DM) and cardiovascular diseases. Thus, understanding of the cellular processes that cause dysfunction of metabolism-regulating body systems is of utmost importance. Everyday fluctuations in both nutrient consumption and physical activity require a tightly controlled mechanism for energy intake and expenditure in order to preserve the metabolic health of the organism. Failure of such mechanism can lead to states of obesity or lipodystrophy.

### **1.1. Obesity**

The prevalence of obesity, which can be defined as a body mass index (BMI) over  $30\text{kg/m}^2$ , is increasing across a large part of the world and is regarded as a major health issue. Obesity lies in the centre of a web of related disorders, namely T2DM, cardiovascular disease, cancer and various other metabolic complications. The strain on the economics and workload of the healthcare system is ever increasing, due to direct costs involved in the diagnosis and treatment of disease related to obesity. Revealing certain mechanisms in the development of obesity will undoubtedly relieve this burden. To achieve this goal it is essential to identify and understand the networks in place that control energy balance and tissue fuel utilization.

Although a number of genetic and environmental factors influence the onset of obesity, the overall cause is a calorific imbalance. In the Western world especially, a tendency towards high daily calorific intake, often mixed with reduced physical exercise, is a prime example of this imbalance. These environmental factors are in addition to the complexities in the metabolic pathways involved in such a multifactorial disease. Studies on obese human subjects and findings from animal models of obesity are slowly expanding our knowledge on potential underlying mechanisms. Here the clear genetic influence on the onset of obesity and its related disorders is made obvious, with human subpopulations, and different genetic

backgrounds of inbred mouse strains, affected differently by changes in diet, and in the progression of obesity and diabetic states.

## **1.2. Adipose tissue**

It is only in the last decade that the perception of adipose tissue as an inert storage tissue has changed to that of a multifunctional secretory organ with a central role in lipid and glucose metabolism. Through para- and endocrine functions, adipocytes are able to influence energy metabolism both in neighboring adipocytes, as well as CNS neurons, hepatocytes, pancreatic  $\beta$ -cells and skeletal myocytes. The two major types of adipose tissue, brown (BAT) and white (WAT), vary in intracellular organization and gene expression profiles, and serve different purposes within the mammalian body.

### *1.2.1. BAT*

Brown adipocytes found within brown adipose tissue (BAT) are multilocular, with small lipid droplets dispersed throughout the cell. These lipids are used as fast-access oxidative fuel by the abundance of mitochondria (the reason for the brown appearance of these adipocytes) found in these cells, where uncoupling protein 1 (UCP-1) acts to uncouple respiration from ATP synthesis at the mitochondrial inner membrane, producing heat (reviewed in (Rousset et al., 2004)). This common heat generating property of BAT is required for non-shivering and diet-induced thermogenesis, vital in new-born babies and hibernating animals (reviewed in (Griggio, 1988; Rothwell and Stock, 1979)).

### *1.2.2. WAT*

WAT consists of a number of cell types, including mature white adipocytes (which make up around a third of the total WAT cell number) as well as preadipocytes, macrophages, stromal cells and vascular cells. WAT is localized in distinct depots around the body, both subcutaneously and within the peritoneum (visceral). These

two major depot-types appear to have slightly different properties with respect to gene expression profiles and role in disease. For example, there are observed differences in expression of both secreted and non-secreted proteins from these depots (Dusserre et al., 2000). Pre-adipocytes isolated from subcutaneous fat depots also differentiate faster and are more responsive to the effects of thiazolidinediones (TZD), a class of peroxisome proliferator-activated receptors (PPAR) agonists used for the treatment of T2DM (Adams et al., 1997). Overall, visceral adiposity appears to play a larger role in downstream metabolic complications than subcutaneous adiposity, possibly due to draining of excess lipids and inflammatory mediators from visceral WAT directly into the portal vein to the liver (Fox et al., 2007). This may also be due to a more pronounced lipolytic effect of catecholamines in visceral depots due to differences at both the receptor and post-receptor levels (Arner et al., 1990; Fisher et al., 2001; Hellmer et al., 1992; Reynisdottir et al., 1997). It has also been demonstrated that the effect of insulin is lower in visceral WAT compared to subcutaneous WAT, owing to differences at both the insulin receptor level and post-receptor signaling (Bolinder et al., 1983; Wu et al., 2001; Zierath et al., 1998).

Although beyond the scope of this work, it is important to understand that WAT also plays an important role in carbohydrate metabolism, exemplified by the phenotype of adipose-specific knockout of GLUT4 in mice. GLUT4 is a glucose transporter protein with an important role in insulin-mediated glucose uptake from the bloodstream, for which translocation of GLUT4 to the cell surface is a crucial process (Bryant et al., 2002). GLUT4 null mutant mice display peripheral insulin resistance and glucose intolerance without any alteration in adiposity (Abel et al., 2001). Although the exact molecular mechanism for this phenotype is unclear, it does point to adipocyte glucose uptake as an important part of whole-body carbohydrate metabolism.

### **1.3. Adipogenesis: adipocyte hypertrophy and hyperplasia**

The process of adipogenesis occurs via two processes, increase of the size of pre-existing mature adipocytes (hypertrophy) and proliferation with subsequent terminal differentiation of preadipocytes (hyperplasia). These preadipocytes derive from multipotent stem cells of mesodermal origin. The differentiation of preadipocytes is controlled by the activity of various hormones, cytokines and transcription factors (Farmer, 2006) and the ability of these precursor cells to become fully differentiated adipocytes decreases with age (Karagiannides et al., 2001). Circulating insulin appears to stimulate preadipocyte differentiation, with factors released from hypertrophied adipocytes such as insulin-like growth factor 1 (IGF-1) also shown to play a role in this process via paracrine effect (Avram et al., 2007). Non-esterified fatty acids (NEFA) released by hypertrophic adipocytes have also been demonstrated to induce differentiation of preadipocytes (Amri et al., 1994). Early *in vivo* animal experiments indicated that hypertrophy occurs prior to hyperplasia, and that this hyperplasia is associated with a more severe and less reversible state of metabolic dysfunction (Bjorntorp et al., 1982; Hirsch et al., 1989).

Stimulation of preadipocyte differentiation triggers expression of a number of key adipocyte transcription factors, most notably of the PPAR, CCAAT-enhancer binding protein (C/EBP) and sterol regulatory element-binding protein (SREBP) families. This transcriptional cascade starts with early expression of C/EBP $\beta$  and C/EBP $\delta$ , followed by C/EBP $\alpha$ , which in turn activates PPAR $\gamma$ . The latter two, as well as SREBP-1c, are central transcriptional players in differentiating adipocytes, activating a number of key adipogenic genes involved in NEFA influx and storage (Kim and Spiegelman, 1996; Vidal-Puig et al., 1996). Ultimately, this lipogenic program results in establishing the gene expression profile characterizing the phenotype of fully differentiated white adipocytes. Adipocyte differentiation can be studied *in vitro* using primary preadipocytes, or immortalized cell lines such as 3T3-L1 and 3T3-F22A fibroblasts. Here, the differentiation program discussed above can be initiated by treatment of cells with a cocktail of pro-differentiation agents (insulin, dexamethasone, Isobutylmethylxanthine (IBMX)), which stimulates the expression of adipocyte specific transcripts, changes in cell morphology and the formation of numerous lipid droplets.

#### **1.4. NEFA storage and release in the white adipocyte**

WAT is the most important organ in the body for the storage and release of energy from lipids, depositing NEFA originating either from the diet or *de novo* synthesis, as triacylglycerols (TAG). In times of energy surplus, WAT sequesters excess lipids into specialised intracellular structures known as lipid droplets (LD). TAG, along with cholesterol esters are stored in the LD core, which is surrounded by a phospholipid monolayer. Equally important is the ability of WAT to hydrolyse stored TAG by the process of lipolysis to release NEFA into the bloodstream as a vital oxidative fuel for other organs in times of energy demand. The LD is coated with a series of proteins involved in both the storage and release of these lipids. The processes of TAG synthesis and hydrolysis are not restricted to the postprandial and fasted states, respectively; both these anabolic and catabolic pathways undergo constant cycling, resulting in rapid turnover of neutral TAG stores (Newsholme, 1978; Vaughan, 1962; Hammond and Johnston, 1987). Moreover, small alterations in TAG synthesis and hydrolysis can have a significant effect on fat mass in a relatively short space of time (Langin and Arner, 2006). Adipose tissue as a whole is highly innervated by the sympathetic nervous system and highly vascularised, meaning that adipose tissue is able to respond rapidly to acute changes in dietary intake via both hormonal and neuronal control, to alter the storage and release of TAG accordingly.

##### *1.4.1. NEFA storage*

The role of WAT is to act as a buffering system for circulating free fatty acids. Circulating TAG is hydrolyzed via the action of lipoprotein lipase (LPL) from very low-density lipoproteins (VLDL) and chylomicrons in the capillary endothelial lumen, liberating NEFA, which are subsequently taken up by the adipocyte by both passive and active mechanisms (Abumrad et al., 1998; Hamilton and Kamp, 1999; Scow and Blanchette-Mackie, 1985). Fatty acid translocase (FAT/CD36) (Abumrad et al., 1993), fatty acid transport protein (FATP) (Schaffer and Lodish, 1994) and calveolin-1 (Trigatti et al., 1999) have all been linked with transport of NEFA transport across the plasma membrane, although further proteins may yet to be identified (Kampf et al., 2007). Here they are esterified using a glycerol backbone, using both glycerol-3-phosphate (produced in glycolysis) and acyl coenzyme A

(produced during adipocyte NEFA uptake), into TAG to reduce their cytotoxic effect. A summary of these processes can be found in Fig. 1.1. This process requires a series of acylation reactions catalysed by three different acyltransferases at the surface of the endoplasmic reticulum, the site of neutral lipid synthesis. Incorporation of TAG into the LD has been suggested to occur through fusion, which appears to be dependent on cytoskeletal elements and soluble N-ethylmaleimide-sensitive factor attachment protein receptor (SNARE) fusion machinery (Bostrom et al., 2007; Bostrom et al., 2005; Olofsson et al., 2009). SNARE proteins are vital components of protein complexes involved in membrane fusion (reviewed in (Jahn and Scheller, 2006)) and may play a role in the control of fusion between neutral TAG packaged within amphipathic lipoproteins and the LD phospholipid monolayer.

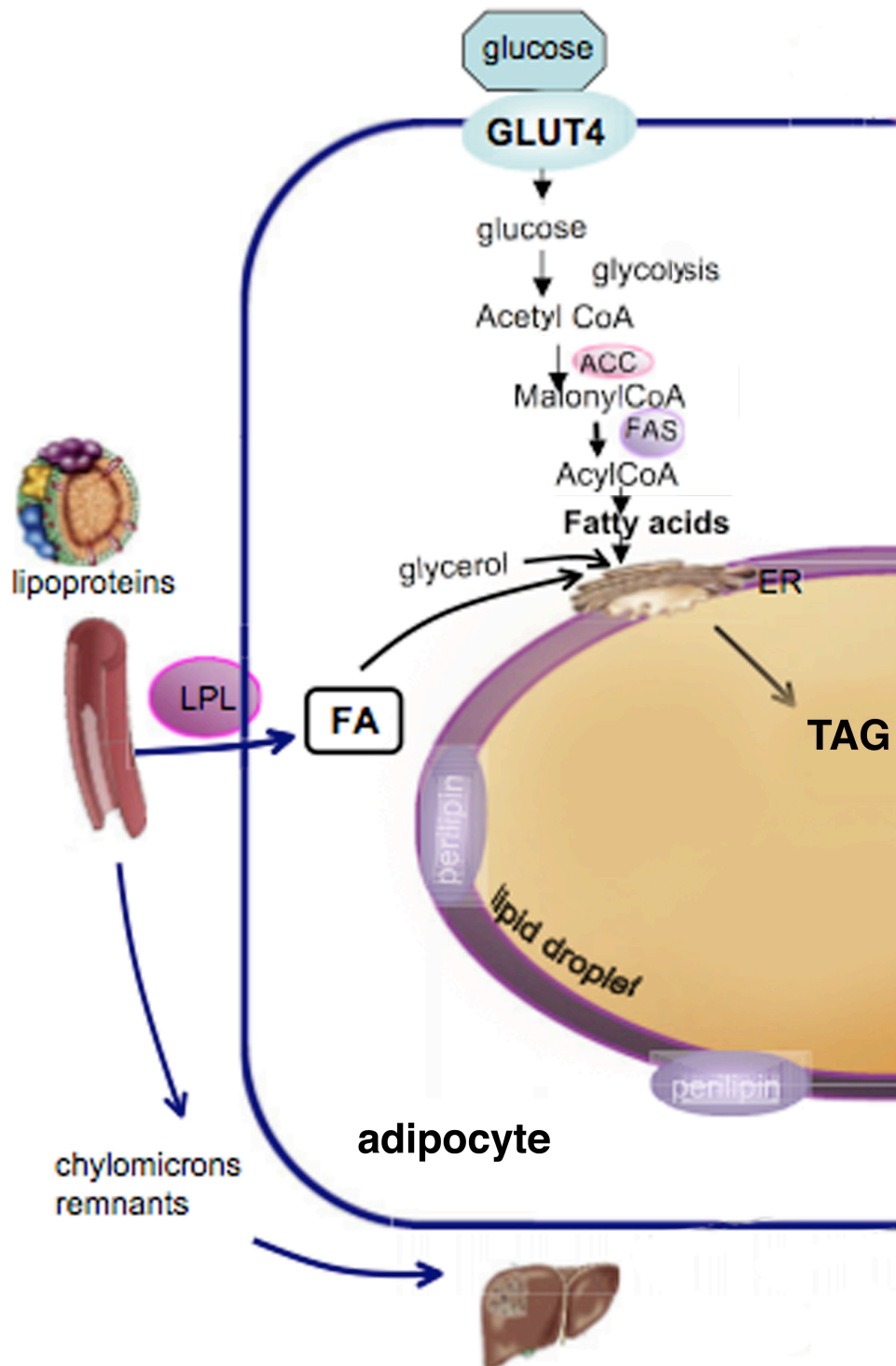


**Fig. 1.1. Overview of lipogenesis.** Fatty acids (FA) obtained from lipoproteins through the action of lipoprotein lipase (LPL) are esterified into triacylglycerols (TAG) in the endoplasmic reticulum (ER) and stored in the lipid droplet. Excess glucose is oxidized to acetyl-CoA by glycolysis, and converted to acyl-CoA, which is also esterified into TAG. ACC, acetyl-CoA carboxylase; FAS, fatty acid synthase. Adapted from (Vazquez-Vela et al., 2008).

### *1.4.2. NEFA release and the major lipolytic pathways*

Catecholamines and insulin are two of the most potent mediators of lipolysis. The classic pathway by which adipocyte TAG is hydrolysed is in response to catecholamine-mediated stimulation of  $\beta$ -adrenergic receptors on the adipocyte cell surface ( $\beta_1$  and  $\beta_2$  being the most active isoforms in human adipocytes and  $\beta_3$  in rodent adipocytes). This in turn activates adenylate cyclase via stimulatory G-proteins ( $G\alpha_s$ ) consequently raising intracellular cAMP levels, activating cAMP-dependent protein kinase (PKA). Stimulated PKA has two key target proteins in this pathway, the major LD-associating lipoprotein, perilipin A, and the rate-limiting enzyme involved in catecholamine-stimulated lipolysis, hormone-sensitive lipase (HSL). This mechanism is discussed in detail below with an overview found in Fig. 1.2.

#### *1.4.2.1. Perilipins and the PAT family*

In addition to various cellular lipases, a number of LD-associated proteins modulate lipid metabolism in adipocytes. Members of a group of proteins known as the PAT family (perilipins, adipophilin, tail-interacting protein of 47kDa (TIP47)) all play roles in the efficient storage of TAG within the adipocyte LD (reviewed in (Bickel et al., 2009; Wolins et al., 2005)). Out of all members of the PAT family proteins, perilipins appear to have the most significant effect on adipocyte lipid storage. A single perilipin transcript gives rise to three distinct isoforms by alternative splicing, with perilipin A the most abundant form in WAT (Greenberg et al., 1993). Perilipin A has a dual role as a LD scaffold protein, under basal conditions it functions to protect TAG within the LD from hydrolysis by cellular lipases, whereas its hyperphosphorylation at up to six serine residues is required for maximally stimulated lipolysis (Brasaemle et al., 2000b; Martinez-Botas et al., 2000; Souza et al., 2002; Tansey et al., 2003; Tansey et al., 2001). In this latter state, perilipin A is required for translocation of a major lipase HSL from the cytosol to the LD (Miyoshi et al., 2006; Sztalryd et al., 2003) where it interacts physically with perilipin A (Shen et al., 2009).

#### *1.4.2.2. Hormone sensitive lipase (HSL)*

For decades after the discovery of HSL in the 1960s (Bjorntorp and Furman, 1962; Rizack, 1964), this enzyme was considered the sole player in adipocyte TAG hydrolysis. Key PKA phosphorylation sites (S563, S659, S660 in rodents, corresponding to S552, S649 S650 in humans (Anthonsen et al., 1998; Contreras et al., 1998)) are responsible for increases in intrinsic enzyme activity and its translocation from a predominantly cytosolic localization to the LD (Brasaemle et al., 2000a; Clifford et al., 2000; Egan et al., 1992; Hirsch and Rosen, 1984; Shen et al., 1998; Su et al., 2003). This translocation is crucial to the access of HSL to stored TAG. As well as the classical activation of HSL by PKA, a number of other protein kinases have been shown to phosphorylate adipocyte HSL at key serine residues, independent of PKA activation, including AMP-dependent protein kinase (AMPK), glycogen synthase kinase 4 (GSK) and extracellular signal-related kinase (ERK) with both pro- and anti-lipolytic effects (Daval et al., 2005; Garton and Yeaman, 1990; Greenberg et al., 2001; Olsson et al., 1986). Accordingly, HSL null mutant mice have blunted catecholamine-stimulated lipolysis (CSL), but with no changes in basal lipolysis (Haemmerle et al., 2002; Harada et al., 2003; Mulder et al., 2003; Osuga et al., 2000).

#### *1.4.2.3. Adipose triglyceride lipase (ATGL)*

Although HSL has broad substrate specificity, with an affinity for TAG and both cholesterol and retinyl esters, it is most active against diacylglycerols (DAG) (Langin et al., 2000). The first hydrolysis reaction to liberate the first fatty acid is in fact performed by another key lipase in this pathway, adipose triglyceride lipase (ATGL). Its discovery in 2004 ended growing doubts that HSL was not the sole adipocyte TAG hydrolase (Jenkins et al., 2004; Villena et al., 2004; Zimmermann et al., 2004). These doubts had stemmed from two particular findings, firstly the disparity between increases in PKA-mediated HSL activity and overall adipocyte lipolysis, and secondly the observed DAG accumulation (and therefore sufficient TAG hydrolysis) in HSL null mutant mice (Haemmerle et al., 2002). In the absence of HSL, ATGL accounts for the majority of TAG hydrolase activity in WAT (Zimmermann et al., 2004). ATGL displays specific activity against TAG, and seems to play an important role in

basal lipolysis (Langin et al., 2005; Miyoshi et al., 2008; Ryden et al., 2007). Although not a direct target of PKA (Zimmermann et al., 2004), nor does it interact with perilipin A itself (Granneman et al., 2007), ATGL is also activated by  $\beta$ -adrenergic stimulation (Miyoshi et al., 2007). Here its coactivator, comparative gene identification 58 (CGI-58), which is normally bound to unphosphorylated perilipin A at the LD, is released from phosphorylated perilipin A following stimulation, binds to ATGL at the LD surface, and increases its activity (Granneman et al., 2007; Lass et al., 2006; Subramanian et al., 2004). Accordingly, ATGL null mutant mice were shown to display reduced CSL (Haemmerle et al., 2006). The potent TAG hydrolase activity of ATGL and its important role in energy homeostasis is demonstrated both *in vitro* and *in vivo*. Overexpression or knockdown of ATGL in 3T3-L1 adipocytes alters TAG hydrolase activity and subsequent cell lipolysis, whilst ATGL null mutant mice display ectopic deposition of TAG in non-adipose tissues including the heart, which results in their premature death (Haemmerle et al., 2006; Kershaw et al., 2006; Villena et al., 2004). Similar pathology is seen in patients with autosomal recessive mutations in either the ATGL or CGI-58 gene, with accumulation of neutral lipids in multiple tissues manifesting in severe myopathy and ichthyosis respectively (Schweiger et al., 2009).

#### *1.4.2.4. Final stages of TAG hydrolysis*

After hydrolysis of TAG and DAG by ATGL and HSL respectively, a third lipase in this chain, monoglyceride lipase (MGL), which is not under hormonal control, is required for hydrolysis of the third and final fatty acid from the glycerol backbone (Fredrikson et al., 1986). Glycerol released from the complete hydrolysis of TAG leaves the cell via facilitated diffusion through the aquaporin 7 receptor (Hibuse et al., 2005) while NEFA is able to cross the plasma membrane into the bloodstream via both passive diffusion or facilitated transport as discussed in section 1.4.1.

#### *1.4.2.5. aP2/fatty-acid binding protein 4 (FABP-4)*

Fatty-acid binding protein 4 (FABP-4), commonly known as aP2, is part of a large family of lipid-binding proteins and is a key NEFA carrier in adipocytes. aP2 has high

affinity for NEFA and is involved in their solubilisation and flux from lipases to cell membranes (Matarese and Bernlohr, 1988). aP2 physically interacts with HSL (Shen et al., 1999) in the cytosol upon PKA-mediated lipolysis, and this aP2/HSL complex migrates to the LD. Here, aP2 is important for the catalytic activity of HSL, and liberated NEFA is shuttled solely by aP2 from LD to the plasma membrane during the process of NEFA efflux (Jenkins-Kruchten et al., 2003). This role in NEFA efflux is supported by studies on aP2 null mutant mice, which demonstrated increases in intracellular NEFA levels as well as reduced lipolysis (Baar et al., 2005; Coe et al., 1999; Scheja et al., 1999).

### *1.4.3. Other pro-lipolytic molecules involved in the regulation of lipolysis*

#### *1.4.3.1. Natriuretic peptides*

As well as extracellular stimulation by catecholamines, circulating natriuretic peptides also play a role in the lipolytic response of adipocytes (reviewed in (Lafontan et al., 2005)). This occurs via a similar yet independent pathway to that of catecholamine-mediated stimulation, involving cGMP and cGMP-dependent protein kinase (PKG) downstream of a natriuretic peptide type A receptor with intrinsic guanylyl cyclase activity, a pathway specific to primate adipocytes (Sengenès et al., 2002). The end result of this natriuretic peptide activation is also phosphorylation of HSL, and subsequent increases in lipolysis *in vitro* and *in vivo* (Sengenès et al., 2000; Sengenès et al., 2003).

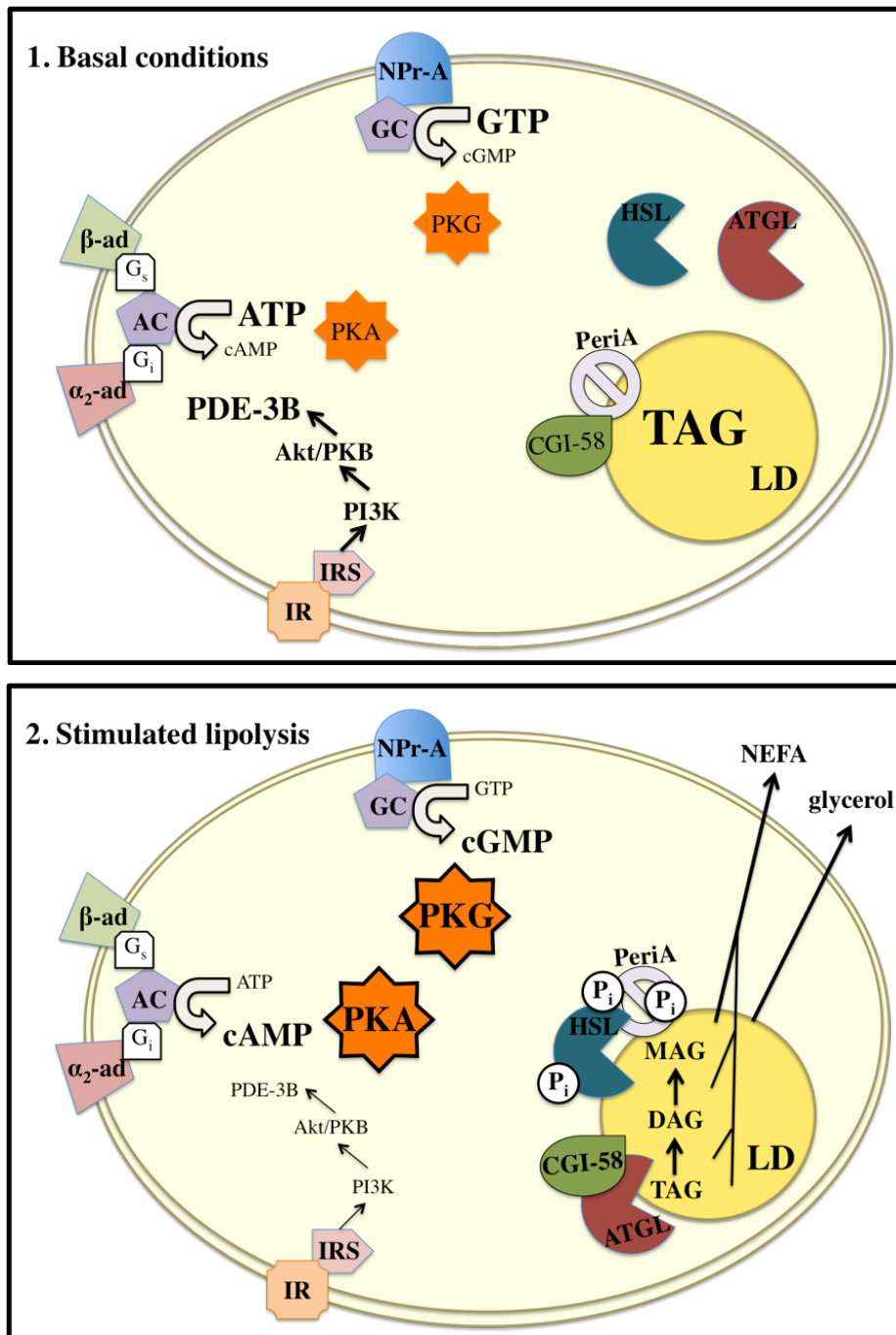


**Fig. 1.2. Lipolytic machinery of the adipocyte.**  $\alpha_2$ -ad,  $\alpha_2$ -adrenergic receptor;  $\beta$ -ad,  $\beta$ -adrenergic receptor; AC, adenylyl cyclase; Akt/PKB, protein kinase B; ATGL, adipose triglyceride lipase; GC, guanylyl cyclase; CGI-58, comparative gene identification 58;  $G_i$ , inhibitory GTP-binding protein;  $G_s$ , stimulatory GTP-binding protein; HSL, hormone-sensitive lipase; NPr-A, natriuretic peptide receptor A; PeriA, perilipin A;  $P_i$ , phosphate group; PI3K, phosphatidylinositol-3-phosphate kinase; PKA, protein kinase A; PKG, protein kinase G; IR, insulin receptor; IRS, insulin receptor substrate.

#### *1.4.3.2. Tumour necrosis factor- $\alpha$*

Tumour necrosis factor- $\alpha$  (TNF- $\alpha$ ) is a pro-inflammatory cytokine released by hypertrophic mature adipocytes and WAT resident macrophages, whose numbers increase in obesity (Weisberg et al., 2003). TNF- $\alpha$  has been shown to affect lipid metabolism via an ERK-dependent pathway in 3T3-L1 cells and human adipocytes (Ryden et al., 2002; Souza et al., 2003; Zhang et al., 2002), and has also been linked with effects on insulin signaling (Fujishiro et al., 2003), perilipin expression (Ryden et al., 2002; Souza et al., 2003) and lipase (HSL and ATGL) expression during an adipocyte 'dedifferentiation' process (Bezaire et al., 2009; Kim et al., 2006; Kralisch et al., 2005; Sumida et al., 1990). The effect of this cytokine on lipid metabolism in states of obesity and insulin resistance is discussed further in chapter 1.6.3.

#### *1.4.4. Anti-lipolytic pathways*

Adipocyte lipolysis is also under inhibitory control by various circulating catecholamines, hormones and factors. Probably the most potent is insulin, which acts via phosphorylation of the insulin receptor and its attached insulin receptor substrate (IRS). This in turn activates the phosphatidylinositol-3-phosphate kinase (PI3K) pathway, resulting in increased activity of a phosphodiesterase, PDE-3B, reducing intracellular cAMP levels. In addition to this cAMP degradation, there may be additional anti-lipolytic mechanisms of insulin, including direct inhibition of adenylate cyclase (Illiano and Cuatrecasas, 1972), internalization of  $\beta$ -adrenergic receptors (Engfeldt et al., 1988) and activation of phosphatases that dephosphorylate HSL (Stralfors and Honnor, 1989). Other molecules shown to possess anti-lipolytic activity include nicotinic acid (Carlson, 1963), adenosine (Dole, 1961), neuropeptide Y and peptide YY (Bradley et al., 2005; Valet et al., 1990).

As mentioned above, catecholamines are able to stimulate lipolysis through a mechanism involving cAMP/PKA downstream of  $\beta$ -adrenoreceptors. Conversely in human adipocytes, catecholamines can also exert a strong anti-lipolytic effect via stimulation of  $\alpha_2$ -adrenergic receptors, with  $G\alpha_i$  activity reducing intracellular cAMP levels. In fact,  $\alpha_2$ -adrenergic receptors are more abundant than  $\beta$ -adrenoreceptors on human subcutaneous fat cells and also have a higher affinity for major catecholamines

such as adrenaline and noradrenaline, suggesting that this pathway plays an important role in control of lipolysis in humans (Lafontan and Berlan, 1995). These findings have since been supported by work demonstrating adrenaline-mediated lipolytic control in human subcutaneous WAT via  $\alpha_2$ -adrenoceptors, as well as their role in the blunted catecholamine-stimulated lipolysis observed in obese patients, an effect which is discussed in the next section (Mauriege et al., 1991; Stich et al., 2000; Stich et al., 1999).

#### *1.4.5. Blunted catecholamine-stimulated lipolysis in obesity*

In states of obesity, it becomes apparent that catecholamine-stimulated lipolysis (CSL) is less efficient (Blaak et al., 1994; Connacher et al., 1991; Horowitz and Klein, 2000; Webber et al., 1994). This has been linked with decreased abundance and function of  $\beta$ -adrenergic receptors (Reynisdottir et al., 1994) possibly combined with an increased effect of  $\alpha_2$ -adrenergic receptors, which have an opposing effect (Stich et al., 2000). Decreased activity and expression of HSL have also been reported (Large et al., 1999). It has also been speculated that WAT depots in obese individuals are less suited to receive an adequate blood supply and/or neuronal input. Whether this blunted CSL is itself a key defect responsible for onset of obesity, or a consequence of the obese state is a topic of much discussion. Some findings suggest a strong genetic component for predisposition of this defect, with impaired CSL a feature of adipocytes from immediate relatives of obese patients and also from adolescent patients with childhood onset obesity (Bougneres et al., 1997; Enoksson et al., 2000; Hellstrom et al., 1996). Moreover, polymorphisms and alterations in expression of genes encoding  $\beta_2$ -adrenoreceptors (Jocken et al., 2007a; Large et al., 1997), HSL (Hoffstedt et al., 2001) and perilipin A (Mottagui-Tabar et al., 2003) are associated with obesity and diminished CSL.

On the other hand, it is also possible that these changes in the lipolytic machinery are a compensatory mechanism to reduce NEFA efflux from adipocytes in order to avoid high levels of circulating NEFA in the bloodstream, which is linked to insulin resistance. In obese patients, fasting plasma insulin concentrations are inversely correlated to NEFA output from adipose tissue (Karpe and Tan, 2005) as are protein expression of HSL and ATGL (Jocken et al., 2007b; Large et al., 1999). If this

compensatory mechanism is the case, it would seem that this 'protective' function would also prevent efficient 'switching' of adipose tissue function from TAG storage to hydrolysis where necessary.

### **1.5. Adipocyte secretion of 'adipokines'**

It is only relatively recently in the work on adipose tissue that research has demonstrated it to not simply be an inert storage tissue for excess lipids, but that it also functions as a major signaling organ, secreting a multitude of so called 'adipocytokines' or simply 'adipokines' (reviewed in (Rosen and Spiegelman, 2006; Trujillo and Scherer, 2006)). These factors play a role in the local responses of WAT via auto-/paracrine effects, as well as an endocrine effect on overall body energy metabolism by modulating food intake, energy expenditure and substrate utilization, mainly via the CNS and other metabolic tissues. These adipokines include peptide hormones (e.g. leptin, adiponectin, resistin), cytokines (interleukin 6 (IL-6), TNF- $\alpha$ ) and enzymes (plasminogen activated inhibitor 1, LPL).

#### *1.5.1. Leptin*

Probably the adipokine that has attracted the most attention since its discovery is leptin, the product of the Ob gene associated with genetically obese (ob/ob) mice (Zhang et al., 1994). Adipocyte leptin expression increases with adipocyte hypertrophy (Considine et al., 1996), and is responsive to insulin, (Saladin et al., 1995), but is not directly affected by food intake itself. Leptin is seen as a signaling molecule able to convey long-term body fat mass status to the CNS (Schwartz et al., 2000). Circulating leptin acts on key leptin-responsive neurons in the hypothalamus to control downstream effectors of satiety and energy expenditure, via inhibition of AMP-activated protein kinase (AMPK) signaling (Long and Zierath, 2006) demonstrating that WAT is able to affect the overall energy balance and nutritional status of the organism. In peripheral tissues, leptin increases lipid utilization in WAT, liver and skeletal muscle, and has been shown to inhibit pancreatic insulin release as well as having an anti-apoptotic effect in pancreatic  $\beta$ -cells (Okuya et al., 2001; Poitout et al., 1998; Shimabukuro et al., 1998). Obese humans have increased levels

of circulating leptin, but without sufficient control of satiety and energy expenditure control. This led to the belief of a state of hypothalamic leptin resistance, which appears to play an important role in the pathophysiology of obesity and its related disorders (Munzberg and Myers, 2005).

### *1.5.2. Adiponectin*

Another key adipokine, adiponectin, is able to modulate insulin sensitivity by inhibiting hepatic glucose production, enhancing glucose uptake in muscle, and increasing NEFA oxidation in both liver and muscle via increased AMPK activity (Goldstein and Scalia, 2004; Kadowaki and Yamauchi, 2005). Adiponectin synthesis is decreased in states of obesity and insulin resistance (Hajer et al., 2007; Lindsay et al., 2002). As with leptin, adiponectin acts peripherally to increase energy expenditure in skeletal muscle, which in turn reduces lipid deposition in non-adipose tissues. However in the severe obese and insulin resistant state, it seems that the effect of both these adipokines is reduced, possibly due to a combination of the reduced levels of circulating adiponectin in obesity as well as a reduced sensitivity to leptin. A summary of the effects of leptin and adiponectin, as well as a few other major adipokines is summarized in Table 1.1 below.

<i>Adipokine</i>	<i>Overall effect on food intake</i>	<i>Effects on lipid metabolism</i>	<i>Levels found in obesity</i>
<i>Leptin</i>	Anorexigenic	Reduction of body lipid stores due to effects on CNS (via AMPK signaling) and enhanced lipid utilization in peripheral tissues (liver, WAT, skeletal muscle)	Increased
<i>Adiponectin</i>	No effect	Reduction of lipid stores due to enhanced utilization in liver and skeletal muscle (via AMPK signaling)	Reduced
<i>Resistin</i>	Anorexigenic	Increases adipocyte lipolysis <i>in vivo</i> , decreased NEFA uptake/metabolism <i>in vitro</i>	Increased
<i>TNF-<math>\alpha</math></i>	Anorexigenic	Increases adipocyte lipolysis and inhibits muscle AMPK signaling	Increased
<i>IL-6</i>	Anorexigenic	Stimulation of adipocyte lipolysis and also lipid oxidation (via AMPK)	Increased

**Table. 1.1. Summary of the major effects of key adipokines secreted from WAT.**

## **1.6. Theories on how obesity leads to insulin resistance**

The expansion of adipose tissue in obesity is associated with metabolic disorders affecting multiple tissues. Given the pandemic of obesity it is critical to understand this link between increased adipose mass and metabolic disturbances in order to identify potential novel therapies. Inhibiting adipose tissue expansion alone is likely to worsen metabolic disease, as evidenced by human syndromes of lipodystrophy, where inappropriately decreased adipose mass causes severe insulin resistance. The insulin resistant state is a key risk factor for the development of cardiovascular disease and T2DM. Although studies have shown that obesity is the single most important predictor of T2DM (Hu et al., 2001), multiple genetic factors play a role in this pathogenesis. Discussed below are some major hypotheses that currently exist, proposing how obesity and WAT dysfunction lead to states of insulin resistance and metabolic disease.

### *1.6.1. 'WAT expansion' hypothesis and downstream lipotoxicity*

As mentioned above, considering that states of severe obesity, but also lipodystrophy, are linked to downstream metabolic complications, it seems likely that lipotoxicity is due, at least in part, to the situation where body WAT has reached an upper limit of potential TAG storage. Lipotoxicity is a mechanism whereby failure to appropriately store lipids in adipose tissue leads to their accumulation in other tissues and the circulation causing hepatic steatosis, insulin resistance and cardiovascular disease. Adipose tissue dysfunction and/or exceeded adipose storage capacity is believed to lead to lipotoxicity in common obesity and therefore a major challenge is to identify pathways via which adiposity can be reduced without concomitant increases in circulating lipids, lipotoxicity and metabolic disease. This phenomenon is perhaps best demonstrated in mice completely lacking adipose tissue (A-ZIP/F-1 mice), which causes extreme metabolic dysfunction including severe insulin resistance in these animals (Moitra et al., 1998). It may be that it is more important to efficiently expand WAT and therefore increase adiposity, and to sequester lipids in this tissue in order to reduce levels of circulating NEFA and ectopic NEFA/TAG deposition. Further evidence for this theory is that insulin resistance appears to correlate with circulating

NEFA and uptake into non-adipose tissues, rather than just excess body fat *per se*. For example, reduction of circulating NEFA in obese patients using the anti-lipolytic drug acipimox, improves peripheral insulin resistance (Santomauro et al., 1999). Furthermore, deficiency of fatty acid binding proteins in either adipocytes or macrophages (therefore reducing NEFA efflux) also improves insulin sensitivity in mice (Furuhashi et al., 2008). Further evidence for the importance of efficient expansion of WAT comes from the use of TDZs in the treatment of T2DM and non-alcoholic fatty liver disease, where this class of drugs actually increases WAT mass whilst improving insulin sensitivity (Nichols and Gomez-Caminero, 2007). Similar findings have also been made in mouse models of genetic obesity. Mice that harbour a dominant negative mutation in the PPAR $\gamma$  gene, when crossed onto the ob/ob background (PPAR $\gamma$  P465L ob/ob mice, aka PLO mice) have less adiposity than ob/ob mice but with a more severe insulin resistant phenotype (Gray et al., 2006). Similarly, mice with adipose specific overexpression of adiponectin (ADN-ad<sup>TG/TG</sup> mice) on ob/ob background have seemingly limitless WAT expansion, are 50% larger than ob/ob alone, but have smaller adipocytes, are completely insulin sensitive with no ectopic lipid deposition (Kim et al., 2007).

### *1.6.2. NEFA impairment of skeletal muscle insulin signaling*

Regardless of the upper limit of WAT expansion, an increased adipose tissue mass in obesity undoubtedly delivers more NEFA into the circulation, resulting in an increased plasma NEFA concentration when compared with lean subjects. This has been linked to peripheral insulin resistance in humans and animals, with concomitant reduction in glucose uptake into skeletal muscle. Elevated NEFA uptake into skeletal muscle has been shown to affect insulin signaling in skeletal myocytes at upstream parts of the pathway such as tyrosine phosphorylation of insulin receptor and insulin receptor substrate (IRS) proteins (Kraegen et al., 2001) as well as promoting inhibitory serine phosphorylation by various protein kinases such as protein kinase C $\theta$  (Griffin et al., 1999) and p70 S6 kinase (Tremblay and Marette, 2001). Consistent with this role for these serine kinases mediating deleterious effects of NEFA, accumulation of intracellular lipid metabolites (e.g. fatty acyl-CoA and DAG) can also activate protein kinase C (PKC). This kinase has been shown to phosphorylate

IRS and inhibit insulin signaling in rodent skeletal muscle (Griffin et al., 1999; Yu et al., 2002). Furthermore, gene disruption of either protein kinase C $\theta$  or p70 S6 kinase 1 in mice gives resistance to high fat diet-induced defects in insulin-stimulated glucose uptake in skeletal muscle (Kim et al., 2004; Um et al., 2004).

The onset of T2DM is most likely due to a combination of insulin resistance and reduced secretory function of insulin itself. To meet demands for increased insulin production, the mass of pancreatic  $\beta$ -cells enlarges. Acute increases in circulating NEFA cause temporary increases in insulin secretion but chronically (i.e. in obesity) they inhibit insulin secretion possibly due to an endoplasmic stress response resulting in apoptosis of  $\beta$ -cells (Zhao et al., 2006). Generally, although increases in weight correlate negatively with insulin sensitivity, it appears that there is a lag time between insulin resistance and the onset of T2DM, a period where circulating glucose levels are maintained by compensatory increases in  $\beta$ -cell insulin secretion. However this hypersecretion is unsustainable and results in  $\beta$ -cell dysfunction and apoptosis, perpetuating a state of worsening insulin resistance, hyperinsulinaemia and hyperglycaemia (Rhodes, 2005).

### *1.6.3. A less beneficial array of adipokine secretion from larger adipocytes*

As mentioned previously, circulating adipokines secreted from adipocytes are an important modulator of energy metabolism and whole-body insulin sensitivity. Adipocytes alter their adipokine production profile upon nutritional overload. At first, increased adiposity appears to be compensated for, however eventually, hypertrophic adipocytes fail to properly secrete a normal balance of adipokines. Moreover they have been shown to secrete pro-inflammatory proteins such as monocyte chemoattractant protein 1 (MCP-1) and TNF- $\alpha$ , which modulate an inflammatory response in WAT. The resultant macrophage infiltration (and the low-grade inflammatory state) is a typical phenomenon associated with obesity (Weisberg et al., 2003), with levels of macrophage infiltration shown to correlate with levels of insulin resistance (Otto and Lane, 2005). Cytokines secreted from macrophages and hypertrophic adipocytes affect lipid metabolism, for example the pro-lipolytic effect of TNF- $\alpha$  via the ERK pathway (Ryden et al., 2002; Souza et al., 2003; Zhang et al.,

2002). The resulting increases in circulating NEFA further aggravate the insulin resistant state. IL-6, another pro-inflammatory cytokine secreted from WAT (Fontana et al., 2007) is increased in obese and diabetic patients (Bastard et al., 2000; Vozarova et al., 2001). Similar to TNF- $\alpha$ , IL-6 is pro-lipolytic (Path et al., 2001; Petersen et al., 2005) and can induce insulin resistance (Lagathu et al., 2003; Rotter et al., 2003). NEFA release from hypertrophic adipocytes also have a paracrine effect in WAT whereby these NEFA are able to bind to toll-like receptors on macrophages, activating the nuclear factor kappa-light-chain-enhancer of activated B cells (NF- $\kappa$ B) pathway and augment TNF- $\alpha$  production (Suganami et al., 2007; Suganami et al., 2005).

## 1.7. Synucleins

The synucleins ( $\alpha$ -,  $\beta$ - and  $\gamma$ -synuclein) are a family of highly homologous and vertebrate-specific proteins, with elusive function and predominantly neuronal expression. Synucleins are probably best known for their involvement in various neurodegenerative conditions, termed ‘synucleinopathies’ (Goedert and Spillantini, 1998; Spillantini and Goedert, 2000), the most notable of these being the role of  $\alpha$ -synuclein in the aetiology and pathogenesis of both familial and sporadic Parkinson’s disease (PD) (reviewed in (Cookson and van der Brug, 2008; Ruiperez et al., 2010; Venda et al., 2010)). Because of this link,  $\alpha$ -synuclein is the most studied member of this family.

### 1.7.1. $\alpha$ -synuclein

#### 1.7.1.1. $\alpha$ -synuclein gene and protein structure

$\alpha$ -synuclein was first identified as a 143 amino acid protein of approximately 17 kDa localized in neuronal presynaptic terminals of the electric ray, *Torpedo californica* (Maroteaux et al., 1988). This group subsequently isolated from a rat brain cDNA library a highly homologous cDNA clone encoding 140 amino acid rat  $\alpha$ -synuclein. The newly identified protein was found to contain a number of imperfect repeats based around a ‘KTKEGV’ motif throughout the first 100 amino acids, as well as an acidic C-terminus. These N-terminal repeats share similarity to the class A2 lipid-binding domains of apolipoproteins and modulate interactions of synucleins with lipid membranes (George et al., 1995). Upon lipid binding, the structure of synucleins shifts from a natively unfolded state to adoption of partial  $\alpha$ -helical structure (Davidson et al., 1998; Eliezer et al., 2001; Perrin et al., 2000). Identification of the highly similar (~95% identity of amino acid sequence) human orthologue came a few years later, originally as the precursor protein of a non-amyloid beta component peptide (NAC) from the amyloid preparation of Alzheimer’s disease brains (Ueda et al., 1993). Subsequent gene mapping showed the human SNCA gene to be located on chromosome 4 (4q21.3-22) containing 6 exons (Jakes et al., 1994; Spillantini et al.,

1995). The expressed  $\alpha$ -synuclein protein is found in various neuronal populations in the CNS, where it is concentrated at presynaptic terminals (George et al., 1995). A summary of some of the key features of synuclein proteins can be found in Fig. 1.3.

#### 1.7.1.2. Proposed function for $\alpha$ -synuclein

As is the case for all three synucleins, the exact role of  $\alpha$ -synuclein is not fully understood. The large proportion of research has been in the area of dopamine metabolism, with early work suggesting an interaction between  $\alpha$ -synuclein and tyrosine hydroxylase, the rate-limiting enzyme in dopamine biosynthesis, both *in vitro* and *in vivo* (Perez et al., 2002). Another study demonstrated interaction of  $\alpha$ -synuclein with the dopamine transporter (DAT), again both *in vitro* and *in vivo*, with resulting alterations in dopamine handling (Lee et al., 2001). Generally, emphasis has been put on the potential role of  $\alpha$ -synuclein, and indeed  $\beta$ - and  $\gamma$ -synuclein, in regulating synaptic function and plasticity, possibly through the suggested chaperone-like activity of synucleins (Ahn et al., 2006; Lee et al., 2004; Park et al., 2002; Souza et al., 2000).

Over the past ten years a number of different groups have produced and studied  $\alpha$ -synuclein null mutant mice, mainly concentrating on the nigrostriatal pathway, but with conflicting results.  $\alpha$ -synuclein null mutant ( $\alpha$ -synuclein<sup>-/-</sup>) mice are viable and fertile, but have been shown to display subtle alterations in dopamine metabolism, such as reduced striatal dopamine levels and attenuation of dopamine-dependent locomotor response to amphetamine (Abeliovich et al., 2000). These findings were however not seen in other studies, but rather various groups showed other alterations in mutant mice, including a reduction of dopaminergic neurons in the substantia nigra pars compacta, and impairments in synaptic response to prolonged electrical stimulation (Cabin et al., 2002; Robertson et al., 2004; Schluter et al., 2003). Interestingly,  $\alpha$ -synuclein<sup>-/-</sup> mice have been shown to have enhanced resistance to the selective dopaminergic neurotoxin 1-methyl-4-phenyl-1,2,3,6-tetrahydropyridine (MPTP) with certain regimes and genetic backgrounds (Dauer et al., 2002; Drolet et al., 2004; Fornai et al., 2005; Robertson et al., 2004) although mice carrying a

spontaneous deletion of a region including the SNCA locus were as sensitive to MPTP as wild type mice (Schluter et al., 2003).

Recently, Burre and colleagues demonstrated that in neuronal synapses,  $\alpha$ -synuclein is involved in regulation of synaptic vesicle fusion with the cell membrane by promoting the assembly of SNARE complexes from its subunits, namely vesicular SNARE protein vesicle-associated membrane protein 2 (VAMP-2/synaptobrevin) and two target membrane-associated SNARE (tSNARE) proteins, syntaxin-1 and synaptosomal-associated protein 25 (SNAP-25) (Burre et al., 2010). These complexes play a pivotal role in synaptic vesicle docking and fusion pore formation at the plasma membrane, for example during neurotransmitter release (reviewed in (Rizo and Rosenmund, 2008; Sudhof and Rothman, 2009). The function of  $\alpha$ -synuclein as a promoter of SNARE complex assembly was suggested to be particularly important during periods of increased synaptic activity (Burre et al., 2010).

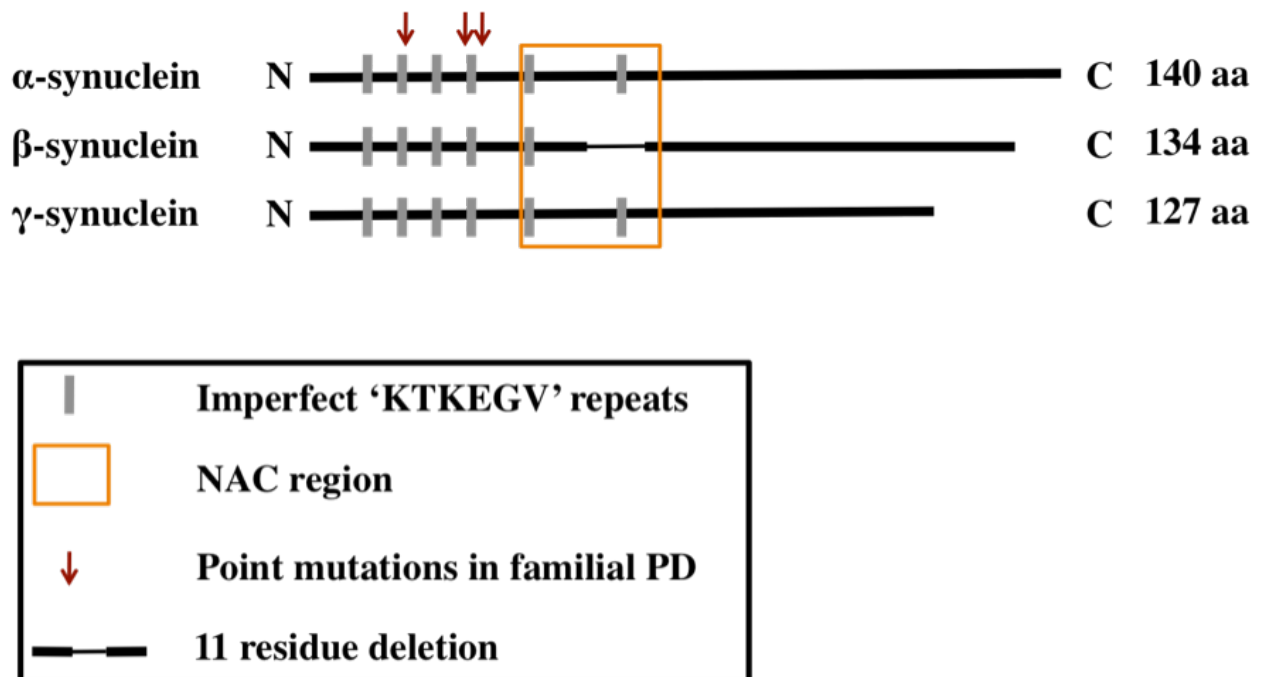


**Fig. 1.3. Overview of some key functional domains of the synuclein family.**

### 1.7.1.3. $\alpha$ -synuclein and neurodegeneration

Links between  $\alpha$ -synuclein and PD were first established in 1997 when a genetic defect causing familial, early onset form of the disease was located in the encoding (SNCA) gene and  $\alpha$ -synuclein protein was found to be the main constituent of histopathological inclusions in the brains of PD sufferers. Firstly, an autosomal dominant mutation in the SNCA gene was discovered in a large Italian kindred and three other (non-related) Greek families. This mutation (A53T) was thought to disrupt the normal structure of  $\alpha$ -synuclein and render the protein more susceptible to aggregation (Polymeropoulos et al., 1997). Since these findings, further discoveries have demonstrated more links with alterations to the SNCA gene sequence and forms of familial PD, including two further autosomal-dominant mutations A30P (Kruger et al., 1998) and E46K (Zarranz et al., 2004), gene duplications and triplications (Chartier-Harlin et al., 2004; Ibanez et al., 2004; Singleton et al., 2004) and polymorphisms in the SNCA promoter (Pals et al., 2004).

A secondly major link between  $\alpha$ -synuclein and PD was made with the discovery that  $\alpha$ -synuclein is a key component of Lewy bodies, the pathological hallmark of both sporadic and familial Parkinson's disease (Spillantini et al., 1997). Accumulation and aggregation of  $\alpha$ -synuclein has since been found in a number of neurodegenerative disorders including dementia with Lewy bodies (DLB) (Galvin et al., 1999; Spillantini et al., 1998b), multiple system atrophy (Spillantini et al., 1998a; Tu et al., 1998) and Hallervorden-Spatz syndrome (Galvin et al., 2000). Purified  $\alpha$ -synuclein aggregates rapidly *in vitro*, and forms fibrils similar to the fibrils found in deposits typical for synucleinopathies, including Lewy Bodies. A number of factors affect the aggregation of  $\alpha$ -synuclein including concentration of the protein itself as well as other various physiological parameters (reviewed in (Dev et al., 2003)). This aggregation appears to be initiated by a seeding mechanism (Uversky et al., 2002) and is exacerbated by A30P and A53T mutated  $\alpha$ -synuclein (Conway et al., 1998). A major question regarding these disorders is the possible varying toxicity of aggregatory intermediates and final products, as well as the identification of toxic mechanisms (Cookson and van der Brug, 2008; Volles and Lansbury, 2003). A key topic of discussion is whether these proteinacious inclusions are cytotoxic themselves

or the result of a form of compensatory protective mechanism to reduce levels of toxic intermediates and sequester dysfunctional protein to a particular part of the cell.

### *1.7.2. $\beta$ -synuclein*

#### *1.7.2.1 $\beta$ -synuclein gene and protein structure*

Along with the identification of  $\alpha$ -synuclein from human brain came the purification and sequencing of a 134 amino acid protein with 61% identity to  $\alpha$ -synuclein that was named  $\beta$ -synuclein (Jakes et al., 1994).  $\beta$ -synuclein is the human orthologue of bovine phosphoneuroprotein 14 (PNP14) and like  $\alpha$ -synuclein was also found to be predominantly expressed in the brain, and enriched in presynaptic terminals (Jakes et al., 1994). The gene encoding  $\beta$ -synuclein, SNCB, maps to chromosome 5q35 and has 6 exons (Spillantini et al., 1995).  $\beta$ -synuclein lacks a string of 11 central hydrophobic residues found in  $\alpha$ - and  $\gamma$ -synuclein which appears to mediate structural differences between the three proteins (Fig. 1.3).  $\beta$ -synuclein exhibits a lower predisposition towards helical structure in this altered region and is the assumed reason for its negligible propensity to aggregate, with the NAC region of  $\alpha$ -synuclein thought to be important for its aggregation (Sung and Eliezer, 2007). *In vitro*,  $\beta$ -synuclein was shown to inhibit the aggregation of  $\alpha$ -synuclein (Park and Lansbury, 2003; Uversky et al., 2002). Moreover, transgenic overexpression of  $\beta$ -synuclein, which does not cause neurological dysfunction, was able to ameliorate  $\alpha$ -synuclein neurotoxicity when the two proteins are co-expressed in bigenic mice (Fan et al., 2006; Hashimoto et al., 2001).

#### *1.7.2.2. $\beta$ -synuclein and neurodegeneration*

Although  $\alpha$ -synuclein is the major component of Lewy bodies as well as other pathological inclusions typical for that of the synucleinopathies, the presence of  $\beta$ -synuclein in these aggregates is yet to be reported. However, in cases of Alzheimer's disease (AD) and Lewy Body disease there do appear to be significant changes in the

levels of expression of  $\beta$ -synuclein (Rockenstein et al., 2001). There is also evidence that  $\beta$ -synuclein can be found within pathological lesions of other neurodegenerative conditions such as Pick's Disease (Mori et al., 2002), in the axonal spheroids typical for Hallervorden-Spatz syndrome (Galvin et al., 2000), as well as in Ubiquitin Carboxyl-terminal Hydrolase-L1 (UCH-L1) deficient *gad* mice (Wang et al., 2004). To date, there have been no reported links between mutations to the SNCB gene and PD (Lincoln et al., 1999a), although two point mutations (V70M and P123H) have been found possibly predisposing to DLB.

### *1.7.2.3. Modelling loss of $\beta$ -synuclein in vivo*

As with  $\alpha$ -synuclein<sup>-/-</sup> mice,  $\beta$ -synuclein<sup>-/-</sup> mice are viable and fertile with no obvious neurological phenotype ((Chandra et al., 2004), and our unpublished observations). Because the high similarity of  $\alpha$ - and  $\beta$ -synuclein might potentially lead to functional redundancy in single null mice,  $\alpha$ -/ $\beta$ -synuclein null mutant mice have been created. These double mutant mice did not exhibit any discernable phenotype although a statistically significant reduction in striatal dopamine levels was found, suggesting a certain degree of functional redundancy between  $\alpha$ - and  $\beta$ -synuclein ((Chandra et al., 2004), and our unpublished observations).

## *1.7.3. $\gamma$ -synuclein*

### *1.7.3.1. $\gamma$ -synuclein gene and protein structure*

The most recently identified and probably the least studied member of the synuclein family is  $\gamma$ -synuclein, which was cloned in three independent laboratories, including our own, a little over ten years ago (Buchman et al., 1998b; Ji et al., 1997; Lavedan et al., 1998b). The human  $\gamma$ -synuclein gene maps to chromosome 10q23 and contains 5 exons encoding a protein of 127 amino acids (Ninkina et al., 1998). Comparison of amino acid sequences shows that human  $\gamma$ -synuclein shares 56% and 54% similarity with human  $\alpha$ - and  $\beta$ -synuclein respectively (Lavedan et al., 1998b) with the highest

degree of similarity within the first 85 amino acid residues, containing six 'KTKEGV' repeats and the region similar to the NAC region found in  $\alpha$ -synuclein. However  $\gamma$ -synuclein differs considerably at the C-terminus from the other two family members (Buchman et al., 1998b; Ji et al., 1997; Lavedan et al., 1998b). It appears that this diversion in C-terminal sequence confers some key differences in structure from the other two synucleins. This is thought to mediate functional variations between the three proteins, with differences in  $\gamma$ -synuclein function expected to result from different protein-protein interactions mediated by its C-terminus (Sung and Eliezer, 2006).  $\gamma$ -synuclein adopts a similar free state residual secondary structure to  $\alpha$ -synuclein (Sung and Eliezer, 2007), which is consistent with the ability of  $\gamma$ -synuclein to aggregate and form fibrils *in vitro* as does  $\alpha$ -synuclein, although aggregates of  $\alpha$ -synuclein form much more readily (Biere et al., 2000; Serpell et al., 2000). The reduced tendency of  $\gamma$ -synuclein to form aggregates may be due to its higher propensity to form secondary structure ( $\alpha$ -helices) in the amyloid-forming region that is critical for the fibrillization of  $\alpha$ -synuclein (Marsh et al., 2006). In its extended mode, the structure of  $\gamma$ -synuclein resembles  $\beta$ -synuclein (Sung and Eliezer, 2007) which can be linked to the ability of both proteins to impede the *in vitro* aggregation of  $\alpha$ -synuclein, although  $\beta$ -synuclein blocks this process much more efficiently than  $\gamma$ -synuclein (Park and Lansbury, 2003; Uversky et al., 2002).

#### 1.7.3.2. $\gamma$ -synuclein expression and function

$\gamma$ -synuclein is found predominantly distributed throughout the cell body and axons of motor and sensory neurons of the peripheral nervous system (PNS) where it is expressed from the earliest stages of neural development (Buchman et al., 1998b). Expression of  $\gamma$ -synuclein can also be found in certain populations of neurons localised in other regions of the central nervous system (CNS), including the cerebral cortex, olfactory bulb, thalamus, hypothalamus, substantia nigra pars compacta (SNpc) and locus coeruleus (Lavedan et al., 1998b; Li et al., 2002). Initial work found that  $\gamma$ -synuclein could influence the neurofilament network, by exposure of neurofilaments to  $\text{Ca}^{2+}$ -dependent proteases (Buchman et al., 1998a). However determining a specific cellular role for  $\gamma$ -synuclein has remained elusive, partly due to

the fact that  $\gamma$ -synuclein knockout ( $\gamma$ -synuclein<sup>-/-</sup>) mice are viable, fertile, and have no evident phenotypical abnormalities (Ninkina et al., 2003, and discussed later). Interestingly, hypothalamic expression of  $\gamma$ -synuclein was recently shown to be responsive to both fasting and leptin administration in mice (Jovanovic et al., 2010; Tung et al., 2008). The hypothalamus is a heterogeneous region of the brain containing a number of anatomically distinct nuclei, each expressing their own individual sets of various neuronal populations. Within the CNS, the hypothalamus is recognised to receive and integrate neural, metabolic and humoral signals from the periphery and provides a major link between the nervous system and endocrine system to finely regulate downstream metabolic homeostatic responses as well as other activities of the autonomic nervous system. Two key regions of the hypothalamus, the arcuate nucleus (ARC) and the paraventricular nucleus (PVN) both include leptin receptor expressing-neurons which are critical for energy homeostasis and are considered key neurons through which leptin exerts its effects (Cone, 2005). Hypothalamic  $\gamma$ -synuclein expression in both the PVN and ARC was substantially downregulated in mice fasted for 48 hours but restored to nearly *ad libitum* fed levels by leptin treatment (Jovanovic et al., 2010; Tung et al., 2008).

#### 1.7.3.3. $\gamma$ -synuclein and cancer

$\gamma$ -synuclein was found to be a differentially expressed gene in advanced human breast cancer, which led to it being termed breast cancer-specific gene 1 (BCSG1) (Ji et al., 1997). It has since been documented that its upregulation occurs during the development of invasive and metastatic carcinomas of the breast, ovary and pancreas amongst others, and that this level of expression correlates strongly with the stage of cancer progression (Bruening et al., 2000; Cao et al., 2005; Guo et al., 2007). This increased expression has been suggested to be caused by demethylation of the CpG island on the SNCG gene (Gupta et al., 2003a; Liu et al., 2005; Liu et al., 2007; Lu et al., 2001), and may lead to the potential inhibition of mitotic checkpoints (Inaba et al., 2005), possibly via binding and subsequent degradation of the mitotic checkpoint protein BubR1 (Gupta et al., 2003b). In addition to this, it has been demonstrated that  $\gamma$ -synuclein is able to block c-Jun N-terminal kinase (JNK) signalling (Pan et al., 2002), a pathway which commonly induces apoptosis.

#### 1.7.3.4. $\gamma$ -synuclein and neurodegeneration

As is the case for  $\beta$ -synuclein, the presence of  $\gamma$ -synuclein in pathological lesions typical for synucleinopathies is yet to be seen. However, in cases of Alzheimer's disease (AD) and Lewy Body disease (Galvin et al., 1999; Mukaetova-Ladinska et al., 2008; Rockenstein et al., 2001), glaucoma (Surgucheva et al., 2002) and Gaucher disease (Myerowitz et al., 2004) there are changes in the levels of expression of  $\gamma$ -synuclein as well as its abnormal distribution.  $\gamma$ -synuclein has also been found in axonal spheroids typical for Hallervorden-Spatz syndrome (Galvin et al., 2000) as well as in Ubiquitin Carboxyl-terminal Hydrolase-L1 (UCH-L1) deficient *gad* mice (Wang et al., 2004).

Unlike the specific mutations found in the SNCA gene coding for  $\alpha$ -synuclein that cause an early onset, hereditary form of PD, no mutations or polymorphisms in the SNCG gene have been found to be associated with familial PD (Flowers et al., 1999; Kruger et al., 2001; Lavedan et al., 1998a; Lincoln et al., 1999b). In addition to this, unlike  $\alpha$ -synuclein, an acute overexpression of  $\gamma$ -synuclein does not induce apoptosis in neuronal cultures (Saha et al., 2000). However  $\gamma$ -synuclein has been implicated in some neurodegenerative conditions in the optic system. Its expression and distribution are altered in retinal ganglion cells and their axons in the optic nerve in human cases and mouse models of glaucoma (Buckingham et al., 2008; Soto et al., 2008; Surgucheva et al., 2002). It is therefore still possible that the accumulation and even aggregation of  $\gamma$ -synuclein may occur in these conditions. Indeed, our laboratory has recently produced a transgenic mouse line with pan neuronal overexpression of  $\gamma$ -synuclein under control of the Thy-1 promoter. These mice display progressive motor deficits from six months onwards and die prematurely. On closer inspection, there is prominent neuronal pathology, most notably in the spinal cord, with accumulation and aggregation of  $\gamma$ -synuclein within the axon and cell body (Ninkina et al., 2009).

#### 1.7.3.5. Modelling loss of $\gamma$ -synuclein *in vivo*

As with both  $\alpha$ - and  $\beta$ -synuclein<sup>-/-</sup> mice,  $\gamma$ -synuclein<sup>-/-</sup> mice are viable, fertile, and do not display any obvious neurological phenotype. Moreover, neurons of the dorsal root ganglion and trigeminal ganglion, regions where  $\gamma$ -synuclein is most highly expressed

do not display any developmental or functional defects (Ninkina et al., 2003; Papachroni et al., 2005; Robertson et al., 2004). Behavioural analysis of these animals did not reveal any motor deficits nor were there any evidence of cell loss in the SNpc or VTA even in aged animals (Al-Wandi et al., 2010). Similar to  $\alpha$ -synuclein<sup>-/-</sup> mice,  $\gamma$ -synuclein<sup>-/-</sup> mice have enhanced resistance to MPTP (Robertson et al., 2004) suggesting potential functional overlap between  $\alpha$ - and  $\gamma$ -synuclein, which is indeed supported by the fact that similar groups of genes are altered in single  $\alpha$ - and  $\gamma$ -synuclein<sup>-/-</sup> mice (Kuhn et al., 2007).

#### 1.7.4. Synucleins and lipids

##### 1.7.4.1. Lipid interaction and multimerisation of synucleins

*In vitro*  $\alpha$ -synuclein interacts with phospholipid vesicles and in cultured HeLa cells is enriched at lipid rafts, where it exhibits preferential interaction for certain phospholipid species (Fortin et al., 2004; Jo et al., 2000; Kubo et al., 2005; Ramakrishnan et al., 2003).  $\alpha$ -synuclein can also associate with lipid droplets and protect internal TAG stores from hydrolysis in lipid-loaded cells (Cole et al., 2002). The binding of  $\alpha$ -synuclein to neutral and charged membranes appears to occur by different mechanisms (Shvadchak et al., 2011). This study showed that binding of  $\alpha$ -synuclein to neutral bilayers increases with membrane curvature and rigidity and decreases in the presence of cholesterol. Furthermore, it was demonstrated that the association of  $\alpha$ -synuclein with negatively charged membranes is much stronger overall, and is much less sensitive to membrane curvature and cholesterol content. In both neutral and charged membranes, the presence of unsaturated lipids was shown to increase binding of  $\alpha$ -synuclein (Shvadchak et al., 2011).

Links between synucleins and polyunsaturated fatty acids (PUFA) have also been documented, including direct *in vitro* interaction of  $\alpha$ -synuclein with PUFA (Karube et al., 2008; Sharon et al., 2001). PUFA also promote multimerisation of  $\alpha$ -synuclein (Perrin et al., 2001; Sharon et al., 2003a) as well as  $\beta$ -, and  $\gamma$ -synuclein (Perrin et al., 2001). The presence of lipid-associated oligomers of  $\alpha$ -synuclein in the brain is

believed to play a role in the development of neuronal dysfunction observed in Parkinson's disease and other synucleinopathies (Fink, 2006; Uversky, 2007). *In vitro* work has shown that oligomerisation of  $\alpha$ -synuclein is dependent both on fatty acid length and saturation, and that these oligomers are cytotoxic to neuronal cells in culture (Assayag et al., 2007). Certain lipid species increase this multimerisation, for example in yeast cells, the aggregation of  $\alpha$ -synuclein is enhanced in yeast mutants that produce high levels of acidic phospholipids (Soper et al., 2011). Similarly, docosahexaenoic acid (DHA) promotes aggregation of  $\alpha$ -synuclein *in vitro*, producing fibrils that are morphologically different from oligomers formed in the absence of DHA. Moreover,  $\alpha$ -synuclein oligomers generated in a dopaminergic cell line were more cytotoxic when formed in the presence of this PUFA (De Franceschi et al., 2011).  $\alpha$ -synuclein interaction with PUFA also affects the properties of PUFA themselves, reducing their micellar size (Broersen et al., 2006). This study also demonstrated that in the presence of PUFA, namely arachidonic acid (ARA) and DHA, and not saturated fatty acids,  $\alpha$ -synuclein undergoes conformational changes adopting  $\alpha$ -helical structure (Broersen et al., 2006). Of importance to normal lipid metabolism and in cases of possible dysfunction, DHA accounts for over half of all esterified fatty acids in plasma membrane phospholipids in neurons, and the levels of this fatty acid are elevated in Parkinson's disease patients (Lukiw and Bazan, 2008; Sharon et al., 2003b). Interestingly, in the brains of rats fed high n-3 PUFA diets (e.g. eicosapentaenoic acid and DHA), the expression of both  $\alpha$ - and  $\gamma$ -synuclein was increased approximately 2-fold (Kitajka et al., 2002).

#### *1.7.4.2. Effects of synucleins on lipid metabolism in the brain*

In the brains of  $\alpha$ -synuclein null mutant mice, there are changes in intracellular lipid metabolism as well as an increase in whole-brain neutral lipid content (Barcelo-Coblijn et al., 2007; Ellis et al., 2005). Alterations in fatty acid handling can also be found in the brains of these  $\alpha$ -synuclein deficient mice. Here there is a reduced incorporation of ARA into phospholipids with a compensatory rise in incorporation of DHA (Golovko et al., 2007). This was attributed to a role for this protein in substrate presentation to acyl-CoA synthetase (ACS), an important enzyme in the fatty acid reacylation pathway, with reduced ACS (ACS-6 isoform) activity demonstrated in

mutant mice (Golovko et al., 2009; Golovko et al., 2006).  $\alpha$ -synuclein deficient mice were also shown to have lower levels of free PUFA in brain, with the same group observing increased free PUFA levels in cultured neurons with overexpression of  $\alpha$ -synuclein (Sharon et al., 2003b).

Various groups have demonstrated direct interaction and inhibition of phospholipase D (PLD) by  $\alpha$ -synuclein *in vitro* (Ahn et al., 2002; Jenco et al., 1998) and *in vivo* (Gorbatyuk et al., 2010). PLD is an enzyme believed to participate in vesicle trafficking, membrane signaling and both endo- and exocytosis, and its activity is responsive to various hormones, factors, neurotransmitters and reactive lipids (Liscovitch et al., 2000). Specifically, PLD hydrolyses phosphatidylcholine at the cell membrane, producing phosphatidic acid and choline, and phosphatidic acid has been shown to mediate a number of processes controlling vesicular transport (Ktistakis et al., 1995; Tsai et al., 1989). In addition to  $\alpha$ -synuclein,  $\beta$ - and  $\gamma$ -synuclein were also able to inhibit PLD *in vitro* (Jenco et al., 1998; Payton et al., 2004). However a different group, who found no evidence of PLD inhibition by  $\alpha$ -synuclein in either cell-free assays or several cell lines, has disputed these findings (Rappley et al., 2009).

#### 1.7.5. Expression of $\gamma$ -synuclein in white adipose tissue

As mentioned previously, there is no clear cellular role for  $\gamma$ -synuclein, and ablation of  $\gamma$ -synuclein causes only minor changes in the nervous system (Ninkina et al., 2003; Papachroni et al., 2005; Robertson et al., 2004). Whilst working on a mouse model of mammary gland tumourigenesis in our laboratory, we unexpectedly discovered that not only is  $\gamma$ -synuclein expressed in certain types of mouse mammary tumours but also in the normal adjacent mammary tissue. Moreover, expression levels appeared to correlate with the number of stromal adipocytes. This prompted us to check the expression in various body fat pad depots using Northern blotting, quantitative RT-PCR and Western blotting, which all confirmed that epididymal and subcutaneous white adipose tissue depots express high levels of  $\gamma$ -synuclein (Fig. 1.4, 1.5, 1.6). Northern blot hybridisation with a highly specific 3' UTR probe revealed the same size (~0.8 kb)  $\gamma$ -synuclein transcripts in mouse neural tissues and WAT depots (Fig.

1.4). Transcript levels were very low in adult brown adipose tissue, however levels in WAT were higher than in the adult mouse central nervous system regions and only slightly lower than in the peripheral sensory ganglia, a tissue with the highest level of  $\gamma$ -synuclein expression in the mouse nervous system (Buchman et al., 1998b; Ninkina et al., 2003) (Fig. 1.5). Western blotting with antibodies against mouse  $\gamma$ -synuclein (Buchman et al., 1998b) confirmed the presence of  $\gamma$ -synuclein protein in subcutaneous and epididymal WAT (Fig. 1.6).

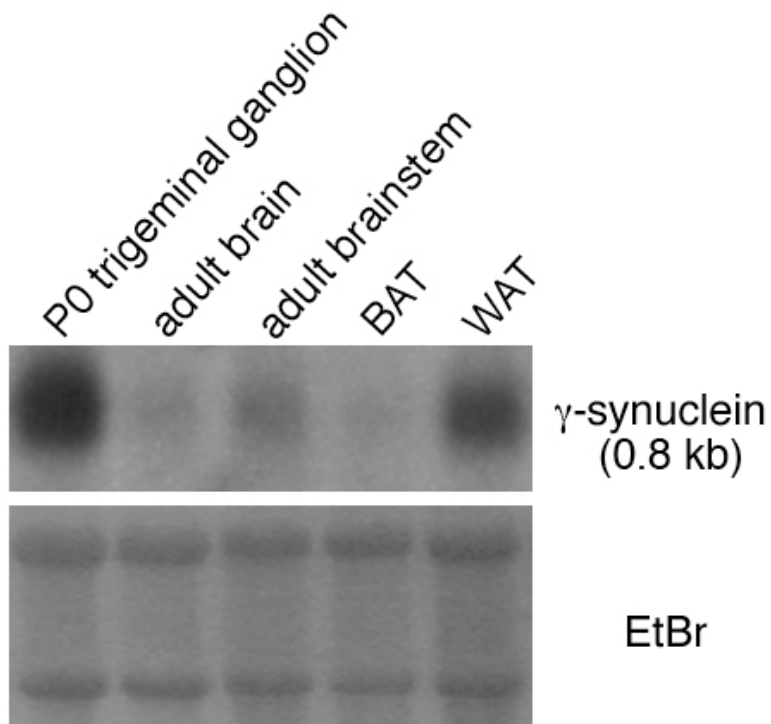


**Fig. 1.4. Northern blot analysis of  $\gamma$ -synuclein mRNA in mouse tissues.** mRNA isolated from wild type adult mouse brown adipose tissue (BAT), subcutaneous white adipose (WAT) as well as neuronal tissues where  $\gamma$ -synuclein is known to be expressed. A specific hybridisation probe derived from the 3'-UTR of mouse  $\gamma$ -synuclein mRNA was used for detection of a 0.8 kb transcript in each tissue. Equal loading was confirmed by ethidium bromide (EtBr) staining of ribosomal RNA bands on the membrane before hybridisation.

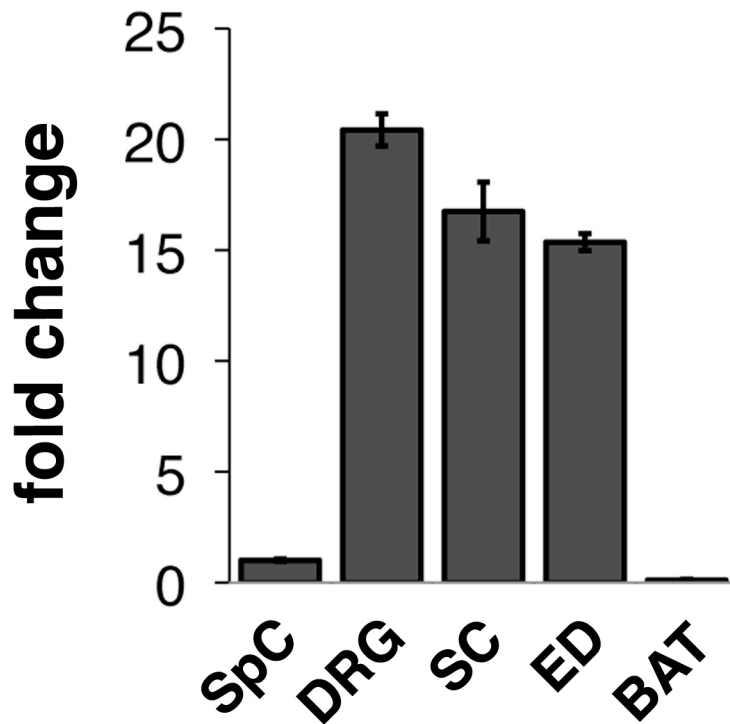


**Fig. 1.5. Quantitative RT-PCR analysis of  $\gamma$ -synuclein mRNA in neuronal and adipose tissues of adult wild type mice.** RNA was extracted from the spinal cord (SpC) and dorsal root ganglia (DRG) as well as subcutaneous (SC), epididymal (ED) and brown (BAT) adipose tissue. Results are shown as mean $\pm$ SEM of fold change normalized to the average level of  $\gamma$ -synuclein mRNA in the spinal cord (n=4).

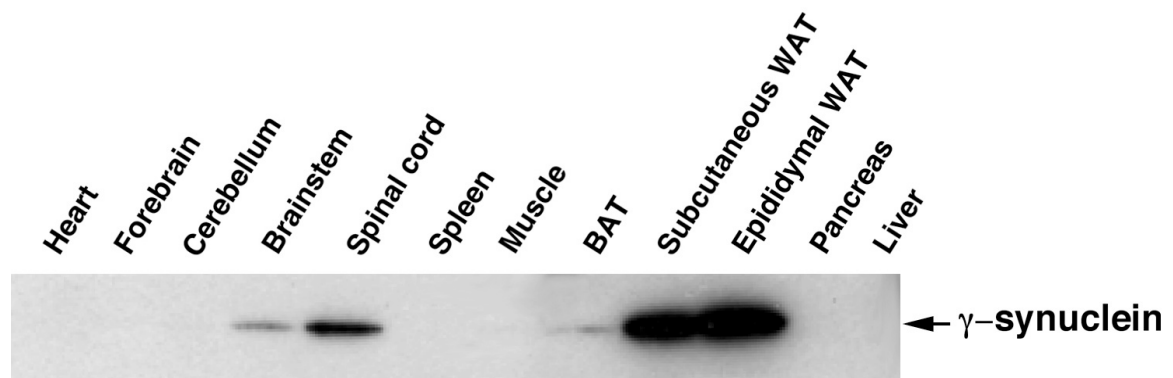


**Fig. 1.6. Analysis of  $\gamma$ -synuclein expression in various mouse tissues using Western blotting.** Total proteins were extracted from tissue taken from adult wild type mice, and detected using an affinity purified anti-mouse  $\gamma$ -synuclein (SK23) antibody (Buchman et al., 1998b). Performed in collaboration with Hiroshi Sakaue (Kobe University, Japan).

Other groups have previously reported high levels of  $\gamma$ -synuclein expression in adipose tissue of both humans and pigs (Frandsen et al., 2009; Oort et al., 2008). Moreover, expression of  $\gamma$ -synuclein is increased in adipose tissue of obese humans and decreased during caloric restriction (Oort et al., 2008). Therefore, we began studying  $\gamma$ -synuclein expression in murine WAT, as outlined in the aims section below.

## 1.8. Aims

In an attempt to understand the role of  $\gamma$ -synuclein in WAT, and its possible involvement in the development of obesity, we planned to investigate the following:

1. To determine whether in mice fed a high fat diet,  $\gamma$ -synuclein expression is nutritionally regulated in WAT, similar to the expression changes seen in obese humans.
2. To test whether  $\gamma$ -synuclein deficiency affects progression of high fat diet-induced obesity in a mouse model. In order to achieve this aim we challenged  $\gamma$ -synuclein null mutant mice with a high fat diet known to cause diet-induced obesity in wild type mice.
3. To describe any alterations in lipid metabolism within WAT resulting from loss of  $\gamma$ -synuclein, and therefore begin to understand a possible role for  $\gamma$ -synuclein in this tissue.
4. To elucidate the involvement of  $\gamma$ -synuclein in molecular mechanisms concerned with lipid handling in adipocytes.
5. To describe any changes in lipid composition in the brain of  $\gamma$ -synuclein null mutant mice.

## **Chapter 2 - Experimental Procedures**

## 2. Experimental Procedures

### 2.1. Solutions

#### *DNA loading dye*

Tris-borate	89 mM
EDTA	2 mM
Glycerol	20% (v/v)
Bromophenol blue	0.02% (w/v)

#### *Diaminobenzidine solution (Sigma-Aldrich)*

3,3'-diaminobenzidine	3.3 mM
Urea hydrogen peroxide	7.0 mM
Tris	60 mM

#### *Enzyme dilution buffer pH 7.0*

KPO <sub>4</sub> pH 7.0	0.1 M
EDTA	1 mM
DTT	1 mM
BSA	0.002% (w/v)

#### *Garbus solution pH 7.4*

KCl	2 M
KPO <sub>4</sub>	0.5 M

*Hypertonic sucrose buffer*

Tris-HCl pH 7.5	50 mM
Sucrose	0.25 M
EDTA	1 mM
DTT	1 mM

*Immunoprecipitation (IP) buffer*

Tris-HCl pH 7.5	50 mM
NaCl	150 mM
Triton X-100	1 % (v/v)
Protease Inhibitors (Complete mini from Roche)	

*Krebs-Ringer Media (KRM) pH 7.4*

NaCl	0.12 M
KCl	4.5 mM
MgCl <sub>2</sub>	0.5 mM
NaH <sub>2</sub> PO <sub>4</sub>	1.5 mM
Na <sub>2</sub> HPO <sub>4</sub>	0.7 mM
D-Glucose	10 mM
* * *	* *
HEPES	25 mM
NaHCO <sub>3</sub>	15 mM
BSA (fraction V)	1% (w/v)

CaCl <sub>2</sub>	2.5 mM
Adenosine	200 nM
Collagenase I (Sigma-Aldrich)	1 mg/ml

*Phosphate buffered saline: Dulbecco A (pH 7.3±0.2) (Oxoid)*

NaCl	0.1 M
KCl	2.6 mM
Sodium phosphate dibasic (HNa <sub>2</sub> O <sub>4</sub> P.2H <sub>2</sub> O)	6.5 mM
Potassium phosphate monobasic (N <sub>2</sub> KO <sub>4</sub> P)	1.2 mM

*SDS-PAGE loading buffer*

Tris-HCl pH 6.8	100 mM
Glycerol	20% (v/v)
SDS	4% (w/v)
Bromophenol blue	0.02% (w/v)
β-mercaptoethanol	200 mM

*SDS-PAGE running buffer (pH 8.5)*

Tris	25 mM
Glycine	192 mM
SDS	0.1% (w/v)

*TBE buffer (pH 8.3) (Sigma-Aldrich)*

Tris-borate	89 mM
EDTA	2 mM

*TBS-T (pH 8.0) (Sigma-Aldrich)*

Tris	50 mM
NaCl	138 mM
KCl	2.7 mM
Tween-20	0.1% (v/v)

## 2.2. Animals

### 2.2.1. *γ-synuclein null mutant mice*

Generation of mice with a targeted deletion of the *Sncg* gene ( $\gamma$ -synuclein null mutant) on a C57Bl6J background was described previously (Ninkina et al., 2003).

### 2.2.2. *Genotyping by conventional PCR*

Genomic DNA (gDNA) was isolated and purified using a Wizard SV gDNA purification system (Promega) and 5  $\mu$ l of gDNA mixed with 45  $\mu$ l of an amplification mastermix yielding a 50  $\mu$ l reaction with the following components:

Tris-HCl pH 9.0	10 mM
MgCl <sub>2</sub>	1.5 mM
KCl	50 mM
Triton X-100	0.1% (v/v)
Primers (fwd/rev)	0.25 $\mu$ M
dNTP	0.2 mM
Taq Polymerase	5 units

DNA was amplified by 40 cycles of conventional PCR with thermal cycling conditions set at:

Denaturation	94°C	15 seconds
Annealing	60°C	30 seconds
Extension	72°C	40 seconds

A common upstream primer (*SAUP*) as well as primers specific for the wild type allele (*GDN*) and the *PGK-neo* cassette (*NeoB'*) were used for amplification:

<i>SAUP</i>	5'-AGTCCTGGCACCTCTAAGCA-3'
<i>GDN</i>	5'-GGGCTGATGTGTGGCTATCT-3'
<i>NeoB'</i>	5'-CTGAAGAACGAGATCAGCAGC-3'

(all sequences produced by Sigma-Genosys)

Amplified fragments were separated on 1.5% (w/v) agarose gels in Tris-borate-EDTA (TBE) buffer:

TBE	100 ml
Agarose	1.5 g
Ethidium Bromide	2 $\mu$ l

10  $\mu$ l of PCR product was mixed with 10  $\mu$ l DNA loading dye and loaded into each well along with 5  $\mu$ l of DNA ladder (Hyperladder I, Bioline). The electrophoresis was run at 130V until sufficient separation had taken place. PCR using these primers generated a 490bp fragment from wild type DNA and a 397bp fragment from  $\gamma$ -synuclein knockout DNA.

### *2.2.3. Husbandry & Diets*

Mice were single housed in standard cages, in a temperature and humidity controlled environment, a 12 hour light/dark cycle, and with free access to water. From the age of 9 week animals were fed either a low fat diet (LFD, equivalent of 10% energy from fat) or a high fat diet (HFD, equivalent of 45% energy from fat) ((Van Heek et al., 1997), both purchased from TestDiet). Dynamics of body mass changes and amount of food consumed were measured weekly. All animal work was carried out in accordance with the United Kingdom Animals (Scientific Procedures) Act (1986).

### *2.2.4. Tissue Collection*

On the day of tissue collection, food was removed 4 hours prior to terminally anaesthetizing mice with barbiturate overdose via i.p. injection (Euthatal, from Merial). Blood was harvested via exsanguination from a cardiac puncture using a syringe presoaked in 1 mg/ml sodium heparin (Sigma-Aldrich), centrifuged at 2,100 x g for 5 minutes at room temperature in Microvette CB300 LH heparinated tubes (Sarstedt), and the plasma pipetted off and snap frozen in liquid nitrogen. Liver, brown adipose tissue (BAT) and also white adipose tissue (WAT) from visceral (epididymal and retroperitoneal) and subcutaneous (femoral) depots were dissected, weighted and processed for subsequent analysis.

## **2.3. Magnetic resonance imaging (MRI) analysis**

MRI is able to provide scans with detailed contrast between various soft tissues of the body, for example the distribution of fat amongst the major organs. Mice were anaesthetised and scanned at 9, 15, 20 weeks of age using a highfield (9.4T) small bore (72mm) Bruker 94/20 MRI/MRS scanner. Two whole-body 2D RARE scans (one with fat suppression on and one with fat suppression off) were acquired per time point (matrix 512 x 256 = 156µm in plane resolution, 64 x 0.5mm slices, TE 12ms, TR 3.9s, RARE factor 4). Fat only images were generated by the subtraction of the fat suppressed image from the non-suppressed image. This subtraction, the 3D image reconstruction and user directed fat pad volume measurement were carried out using

'FAT' (Fat Analysis Tool), a small GUI application custom written in IDL at Cardiff University Experimental MRI Centre.

#### **2.4. Whole-body metabolic analysis**

A comprehensive lab animal monitoring system (CLAMS) can be used to measure simple parameters such as body weight and water/food consumption, as well as other, more complex measurements, including free physical activity and respiration rates, all over a set period of time. Metabolic rate in mice in the 8<sup>th</sup> week of HFD feeding was determined by indirect calorimetry with the use of a CLAMS (Columbus Instruments) attached to a custom built O<sub>2</sub> and CO<sub>2</sub> monitoring system, based in the Institute of Metabolic Science, Cambridge University. Mice were single housed, and were acclimatised to the cages a few days before testing period. Cages were maintained at constant temperature, air-flow was set at 0.4 L/min, and the O<sub>2</sub> and CO<sub>2</sub> concentration in room air and air leaving each cage was measured every 18 minutes to determine respiratory exchange ratio (RER,  $v\text{CO}_2/v\text{O}_2$ ) and also energy expenditure (using constants according to (Elia and Livesey, 1992)) over a 72-hour period. Data was averaged for 3-hour intervals.

#### **2.5. Glucose- / Insulin Tolerance Testing**

Glucose- (GTT) and insulin tolerance tests (ITT) were performed on non-anaesthetised mice in the 9<sup>th</sup> and 10<sup>th</sup> week of HFD feeding, respectively. Mice were fasted overnight before GTT or for 4 hours before ITT. For GTT, glucose levels in tail vein blood were measured at baseline, and 30, 60, 90 and 120 minutes after a single i.p. injection of D-glucose (1 g/kg body weight, from Sigma-Aldrich) using an Accutrend Plus glucometer (Roche Diagnostics). For ITT, mice received an i.p. injection of human insulin (Sigma-Aldrich) in 0.9% (w/v) NaCl (0.75 U/kg body weight). The blood glucose levels were measured at baseline, and 15, 30, 45 and 60 minutes after injection. Data was plotted on graphs of blood glucose concentration over time with the area under the curve calculated for each genotype, for both GTT and ITT to quantify clearance of glucose from the blood, and insulin sensitivity respectively.

## 2.6. Lentiviral expression of $\gamma$ -synuclein

### 2.6.1. DNA fragment amplification

A 414 bp fragment of human  $\gamma$ -synuclein cDNA that included the coding region and 20 nucleotides upstream of the start codon, including the Kozak sequence, was amplified from a previously obtained plasmid clone (Ninkina et al., 1998) by PCR using primers with BamHI restriction endonuclease recognition site added at their 5' end:

*hgamma\_for\_Bam* 5'-ggatccCACAACCCTGCACACCCACCATGGATG-3'

*h\_gamma\_rev\_Bam* 5'-ggatccCTAGTCTCCCCCACTCTG-3'

This fragment was cloned into a pCR-Blunt II-TOPO vector using One Shot chemically competent cells according to manufactures protocol (Invitrogen). Transformants were grown on LB agar plates with 50  $\mu$ g/ml of kanamycin overnight at 37°C. Individual bacteria colonies were inoculated into 5 ml of LB medium with kanamycin and grown overnight at 37°C with intensive shaking. Plasmid DNA was extracted from 4 ml of bacteria suspension using a NucleoSpin mini-prep kit according to the manufactures (Macherey-Nagel GmbH) instructions. The presence of eukaryotic insert was checked by digestion of each plasmid DNA with BamHI and analysis of digestion products by electrophoresis in 1.2% (w/v) agarose gels. Inserts of several individual clones were fully sequenced to select those with correct nucleotide sequence.

### *2.6.2. Purification of insert DNA, and ligation, transformation and plasmid analysis*

Selected recombinant TOPO plasmid DNA was digested with BamHI prior to purification by electrophoresis in 1.2% (w/v) agarose gels. Correct molecular weight bands representing insert DNA were excised and purified using a gel extraction kit according to manufacturers protocols (Qiagen). Ligations were performed using T4 DNA ligase (Invitrogen), with the DNA insert containing the coding region of human  $\gamma$ -synuclein subcloned into the unique BamHI site of the pRRLsin.cPPT.hPGK-eGFP lentiviral expression vector (Follenzi et al., 2000, see Appendix 1). Prior to ligation, this vector was digested, treated with alkaline phosphatase and purified in agarose gels as above. Plasmids were transformed into DH5 $\alpha$  competent cells with growth of transformants on LB agar plates, inoculation of individual colonies and extraction of plasmid DNA performed as in section 2.6.1. Insertion of the DNA insert in the correct orientation was checked by digestion of plasmid DNA with NcoI and XhoI and analysis of the digestion products by electrophoresis in 1.2% (w/v) agarose gels as well as sequencing using an oligonucleotide primer 'p305for' located in the hPGK-1 promoter, 88 bp upstream of the cloning BamHI site.

*p305for*                      5'-GTTCCGCATTCTGCAAGC-3'

### *2.6.3. Lentiviral production*

Selected plasmids were used for production of recombinant lentivirus particles. All work involving lentiviral production was performed in the laboratory of Dr Riccardo Brambilla in the Institute of Experimental Neurology, San Raffaele Foundation and University, Milano. Virus particles were produced and tittered according to the previously described protocols (Indrigo et al., 2010).

#### *2.6.4. Lentiviral transduction of cells in vivo and in vitro*

For expression of  $\gamma$ -synuclein in cultured cells,  $1.5 \times 10^6$  virus transducing units in one millilitre of the full culture medium were incubated for 48 hours with cells growing on culture dishes or coverslips. For expression in mouse WAT adipocytes, 5  $\mu$ l of F12 medium containing  $5 \times 10^5$  virus transducing units were injected into an exposed subcutaneous femoral WAT pad of anaesthetized 9-week-old male mouse. 3-5 injections of  $\gamma$ -synuclein expressing viruses were made per right fat pad and 3-5 injections of GFP-only expressing viruses – per left fat pad. After HFD feeding protocol, these fat pads were dissected out, fixed and immunostained as described in ‘histological techniques’.

#### **2.7. Blood chemistry**

Commercially available kits were used to measure plasma levels of glucose, insulin, leptin and adiponectin (Linco Research), as well as plasma ketone body levels by  $\beta$ -hydroxybutyrate content (Cayman Chemicals), all according to manufacturers instructions.

#### **2.8. Isolation of cell populations from WAT**

Mature adipocytes as well as the preadipocyte-containing stromal cell fraction were isolated from epididymal fat depots based on the method of (Rodbell, 1964) as modified by (Honnor et al., 1985). All cell processing was performed in Krebs-Ringer bicarbonate medium (KRM) buffered with 25 mM HEPES at pH 7.4 containing 2.5 mM  $\text{CaCl}_2$ , 10 mM glucose and 200 nM adenosine (to suppress cAMP production during cell isolation). Briefly, WAT was incubated in KRM containing 1% (w/v) fatty acid free bovine serum albumin (BSA) and 1 mg/ml collagenase, for 45 minutes at 37°C with gentle shaking. Cells were filtered through a nylon mesh and centrifuged 3 times for 1 minute at 250 x g and room temperature to sediment stromal-vascular cells, each time with aspiration of infranate, and resuspension of the floating adipocytes in KRM without collagenase.

## **2.9. Adipocyte lipolysis**

Mature adipocytes (isolated from 500 mg of epididymal WAT) were suspended at approximately 20% (v/v) in KRM, aliquoted in triplicate, and lipolysis measured under basal (200 nM (R)-(-)-N<sup>6</sup>-(2-phenylisopropyl)adenosine, PIA) and catecholamine-stimulated (200 nM PIA + 10 μM isoproterenol) conditions. Lipolytic rate was quantified by glycerol release into the media over a 2-hour period at 37°C using a free glycerol determination kit (Sigma-Aldrich). Results were normalized to the level of endogenous GAPDH expression in each suspension measured using semi-quantitative Western blotting.

## **2.10. Semi Quantitative Western blotting**

Western blotting is an important tool used to measure the abundance of a certain protein with the use of a specific antibody.

### *2.10.1. Protein extraction*

Total tissue proteins were extracted from cells cultured on tissue culture plates or isolated mouse cell populations by direct homogenisation in SDS-PAGE loading buffer using a pellet pestle and motor, followed by incubation at 100°C for 10 minutes. For WAT depots, 50 mg of tissue was homogenized into 350 μl SDS-PAGE loading buffer, vortexed, incubated at 37°C for 5 minutes and finally centrifuged at 6,000 x g. The infranate was removed from underneath the fat cake, and incubated at 100°C for 10 minutes.

To analyse separately nuclear, cytosolic and lipid droplet-associated proteins, purified WAT mature adipocytes were lysed in a hypotonic sucrose buffer at 4°C using a glass Porter homogeniser. Lysates were centrifuged at 1,000 x g for 10 minutes at 4°C, and the infranate removed. The pellet and fat cake were washed three times with fresh lysis buffer, each time with centrifugation as above. All fractions were diluted or re-suspended in SDS-PAGE loading buffer followed by incubation at 100°C for 10 minutes.

### 2.10.2. Total protein quantification

Levels of total proteins in each sample were estimated prior to analysis, using a commercial kit (BioRad) based on the Bradford protein assay (Bradford, 1976) and measuring absorbance at 590 nm using a multiwell plate reader (BioTek).

### 2.10.3. SDS-Polyacrylamide gel electrophoresis (SDS-PAGE) & protein transfer

Proteins were separated by SDS-PAGE using resolving gels of various acrylamide concentration (8-18%, w/v) and a 6% (w/v) stacking gel cast into BioRad plates and moulds.

#### *Resolving gel*

Acrylamide/bis-acrylamide	8-18% (w/v)
Tris-HCl pH 8.8	313 mM
Sodium dodecyl sulphate (SDS)	0.1% (w/v)
Ammonium persulphate (APS)	0.1% (w/v)
Tetramethylethylenediamine (TEMED)	0.1% (v/v)

#### *Stacking gel*

Acrylamide/bis-acrylamide	6% (w/v)
Tris-HCl pH 6.8	156 mM
SDS	0.1% (w/v)
APS	0.1% (w/v)
TEMED	0.1% (v/v)

Loaded proteins, along with 5  $\mu$ l protein ladder (10-250 kDa, PageRuler, Fermentas) were separated at 200V using a Tris-glycine SDS-PAGE running buffer and electrophoretically transferred to polyvinylidene difluoride (PVDF) using iBlot technology (Invitrogen) according to manufacturer's protocol.

#### *2.10.4. Antibodies and detection*

Subsequent membranes were blocked in 4% (w/v) non-fat dry milk (Marvel) in Tris-buffered saline with 0.1% Tween-20 (v/v, TBS-T) followed by incubation with specific primary antibodies and appropriate horseradish peroxidase (HRP)-conjugated secondary antibodies (1:3000, Amersham), both diluted in 4% (w/v) non-fat dry milk in TBS-T. Membranes were washed for 20 minutes in TBS-T after both primary and secondary antibody incubation. All antibodies used in Western blotting experiments are listed below in table 2.1. Enhanced chemiluminescence (ECL) and ECL plus reagents (Amersham) were used for detection of protein bands. Membranes were exposed to X-ray film (Fuji). Band intensities were obtained using an AlphaImager™ 2200 and quantified using AlphaEase 2200 software (both AlphaInnotec). After subtracting background values, intensities of bands were normalised relative to the levels of GAPDH on the same membrane, to control variations in loading and confirm uniform efficiency of transfer.

*Antibodies used for Western blotting*

<b>Target</b>	<b>Type / Clone</b>	<b>Source</b>	<b>Dilution</b>
<b><math>\gamma</math>-synuclein (mouse)</b>	Rabbit polyclonal	(Buchman et al., 1998b)	1:1000
<b><math>\gamma</math>-synuclein (human)</b>	Rabbit polyclonal	(Ninkina et al., 1998)	1:1000
<b>GAPDH</b>	Mouse monoclonal (6C5)	Santa Cruz Biotechnology	1:3000
<b>HSL</b>	Rabbit polyclonal	Cell Signaling	1:1000
<b>phospho-HSL</b>	Rabbit polyclonal	Cell Signaling	1:1000
<b>perilipin A</b>	Rabbit polyclonal	Cell Signaling	1:1000
<b>ATGL</b>	Rabbit monoclonal (30A4)	Cell Signaling	1:1000
<b>histone 3 (H3)</b>	Rabbit polyclonal	Abcam	1:5000
<b>phospho-AMPK<math>\alpha</math></b>	Rabbit monoclonal (40H9)	Cell Signaling	1:500
<b>Akt/PKB</b>	Rabbit polyclonal	Cell Signaling	1:1000
<b>phospho-Akt/PKB</b>	Rabbit monoclonal (D9E)	Cell Signaling	1:1000
<b>Phospho-p70 S6 kinase</b>	Rabbit polyclonal	Cell Signaling	1:1000
<b>ERK</b>	Rabbit polyclonal	Cell Signaling	1:1000
<b>Phospho-ERK</b>	Rabbit monoclonal (20G11)	Cell Signaling	1:1000
<b>VAMP-4</b>	Rabbit polyclonal	Abcam	1:1000
<b>Syntaxin-5</b>	Rabbit polyclonal	Synaptic Systems	1:3000
<b>SNAP-23</b>	Rabbit polyclonal	Synaptic Systems	1:3000
<b>Anti-mouse IgG</b> (produced in sheep)		Amersham	1:3000
<b>Anti-rabbit IgG</b> (produced in donkey)		Amersham	1:3000

**Table 2.1. Antibodies used in Western blotting experiments.**

## 2.11. RNA expression analysis

mRNA levels of a particular gene can be measured by purification of total RNA from tissues or cells, synthesis of first strand cDNA and finally quantitative amplification using specific oligonucleotide primers and a DNA-binding fluorescent dye.

### 2.11.1. RNA extraction and cDNA synthesis

Total RNA was extracted from 50 mg of epididymal and subcutaneous white adipose tissue or directly from cells growing on a tissue culture plate using an RNeasy™ lipid tissue kit (Qiagen) according to manufacturer's protocol. Levels of the resultant purified RNA was quantified using a Nanodrop ND-1000 spectrophotometer (Labtech). First-strand cDNA was synthesized from 0.3 µg of total RNA using 0.5 µg of random hexadeoxynucleotide primers (Promega) incubated at 68°C for 10 minutes to denature RNA secondary structure, followed by a 1 hour incubation at 39°C in a 20 µl reverse transcription reaction containing:

Tris-HCl pH 8.3	50 mM
KCl	75 mM
MgCl <sub>2</sub>	3 mM
Dithiothreitol (DTT)	10 mM
dNTPs	0.5 mM
SuperScript™ III reverse transcriptase (Invitrogen)	200 units

### 2.11.2. Quantitative PCR

Gene expression was analysed by quantitative PCR (qPCR) using a StepOne Real-Time PCR System (Applied Biosystems). Quantitative amplification of 2  $\mu$ l of reverse transcriptase product was carried out in a 20  $\mu$ l reaction mixture using thin-wall fast optical 48 well qPCR plates (Applied Biosystems) and a SYBR Green I based mastermix containing:

SYBR Green I	0.001% (v/v)
Tris-HCl pH 8.3	20 mM
KCl	20 mM
(NH <sub>4</sub> ) <sub>2</sub> SO <sub>4</sub>	5 mM
MgCl <sub>2</sub>	2.5 mM
dNTPs	0.25 mM
Primers (fwd/rev)	0.5 $\mu$ M
ROX	0.1 $\mu$ M
TrueStart Taq Polymerase (Fermentas)	15 units

ROX was used as a passive reference dye to control for non-specific fluorescent signal variations, and amplification of GAPDH cDNA used as an internal gene control. After an initial 95°C hot start, cDNA underwent 40 cycles of amplification, with thermal reaction conditions set at 95°C for 15 seconds and 60°C for 60 seconds, followed by melt curve determination in increments of 0.3°C. Changes in fluorescence were plotted against reaction cycle using StepOne v2.0 software. Fold changes in gene expression were calculated using the  $2^{-\Delta\Delta C_T}$  method (Livak and Schmittgen, 2001) with the threshold cycle value ( $C_T$ ) taken from the mid-exponential phase of amplification. All primers were designed using *Primer3* software (<http://fokker.wi.mit.edu/primer3/input.htm>) and mRNA sequences available through

NCBI. Primers in each pair used for qPCR were located in different exons separated by large intronic sequences to prevent the influence of potential gDNA contamination. gDNA sequences were first aligned to mRNA sequences using Spidey mRNA-to-genomic alignment program (<http://www.ncbi.nlm.nih.gov/spidey>). All primers were first checked by amplifying cDNA using standard PCR and checking for the presence of a single product on 1.5% (w/v) agarose gels. All primers were produced by Sigma-Genosys and a summary of the sequences used is shown in table 2.2. below:

*Sequences of primers used for qPCR*

<b>Target</b>	<b>Forward</b>	<b>Reverse</b>
<b><math>\gamma</math>-synuclein</b>	5'-CCATGGACGTCTTCAAGAAAGG-3'	5'-CGTTCTCCTTGGTTTTGGTG-3'
<b>GAPDH</b>	5'-CACTGAGCATCTCCCTCACA-3'	5'-GTGGGTGCAGCGAACTTTAT-3'
<b>leptin</b>	5'-TGACACCAAACCCTCATCA-3'	5'-TGAAGCCCAGGAATGAAGTC-3'
<b>HSL</b>	5'-ACGCTACACAAAGGCTGCTT-3'	5'-TCGTTGCGTTTGTAGTGCTC-3'
<b>perilipin A</b>	5'-CACTCTCTGGCCATGTGGAT-3'	5'-AGAGGCTGCCAGGTTGTG-3'
<b>ATGL</b>	5'-CAACGCCACTCACATCTACG-3'	5'-ATGCAGAGGACCCAGGAAC-3'
<b>aP2</b>	5'-TCACCTGGAAGACAGCTCCT-3'	5'-AATCCCCATTTACGCTGATG-3'
<b>3-KAT</b>	5'-GGTCTTATGACATTGGCATGG-3'	5'-TCTCTGGCCTTCTCGTTCTC-3'
<b>UCP-1</b>	5'-GGCAAAAACAGAAGGATTGC-3'	5'-TAAGCCGGCTGAGATCTTGT-3'
<b>ACC-1</b>	5'-TGGTATTGGGGCTTACCTTG-3'	5'-AAGCTGGTTGTTGGAGGTGT-3'
<b>C/EBP<math>\beta</math></b>	5'-CAAGCTGAGCGACGAGTACA-3'	5'-AGCTGCTCCACCTTCTTCTG-3'
<b>LPL</b>	5'-CTCTGTGTCTAACTGCCACTTCA-3'	5'-AGTTTGGGCACCCAACCTCTC-3'
<b>PPAR<math>\gamma</math></b>	5'-TTCAGAAGTGCCTTGCTGTG-3'	5'-TCAGCAGACTCTGGGTTTCAG-3'

**Table 2.2. Summary of primer sequences used in qPCR experiments.**

For PCR analysis of  $\gamma$ -synuclein mRNA transcripts in WAT and MEF, PCR reactions, cycling conditions and agarose gel analysis were all performed as in section 2.2.2. Primers specific for  $\gamma$ -synuclein cDNA representing the entire coding region of the gene, as well as primers specific for GAPDH cDNA were used for amplification:

*$\gamma$ -synuclein for* 5'-CCATGGACGTCTTCAAGAAAGG-3'

*$\gamma$ -synuclein rev* 5'-CTAGTCTTCTCAACTCTTGG-3'

*GAPDH for* 5'-CACTGAGCATCTCCCTCACA-3'

*GAPDH rev* 5'-GTGGGTGCAGCGAACTTTAT-3'

## 2.12. Co-immunoprecipitation

Co-immunoprecipitation (coIP) can be used to determine whether or not two proteins permanently bind within the cell. Co-immunoprecipitation of SNARE proteins vesicle-associated membrane protein 4 (VAMP-4) and syntaxin-5 in WAT was performed according to a protocol described previously for synaptic SNARE complexes (Burre et al., 2010). Briefly, 150 mg WAT was homogenised in 0.6 ml of IP buffer and lysates cleared by centrifugation at 16,000 x g for 10 minutes at 4°C. 250  $\mu$ l of supernatant was incubated with 5  $\mu$ l of rabbit polyclonal anti-syntaxin-5 antibody (Synaptic Systems) and 50  $\mu$ l of Protein G Sepharose (Amersham). This suspension was rotated for 2 hours at 4°C after which Sepharose beads were sedimented by centrifugation for 1 minute at 500 x g and washed four times with IP buffer. Bound proteins were eluted by incubation at 100°C for 10 minutes in 50 $\mu$ l of SDS-PAGE loading buffer.

### 2.13. Histological techniques

Dissected WAT, BAT and liver samples were fixed overnight in 10% (w/v) neutral buffered formalin (Sigma-Aldrich) at 4°C and dehydrated in a graded alcohol series:

PBS	15 minutes (x3)
95% ethanol	5 minutes (x3)
100% ethanol	30 minutes
1:1 ethanol:chloroform	30 minutes
Chloroform	60 minutes
Chloroform (4°C)	Overnight

After dehydration, tissues were left in paraffin wax (RA Lamb) for 3 hours at 60°C before being embedded in fresh wax. 8 µm sections were cut using a HM 310 microtome (Microm International) and mounted onto poly-L-lysine coated slides (Mendel Glazer) by floating cut sections onto the surface of dH<sub>2</sub>O heated in a 40°C water bath. Slides were left to dry overnight at room temperature.

#### 2.13.1. Haematoxylin & Eosin (H&E) staining

Paraffin sections were cleared in xylene, rehydrated, stained with Mayers haematoxylin and 1% (w/v) aqueous eosin (both Leica) for 5 minutes each, both followed by washing with dH<sub>2</sub>O. Stained sections were brought to xylene through a graded alcohol series and mounted with di-n-butylphthalate in xylene (DPX, RA Lamb).

### *2.13.2. Immunohistochemistry*

Rehydrated tissues were subjected to an antigen retrieval process by microwaving for 10 minutes at 750W in 10 mM sodium citrate pH 6.0. Endogenous peroxidase activity was quenched with 3% (v/v) hydrogen peroxide in methanol and slides washed three times with PBS. Tissues were blocked with 10% (v/v) horse serum in phosphate-buffered saline (PBS) containing 0.4% (v/v) Triton X-100 (T-PBS) for 30 minutes before incubation with primary antibodies against GFP (1:1000, rabbit polyclonal, Living Colours from Clontech) in blocking solution for 2 hours at room temperature. Slides were washed with PBS before applying appropriate biotinylated secondary antibodies (Vector) diluted in T-PBS for 1 hour at room temperature. Slides were once again washed with PBS before incubation with Elite plus ABC solution (Avidin-biotin HRP complex, Vector) for 30 minutes at room temperature. Detection of immune complexes was performed using 3,3'-diaminobenzidine (DAB, Sigma-Aldrich) as a substrate until sufficient staining had taken place. Stained sections were brought to xylene through a graded alcohol series and mounted with DPX.

### *2.13.3. Adipocyte size measurement*

Two different methods were used to estimate adipocyte cell size. Live images were obtained using an Olympus U-CMAD3 ColorView III camera fixed upon an Olympus BX41 microscope. Care was taken to choose fields of view that almost exclusively contained adipocytes to minimize stromal and vascular areas, and all counts and measurements were performed blindly.

#### *2.13.3.1. Using Image J*

White adipocyte area was measured from images of subcutaneous WAT loaded onto Image J software by using the 'polygon selections' tool and a calibrated 50  $\mu\text{m}$  scale bar. Four randomly selected fields of view were used per section, with two sections taken at two different medial points through the embedded tissue. Data was averaged per medial point, in  $\mu\text{m}^2$ .

### 2.13.3.2. According to Ashwell et al. (1976)

This method estimates adipocyte diameter from the number of cells in a given area.

Epididymal WAT images were loaded onto analySIS-3.2 software, and counts were performed on random fields of view (350 x 263  $\mu\text{m}$ ) using four different fields per section, with two sections taken from two different medial points through each fat pad. Cells were included if they crossed the top or left boundaries of the field of view and excluded if crossing the bottom or right boundaries.

Cell counts were entered into the following formula:

$$d' = (2 \times \sqrt{A}) / (m \times \sqrt{\pi n})$$

Where  $d'$  = estimated cell diameter ( $\mu\text{m}$ );  $A$  = area of region from which cells are counted ( $\mu\text{m}^2$ );  $m$  = magnification of section;  $n$  = number of cells counted in region.

## 2.14. Lipid analysis

### 2.14.1. Lipid extraction and separation

Levels of lipids in biological samples were analysed using gas chromatography, in collaboration with the laboratory of Prof. John Harwood in the Cardiff University School of Biosciences, with assistance from Dr Irina Guschina. Lipids were extracted with 2.5 ml chloroform/methanol (2:1, v/v), before addition of 1.25 ml chloroform and 1.25 ml Garbus solution. Extracts were centrifuged at 250 x g, with the lower (organic) phase dried down under a stream of nitrogen and lipids reconstituted in chloroform. Non-polar (e.g. triacylglycerols) and polar lipids were separated by one-dimensional and two-dimensional thin-layer chromatography on silica gel G plates (Merck) respectively. Individual lipids were scraped from TLC plates and fatty acid

methylation performed by incubation in 3 ml H<sub>2</sub>SO<sub>4</sub> in methanol:toluene (2:1, v/v) for 2 hours at 70°C.

#### *2.14.2. Gas chromatography*

Methylated fatty acids were extracted twice with hexane and fatty acid profiles determined using a Clarus 500 gas chromatograph with a flame ionising detector (Perkin-Elmer 8500) fitted with a 30 cm x 0.25 mm i.d. Elite 225 capillary column. The oven temperature was programmed: 170°C for 3 minutes, heated to 220°C at 4°C/minute, held at 220°C for 15 minutes. Pentadecanoate (15:0) and heptadecenoate (17:1) were used as internal standards and fatty acids were identified using retention times of fatty acid standards (Nu-Chek-Pre. Inc.).

### **2.15. *In vitro* experiments**

#### *2.15.1. Cell culture*

##### *2.15.1.1. Mouse embryonic fibroblasts*

Primary cultures of mouse embryonic fibroblasts (MEF) from E12.5 embryos were maintained and differentiated as described by (Soukas et al., 2001) with slight modifications. Briefly, embryos were removed from the uterine horn into PBS with the yolk sac, head, and internal organs discarded. Remaining tissue was sheared through the barrel of an 18-gauge needle attached to a 2 ml syringe into cell culture medium, a total of three times. These cell suspensions from each individual embryo were plated into separate wells on 6 well tissue culture plates (Nunclon), incubated for 24 hours (37°C, 5% CO<sub>2</sub>) and split (using 0.05% w/v trypsin/EDTA) onto 10 cm plates. Cells were maintained in Dulbecco's modified Eagle's medium (DMEM) and F12 (1:1) containing:

Fetal bovine serum (FBS)	10% (v/v)
L-glutamine	1.8 mM
Penicillin G	100 units/ml
Streptomycin	100 µg/ml
(all Gibco)	

At confluence cells were split onto 6 well tissue culture plates or poly-L-lysine coated 13 mm coverslips. Two days post-confluence, media was changed to a pro-differentiation media containing:

Insulin	170 nM
Dexamethasone	250 nM
Isobutylmethylxanthine (IBMX)	0.5 mM
(all Sigma-Aldrich)	
Rosiglitazone (Axxora)	2.5 nM

After 2 days, this media was removed and cells were fed media containing only insulin and rosiglitazone for a further 6 days. Cells were fixed, or harvested for RNA on day 0, 2, 5 and 8 respective to addition of the first differentiation regimen.

#### *2.15.1.2. Stable cell lines*

3T3-L1 preadipocytes were a kind gift from Dr Justin Rochford, Institute of Metabolic Science, Cambridge University. Both 3T3-L1 preadipocytes and 3T3 fibroblasts were maintained in DMEM containing:

Newborn calf serum (Sigma-Aldrich)	10% (v/v)
L-glutamine	1.8 mM
Penicillin G	100 units/ml
Streptomycin	100 µg/ml

3T3-L1 preadipocytes were always passaged before they reached 70% confluence. For differentiation of 3T3-L1 preadipocytes, 2 day post confluent cells were switched to media containing 10% FBS rather than new born calf serum, and also:

Insulin	1 µM
Dexamethasone	1 µM
Isobutylmethylxanthine (IBMX)	0.5 mM

Cells were incubated in this pro-differentiation media for 2 days and then switched to the same differentiation media but without dexamethasone or IBMX for 2 further days. After this point cells were fed media containing FBS but with no pro-differentiation agents for 6 more days, with media changed every 2 days.

MG1361 cells were cultured in Williams E media containing:

FBS	10% (v/v)
L-glutamine	1.8 mM
Penicillin G	100 units/ml
Streptomycin	100 µg/ml
Non essential amino acids	0.1 mM

For experiments involving expression analysis in response to IBMX treatment, subconfluent cultures of 3T3, 3T3-L1 and MG1361 cells were fed respective passage media plus 0.5 mM IBMX, with cells harvested for RNA after 2, 12 and 48 hours after introduction of IBMX.

#### *2.15.2. ERK activation assay*

3T3 cells were incubated with lentivirus particles for 48 hours at approximately 40% confluence as described in section 2.6.4. Subconfluent cultures were serum-starved overnight for 16 hours and cells harvested for protein analysis prior to re-feeding, and 15, 30, 60 and 120 minutes after re-feeding with serum-containing passage media.

#### *2.15.3. Immunocytochemistry*

Cells growing on 13 mm coverslips were fixed with 4% (w/v) paraformaldehyde (Sigma-Aldrich) in PBS for 10 minutes at 4°C, washed twice with PBS, and blocked in 10% (v/v) goat serum and 0.1% (v/v) Triton X-100 in PBS for 1 hour at room temperature. After blocking, coverslips were incubated with primary antibodies against mouse  $\gamma$ -synuclein (1:100, SK23, (Buchman et al., 1998b)) for 2 hours at room temperature, followed by washing twice with PBS. Appropriate AlexaFluor fluorescent secondary antibodies were then applied including counterstaining with 1  $\mu$ M Bodipy 493/505 (both Molecular Probes). Coverslips were subsequently washed with PBS, and mounted using Immu-mount aqueous mounting media (Thermo Scientific), and left to dry overnight in the dark. Fluorescent images were captured on a Leica TCS SP2 laser scanning confocal microscope.

## **2.16. Statistical analysis**

One Way Analysis of Variance tests (ANOVA) were employed to test for statistical differences between data sets, with data checked for normal distribution and equal variance using Anderson-Darling and Bartlett's tests respectively. Data sets meeting both these criteria were considered to be parametric, and so ANOVA used in these cases. Where data was non-parametric, a Kruskal-Wallis test was used on untransformed data, with post hoc pair wise comparison made using a Fisher's a priori test. Differences between pairs of data were analysed using two-sample Student t-tests or the Mann-Whitney U-test as the non-parametric equivalent. In these cases, distribution of normality and equality of variance were tested by Anderson-Darling and an F-test respectively. As previously, data that did not conform to these parameters were considered non-parametric. All calculations were made using Minitab 15, with a probability of error less than 5% considered significant ( $p < 0.05$ ).

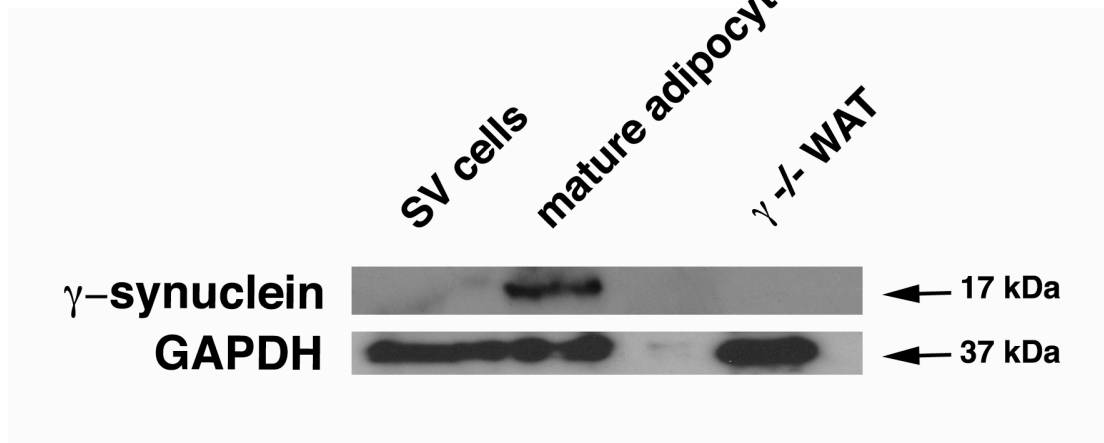
### **Chapter 3 - WAT expression of $\gamma$ -synuclein**

### **3.1. Overview**

Previous studies have demonstrated significant levels of  $\gamma$ -synuclein in white adipose tissue (Frandsen et al., 2009; Oort et al., 2008). Moreover, the expression of  $\gamma$ -synuclein in WAT of obese humans is increased, and this upregulation is reversed upon calorific restriction (Oort et al., 2008). We have demonstrated high levels of both  $\gamma$ -synuclein RNA and proteins in epididymal and subcutaneous fat depots in mice using Northern blotting, quantitative RT-PCR and Western blotting (Fig. 1.5-1.7). To determine whether  $\gamma$ -synuclein expression in murine WAT is nutritionally regulated, as is the case in human WAT, we employed a mouse model of diet-induced obesity, using a high fat diet known to cause obesity in wild type mice (Van Heek et al., 1997). This chapter discusses both the cell-type specific expression of  $\gamma$ -synuclein in WAT and its subcellular localization, followed by the dynamics of  $\gamma$ -synuclein expression in response to high fat diet feeding and calorific restriction in wild type mice.

#### **3.2.1. Results: Cell-specificity and subcellular localisation of $\gamma$ -synuclein in murine WAT**

WAT is made up of a number of cell types, including mature adipocytes, preadipocytes, vascular cells and immune cells. To determine whether expression of  $\gamma$ -synuclein is restricted to the mature adipocytes or could also be found in WAT stromal cells, we obtained fractions enriched in these cell populations. Epididymal WAT from wild type mice was digested with collagenase in Krebs-Ringer bicarbonate medium and stromal cells pelleted by centrifugation, whilst mature adipocytes floated to the top of the buffer. These cell fractions were homogenized directly in SDS-PAGE loading buffer and proteins analysed by semi-quantitative Western blotting using antibodies against mouse  $\gamma$ -synuclein (Buchman et al., 1998b). This work demonstrated that  $\gamma$ -synuclein is expressed in the mature adipocyte but not the preadipocyte-containing stromal cell fraction of this tissue, with levels of GAPDH protein used to confirm similar levels of total protein in each lane (Fig. 3.1).

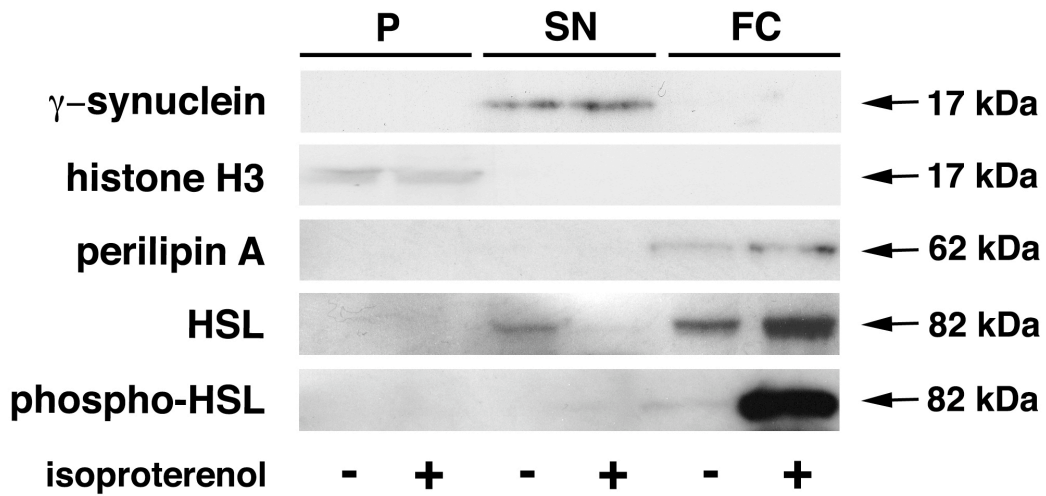
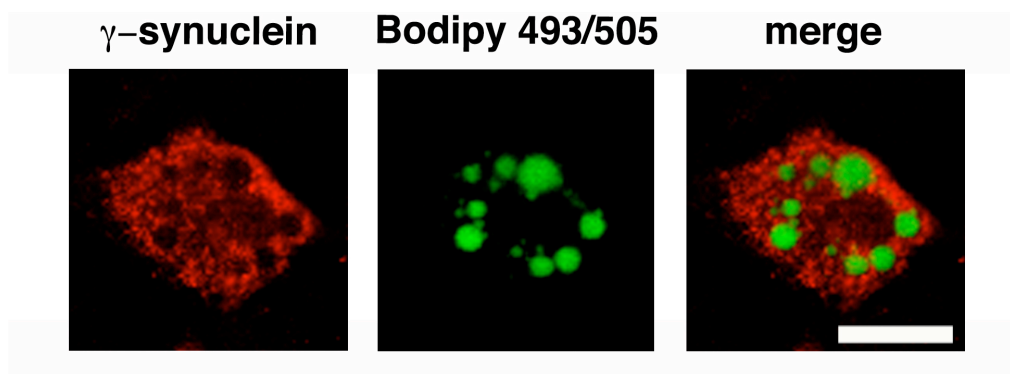


**Fig. 3.1. Cell-specific expression of  $\gamma$ -synuclein in murine WAT.** Western blot analysis of  $\gamma$ -synuclein expression in the total cell lysates of stromal-vascular (SV) and mature adipocyte fractions from epididymal WAT of wild type mice. A lysate of epididymal WAT of a  $\gamma$ -synuclein<sup>-/-</sup> mouse ( $\gamma$ <sup>-/-</sup> WAT) was included as control for specificity of antibodies. GAPDH was used as a loading control.

\*                      \*                      \*

Subcellular fractionation was employed to reveal compartmentalisation of  $\gamma$ -synuclein in murine white adipocytes. Isolated mature adipocytes from epididymal WAT of wild type mice were subjected to subcellular fractionation, first by lysis in a hypotonic sucrose buffer followed by centrifugation to pellet nuclei, whilst the lipid droplet-containing fat cake fraction rose to the top of the buffer. Both these fractions, as well as the supernatant beneath the fat cake (infranate), were diluted or re-suspended in SDS-PAGE loading buffer and the proteins contained within each fraction were analysed by semi-quantitative Western blotting. Presence of marker proteins histone 3 and perilipin A were used to demonstrate efficient fractionation of nuclear and lipid-droplet fractions respectively (Fig. 3.2A).  $\gamma$ -synuclein was recovered in the infranate containing cytosol and membranes and was absent from the nuclear fraction (Fig. 3.2A). No  $\gamma$ -synuclein was detected in the fraction containing lipid droplet-associated proteins either in the presence or absence of lipolytic stimulation,

achieved by incubation of purified mature adipocytes with the non-specific  $\beta$ -adrenergic agonist, isoproterenol prior to cell lysis. This stimulation was sufficient to induce the translocation of hormone sensitive lipase (HSL) and phosphorylation at its catecholamine-sensitive regulatory phosphorylation site, serine 563 (Garton et al., 1988; Stralfors et al., 1984) (Fig. 3.2A). Immunofluorescent staining of adipocytes differentiated from MEFs *in vitro*, using antibodies against mouse  $\gamma$ -synuclein (Buchman et al., 1998b) also did not suggest an association of  $\gamma$ -synuclein with lipid droplets, which were revealed by staining with the fluorescent neutral lipid stain, Bodipy 493/505. Instead,  $\gamma$ -synuclein immunostaining revealed a diffuse, partly punctuate pattern throughout the cell cytoplasm (Fig. 3.2B).

**A****B**

**Fig. 3.2. Subcellular localization of  $\gamma$ -synuclein in WAT and MEF adipocytes.** (A) Subcellular localization of  $\gamma$ -synuclein in mature white adipocytes isolated from epididymal WAT of wild type mice and incubated for 30 minutes in the presence or absence of 10  $\mu$ M isoproterenol. Proteins in the pellet (P), supernatant (SN) and fat cake (FC) fractions obtained after cell lysis in a hypotonic sucrose buffer were analysed by Western blotting using antibodies against  $\gamma$ -synuclein and protein markers for each fraction. (B) Immunofluorescent staining of MEF differentiated into adipocytes in culture with antibodies against  $\gamma$ -synuclein (red) and counterstained with the neutral lipid stain, Bodipy 493/505 (green). Scale bar = 20  $\mu$ m.

### 3.2.2. Results: Nutritional regulation of $\gamma$ -synuclein in murine WAT

To determine whether  $\gamma$ -synuclein expression in murine WAT is nutritionally regulated we used a mouse model of high fat diet (HFD)-induced obesity. From the age of 9 weeks wild type mice were fed either a low fat (LFD) or HFD for 11 weeks (Van Heek et al., 1997) and expression of  $\gamma$ -synuclein mRNA in WAT depots was measured by quantitative RT-PCR. Consistent with what was found in human adipose tissue, the level of  $\gamma$ -synuclein mRNA was dramatically increased in both epididymal and subcutaneous adipose tissue (approximately 3 and 4-fold respectively) of mice fed a high fat diet for 11 weeks comparing with mice fed a control LFD for 11 weeks (Fig. 3.3A). This upregulation was also reversible upon calorific restriction. Levels of  $\gamma$ -synuclein mRNA in both epididymal and subcutaneous WAT depots were decreased by approximately 50% after mice fed a HFD for 10 days were switched to a low fat diet (LFD) for 36 hours. When mice fed HFD for 10 days were switched to a LFD for 1 week or fasted for 36 hours, this reduction was more prominent, with levels of  $\gamma$ -synuclein mRNA decreased by approximately 80% and 65% in epididymal and subcutaneous WAT depots respectively (Fig. 3.3B). Using semi-quantitative Western blotting and antibodies against mouse  $\gamma$ -synuclein (Buchman et al., 1998b), levels of  $\gamma$ -synuclein protein in epididymal WAT depots from these mice were also measured. Generally, changes in  $\gamma$ -synuclein protein abundance following dietary manipulation were congruent with the changes in mRNA expression in this depot, with a similar 3-fold increase of  $\gamma$ -synuclein protein levels in mice fed a HFD for 11 weeks comparing with mice fed a control LFD for 11 weeks (Fig. 3.3C and Appendix 2). Consistently with results of mRNA expression analysis, we observed a similar (~75%) reduction in  $\gamma$ -synuclein protein abundance when mice fed HFD for 10 days were switched to a LFD for 1 week or fasted for 36 hours (Fig. 3.3C and Appendix 2). The only obvious disparity between changes in mRNA and protein abundance observed in these experiments was for a group of mice switched from a 10 day HFD feed to a LFD for 36 hours. The ~50% decrease in mRNA levels in epididymal WAT of this group was not followed by similar decrease at the protein level (Fig. 3.3C and Appendix 2).

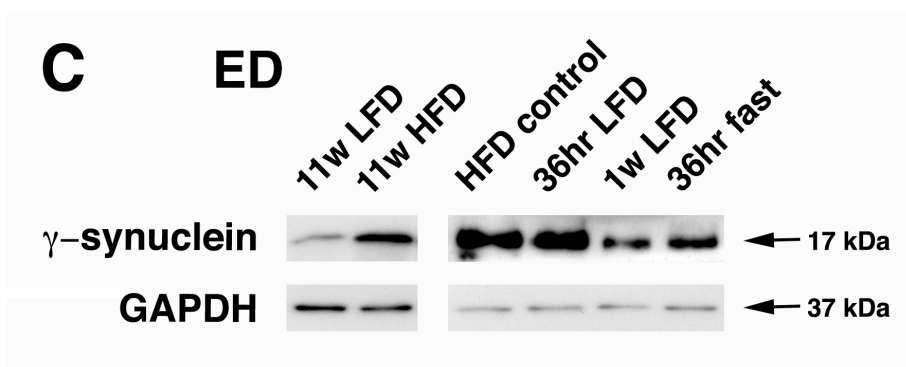
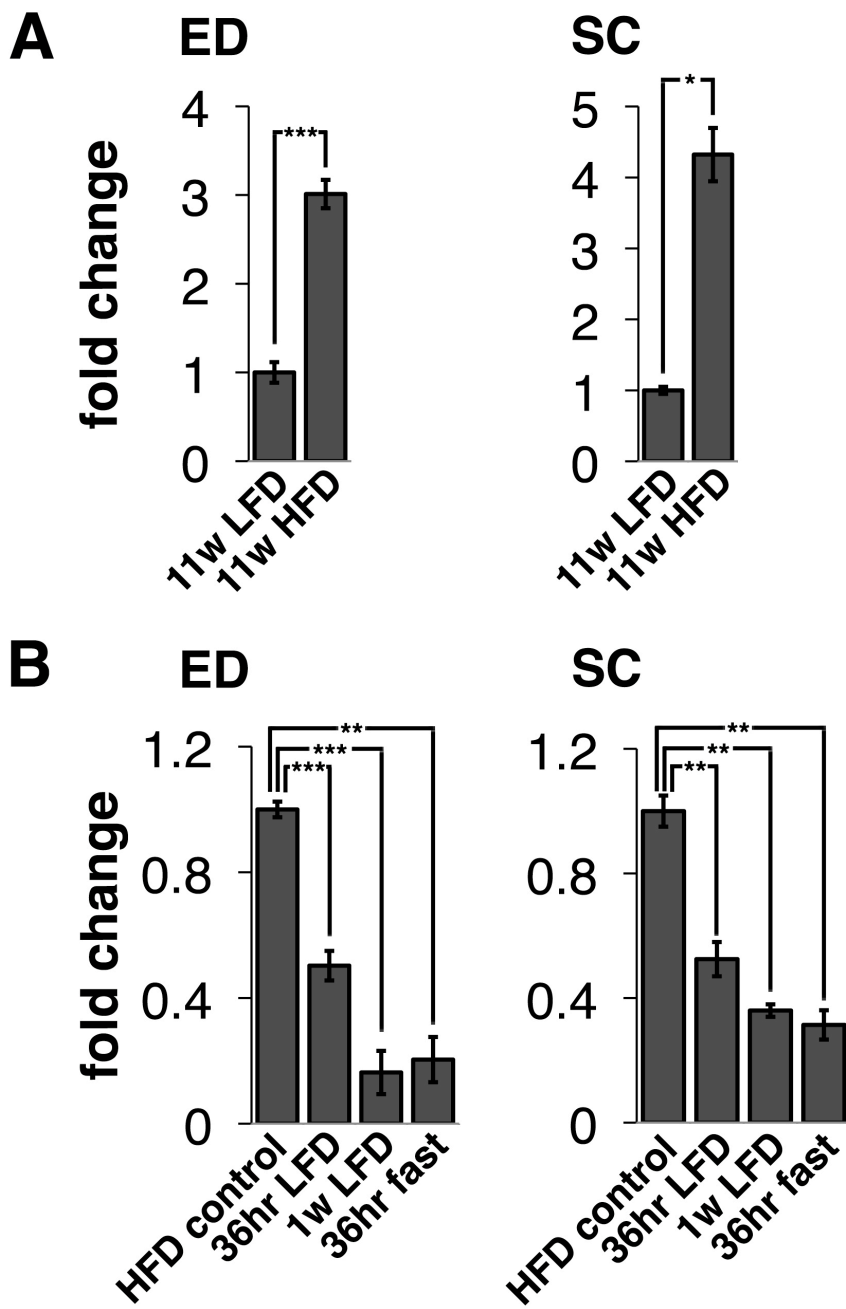


**Fig. 3.3. WAT expression of  $\gamma$ -synuclein in response to changes in nutritional status in mice** – previous page. (A) Quantitative RT-PCR analysis of  $\gamma$ -synuclein mRNA expression in epididymal (ED, n=8) and subcutaneous (SC, n=4) WAT of wild type mice fed a low fat (LFD) or high fat diet (HFD) for 11 weeks. Results are shown as mean $\pm$ SEM of fold change compared with LFD fed mice. (B) Quantitative RT-PCR analysis of changes  $\gamma$ -synuclein mRNA expression in epididymal and subcutaneous WAT of mice fed a HFD for 10 days and then given LFD for 36 hours, 1 week, fasted for 36 hours or maintained on HFD as controls. Results are shown as mean $\pm$ SEM fold change compared with HFD fed controls (n=3-5). (C) Western blot analysis of  $\gamma$ -synuclein expression in epididymal WAT of the same wild type mice that were used for RT-PCR analysis shown in panels D and E. GAPDH was used as a loading control. Non-parametric Mann-Whitney U-test analysis demonstrated statistically significant differences between groups (\* p < 0.05, \*\* p < 0.01, \*\*\* p < 0.001).

### 3.3. Summary of results and discussion

To assess whether expression of  $\gamma$ -synuclein in murine WAT is nutritionally regulated, as is the case in human WAT (Oort et al., 2008), we employed a mouse model of HFD-induced obesity and measured dynamics of  $\gamma$ -synuclein expression. Similar to the upregulation seen in obese humans, wild type mice fed HFD showed increased expression of  $\gamma$ -synuclein compared to wild type mice fed a control LFD, both at the RNA and protein level. (Oort et al., 2008) also demonstrated that this upregulation could be reversed upon calorific restriction of obese patients. In wild type mice fed HFD, we have shown rapid reduction of  $\gamma$ -synuclein mRNA and protein levels upon introduction of feeding with LFD or fasting. Overall, expression dynamics of  $\gamma$ -synuclein in WAT appear to be under similar nutritional regulation in both humans and mice.

In this section we have also demonstrated that  $\gamma$ -synuclein expression is restricted to the mature adipocyte fraction of WAT, with no expression detected in the preadipocyte-containing stromal fraction. In addition we have shown that  $\gamma$ -synuclein is localized exclusively to the cytosol of adipocytes both *in vivo* and *in vitro*, and no apparent association with lipid droplets.

Overall, results in this section suggest that the high levels of  $\gamma$ -synuclein in WAT may play a role in lipid metabolism in mature white adipocytes, but probably not by direct influence on TAG storage at the lipid droplet surface. This data also indicates a possible role for  $\gamma$ -synuclein in the development of certain forms of obesity. To address this possibility, we investigated the effect of  $\gamma$ -synuclein deficiency in a mouse model of HFD-induced obesity and these findings are discussed in the next chapter.

**Chapter 4 – Effect of  $\gamma$ -synuclein<sup>-/-</sup>  
in a mouse model of HFD-induced obesity**

## 4.1. Overview

The previous chapter described nutritional regulation of  $\gamma$ -synuclein expression in mature white adipocytes, with upregulation both at the RNA and protein level upon introduction of HFD feeding in mice. This led us to investigate whether  $\gamma$ -synuclein plays a role in the development of certain forms of obesity. To achieve this, we used mice with targeted inactivation of the  $\gamma$ -synuclein gene ( $\gamma$ -synuclein<sup>-/-</sup> mice), which have been previously created and characterised in our laboratory (Ninkina et al., 2003). These animals do not show any obvious neuronal phenotype, even in neuronal populations where  $\gamma$ -synuclein is most highly expressed (Ninkina et al., 2003; Papachroni et al., 2005). Moreover they do not display any sign of metabolic abnormalities when kept in conventional husbandry and diet conditions (our unpublished observations). We challenged these  $\gamma$ -synuclein<sup>-/-</sup> mice and their wild type littermates with the same HFD as discussed in the previous chapter, to determine whether deficiency of  $\gamma$ -synuclein affects HFD-induced WAT accumulation and overall body weight gain. Mouse weights and food consumption during the HFD feeding protocol were recorded, with MRI employed to monitor body fat composition. This chapter discusses the effect of  $\gamma$ -synuclein deficiency in a mouse model of HFD-induced obesity, as well as the analysis of obesity-related metabolic disorders in these mice.

### 4.2.1. Results: $\gamma$ -synuclein<sup>-/-</sup> mice are resistant to diet-induced obesity

9-week old  $\gamma$ -synuclein<sup>-/-</sup> and wild type male mice were fed a HFD or a control LFD for a period of 11 weeks. Mice were single caged and both body weights and food consumption were measured weekly. At the beginning of the feeding protocol, no statistically significant differences in animal weight existed between any of the four groups. Mice of both genotypes fed LFD did not show any differences in weight gain throughout the duration of the 11 weeks, and indeed, at the end of the LFD-feeding protocol, there was no statistically significant difference in weights between wild type and  $\gamma$ -synuclein<sup>-/-</sup> mice (Fig. 4.1). As expected, HFD feeding caused weight gain in both HFD-fed groups. However, HFD-feeding caused only modest gradual weight gain in  $\gamma$ -synuclein<sup>-/-</sup> mice and they remained substantially leaner than their HFD-fed

wild type counterparts throughout the duration of the feeding protocol (Fig. 4.1). This difference was already statistically significant after 1 week of HFD feeding ( $p < 0.01$ ). After 11 weeks of HFD feeding, wild type mice gained on average 53% of their original weight, compared to 34% in  $\gamma$ -synuclein<sup>-/-</sup> mice. Further calculations showed that at the end of the study,  $\gamma$ -synuclein<sup>-/-</sup> mice were on average only 16% heavier on HFD compared to LFD, compared to an average of 33% in wild type mice. Quantitative MRI analysis of body fat volume was performed on at the start of the dietary intervention or after 6 or 11 weeks on LFD or HFD. MRI scans of anaesthetized mice were uploaded onto custom written software 'FAT' which was provided for us by Stephen Paisey and Pavel Tokarchuk of the Experimental MRI Centre, Cardiff University. This software enabled generation of fat only images as well as user directed fat pad volume measurement. This analysis firstly revealed no differences in total body fat pad volume between all four experimental groups at the beginning of the experiment (Fig. 4.2). In addition to this, we observed a similar total fat pad volume between mice of both genotypes on LFD throughout the feeding protocol. As expected, HFD feeding caused substantial WAT accumulation, however this increase was attenuated in HFD-fed  $\gamma$ -synuclein<sup>-/-</sup> mice compared to HFD-fed wild type mice (~8 fold increase in wild type and ~6 fold in  $\gamma$ -synuclein<sup>-/-</sup> mice) (Fig. 4.2). This attenuation was statistically significant after 11 weeks of HFD feeding ( $p < 0.05$ ) and was consistent with overall changes in total mouse body weight between the two HFD-fed groups. The reduced WAT accumulation seen in HFD-fed  $\gamma$ -synuclein<sup>-/-</sup> compared to HFD-fed wild type mice was confirmed at the end of the feeding protocol following Schedule 1 sacrificing of experimental mice, and determining whole fat pad mass of dissected epididymal, subcutaneous and retroperitoneal depots, as well as fat pad mass to body mass ratios for all three depots (Fig. 4.3 and Appendix 3). These data also demonstrated the increase in both fat pad mass and fat pad mass to body mass ratio of these three major depots upon HFD feeding in both genotypes (Fig. 4.3 and Appendix 3).

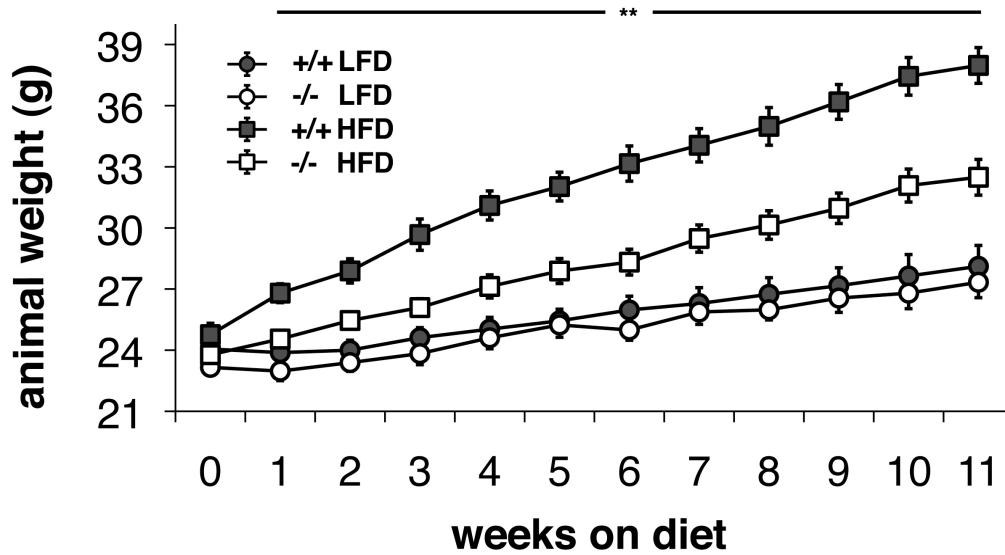


**Fig. 4.1. Raw weights of wild type and  $\gamma$ -synuclein<sup>-/-</sup> mice fed LFD or HFD.** Dynamics of total body weight changes of wild type (+/+) and  $\gamma$ -synuclein<sup>-/-</sup> mice (-/-) fed a LFD or HFD for 11 weeks. Results are shown as mean weight $\pm$ SEM (n=12-15). Non-parametric Mann-Whitney U-test analysis demonstrated a statistically significant difference between wild type and  $\gamma$ -synuclein<sup>-/-</sup> mice on HFD (\*\* p < 0.01).

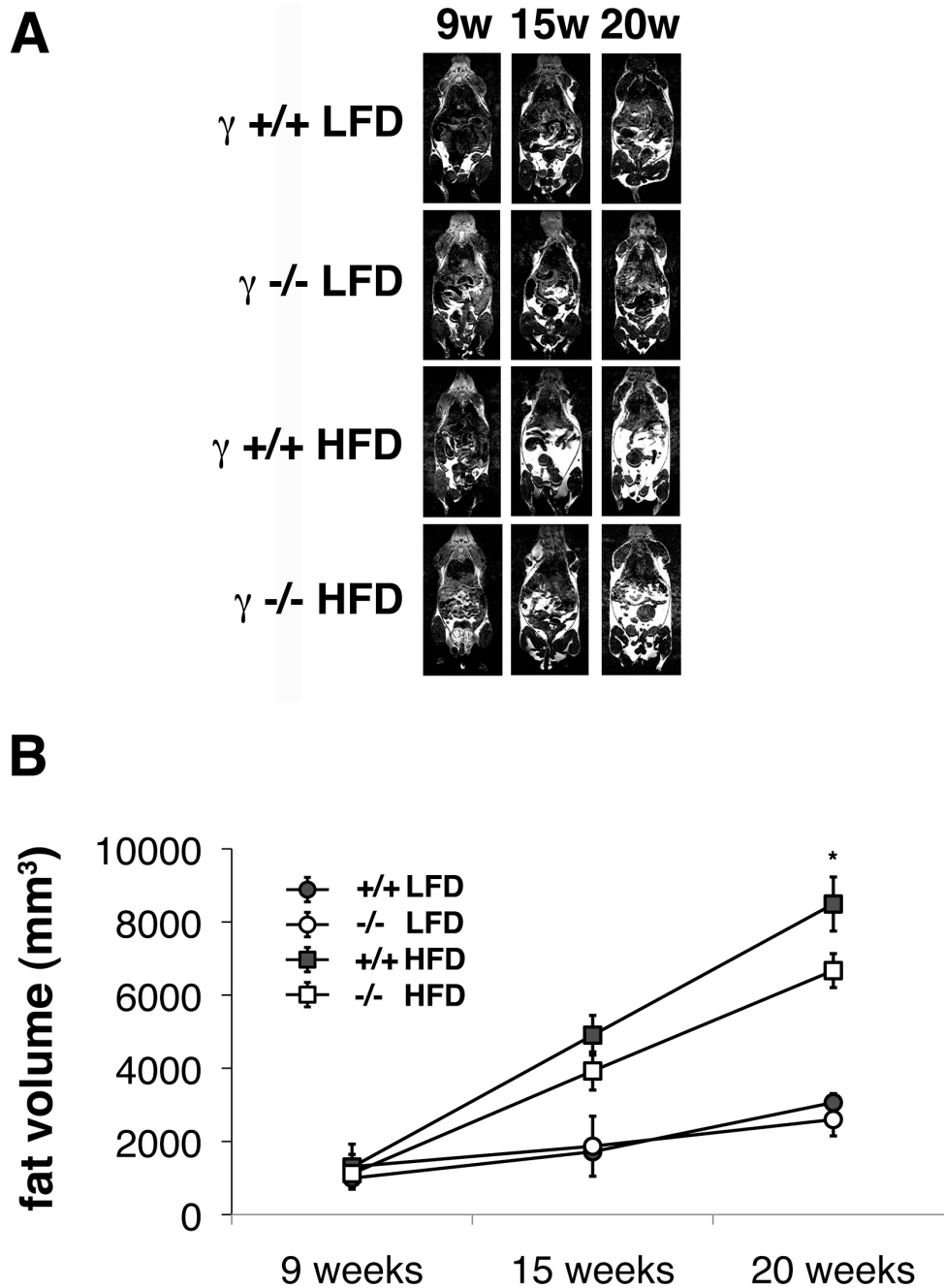


**Fig. 4.2. Quantification of body fat volume by MRI.** (A) MRI scans of wild type and  $\gamma$ -synuclein<sup>-/-</sup> mice at the beginning (9w), middle (15w) and end (20w) of an 11 week feed with either LFD or HFD. Two whole-body 2D RARE scans were used to generate fat only images (fat shown in white) by the subtraction of the fat suppressed image from the non-suppressed image. (B) MRI scans were used to quantify fat volume using custom written software ‘FAT’ (n=4 animals). Non-parametric Mann-Whitney U-test analysis demonstrated a statistically significant difference between wild type and  $\gamma$ -synuclein<sup>-/-</sup> mice on HFD (\* p < 0.05).

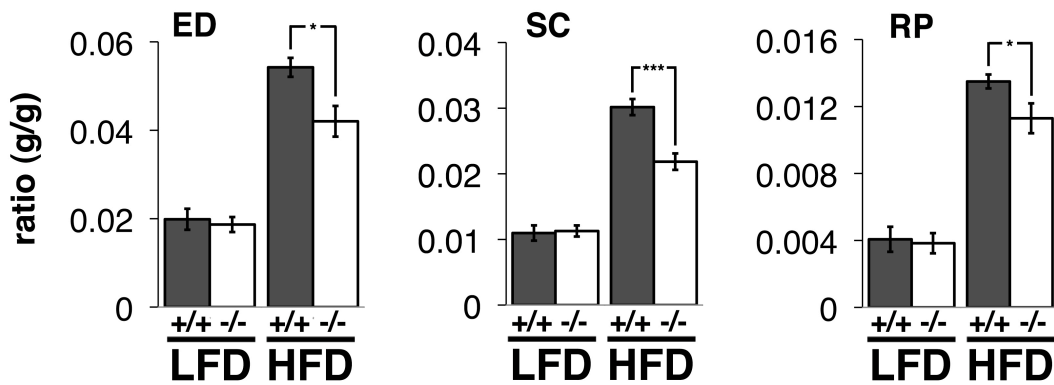


**Fig. 4.3. WAT mass to body mass ratios.** Total epididymal (ED), subcutaneous (SC) and retroperitoneal (RP) WAT mass to body mass ratios of wild type (+/+) and  $\gamma$ -synuclein<sup>-/-</sup> (-/-) mice fed a LFD or HFD for 11 weeks (n=12-14). Bar charts represent mean $\pm$ SEM. Non-parametric Mann-Whitney U-test analysis demonstrated statistically significant differences between groups (\* p < 0.05, \*\*\* p < 0.001).

To check whether or not the observed differences in WAT accumulation between HFD-fed wild type and  $\gamma$ -synuclein<sup>-/-</sup> mice were due to any differences in calorific intake or absorption of lipids from the diet, we assessed both, by measuring food consumption as well as faecal lipid content. Taking into consideration the calorific value of each diet, we did not observe any statistically significant differences in calorific intake between all four experimental groups (Fig. 4.4A). To measure absorption of lipids from the diet, 3-4 faecal pellets were collected per day from each mouse cage over week 8 of the HFD feeding protocol, and following extraction the total lipid content was assessed using gas chromatography. We did not observe any difference between the levels of total lipids in faecal pellets from HFD-fed wild type and  $\gamma$ -synuclein<sup>-/-</sup> mice, suggesting that lipid absorption from the diet is similar in both groups of mice (Fig. 4.4B).

To determine whether reduced WAT accumulation on HFD in  $\gamma$ -synuclein<sup>-/-</sup> mice is due to reduced adipocyte size or number, we measured the area (using ImageJ, see Experimental Procedures) of individual white adipocytes in H&E stained histological sections of subcutaneous WAT, taken from wild type or  $\gamma$ -synuclein<sup>-/-</sup> mice fed LFD or HFD for 11 weeks. White adipocytes were of similar size in LFD-fed mice of both genotypes (Fig. 4.5A, B). However, upon HFD-feeding the average adipocyte size increased by  $\sim$ 4.5 fold in subcutaneous WAT of wild type mice compared to an increase of  $\sim$ 2.4 fold in  $\gamma$ -synuclein<sup>-/-</sup> mice (Fig. 4.5A, B). Similar differences between the four experimental groups were observed when cell diameter was quantified using H&E stained sections through epididymal WAT, using a different quantification method (according to (Ashwell et al., 1976), see Experimental Procedures) (Fig. 4.5C). Using this method, we observed a  $\sim$ 2.2 fold increase in cell diameter upon HFD-feeding in epididymal WAT of wild type mice compared to an increase of  $\sim$ 1.8 fold in  $\gamma$ -synuclein<sup>-/-</sup> mice (Fig. 4.5C). To investigate whether the lack of  $\gamma$ -synuclein affected adipocyte size in a cell-autonomous manner we performed localised rescue of  $\gamma$ -synuclein expression by local injection of  $\gamma$ -synuclein-expressing lentivirus in the subcutaneous adipose tissue of  $\gamma$ -synuclein<sup>-/-</sup> mice prior to the 11-week HFD feeding protocol. We employed a recombinant lentivirus expressing a single mRNA that translated into both  $\gamma$ -synuclein and GFP due to the presence of an internal ribosome binding site (IRES) upstream of the GFP open reading frame. Each animal also received injections of control lentivirus expressing only GFP into their contralateral subcutaneous WAT depot. Thus, we were able to identify transduced adipocytes in both ipsilateral and contralateral subcutaneous fat depots by immunostaining with the same anti-GFP antibody. Lentivirus particles were produced in collaboration with the laboratory of Dr Riccardo Brambilla based in the Institute of Experimental Neurology, San Raffaele Foundation and University, Milano. At the end of the feeding protocol we dissected out parts of the ipsilateral and contralateral subcutaneous WAT depots surrounding the injection site under a fluorescent dissecting microscope (Fig. 4.6Ai). Fixed WAT was then sectioned and immunostained with antibodies against GFP to identify transduced and non-transduced cells in both subcutaneous WAT depots. Light microscope images were uploaded onto Image J to quantify cell area (Fig. 4.6Aii). Following 11 weeks on HFD we observed a statistically significant increase in size of adipocytes transduced

with  $\gamma$ -synuclein-expressing lentivirus when compared either to adjacent non-transduced cells (~27% increase) or to cells transduced with a control lentivirus expressing only GFP in the contralateral WAT depot of the same animal (~21% increase) (Fig. 4.6B). Overall this data strongly suggests that regulation of  $\gamma$ -synuclein within the fat cell specifically and cell-autonomously affects adipocyte size *in vivo*.

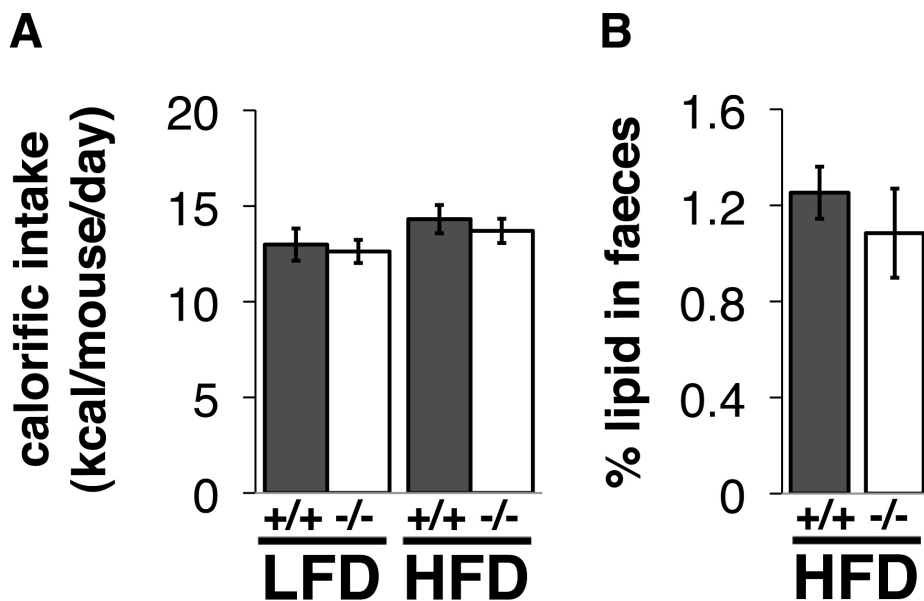


**Fig. 4.4. Calorific intake and faecal lipid content.** (A) Calorific intake of wild type (+/+) and  $\gamma$ -synuclein<sup>-/-</sup> (-/-) mice fed either LFD or HFD for 11 weeks (n=12-15). (B) Faecal lipid content of wild type and  $\gamma$ -synuclein<sup>-/-</sup> mice fed HFD. Samples were collected over the 8<sup>th</sup> week of an 11-week HFD feed (n=3 animals). Bar charts represent mean  $\pm$  SEM.

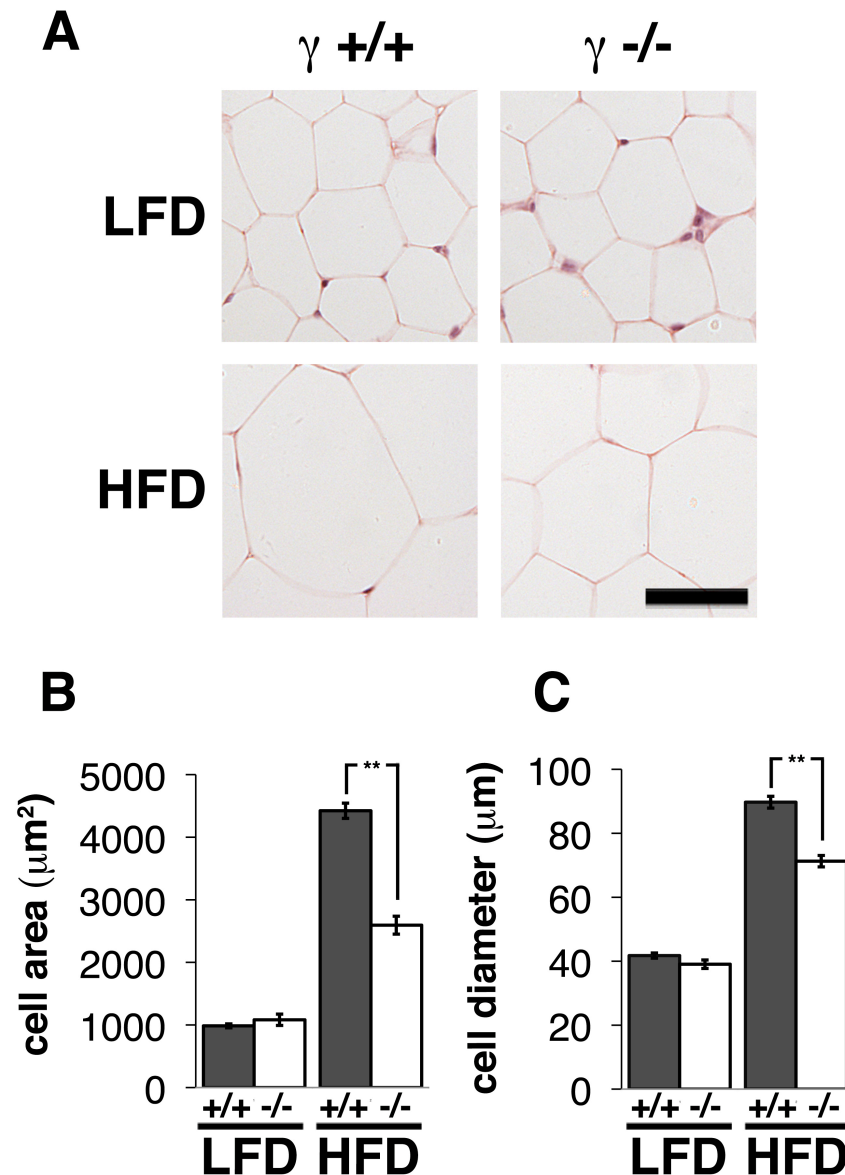


**Fig. 4.5. Adipocyte size quantification in epididymal and subcutaneous WAT.** (A) H&E stained sections through subcutaneous WAT taken from wild type ( $\gamma$  +/+) and  $\gamma$ -synuclein<sup>-/-</sup> ( $\gamma$  -/-) mice fed a LFD or HFD for 11 weeks, scale bar = 50  $\mu\text{m}$ . (B) Using these images, average white adipocyte area for these groups was quantified using ImageJ (n=3 animals/12 sections, per group). (C) White adipocyte diameter was also quantified using H&E stained sections through epididymal WAT of wild type and  $\gamma$ -synuclein<sup>-/-</sup> mice fed a LFD or HFD for 11 weeks (n=3 animals/12 sections, per group). Bar charts represent mean $\pm$ SEM. Non-parametric Mann-Whitney U-test analysis demonstrated statistically significant differences between groups (\*\* p < 0.01).

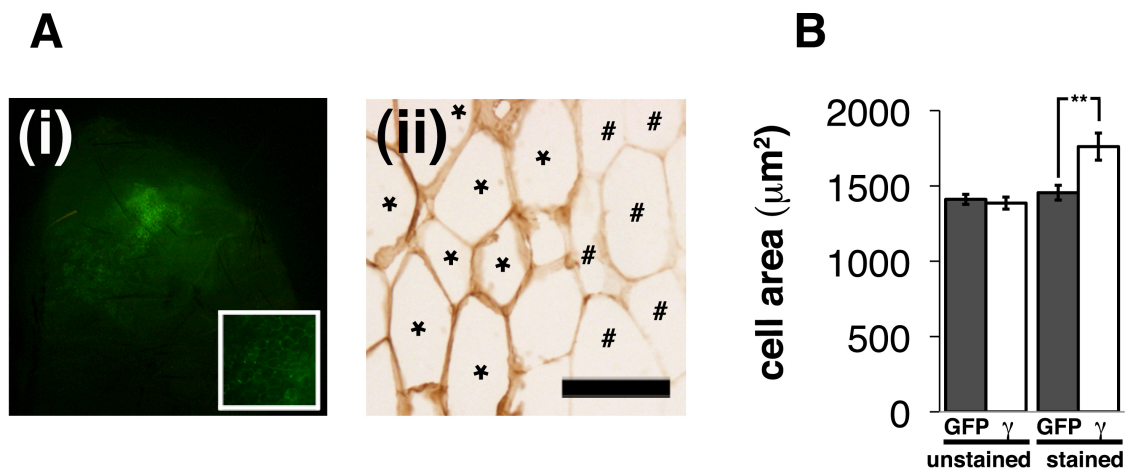


**Fig. 4.6. Size of adipocytes from  $\gamma$ -synuclein<sup>-/-</sup> mice with local re-expression of  $\gamma$ -synuclein by lentivirus delivery.** (A) (i) Fluorescent microscope image of a whole subcutaneous fat pad from a  $\gamma$ -synuclein<sup>-/-</sup> mouse showing adipocytes transduced with GFP-expressing lentivirus (inset). (ii) Histological sections through these subcutaneous fat pads were immunostained with antibodies against GFP to identify transduced (\*) and non-transduced (#) cells (see Experimental Procedures). Scale bar = 50  $\mu$ m. (B) Average adipocyte area was quantified using ImageJ on anti-GFP antibody-stained sections of subcutaneous WAT of  $\gamma$ -synuclein<sup>-/-</sup> mice that received local injection of either  $\gamma$ -synuclein-expressing lentivirus ( $\gamma$ ) or control GFP-only-expressing lentivirus (GFP) into subcutaneous WAT followed by feeding HFD for 11 weeks (see Experimental Procedures for details, n=3 animals/12 sections per group, minimum of 600 adipocytes). Bar chart shows means $\pm$ SEM (\*\* p < 0.01, Mann-Whitney U-test).

WAT depots expand by hypertrophy of mature adipocytes, but also by hyperplasia and terminal differentiation of preadipocytes. We planned to determine whether adipocyte development might also contribute to differences in WAT accumulation between HFD-fed  $\gamma$ -synuclein<sup>-/-</sup> and wild type mice. To do this we used mouse embryonic fibroblasts (MEFs) isolated from E12.5 embryos of wild type or  $\gamma$ -synuclein<sup>-/-</sup> mice and differentiated these cells into adipocytes in culture. cDNA synthesized using total RNA extracted from these cells was first used to identify if the same  $\gamma$ -synuclein mRNA transcript found in WAT was present in MEFs from wild type mice. Indeed, primers specific for amplification of regions representing either a 5' or 3' region of the mouse  $\gamma$ -synuclein mRNA transcript produced the same (126 and 112 bp respectively) fragment using cDNA from MEFs as was seen using cDNA from WAT (Fig. 4.7). Following differentiation, MEF adipocytes were harvested for total RNA with subsequent cDNA synthesis. Quantitative PCR analysis revealed the appearance of adipocyte-specific transcripts over the differentiation period, including the fatty acid transporter aP2, the critical adipogenic transcription factor peroxisome proliferator-activated receptor- $\gamma$  (PPAR $\gamma$ ) and the lipid droplet protein perilipin A. However, no differences were observed in the induction of these adipocyte genes during cell differentiation between  $\gamma$ -synuclein<sup>-/-</sup> and wild type MEFs (Fig. 4.8). These data suggest that loss of  $\gamma$ -synuclein does not affect the adipogenic capacity of precursor cells.

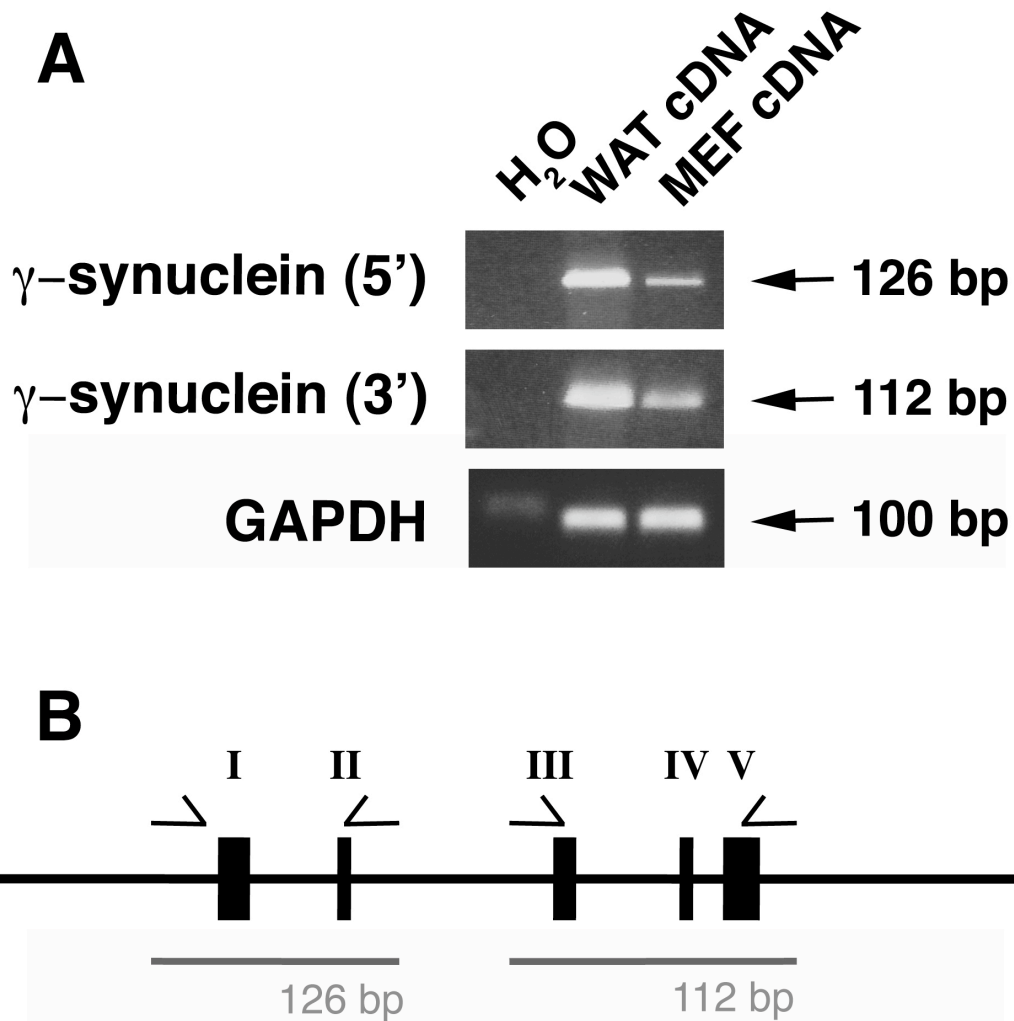


**Fig. 4.7. PCR analysis of the  $\gamma$ -synuclein mRNA transcript using cDNA from WAT and MEFs.** (A) cDNA was synthesized using total RNA from wild type adult mouse epididymal white adipose tissue (WAT cDNA) and mouse embryonic fibroblasts (MEF cDNA) from E12.5 embryos. Specific primers were used to amplify fragments at the 5' (5', 126 bp) or 3' (3', 112 bp) end of the mouse  $\gamma$ -synuclein mRNA transcript. Amplification of GAPDH cDNA was used as a control. (B) Structure of the mouse  $\gamma$ -synuclein locus with 5 exons (black boxes, numbered with roman numerals). Two pairs of primers were used to amplify fragments at either the 5' end (between the ATG site and the start of exon II) or the 3' end (between the end of exon III and the start of exon V).

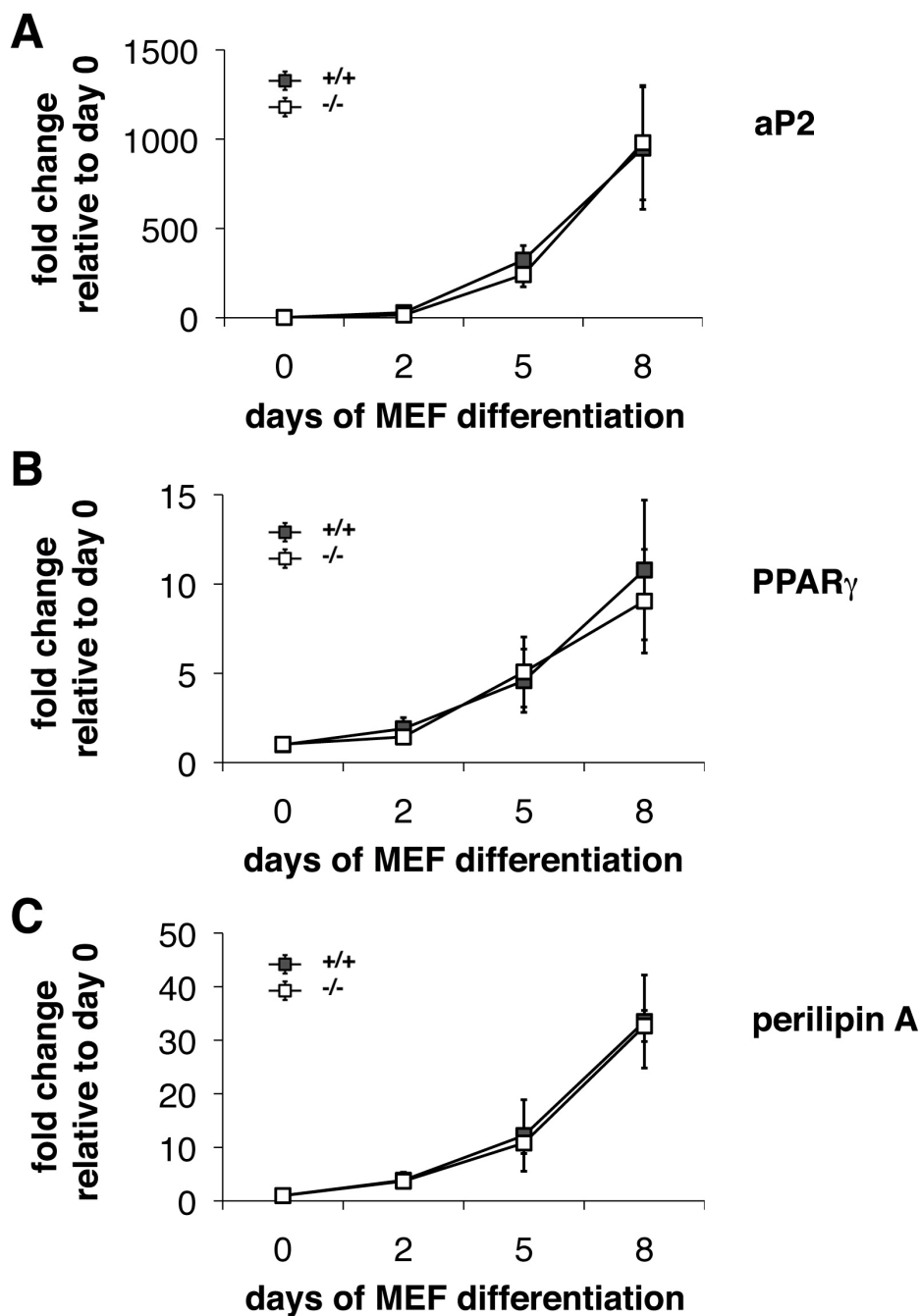


**Fig. 4.8. Adipocyte differentiation of mouse embryonic fibroblasts (MEFs) in culture.** (A-C) MEFs were isolated from E12.5 embryos of wild type (+/+) and  $\gamma$ -synuclein<sup>-/-</sup> (-/-) mice and exposed to a pro-differentiation regimen in culture for 8 days. mRNA expression of adipocyte-specific transcripts during MEF differentiation was analysed by quantitative RT-PCR. Results are shown as mean fold change compared with transcript levels at day 0 of wild type MEFs (n=6). In all graphs, means $\pm$ SEM is shown.

#### **4.2.2. Results: Loss of $\gamma$ -synuclein rescues mice from HFD-induced hyperinsulinaemia and hepatosteatosis**

We next assessed the effect of  $\gamma$ -synuclein deficiency on whole-body metabolism. Restricting adiposity in the face of nutrient excess may lead to an increase in circulating lipids and ectopic lipid accumulation in non-adipose tissues, causing or exacerbating insulin resistance and metabolic disorders. Therefore, we determined triacylglycerol (TAG) levels in the liver and plasma of wild type and  $\gamma$ -synuclein<sup>-/-</sup> mice fed LFD or HFD for 11 weeks. To do this, total lipids were extracted from either liver tissue or plasma and TAG separated by thin-layer chromatography (TLC). TAG levels were measured using gas chromatography, by quantifying total fatty acid methyl esters (see Experimental Procedures). No differences were observed in the levels of hepatic or plasma TAG in wild type and  $\gamma$ -synuclein<sup>-/-</sup> mice fed a LFD (Fig. 4.9A, B). In contrast, whilst HFD feeding resulted in an approximately two-fold increase in both hepatic and plasma TAG levels in wild type mice, no increase in liver or plasma TAG was observed in  $\gamma$ -synuclein<sup>-/-</sup> mice (Fig. 4.9A, B). We also performed histological examination of H&E stained sections through fixed liver and BAT. This analysis revealed that the absence of  $\gamma$ -synuclein protected the liver from the development of extensive hepatosteatosis, which was a characteristic feature of HFD-fed wild type mice (Fig. 4.9C). Similarly, whilst HFD-feeding dramatically altered the morphology of BAT in wild type mice with the appearance of much larger lipid droplets, this was significantly attenuated in  $\gamma$ -synuclein<sup>-/-</sup> mice (Fig. 4.9C).

We also measured the levels of plasma non-esterified fatty acids (NEFA), ketone bodies and adiponectin in all four experimental groups of mice. Plasma NEFA levels were determined by extraction of total lipids from plasma, separation of NEFA from other lipid species by TLC and quantification by gas chromatography. Plasma levels of ketone bodies and adiponectin were measured using commercially available kits. Overall, the absence of  $\gamma$ -synuclein had no effect on the levels of plasma NEFA, ketone bodies or adiponectin on LFD or HFD for 11 weeks (Table 4.1). We also performed i.p. glucose and insulin tolerance tests to determine whether  $\gamma$ -synuclein deficient mice on HFD displayed any differences in the ability to clear glucose from the blood, or any differences in insulin sensitivity, respectively, compared to HFD-fed wild type control mice. GTT and ITT were performed on fasted mice during the 9<sup>th</sup>

and 10<sup>th</sup> week of an 11-week HFD feed respectively. GTT involved initial injection of D-glucose i.p. and measurement of blood glucose levels over the 2-hour period that followed. For ITT, mice received i.p. injection of human insulin with measurement of blood glucose levels over the following 1-hour period. GTT and ITT data were used to create curves representing blood glucose levels over time, from which the area under the curve (AUC) was calculated for each genotype to represent a value of glucose and insulin tolerance. This analysis revealed no significant differences between HFD-fed  $\gamma$ -synuclein<sup>-/-</sup> and wild type mice for either GTT or ITT (Table 4.1). Next we assessed plasma leptin and insulin levels in wild type and  $\gamma$ -synuclein<sup>-/-</sup> mice fed LFD or HFD for 11 weeks using commercially available kits. This analysis was performed by Dr Pieter Oort in the laboratory of Dr Sean Adams based in the USDA/Agricultural Research Service Western Human Nutrition Research Centre, California. No differences were observed in the levels of plasma leptin or insulin in wild type and  $\gamma$ -synuclein<sup>-/-</sup> mice fed a LFD (Fig. 4.10A and B). Plasma leptin levels increased substantially in both genotypes upon HFD-feeding. However this increase was substantially attenuated in  $\gamma$ -synuclein<sup>-/-</sup> mice (~5.5 fold increase in wild type compared to ~2.9 fold in  $\gamma$ -synuclein<sup>-/-</sup> mice), consistent with the observed decrease in adiposity in these mice (Fig. 4.10A). Fasting plasma insulin levels were increased almost 3-fold following HFD-feeding of wild-type mice but were not raised in HFD-fed  $\gamma$ -synuclein<sup>-/-</sup> mice (Fig. 4.10B). Taken together, these data suggest that the reduced adiposity observed in  $\gamma$ -synuclein<sup>-/-</sup> mice is associated with an improved metabolic profile compared with wild type mice when both are fed a HFD.

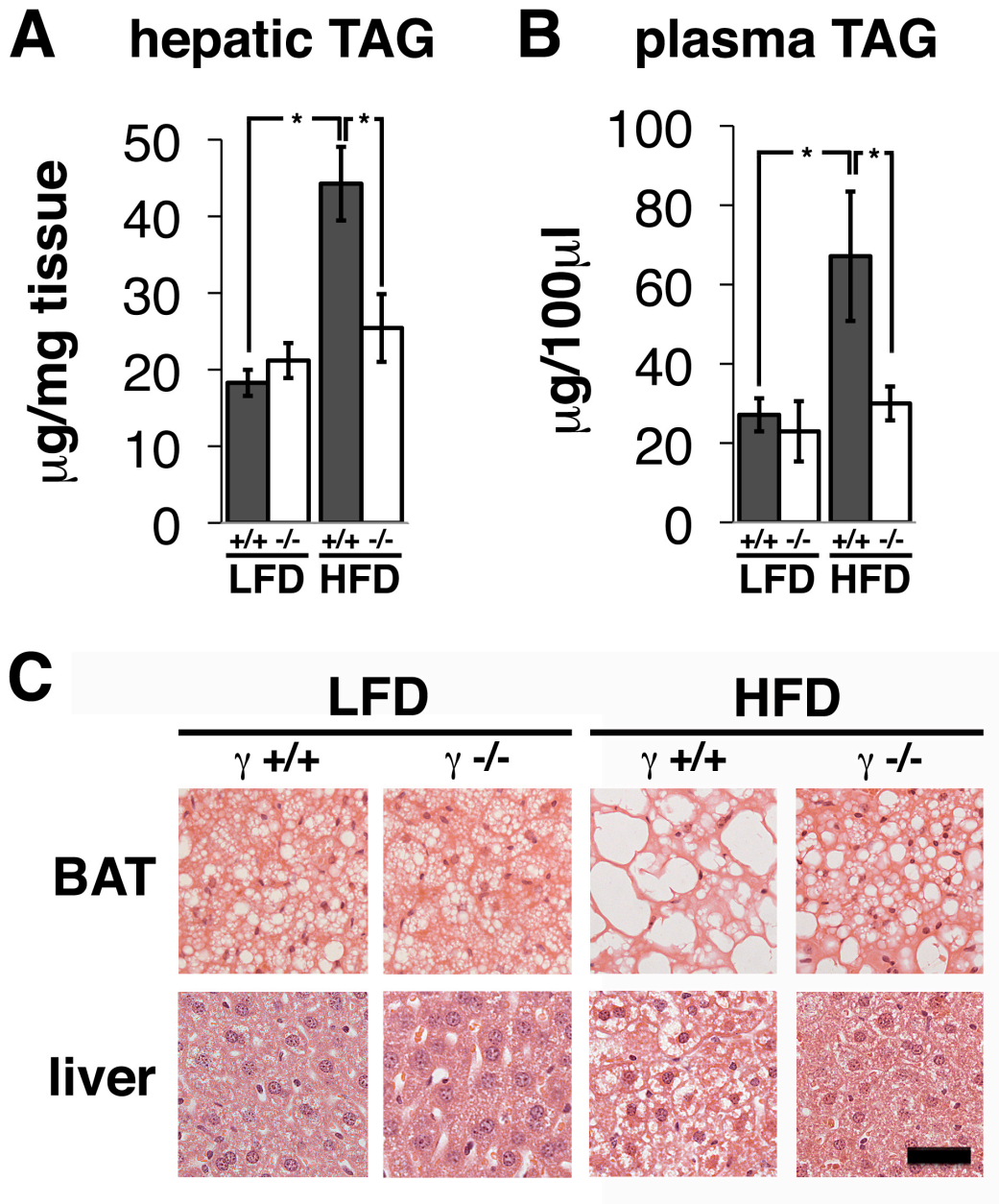


**Fig. 4.9. Effect of  $\gamma$ -synuclein<sup>-/-</sup> on lipid accumulation outside WAT.** (A, B) Levels of triacylglycerols (TAG) in liver (n=5-8) and plasma (n=5-7) of wild type (+/+) and  $\gamma$ -synuclein<sup>-/-</sup> mice (-/-) fed a LFD or HFD for 11 weeks. Bar charts represent mean $\pm$ SEM. Non-parametric Mann-Whitney U-test analysis demonstrated statistically significant differences between groups (\* p < 0.05). (C) H&E stained sections through brown adipose tissue (BAT) and liver taken from wild type and  $\gamma$ -synuclein<sup>-/-</sup> mice fed a LFD or HFD for 11 weeks. Scale bar = 50  $\mu$ m.

<b>Genotype</b>	<b>+/+</b>	<b>-/-</b>	<b>+/+</b>	<b>-/-</b>
<b>Diet</b>	<b>11 week LFD</b>		<b>11 week HFD</b>	
<b>pl. NEFA (<math>\mu\text{g}/100\mu\text{l}</math>, n=6)</b>	<b>15.9 <math>\pm</math> 3.5</b>	<b>19.5 <math>\pm</math> 3.3</b>	<b>16.0 <math>\pm</math> 2.0</b>	<b>20.5 <math>\pm</math> 3.7</b>
<b>pl. adiponectin (<math>\mu\text{g}/\text{ml}</math>, n=12)</b>	<b>77.1 <math>\pm</math> 8.7</b>	<b>68.7 <math>\pm</math> 7.6</b>	<b>58.3 <math>\pm</math> 5.6</b>	<b>62.5 <math>\pm</math> 3.2</b>
<b>pl. ketone bodies (mM, n=6-9)</b>	<b>0.27 <math>\pm</math> 0.05</b>	<b>0.31 <math>\pm</math> 0.03</b>	<b>0.27 <math>\pm</math> 0.04</b>	<b>0.24 <math>\pm</math> 0.03</b>
<b>GTT (area under curve, n=7)</b>	-	-	<b>588 <math>\pm</math> 107</b>	<b>532 <math>\pm</math> 52</b>
<b>ITT (area under curve, n=7)</b>	-	-	<b>224 <math>\pm</math> 39</b>	<b>263 <math>\pm</math> 37</b>

**Table 4.1. Analysis of various metabolic markers in plasma and glucose/insulin tolerance testing.** Levels of non-esterified fatty acids (NEFA), adiponectin and ketone bodies in plasma (pl.) of wild type (+/+) and  $\gamma$ -synuclein<sup>-/-</sup> mice (-/-) fed a LFD or HFD for 11 weeks (GTT glucose tolerance test, ITT insulin tolerance test).

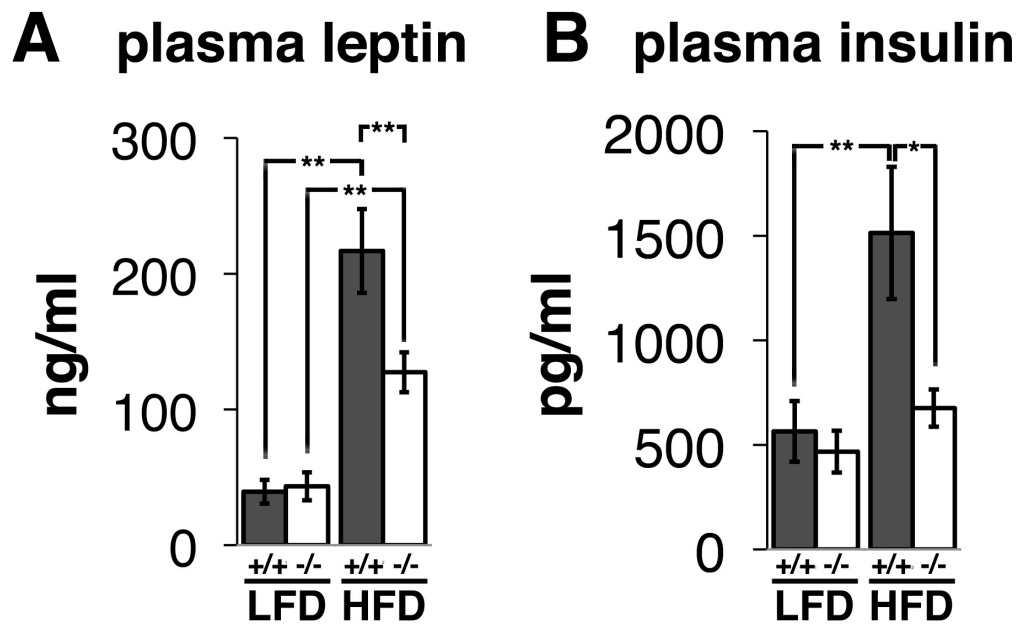


**Fig. 4.10. Plasma levels of leptin and insulin.** (A, B) Levels of leptin and insulin in plasma of wild type (+/+) and  $\gamma$ -synuclein<sup>-/-</sup> (-/-) mice fed a LFD or HFD for 11 weeks (n=11-14). Bar charts represent mean $\pm$ SEM (\* p < 0.05, \*\* p < 0.01, Mann-Whitney U-test).

### **4.2.3. Results: Increased whole-body lipid utilisation and energy expenditure in $\gamma$ -synuclein<sup>-/-</sup> mice**

Given that the observed decreases both in adipose and ectopic lipid storage are not attributed to decreased caloric intake in the absence of  $\gamma$ -synuclein we next examined substrate utilisation and energy expenditure in these mice. During week 8 of the 11-week HFD-feeding protocol, wild type and  $\gamma$ -synuclein<sup>-/-</sup> mice were housed for 72 hours in metabolic cages as part of a Comprehensive Lab Animal Monitoring System (CLAMS), based in the Institute of Metabolic Science, Cambridge University. Mice were given an acclimatisation period in these cages prior to the testing period. Exchange of CO<sub>2</sub> and O<sub>2</sub> in and out of individual cages was used to evaluate CO<sub>2</sub> production and O<sub>2</sub> consumption by individual mice, which were in turn used to calculate respiratory exchange ratio (RER) and energy expenditure by indirect calorimetry. Over this 72-hour testing period,  $\gamma$ -synuclein<sup>-/-</sup> mice had a significantly lower average RER (0.779 compared with 0.807 in wild type mice, Fig. 4.11A). A RER closer to 1.0 is indicative of carbohydrate usage as the main fuel source, whereas a RER nearer to 0.7 indicates that fat is being used primarily. HFD-fed  $\gamma$ -synuclein<sup>-/-</sup> mice also exhibited increased energy expenditure, during the light cycles (Fig. 4.11B). Consistent with this difference in RER between genotypes, further analysis to calculate both lipid and carbohydrate oxidation (again using VCO<sub>2</sub> and VO<sub>2</sub>, as well as known constants, see Experimental Procedures) demonstrated both increased lipid oxidation and reduced carbohydrate oxidation in  $\gamma$ -synuclein<sup>-/-</sup> compared to wild type mice (Fig. 4.12A, B). During the 72-hour testing period, the physical activity of individual mice was also measured using the number of horizontal beam breaks. Analysis of this data showed that, surprisingly, the increased energy expenditure observed in  $\gamma$ -synuclein<sup>-/-</sup> mice was despite lower levels of physical activity, mainly during the dark cycles (Fig. 4.13).

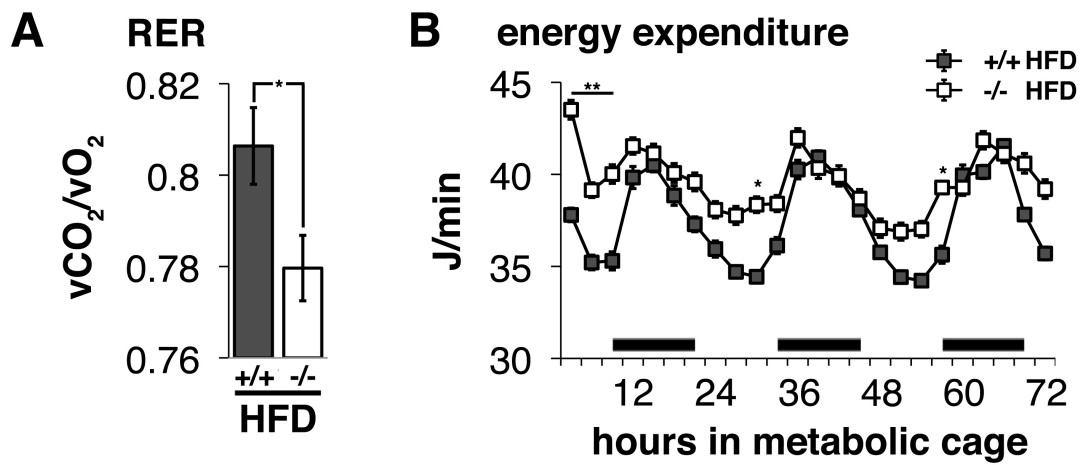


**Fig. 4.11. Whole-body metabolic analysis.** (A) Respiratory exchange ratio (RER) calculated by indirect calorimetry using CLAMS over a period of 72 hours in wild type (+/+) and  $\gamma$ -synuclein<sup>-/-</sup> (-/-) mice fed a HFD for 8 weeks at time of trial (n=8 per genotype). (B) Energy expenditure by these animals over the same period. Black bars indicate periods of dark cycles. In both panels, individual values represent mean±SEM (\* p < 0.05, \*\* p < 0.01, Student's *t*-test).

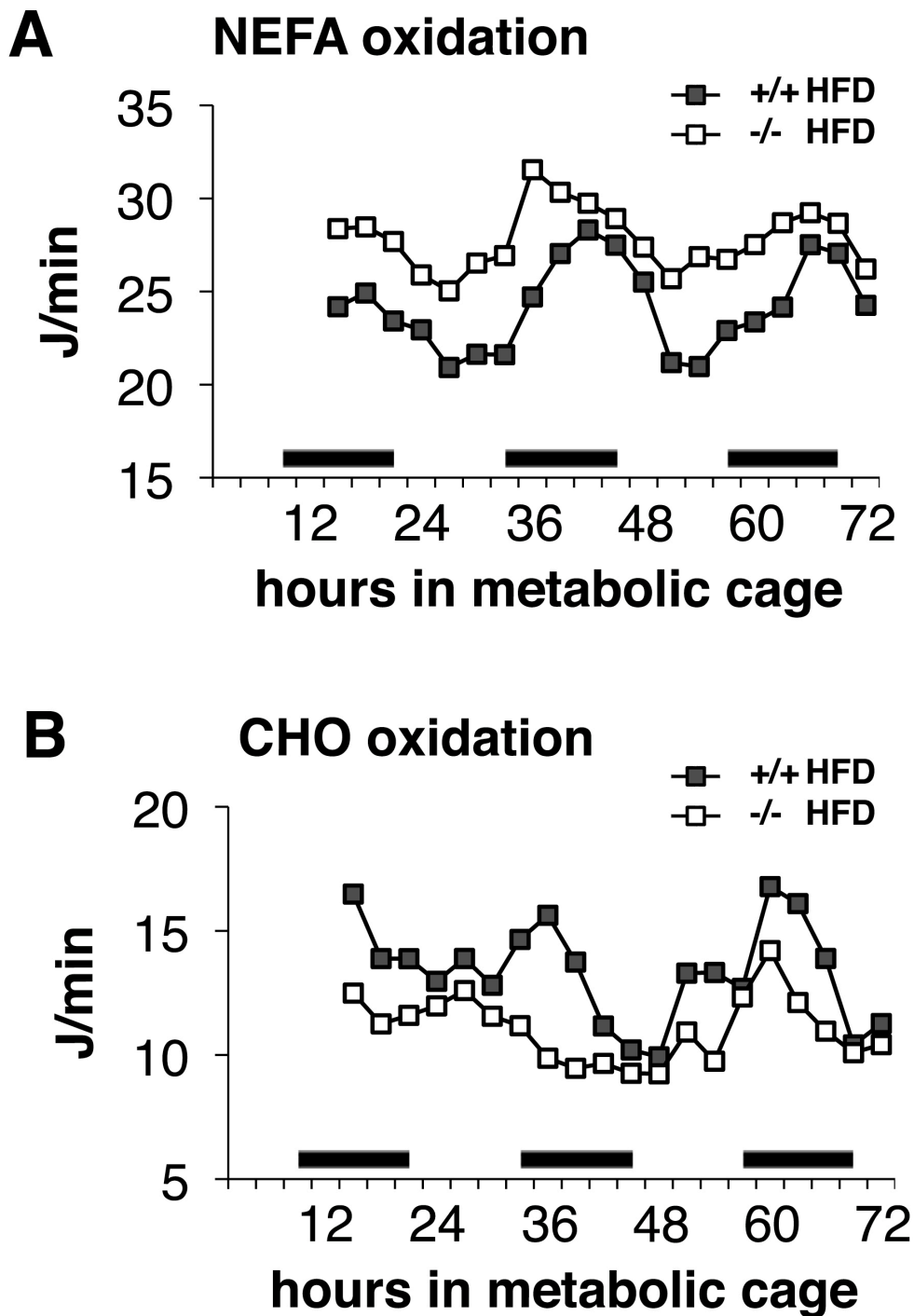


**Fig. 4.12. Substrate utilization during CLAMS analysis.** (A, B) Fatty acid (NEFA) and carbohydrate (CHO) oxidation calculated by indirect calorimetry using CLAMS over a period of 72 hours in wild type (+/+) and  $\gamma$ -synuclein<sup>-/-</sup> (-/-) mice fed a HFD for 8 weeks at time of trial (n=8 per genotype). Black bars indicate periods of dark cycles.

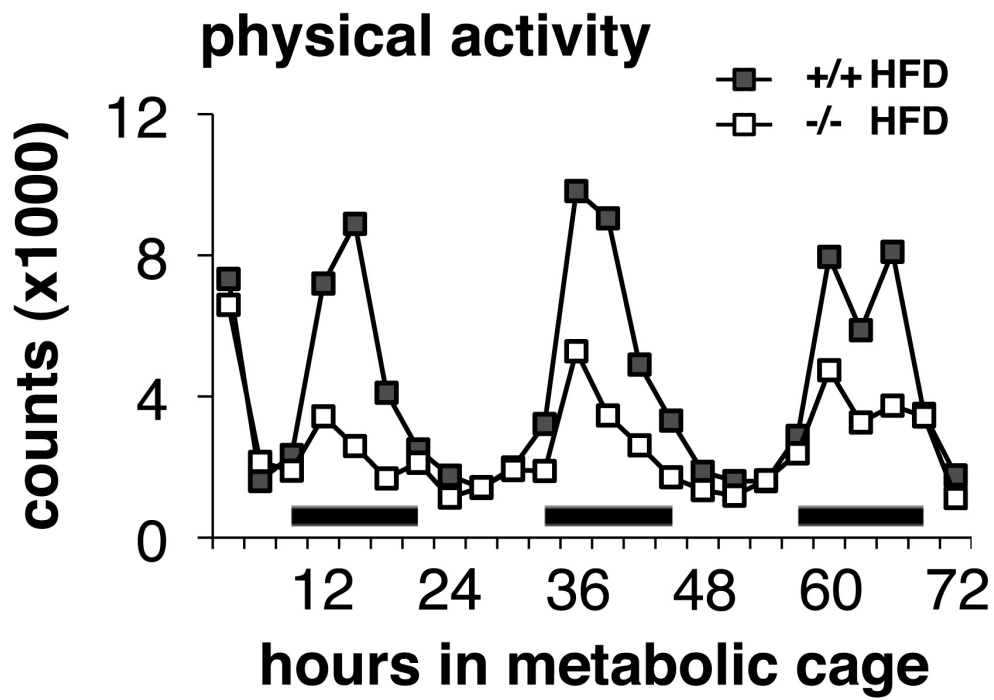


**Fig. 4.13. Physical activity during CLAMS analysis.** Physical activity during 72-hour CLAMS analysis of wild type (+/+) and  $\gamma$ -synuclein<sup>-/-</sup> (-/-) mice fed a HFD for 8 weeks at time of trial (n=8 per genotype). Black bars indicate periods of dark cycles.

### 4.3. Summary of results and discussion

With the observed nutritional regulation of  $\gamma$ -synuclein in murine and human WAT, we hypothesized that expression of  $\gamma$ -synuclein may be required for the development of at least certain forms of obesity. To test this we used  $\gamma$ -synuclein<sup>-/-</sup> mice that had previously been produced and characterized in our laboratory. Under conventional husbandry and diet conditions, these animals do not show any obvious neuronal (Ninkina et al., 2003; Papachroni et al., 2005) or metabolic abnormalities (our unpublished observations). These  $\gamma$ -synuclein<sup>-/-</sup> mice were challenged with a HFD known to cause diet-induced obesity in wild type mice.

Following the control LFD-feeding protocol, wild type and  $\gamma$ -synuclein<sup>-/-</sup> mice showed no differences in weight gain, consistent with the lack of any difference in animal weight that we have previously observed in our cohorts of  $\gamma$ -synuclein<sup>-/-</sup> mice compared with their wild type littermates. In contrast to this, HFD-fed  $\gamma$ -synuclein<sup>-/-</sup> mice were substantially leaner than their HFD-fed wild type counterparts throughout the duration of the feeding protocol. This difference was mirrored by a reduction in the amount of WAT accumulated by  $\gamma$ -synuclein<sup>-/-</sup> compared to wild type mice on HFD. Reduced WAT accumulation in  $\gamma$ -synuclein<sup>-/-</sup> mice was not due to reductions in either food intake or absorption of lipids from the diet. At the cellular level, measuring the size of white adipocytes from epididymal and subcutaneous WAT revealed that the increase of adipocyte size upon HFD-feeding in wild type mice was attenuated in  $\gamma$ -synuclein<sup>-/-</sup> mice. Moreover, injection of  $\gamma$ -synuclein-expressing lentiviral particles into the fat pads of  $\gamma$ -synuclein<sup>-/-</sup> mice before challenging them with HFD partially reversed this observed decrease in adipocyte size. Critically, this was only seen in those adipocytes re-expressing  $\gamma$ -synuclein and not in non-transduced cells in the same depot, nor cells transduced with a control lentivirus expressing only GFP. This data suggests that regulation of  $\gamma$ -synuclein within the fat cell specifically and cell-autonomously affects adipocyte size *in vivo*. As expression of  $\gamma$ -synuclein is not restricted to white adipocytes, but is also found within various regions of the central and peripheral nervous system, we cannot exclude that the absence of  $\gamma$ -synuclein in non-WAT tissues also contributes to observed differences between wild type and  $\gamma$ -synuclein<sup>-/-</sup> mice on HFD described in this chapter, such as the increased energy expenditure or decreased hepatic steatosis. However this finding demonstrates

the importance of WAT  $\gamma$ -synuclein expression on expansion of this tissue during periods of increased intake of lipids from the diet.

As well as hypertrophy of mature adipocytes, expansion of WAT depots occurs by hyperplasia and terminal differentiation of preadipocytes. We have observed that reduced adiposity between  $\gamma$ -synuclein<sup>-/-</sup> and wild type mice on HFD is due to differences in mature adipocyte hypertrophy, however our data suggests that  $\gamma$ -synuclein does not appear to play a major role in adipocyte differentiation from precursor cells. We have demonstrated that  $\gamma$ -synuclein<sup>-/-</sup> mouse embryonic fibroblasts (MEFs) differentiated into adipocytes as efficiently and with the same kinetics as wild type MEFs. Hence it seems that the decreased WAT accumulation in  $\gamma$ -synuclein<sup>-/-</sup> mice on HFD is not caused by a reduced capacity to expand adipose depots when required, but that lipid storage in individual adipocytes is reduced. This is important as human syndromes of lipodystrophy as well as mouse models of limited WAT expansion, demonstrate that restricting adipose mass leads to dyslipidaemia, insulin resistance and metabolic disease (Schweiger et al., 2009; Moitra et al., 1998). Therefore, if modification of  $\gamma$ -synuclein expression was to be employed as a therapeutic intervention aimed at improving obesity related metabolic disease; it is important to note that this method would not affect adipocyte formation.

Reduced adiposity does not always coincide with an improvement in whole-body metabolic function. Moreover these alterations in fat metabolism can result in aberrant increase of lipids in the circulation and their deposition in non-adipose tissues, which are metabolically vulnerable. This however was not the case in HFD-fed  $\gamma$ -synuclein<sup>-/-</sup> mice. Instead we found that  $\gamma$ -synuclein ablation rescues mice from HFD-induced metabolic disturbances, with protection from hypertriglyceridaemia, hepatic steatosis, hyperinsulinaemia and hyperleptinaemia. All of these signs of a metabolic disorder were a characteristic feature of HFD-fed wild type mice. Similar food intake between HFD-fed wild type and  $\gamma$ -synuclein<sup>-/-</sup> mice despite significantly reduced plasma leptin levels in  $\gamma$ -synuclein<sup>-/-</sup> mice, suggests that  $\gamma$ -synuclein<sup>-/-</sup> mice are more leptin sensitive than their wild type counterparts on HFD. Although fasting plasma insulin levels in HFD-fed groups suggest that unlike their wild type counterparts,  $\gamma$ -synuclein<sup>-/-</sup> mice do not display insulin resistance, we saw no improvement in glucose or insulin tolerance in these  $\gamma$ -synuclein<sup>-/-</sup> mice. Overall,

although deficiency of  $\gamma$ -synuclein may render mice resistant to HFD-induced obesity, and rescue them from obesity-related hyperinsulinaemia, it does not cause these mice to be any more insulin-sensitive on HFD. Upon metabolic analysis of HFD-fed mice, we have also revealed that reduced adiposity in  $\gamma$ -synuclein<sup>-/-</sup> mice was associated with increased whole-body lipid oxidation and energy expenditure, despite reduced levels of physical activity, all compared to HFD-fed wild type mice. A number of other mouse models, reported to be lean compared to control animals, also have elevated WAT NEFA oxidation with no increase in plasma NEFA (Martinez-Botas et al., 2000; Nishino et al., 2008; Puri et al., 2007; Tansey et al., 2001). Although NEFA oxidation is not commonly considered to be a major metabolic pathway in WAT, these findings have led to speculation that increased adipocyte NEFA oxidation may play a significant role in energy metabolism and adiposity (discussed in (Lafontan, 2008)). It is feasible to hypothesise that increased lipid utilisation and energy expenditure in these  $\gamma$ -synuclein<sup>-/-</sup> mice may therefore be a compensatory mechanism in response to reduced lipid storage in adipocytes, to prevent increased levels of circulating lipids and their deposition in non-adipose tissues, factors that are thought to cause or worsen metabolic disease.

In conclusion, knockout of  $\gamma$ -synuclein leads to decreased weight gain and WAT accumulation in mice fed a HFD and this is associated with increased energy expenditure and lipid oxidation. These alterations in lipid/energy metabolism rescued  $\gamma$ -synuclein<sup>-/-</sup> mice from various HFD-induced metabolic disturbances commonly associated with obesity. In the next chapter we will describe in more detail the changes in WAT of  $\gamma$ -synuclein<sup>-/-</sup> mice.

**Chapter 5 –  $\gamma$ -synuclein and lipid  
metabolism in *in vivo* and *in vitro* fat cells**

## 5.1. Overview

In the previous chapter we demonstrated that  $\gamma$ -synuclein deficiency in mice results in resistance to HFD-induced obesity, with reduced WAT accumulation, smaller adipocytes and increased lipid utilisation, all compared to HFD-fed wild type mice. To determine whether this reduction in adipocyte lipid storage was due to any specific alterations in  $\gamma$ -synuclein deficient fat cells, we analysed lipid metabolism in WAT from  $\gamma$ -synuclein<sup>-/-</sup> and wild type mice fed LFD or HFD. Furthermore, this chapter discusses findings concerning the expression of  $\gamma$ -synuclein in differentiating 3T3-L1 cells, a stable cell line frequently used to study gene function during and following adipocyte differentiation.

### 5.2.1. Results: Increased adipocyte lipolysis in $\gamma$ -synuclein<sup>-/-</sup> mice

We first investigated whether differences in lipid storage and lipid utilisation in  $\gamma$ -synuclein<sup>-/-</sup> mice fed HFD could be associated with alterations in adipocyte lipolysis. To do this, epididymal WAT from  $\gamma$ -synuclein<sup>-/-</sup> and wild type mice fed HFD for 11 weeks was dissected out, and mature white adipocytes were isolated. The procedure included collagenase digestion of WAT in Krebs-Ringer bicarbonate medium followed by centrifugation to pellet stromal cells, whilst mature adipocytes floated to the top of the buffer. Purified mature white adipocytes were incubated in the presence or absence of lipolytic stimulation using the non-specific  $\beta$ -adrenergic agonist, isoproterenol. Following this incubation period, media was collected from each suspension with subsequent determination of glycerol content. This was used as an index of lipolysis, with values normalized to the endogenous protein content of each suspension (see Experimental Procedures). The *ex vivo* glycerol release was approximately 3-fold higher in adipocytes isolated from HFD-fed  $\gamma$ -synuclein<sup>-/-</sup> mice compared to adipocytes from HFD-fed wild type mice under basal (no lipolytic stimulation) conditions (Fig. 5.1A). Moreover, whilst isoproterenol dramatically stimulated glycerol release in adipocytes of both genotypes, this remained significantly higher (~2-fold) in adipocytes from  $\gamma$ -synuclein<sup>-/-</sup> mice (Fig. 5.1A). These results suggest that the intracellular lipolytic capacity of adipocytes is greater in the absence of  $\gamma$ -synuclein. We also looked at levels of NEFA in WAT from  $\gamma$ -synuclein<sup>-/-</sup>

and wild type mice fed HFD for 11 weeks. This involved extraction of total lipids from epididymal WAT, separation of NEFA from other lipid species by TLC and quantification using gas chromatography. Interestingly, and consistent with our observations of increased adipocyte lipolysis, we observed increased levels of NEFA in WAT of HFD-fed  $\gamma$ -synuclein<sup>-/-</sup> compared with wild type mice (Fig. 5.1B).

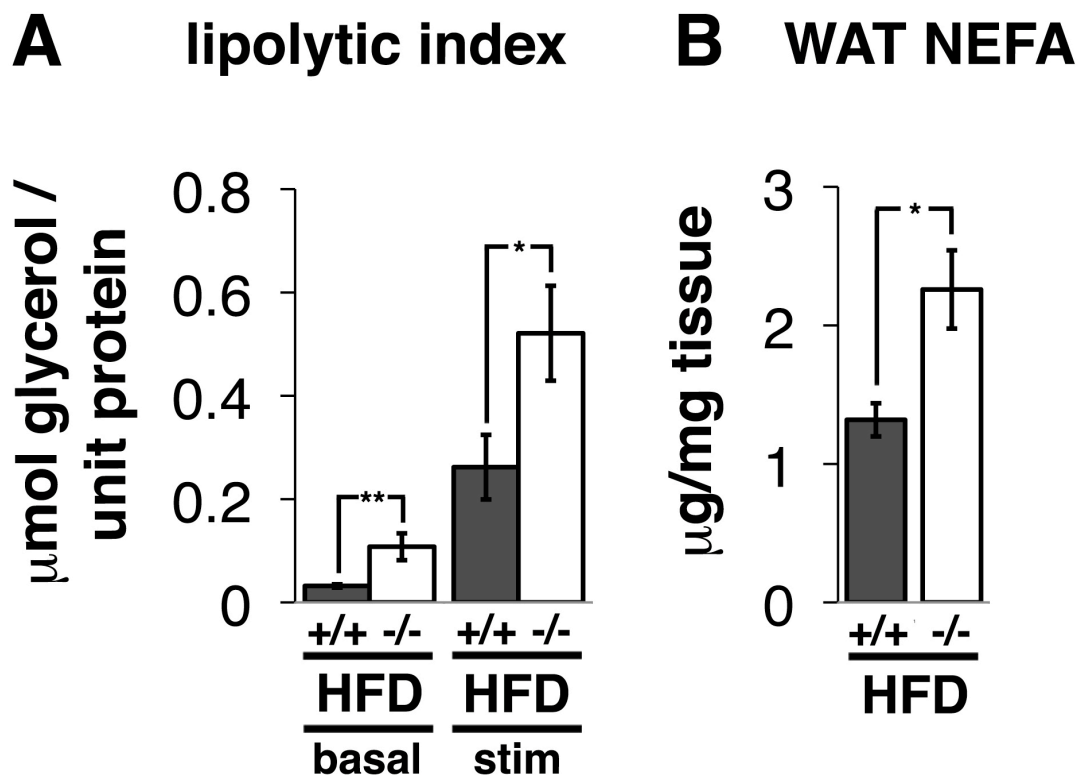


**Fig. 5.1. Lipolysis and NEFA levels in epididymal WAT.** (A) Measurement of cellular lipolysis in white adipocytes isolated from epididymal WAT of wild type (+/+) and  $\gamma$ -synuclein<sup>-/-</sup> (-/-) mice fed a HFD for 11 weeks. White adipocytes were incubated for 2 hours under basal or catecholamine-stimulated (stim) conditions (in the absence or presence of 10 $\mu$ M isoproterenol, correspondingly) and the lipolytic index was determined by measuring glycerol released from cells (n=8 animals per genotype/condition). Values obtained were normalized against levels of endogenous GAPDH protein expression (see Experimental Procedures). (B) Levels of non-esterified fatty acids (NEFA) in epididymal WAT depots of wild type and  $\gamma$ -synuclein<sup>-/-</sup> mice fed a HFD for 11 weeks (n=5). Bar charts represent mean $\pm$ SEM (\* p < 0.05, \*\* p < 0.01, Mann-Whitney U-test).

### **5.2.2. Results: The expression of proteins involved in lipid metabolism is not altered in WAT of $\gamma$ -synuclein<sup>-/-</sup> mice**

We next determined the effect of  $\gamma$ -synuclein loss on the expression of genes known to play a role in adipocyte lipid storage and metabolism. For this we used epididymal WAT from  $\gamma$ -synuclein<sup>-/-</sup> and wild type mice fed either LFD or HFD for 11 weeks. For mRNA expression studies, total RNA was extracted from WAT with subsequent cDNA synthesis. Relative abundance of adipocyte transcripts was measured by quantitative PCR. For protein expression, total proteins were extracted by direct homogenization of WAT into SDS-PAGE loading buffer and analysed by semi-quantitative Western blotting. At the RNA level we found that, consistent with the circulating leptin levels observed in these mice (Fig. 4.10A), leptin mRNA was increased by HFD-feeding in wild type animals and was blunted in  $\gamma$ -synuclein<sup>-/-</sup> mice (Fig. 5.2A). We observed no effect of either  $\gamma$ -synuclein loss or HFD-feeding on the mRNA expression of perilipin A, hormone sensitive lipase (HSL), adipose-triglyceride lipase (ATGL) and lipoprotein lipase (LPL), nor the genes encoding aP2, or the transcription factors peroxisome proliferator-activated receptor- $\gamma$  (PPAR $\gamma$ ) and CCAAT-enhancer binding protein- $\beta$  (C/EBP $\beta$ ) (Fig. 5.2B). The only statistically significant differences in this mRNA expression study were the similar (~1.5-fold) increases of aP2 mRNA levels in both  $\gamma$ -synuclein<sup>-/-</sup> and wild type mice following HFD feeding (Fig. 5.2B). Further mRNA expression studies included other factors known to affect lipid metabolism, including enzymes involved in lipid oxidation (3-ketoacyl-CoA thiolase B, 3-KAT), lipid synthesis (acetyl-CoA carboxylase, ACC-1) and mitochondrial uncoupling (uncoupling protein-1, UCP-1). This analysis revealed that the majority of these genes showed similar changes, with a similar 2-fold increase in WAT mRNA levels of 3-KAT in both wild type and  $\gamma$ -synuclein<sup>-/-</sup> mice following HFD feeding (Fig. 5.3A). UCP-1 mRNA expression was unaltered by both  $\gamma$ -synuclein deficiency and HFD (Fig. 5.3A). However, whilst ACC-1 expression was significantly reduced following HFD-feeding in WAT of wild-type mice, this reduction was not significant in mice lacking  $\gamma$ -synuclein (Fig. 5.3A). In BAT and liver, mRNA expression of 3-KAT was not affected by  $\gamma$ -synuclein loss in HFD-fed mice, nor was the expression of uncoupling protein UCP-1 in BAT of HFD-fed mice (Fig. 5.3B-D).

At the protein level, there were no alterations in expression of perilipin A or HSL between all four experimental groups, nor any evidence of altered phosphorylation of HSL at its catecholamine-sensitive regulatory phosphorylation site, serine 563 (Garton et al., 1988; Stralfors et al., 1984). There was however, a significant (~1.8-fold) increase in the level of ATGL in epididymal WAT of HFD-fed  $\gamma$ -synuclein<sup>-/-</sup> mice compared to HFD-fed wild type mice (Fig. 5.4, Appendix 4).

We also investigated whether  $\gamma$ -synuclein loss affected any major intracellular signaling pathways that might contribute to the protective phenotype in the null mice. As described above, total proteins were extracted from epididymal WAT of  $\gamma$ -synuclein<sup>-/-</sup> and wild type mice fed HFD for 11 weeks, and analysed by semi-quantitative Western blotting. We found no differences in phosphorylation of AMP-activated protein kinase (AMPK $\alpha$ , Thr172) or Akt/PKB (Ser473), nor any alteration in mTOR signaling as measured by phosphorylation of p70 S6 kinase (Thr421/Ser424) (Fig. 5.5). However we did observe a 1.9-fold increase in phosphorylation of extracellular signal-regulated kinase (ERK, Thr202/Tyr204) in epididymal WAT of HFD-fed  $\gamma$ -synuclein<sup>-/-</sup> compared to HFD-fed wild type mice (Fig. 5.5).

To determine whether  $\gamma$ -synuclein is able to directly affect the phosphorylation of ERK, we employed an ERK phosphorylation response to serum-starvation and re-feeding in cultured 3T3 fibroblasts. Dividing cells were transduced with the same  $\gamma$ -synuclein- or GFP-expressing lentivirus particles as discussed in the *in vivo* experiments in section 4.2.1 (for details about transduction see Experimental Procedures). Cells were serum-starved overnight and proteins harvested for analysis prior to re-feeding, and at various intervals up to 2 hours after re-feeding with serum. Analysis of proteins by semi-quantitative Western blotting firstly revealed that cells transduced with  $\gamma$ -synuclein-expressing lentivirus particles showed significant overexpression of  $\gamma$ -synuclein protein (Fig. 5.6A). Serum re-feeding caused rapid ERK phosphorylation within 15 minutes in cells transduced with either  $\gamma$ -synuclein- or GFP-expressing lentivirus particles, with levels of phosphorylated ERK starting to diminish around an hour following serum re-feeding (Fig. 5.6B, C). However, the lentivirus-mediated overexpression of  $\gamma$ -synuclein caused no difference in the dynamics of this ERK phosphorylation over the 2-hour period following serum re-

feeding, as compared with cells transduced with GFP-only expressing lentivirus (Fig. 5.5B, C).

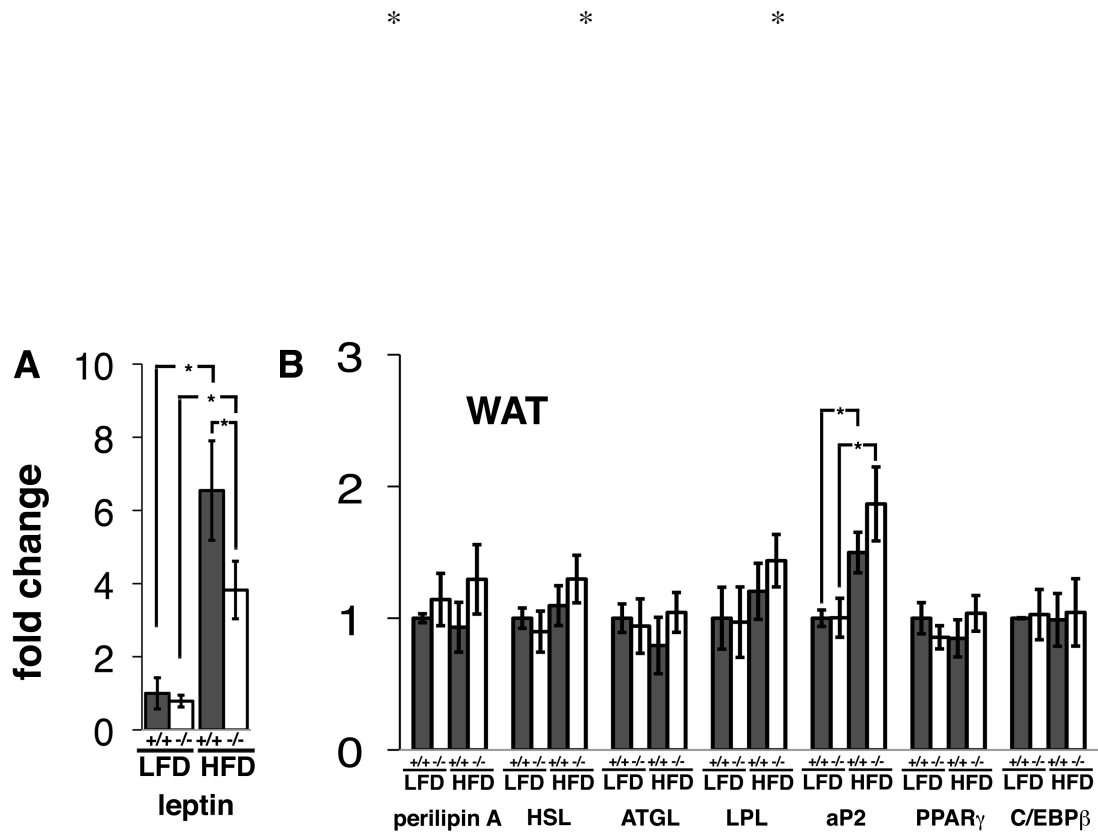


**Fig. 5.2. mRNA expression analysis of genes known to affect fat storage.** (A, B) Bar charts show mean fold change ( $\pm$ SEM) of mRNA expression levels in epididymal WAT of wild type (+/+) and  $\gamma$ -synuclein<sup>-/-</sup> (-/-) mice fed a LFD or HFD for 11 weeks, measured by quantitative RT-PCR and normalised to the mean level of each mRNA expression in wild type mice fed a LFD (n=5-9; \* p < 0.05, Mann-Whitney U-test).

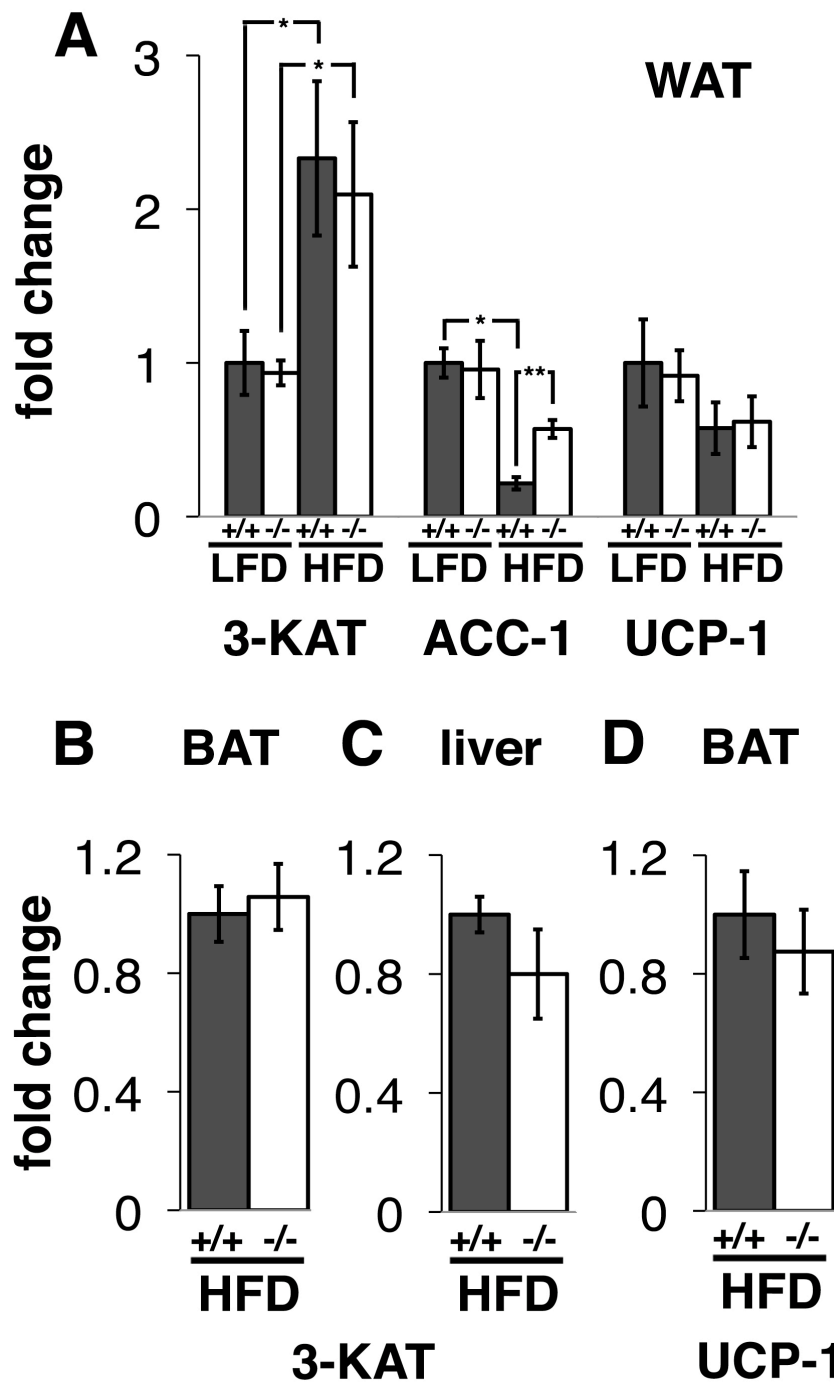


**Fig. 5.3. Quantitative RT-PCR analysis of mRNA encoding proteins involved in lipid metabolism in WAT, BAT and liver.** (A) Levels of 3-KAT, ACC-1 and UCP-1 mRNA in epididymal WAT of wild type (+/+) and  $\gamma$ -synuclein<sup>-/-</sup> (-/-) mice fed a LFD or HFD for 11 weeks (n=5-9). Results are shown as average fold change $\pm$ SEM (\* p < 0.05, \*\* p < 0.01, Mann-Whitney U-test) compared with LFD-fed wild type mice. (B-D) mRNA expression of 3-KAT and UCP-1 in BAT and liver of wild type and  $\gamma$ -synuclein<sup>-/-</sup> mice fed a HFD for 11 weeks (n=4). Results are shown as average fold change $\pm$ SEM compared with wild type mice.

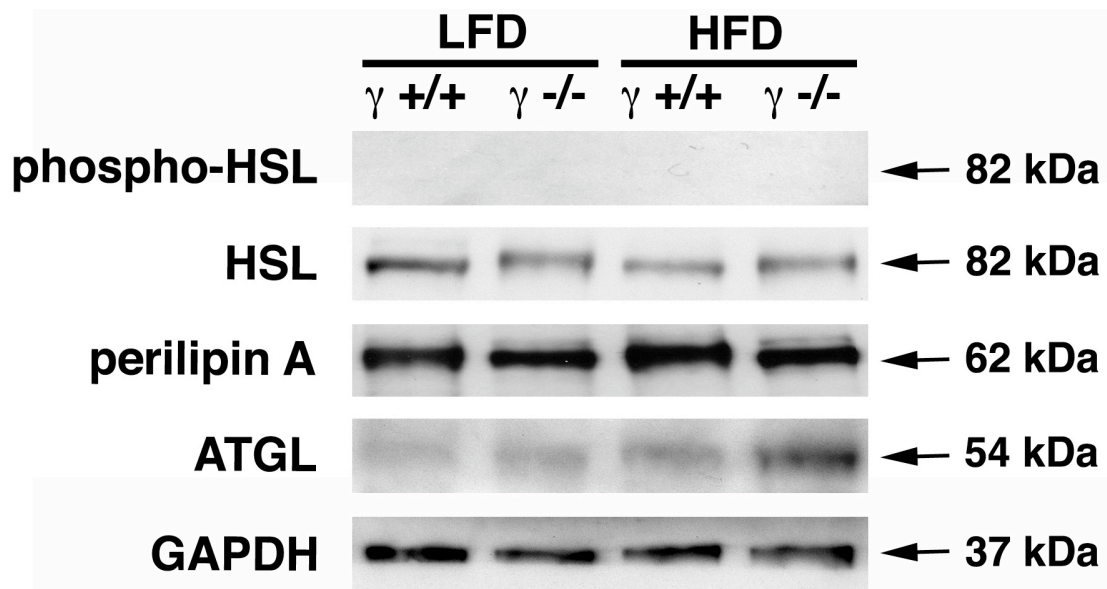


**Fig. 5.4. Protein expression analysis of genes known to affect fat storage.** A representative Western blot of total proteins samples extracted from the epididymal WAT of wild type and  $\gamma$ -synuclein<sup>-/-</sup> mice fed a LFD or HFD for 11 weeks. GAPDH was used as a loading control.

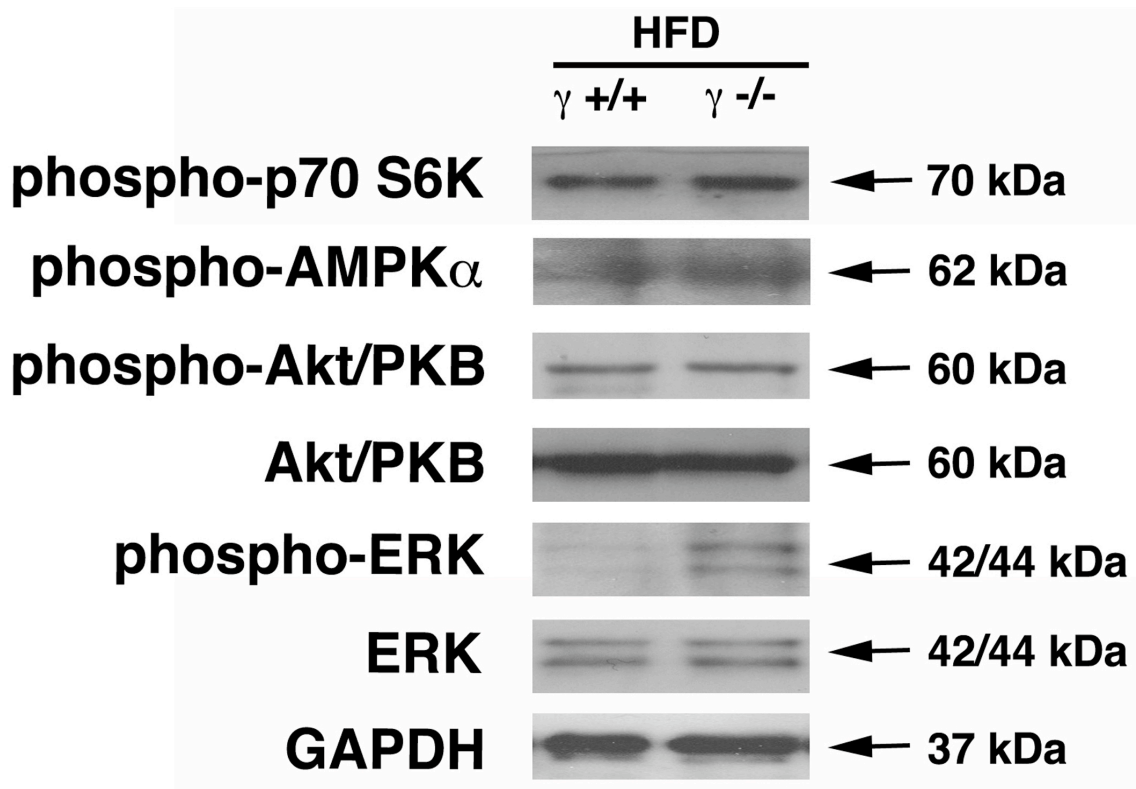


**Fig. 5.5. Expression analysis of proteins involved in nutrient sensing and cell growth.** A representative Western blot of total proteins samples extracted from the epididymal WAT of wild type and  $\gamma$ -synuclein<sup>-/-</sup> mice fed HFD for 11 weeks. GAPDH was used as a loading control.

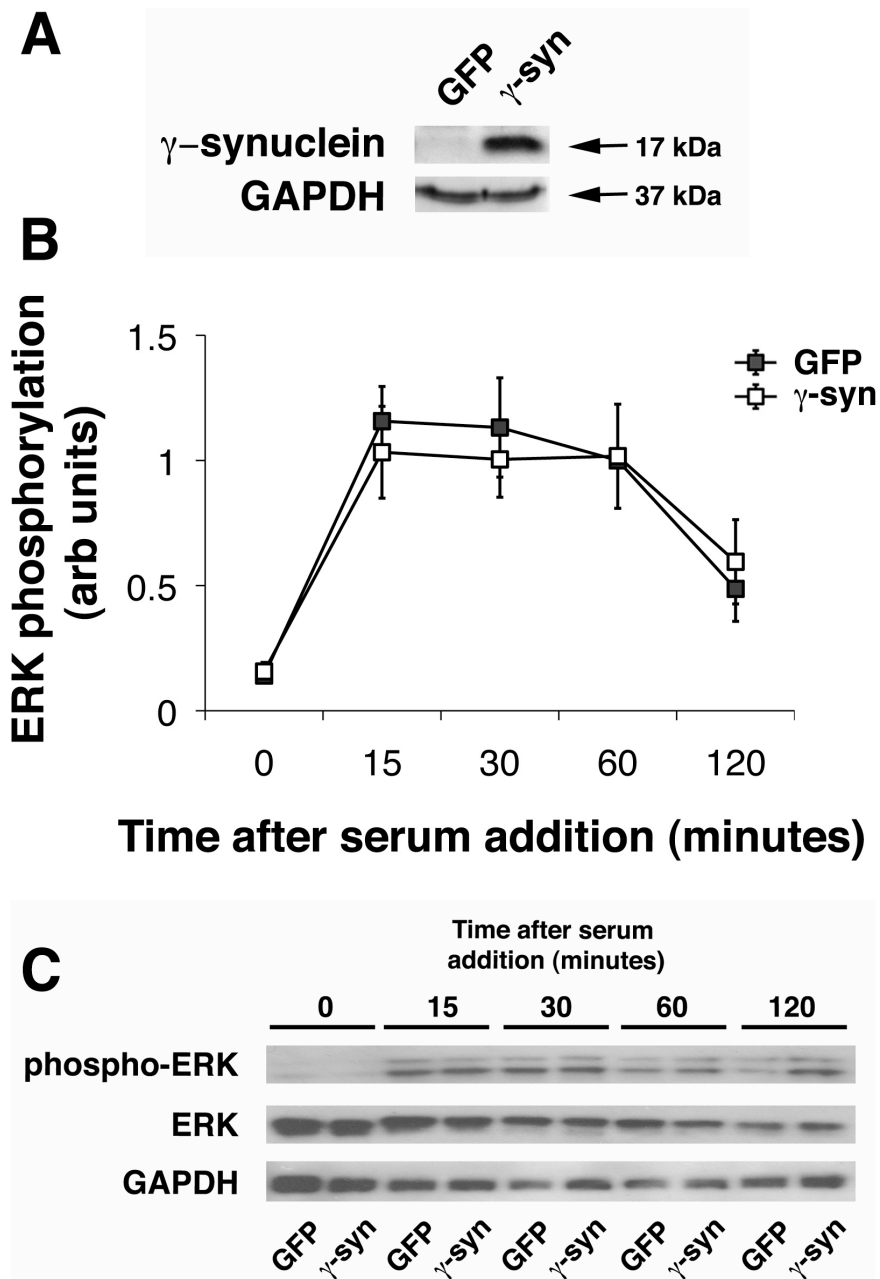


**Fig. 5.6. Dynamics of ERK phosphorylation following lentivirus-mediated overexpression of  $\gamma$ -synuclein.** (A) Western blot analysis of  $\gamma$ -synuclein expression in 3T3 cells transduced with  $\gamma$ -synuclein- ( $\gamma$ -syn) or GFP- (GFP) expressing lentivirus. GAPDH was used as a loading control. (B, C) ERK phosphorylation in 3T3 cells was analysed by measuring abundance of phosphorylated and non-phosphorylated ERK by semi-quantitative Western blotting. Subconfluent 3T3 fibroblasts were transduced with  $\gamma$ -synuclein- ( $\gamma$ -syn) or GFP- (GFP) expressing lentivirus particles as described in Experimental Procedures. Cells were then serum-starved for 16 hours and total proteins extracted prior to re-feeding and 15, 30, 60 and 120 minutes after re-feeding with serum-containing media (n=6).

### **5.2.3. Results: $\gamma$ -synuclein mRNA expression is not altered during differentiation of 3T3-L1 cells, nor is there any detectable level of $\gamma$ -synuclein proteins from these cells**

The 3T3-L1 stable cell line is a useful tool for studying gene function during and following adipocyte differentiation *in vitro*. Upon the addition of certain pro-differentiation factors in culture, 3T3-L1 fibroblasts begin to accumulate and store neutral lipids, along with the parallel induction of the expression of a number of adipocyte-specific transcripts. It has previously been demonstrated that  $\gamma$ -synuclein mRNA levels increase from their relatively low abundance in 3T3-L1 fibroblasts to considerably higher levels (~25 fold increase by the time of full maturation) during their differentiation into mature 3T3-L1 adipocytes (Oort et al., 2008). We decided to also look at the dynamics of  $\gamma$ -synuclein mRNA abundance during differentiation of 3T3-L1 cells in culture, as well as levels of  $\gamma$ -synuclein protein in both 3T3-L1 fibroblasts and mature 3T3-L1 adipocytes. To do this, we harvested cells for total RNA and protein at various stages throughout the differentiation process, and measured mRNA and protein levels of  $\gamma$ -synuclein using RT-PCR and semi-quantitative Western blotting respectively. However, unlike what was found by (Oort et al., 2008), when measuring dynamics of  $\gamma$ -synuclein expression during 3T3-L1 adipocyte differentiation in our laboratory, we found that abundance of  $\gamma$ -synuclein mRNA was low and did not alter significantly during any stage of the differentiation process (Fig. 5.7A). This was alongside the appearance, and a subsequent large increase, of perilipin A mRNA expression in the same cultures over this period (Fig. 5.7A). We also observed the appearance of multiple intracellular lipid droplets when cells were viewed under a light microscope during the differentiation procedure. Both the increase in abundance of perilipin A mRNA and appearance of visible lipid droplets prove that adipocyte differentiation did indeed occur in these cultures. When analysing protein expression in 3T3-L1 cells, either as fibroblasts or mature adipocytes, we did not observe any detectable level of  $\gamma$ -synuclein (Fig. 5.7B). We did however observe the appearance of perilipin A protein expression in the same cultures of mature 3T3-L1 adipocytes (Fig. 5.7B).

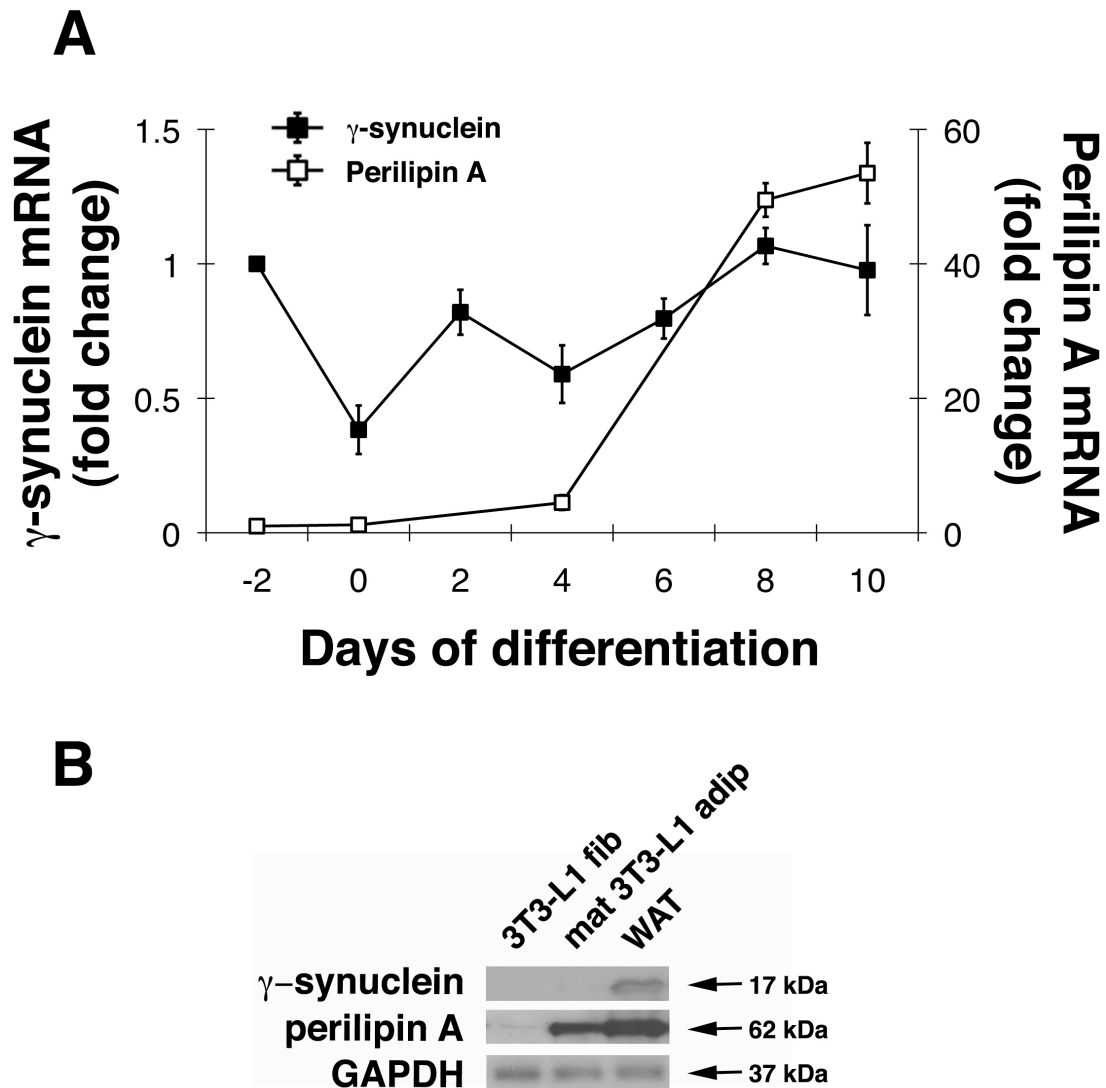


**Fig. 5.7.  $\gamma$ -synuclein mRNA expression during differentiation of 3T3-L1 cells.** (A) Expression of  $\gamma$ -synuclein and perilipin A mRNA in 3T3-L1 cells during their differentiation, measured by quantitative RT-PCR. 2-day post-confluent monolayers of 3T3-L1 fibroblasts (day 0) were exposed to a pro-differentiation medium as described in Experimental Procedures. Values are normalised to the mean level of mRNA expression at day -2 with individual values representing mean $\pm$ SEM (n=4). (B) Western blot analysis of  $\gamma$ -synuclein and perilipin A protein expression in 3T3-L1 fibroblasts (3T3-L1 fib), mature 3T3-L1 adipocytes (mat 3T3-L1 adip) and white adipose tissue (WAT). GAPDH was used as a loading control.

#### **5.2.4. Results: $\gamma$ -synuclein mRNA expression is downregulated by isobutylmethylxanthine (IBMX) in certain cell lines in culture**

Whilst performing experiments regarding adipocyte differentiation of precursor cells in culture, we noticed that 48 hours after introduction of the pro-differentiation regimen, there was a rapid and significant downregulation of  $\gamma$ -synuclein mRNA in MEFs, as analysed by RT-PCR ( $20\pm 8\%$  of levels detected before induction of differentiation,  $p < 0.05$ , Mann-Whitney U-test). We decided to check if one or more agents included in this pro-differentiation medium were responsible for this downregulation. To do this we cultured MEFs in growth medium including only one of insulin, dexamethasone, rosiglitazone or isobutylmethylxanthine (IBMX), all at the same concentration as in the pro-differentiation cocktail. After 48 hours, total RNA was extracted from these cells, followed by synthesis of cDNA and determination of  $\gamma$ -synuclein mRNA levels by quantitative PCR. This analysis showed no changes in abundance of  $\gamma$ -synuclein mRNA following exposure to insulin, dexamethasone or rosiglitazone ( $104\pm 21\%$ ,  $82\pm 32\%$ ,  $92\pm 18\%$  all compared to parallel cultures treated with DMSO, respectively). However, cultures treated with IBMX showed a significant downregulation of  $\gamma$ -synuclein mRNA compared to DMSO-treated cultures, which was of similar magnitude to what was seen when all four pro-differentiation agents were used in cocktail ( $23\pm 8\%$ ,  $p < 0.05$ , Mann-Whitney U-test). We repeated this experiment with the same IBMX treatment in three stable cell lines, namely 3T3 fibroblasts, mature 3T3-L1 adipocytes and MG1361 cells (a murine cell line established from mammary adenocarcinomas, (Sacco et al., 1998)). During studies involving mammary tumourigenesis in our laboratory, we had previously seen that this breast cancer cell line expresses relatively high levels of  $\gamma$ -synuclein mRNA. These three cell lines were grown in their respective culture media, with total RNA extracted 2, 12 and 48 hours following exposure to IBMX. RT-PCR analysis showed that 2 hours after addition of IBMX to the culture media, there were no differences in the levels of  $\gamma$ -synuclein mRNA in any of the three cell lines when compared to DMSO-treated control cultures (Fig. 5.8). In contrast to this, we observed a considerable downregulation ( $\sim 85\%$  reduction) of  $\gamma$ -synuclein mRNA in 3T3 fibroblasts and mature 3T3-L1 adipocytes 12 hours following exposure to IBMX, again compared to DMSO-treated cultures (Fig. 5.8). However, this downregulation was not present in MG1361 cells after either 12 or indeed 48 hours after addition of

IBMX. In 3T3 fibroblasts and mature 3T3-L1 adipocytes, the substantial downregulation of  $\gamma$ -synuclein mRNA was still present 48 hours after the introduction of IBMX (Fig. 5.8).

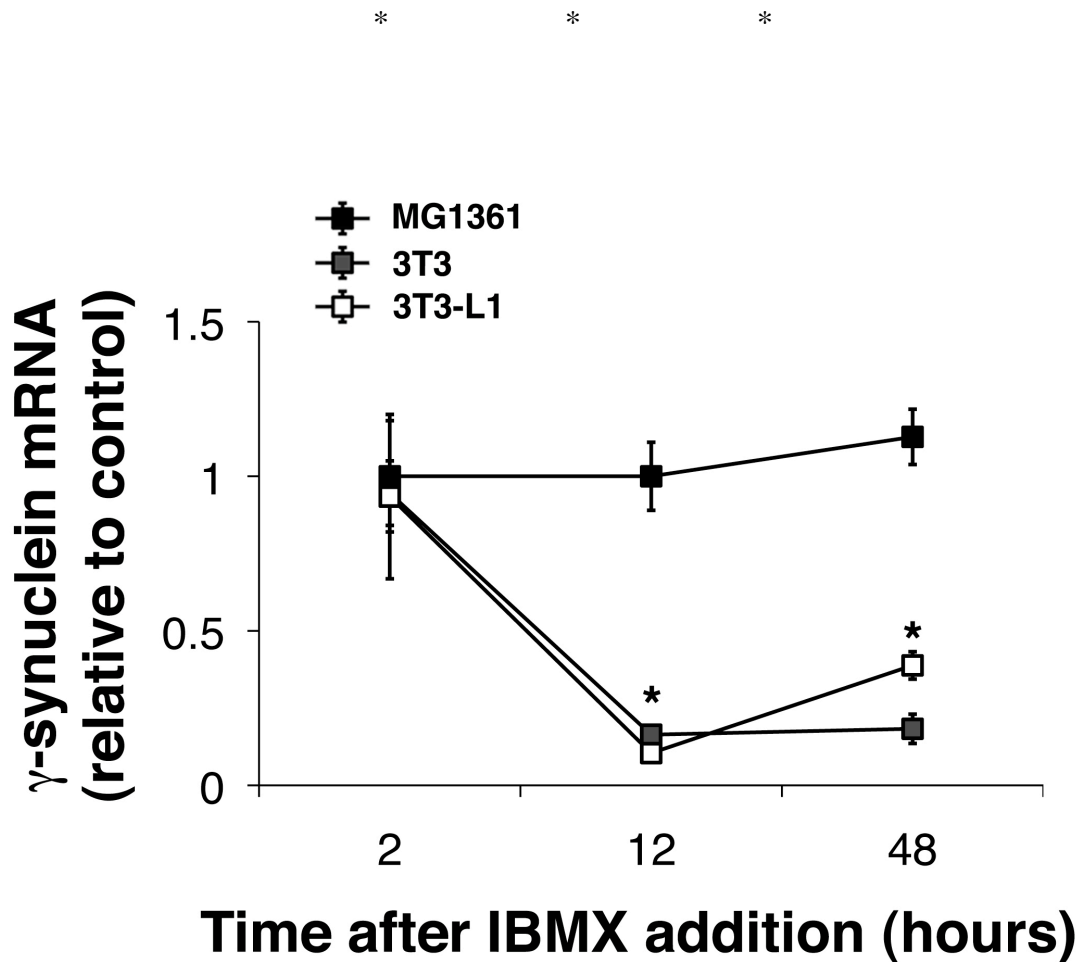


**Fig. 5.8. Effect of IBMX on  $\gamma$ -synuclein mRNA expression in various cell types in culture.** Levels of  $\gamma$ -synuclein mRNA in MG1361 cells, 3T3 fibroblasts and mature 3T3-L1 adipocytes upon exposure to IBMX, measured by quantitative RT-PCR. Values are compared to  $\gamma$ -synuclein mRNA in parallel cultures treated with DMSO for each time point, with individual values representing mean $\pm$ SEM (n=4-5 cultures per cell type/treatment, \* p < 0.05 for both 3T3 fibroblasts and mature 3T3-L1 adipocytes, Mann-Whitney U-test).

### 5.3. Summary of results and discussion

The finding that deficiency of  $\gamma$ -synuclein in mice confers resistance to HFD-induced obesity, with knockout mice displaying reduced WAT accumulation and adipocyte lipid storage, it was logical to look more closely at lipid metabolism in  $\gamma$ -synuclein deficient white adipocytes. We also looked at expression of  $\gamma$ -synuclein mRNA and protein in 3T3-L1 fibroblasts, a stable cell line capable of differentiating into mature adipocytes in culture.

In isolated white adipocytes, we demonstrated that the absence of  $\gamma$ -synuclein leads to increased basal and isoproterenol-stimulated lipolysis, suggesting a larger intracellular lipolytic capacity of  $\gamma$ -synuclein<sup>-/-</sup> adipocytes. In addition to this, in HFD-fed mice we also found increased NEFA levels in WAT from  $\gamma$ -synuclein<sup>-/-</sup> mice. It is possible that in  $\gamma$ -synuclein<sup>-/-</sup> adipocytes, reduced intracellular lipid storage is primarily due to increased lipolysis, represented by increased WAT NEFA levels and efflux of these NEFA from this tissue. Consistent with this idea, we also observed increased levels of ATGL in WAT, the key triglyceride lipase in this tissue, in HFD-fed  $\gamma$ -synuclein<sup>-/-</sup> compared to HFD-fed wild type mice. Similar to our  $\gamma$ -synuclein<sup>-/-</sup> mice, transgenic mice that overexpress ATGL specifically in adipose tissue are also resistant to obesity and have smaller white adipocytes compared to wild type mice following high fat diet feeding (Ahmadian et al., 2009). The overlap of the phenotypes between these two mutant strains of mice suggest that the increased WAT ATGL expression in  $\gamma$ -synuclein<sup>-/-</sup> mice at least contributes to the decreased WAT accumulation in mice lacking  $\gamma$ -synuclein. We observed no effect of  $\gamma$ -synuclein loss on the expression of a number of genes known to play a role in adipocyte lipid storage and metabolism in WAT, BAT or liver, either at the RNA or protein level. Exceptions to this were changes to levels of leptin and acetyl-CoA carboxylase (ACC-1) mRNA in WAT. Changes in leptin mRNA abundance were consistent with both adipocyte size and circulating leptin levels in all four groups of experimental mice. Significant reduction of ACC-1 mRNA expression after HFD feeding in wild type mice was not found in  $\gamma$ -synuclein<sup>-/-</sup> mice, possibly representing that downregulation of the lipid synthesis pathway in WAT of wild type mice was not necessary in  $\gamma$ -synuclein<sup>-/-</sup> mice.

In mouse WAT,  $\gamma$ -synuclein loss did not affect major intracellular signaling pathways involved in nutrient signaling (AMPK), cell growth (mTOR) or insulin signaling

(Akt/PKB). These data suggest that in adipocytes,  $\gamma$ -synuclein functions independent or downstream of these pathways. Interestingly, in WAT of HFD-fed mice,  $\gamma$ -synuclein loss resulted in a significant increase in the phosphorylation of ERK, suggesting that ERK activity in this tissue is increased. However overexpression of  $\gamma$ -synuclein in cultured non-adipose cells did not affect the ERK phosphorylation response to serum-starvation and re-feeding, suggesting modulation of ERK phosphorylation by  $\gamma$ -synuclein is cell-type specific. Although it is possible that this increased ERK activity is a compensatory mechanism in response to restricted adipocyte size in HFD-fed  $\gamma$ -synuclein<sup>-/-</sup> mice, it is unclear at this time the exact reason for this observed increase.

Previous work performed in another laboratory demonstrated a considerable increase of  $\gamma$ -synuclein mRNA levels during the differentiation of 3T3-L1 fibroblasts into mature 3T3-L1 adipocytes (Oort et al., 2008). However, when performing a similar experiment in our laboratory, we found that abundance of  $\gamma$ -synuclein mRNA was low and did not change significantly during any stage of the differentiation process. Moreover, we did not observe a detectable level of  $\gamma$ -synuclein proteins in either 3T3-L1 fibroblasts or mature 3T3-L1 adipocytes, probably reflecting the relatively low expression of  $\gamma$ -synuclein mRNA and, consequently,  $\gamma$ -synuclein protein expression. These experiments were performed using the same methods for determining expression at both the RNA and protein level that were carried out during work in previous chapters, and so it appears unlikely that these observations are false. Although there is no obvious reason for the disparity between findings in different laboratories concerning  $\gamma$ -synuclein mRNA expression during 3T3-L1 differentiation, it is possible that the various sub-lines of 3T3-L1 cells propagated for a long time in different laboratories acquire different properties. If this is the case, then upregulation of  $\gamma$ -synuclein expression during the differentiation procedure is an example of this. Regardless, these findings do further demonstrate (alongside our studies involving adipocyte differentiation of  $\gamma$ -synuclein<sup>-/-</sup> MEFs – section 4.2.1) that  $\gamma$ -synuclein is not required for adipocyte differentiation, and also that this cell line is not an ideal model for the study of  $\gamma$ -synuclein function in cultured adipocytes.

During these *in vitro* experiments we also performed a small separate study that does not have direct link with the function of  $\gamma$ -synuclein in white adipocytes, but might have potential implications for any, possibly therapeutic, reason to regulate expression of  $\gamma$ -synuclein. We noticed that cultured undifferentiated MEFs express relatively high levels of  $\gamma$ -synuclein mRNA but introduction of the pro-differentiation regimen used for their differentiation into adipocytes, induced a substantial downregulation of its expression. Functional dissection of components in the differentiation medium revealed that the isobutylmethylxanthine (IBMX) present in this differentiation cocktail was responsible for the downregulation of  $\gamma$ -synuclein mRNA. IBMX is a non-specific cyclic nucleotide phosphodiesterase inhibitor capable of drastically elevating intracellular cAMP levels. In adipocytes, IBMX treatment promotes a lipolytic response, due to inhibition of phosphodiesterase 3B, raised intracellular cAMP levels and activation of protein kinase A (PKA). Downregulation of  $\gamma$ -synuclein mRNA was highly pronounced in both 3T3 fibroblasts and mature 3T3-L1 adipocytes, but absent in a breast cancer cell line known to express  $\gamma$ -synuclein mRNA, MG1361. Further investigation is required to determine whether this downregulation is a direct cellular response to increased cAMP levels, or via an independent pathway. It is possible that these different cell-types, each with their own properties and gene expression profile, respond differently to IBMX in terms of  $\gamma$ -synuclein expression. To better understand the regulation of  $\gamma$ -synuclein expression by IBMX in various cell types, further analysis is required into the precise mechanism of this regulation, and the cellular pathways/molecules involved.

Experimental results described in this chapter demonstrate that the intracellular lipolytic capacity of white adipocytes is greater in the absence of  $\gamma$ -synuclein. We have also shown that a number of genes known to play a role in adipocyte lipid storage and metabolism are unaltered by loss of  $\gamma$ -synuclein. However we did observe a significant increase in protein levels of the lipase ATGL in WAT between HFD-fed  $\gamma$ -synuclein<sup>-/-</sup> and wild type mice, consistent with increases in adipocyte lipolysis in WAT of these mice. Interestingly, although not fully understood,  $\gamma$ -synuclein loss in HFD-fed mice caused increased phosphorylation of ERK in WAT. Analysis of  $\gamma$ -synuclein expression in 3T3-L1 cells demonstrated that unlike documented in previous reports (Oort et al., 2008),  $\gamma$ -synuclein mRNA levels did not alter significantly during differentiation of 3T3-L1 cells. In addition to this, we did not see

any detectable level of  $\gamma$ -synuclein protein in either immature 3T3-L1 fibroblasts or fully mature 3T3-L1 adipocytes. In a separate experiment we demonstrate that treatment of certain cultured cells (3T3 fibroblasts, 3T3-L1 mature adipocytes) but not all (MG1361), with the non-specific phosphodiesterase inhibitor IBMX significantly downregulates mRNA expression of  $\gamma$ -synuclein, although the precise mechanism involved requires further investigation. In the following chapter we look at an intriguing link between the functions of  $\alpha$ -synuclein in neuronal synapses and  $\gamma$ -synuclein in adipocytes that may help to explain how the latter protein affects lipolysis and the size of mature adipocytes in conditions of nutrient excess.

**Chapter 6 - Effect of  $\gamma$ -synuclein<sup>-/-</sup> on  
SNARE complex formation in white adipocytes**

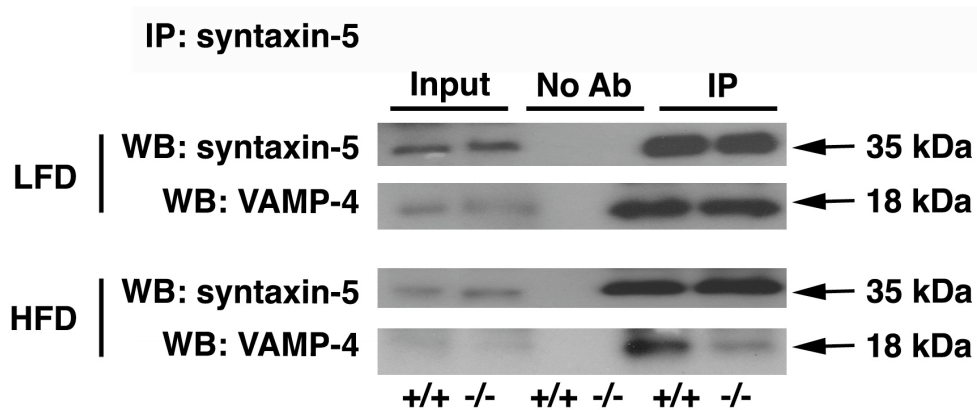
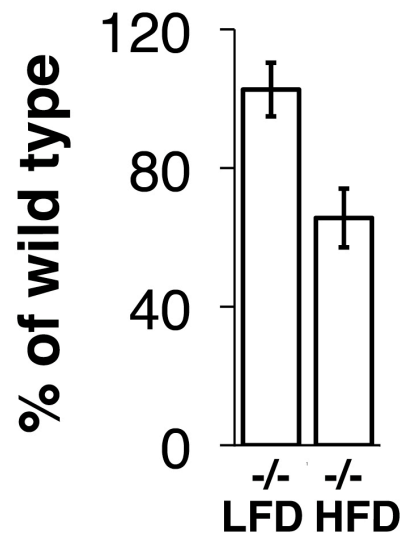
## **6.1. Overview.**

In the previous chapters we have shown that in HFD-fed mice, loss of  $\gamma$ -synuclein leads to reduced WAT accumulation and smaller adipocytes, with increases in WAT lipolysis, whole-body lipid utilisation and energy expenditure. Recently, (Burre et al., 2010) published work concerning the role of another member of the synuclein family  $\alpha$ -synuclein, in the assembly of SNARE complexes in neurons. This chapter discusses a possible role for  $\gamma$ -synuclein involving the assembly of SNARE complexes in adipocytes, and a suggested mechanism for the reduced lipid storage seen in  $\gamma$ -synuclein<sup>-/-</sup> white adipocytes.

## **6.2. Results: $\gamma$ -synuclein promotes assembly of SNARE complexes in WAT**

$\alpha$ - and  $\gamma$ -synuclein are closely related proteins, with potential functional redundancy (Robertson et al., 2004; Senior et al., 2008). In neuronal synapses,  $\alpha$ -synuclein is involved in regulation of synaptic vesicle fusion with the cell membrane by promoting the assembly of SNARE complexes from its subunits, namely vesicular SNARE (vSNARE) protein VAMP-2 and two target membrane-associated SNARE (tSNARE) proteins, syntaxin-1 and SNAP-25 (Burre et al., 2010). In adipocytes, SNARE complexes comprise of different, although structurally and functionally related SNARE proteins. Adipocyte SNARE complexes have been implicated in lipid droplet formation and growth by fusion between neutral TAG packaged within amphipathic lipoproteins and the lipid droplet phospholipid monolayer (Andersson et al., 2006; Bostrom et al., 2007; Bostrom et al., 2005; Olofsson et al., 2009). We hypothesised that in adipocytes,  $\gamma$ -synuclein plays a similar role to that of  $\alpha$ -synuclein in neurons. To determine whether  $\gamma$ -synuclein functions as a regulator for the efficiency of SNARE complex formation in WAT, we quantified the assembled SNARE complexes in WAT lysates by measuring the amount of VAMP-4 (vSNARE) that co-immunoprecipitated with syntaxin-5 (tSNARE). To do this we used epididymal WAT from  $\gamma$ -synuclein<sup>-/-</sup> and wild type mice fed LFD or HFD for 11 weeks. WAT lysates were used for co-immunoprecipitation reactions, and VAMP-4 and syntaxin-5 protein levels pulled down during immunoprecipitation were analysed by semi-quantitative Western blotting. Amounts of co-immunoprecipitated VAMP-4

were normalised per lysate by the amount of immunoprecipitated syntaxin-5. Although we found no differences in the number of assembled SNARE complexes between genotypes for LFD-fed mice, the number of SNARE complexes was reduced by approximately 35% in  $\gamma$ -synuclein<sup>-/-</sup> mice fed HFD compared with HFD-fed wild type mice (Fig. 6.1A, B). To test whether this difference was caused by reduced expression of either VAMP-4, syntaxin-5 or SNAP-23 in WAT of  $\gamma$ -synuclein<sup>-/-</sup> mice we measured levels of these proteins in lysates of epididymal WAT from HFD-fed mice of both genotypes. Levels of these proteins were analysed by semi-quantitative Western blotting using the same VAMP-4 and syntaxin-5 antibodies as in co-immunoprecipitation experiments. This analysis showed that the decreased number of SNARE complexes in  $\gamma$ -synuclein<sup>-/-</sup> mice fed HFD compared with HFD-fed wild type mice was not due to any reduction in protein levels of VAMP-4, syntaxin-5 or SNAP-23 (Fig. 6.2).

**A****B SNARE complexes**

**Fig. 6.1. Quantification of SNARE complexes in WAT.** (A) Representative Western blots showing co-immunoprecipitation of VAMP-4 with syntaxin-5 used to assess SNARE complex abundance in epididymal WAT of wild type (+/+) and  $\gamma$ -synuclein<sup>-/-</sup> (-/-) mice fed a LFD or HFD for 11 weeks. (B) Bar chart shows amount of VAMP-4 in syntaxin-5 immunoprecipitates normalized to the amount of immunoprecipitated syntaxin-5 and expressed as a percentage of wild type samples in each experiment ( $\pm$ SEM, total of 5 independent experiments). No changes were found in  $\gamma$ -synuclein<sup>-/-</sup> mice fed LFD but the difference between values for wild type and  $\gamma$ -synuclein<sup>-/-</sup> mice fed HFD was statistically significant ( $p < 0.05$ , Mann-Whitney U-test).

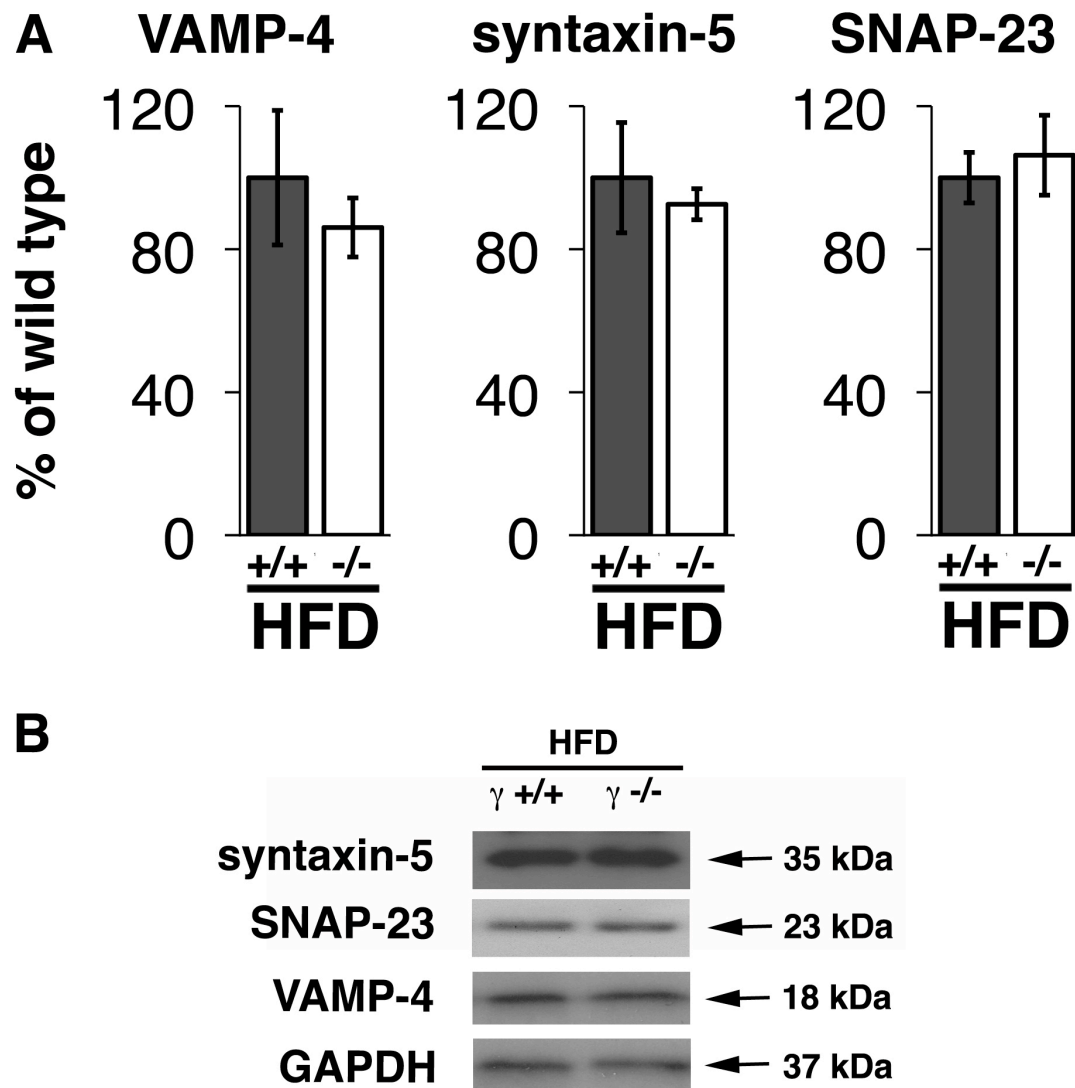


**Fig. 6.2. Analysis of SNARE protein expression in WAT.** Western blot analysis of VAMP-4, syntaxin-5 and SNAP-23 protein expression in epididymal WAT of wild type (+/+) and  $\gamma$ -synuclein<sup>-/-</sup> (-/-) mice fed a HFD for 11 weeks. GAPDH was used as a loading control (n=4). (A) Bar charts show means $\pm$ SEM compared with wild type mice fed HFD. (B) A representative Western blot is shown in the bottom panel.

### 6.3. Summary of results and discussion.

Recently (Burre et al., 2010) published work on  $\alpha$ -synuclein, a closely related protein to  $\gamma$ -synuclein, showing that in neuronal synapses,  $\alpha$ -synuclein enhances neurotransmitter exocytosis by promoting the assembly of SNARE complexes. These complexes play a crucial role in synaptic vesicle docking and fusion pore formation at the plasma membrane, and this group demonstrated how this function of  $\alpha$ -synuclein becomes particularly important during periods of increased synaptic activity. In presynaptic terminals, the vSNARE protein VAMP-2/synaptobrevin and two tSNARE proteins, syntaxin-1 and SNAP-25 are the subunits that make up SNARE complexes in these neurons (summarised in (Rizo and Rosenmund, 2008; Sudhof and Rothman, 2009)). In adipocytes, the functional homologs of these proteins are the vSNARE protein VAMP-4 and tSNARE proteins syntaxin-5 and SNAP-23. These adipocyte SNARE complexes are involved in fusion between neutral TAG packaged within amphipathic lipoproteins and the lipid droplet phospholipid monolayer, a process responsible for adipocyte lipid accumulation and subsequent lipid droplet growth (Andersson et al., 2006; Bostrom et al., 2007; Bostrom et al., 2005; Olofsson et al., 2009).

Work in this chapter has demonstrated that in conditions of increased lipid supply, i.e. in HFD-fed mice, SNARE complex formation in WAT is substantially attenuated in the absence of  $\gamma$ -synuclein. This difference was not due to decreased expression and therefore availability of individual SNARE complex subunits in WAT. Our findings suggest that in HFD-fed mice, the decreased SNARE complex formation seen in  $\gamma$ -synuclein<sup>-/-</sup> adipocytes reduces incorporation of excess TAG (from increased dietary NEFA) into the lipid droplet, which contributes to the decreased adipocyte size (and WAT accumulation) in  $\gamma$ -synuclein<sup>-/-</sup> mice. Overall, this suggests that both  $\alpha$ -synuclein and  $\gamma$ -synuclein have the ability to potentiate SNARE complex-mediated fusion in two different cell types. Both neurons and adipocytes require this process for increased efficiency of cellular mechanisms that depend on this fusion,  $\alpha$ -synuclein-potentiated synaptic transmission in neuronal synapses and similarly  $\gamma$ -synuclein-potentiated lipid droplet formation in adipocytes. In the next chapter we will switch focus from WAT, and look at the effect of  $\gamma$ -synuclein deficiency on lipid classes and fatty acid composition in the brain.

**Chapter 7 – Lipid classes and fatty acid patterns  
in the brains of  $\gamma$ -synuclein<sup>-/-</sup> mice**

## 7.1. Overview

Alterations in brain lipid biochemistry have been previously linked to deficiency of  $\alpha$ -synuclein (Barcelo-Coblijn et al., 2007; Rappley et al., 2009). Since  $\gamma$ -synuclein and  $\alpha$ -synuclein are closely related proteins, whose functions are potentially redundant (Robertson et al., 2004; Senior et al., 2008), it was clearly important to evaluate if  $\gamma$ -synuclein might also play a role in brain lipid homeostasis. In chapters 5 and 6, we focused on  $\gamma$ -synuclein expression in WAT, and the effect of loss of expression on lipid metabolism in this tissue. In this chapter, we look at the effect of  $\gamma$ -synuclein deficiency on the lipid composition and fatty acid patterns of individual lipids from two different brain regions, the cerebral cortex and the midbrain. The midbrain exhibits relatively high levels of  $\gamma$ -synuclein expression, whereas in the cerebral cortex, the expression level of this protein is substantially lower (Abeliovich et al., 2000; Ninkina et al., 2003).

### 7.2.1. Results: Increased oleic acid levels in plasma of $\gamma$ -synuclein<sup>-/-</sup> mice

For analysis of the effect of  $\gamma$ -synuclein deficiency on lipid composition in the brain, we fed 9-week old male  $\gamma$ -synuclein<sup>-/-</sup> and wild type mice low fat diet (LFD) for 11 weeks. Subsequently, tissues of young but mature (20 week old) adult mice with a fully developed nervous system were analysed. We began by looking at the effect, if any, that loss of  $\gamma$ -synuclein had on lipid composition in blood plasma of these mice. To do this, whole blood was taken immediately after sacrificing experimental animals, and plasma collected by centrifugation. Total lipids were extracted from samples of plasma with NEFA separated by TLC and the relative amount of each fatty acid determined by gas chromatography. Palmitic, stearic, oleic, linoleic and arachidonic acids were the major fatty acids in plasma together with a moderate amount of docosahexaenoic acid (DHA) in both wild type and  $\gamma$ -synuclein<sup>-/-</sup> mice. The relative amount of oleic acid was increased significantly in the plasma of  $\gamma$ -synuclein<sup>-/-</sup> compared to wild type mice (Table 7.1).

Fatty acids (% of total fatty acids)	Plasma	
	wild type	$\gamma$ -synuclein <sup>-/-</sup>
<b>C16:0</b>	17.8 ± 4.7	19.8 ± 2.6
<b>C16:1 (n-7)</b>	2.0 ± 0.7	3.1 ± 0.8
<b>C18:0</b>	13.0 ± 2.2	13.0 ± 4.8
<b>C18:1 (n-9)</b>	16.0 ± 1.9	20.5 ± 2.8*
<b>C18:1 (n-7)</b>	2.2 ± 0.2	3.0 ± 0.8
<b>C18:2 (n-6)</b>	17.3 ± 1.8	15.1 ± 1.8
<b>C18:3 (n-3)</b>	0.5 ± 0.2	0.5 ± 0.3
<b>C20:3 (n-6)</b>	1.6 ± 0.8	2.0 ± 0.7
<b>C20:4 (n-6)</b>	20.3 ± 4.5	15.9 ± 4.4
<b>C22:6 (n-3)</b>	7.3 ± 2.4	5.2 ± 1.9

**Table 7.1. Fatty acid composition in the plasma of wild type and  $\gamma$ -synuclein<sup>-/-</sup> mice.** Data as means ± S.D (number of mice = 5, \* p < 0.05) as a % of total fatty acids. Fatty acids are indicated with the number before the colon showing the number of carbon atoms, the figure afterwards denoting the number of double bonds. The position of the first double bond is shown in brackets.

### 7.2.2. Results: Increased proportion of phosphatidylserine in midbrain polar lipids of $\gamma$ -synuclein<sup>-/-</sup> mice

Table 7.2 below shows the fatty acid profile of the total polar lipid fraction from cortex or midbrain in wild type and  $\gamma$ -synuclein<sup>-/-</sup> mice. Total lipids were extracted from dissected cerebral cortex or midbrain samples with polar lipids separated from other lipid species by TLC, and the fatty acid composition of total polar lipids determined by gas chromatography. Palmitic and stearic acids were the dominant fatty acids in cortex followed by DHA, oleic acid and arachidonic acid (ARA). In midbrain, stearic and oleic acids were the major compounds followed by palmitic, DHA and ARA. The percentages of palmitic, ARA and DHA in total polar lipids were significantly higher in the cortex region compared to midbrain in both wild type and  $\gamma$ -synuclein<sup>-/-</sup> mice, whereas proportions of oleic and nervonic (C24:1) acids were higher in this lipid fraction from midbrain. There were no statistically significant differences in the relative proportions of fatty acids from the total polar lipid fraction between wild type and  $\gamma$ -synuclein<sup>-/-</sup> mice in either brain region.

The relative proportions of different polar lipids in the two brain regions are shown below in Fig. 7.1. Extraction of total lipids from either brain region was followed by separation of polar lipids by two-dimensional TLC. Three phospholipids, namely phosphatidylcholine (PtdCho), ethanolamine phospholipids (PtdEtn) and phosphatidylserine (PtdSer), were the major polar lipids in both brain regions (accounting for about 70-80% of the total polar lipids). Phosphatidylinositol (PtdIns), sphingomyelin (CerPCho), diphosphatidylglycerol (Ptd<sub>2</sub>Gro, cardiolipin) as well as sulfatide and cerebroside were present in smaller proportions and were each less than 5% of the total polar lipids. The relative amounts of polar lipids did not vary substantially between midbrain and cortex samples from wild type animals, although the levels of sulfatides and PtdCho showed a statistically significant increase and decrease, respectively, in the midbrain region (Fig. 7.1). In this brain region,  $\gamma$ -synuclein deficiency resulted in a statistically significant (~40%) increase in the relative proportion of PtdSer compared to wild type mice, whereas the proportions of other lipids were not altered significantly (Fig. 7.1). No differences in the polar lipid composition were found in the cortex of wild type compared to  $\gamma$ -synuclein<sup>-/-</sup> mice (Fig. 7.1). Also, no differences in the concentrations of total polar lipids and

triacylglycerol (TAG) were observed for these brain regions as a result of  $\gamma$ -synuclein deficiency (data not shown).

\*                      \*                      \*

Fatty acid (% of total fatty acids)	Cortex		Midbrain	
	wild type	$\gamma$ -synuclein <sup>-/-</sup>	wild type	$\gamma$ -synuclein <sup>-/-</sup>
<b>C16:0</b>	22.2 ± 0.5	22.6 ± 0.8	16.8 ± 0.2 <sup>#</sup>	17.5 ± 0.8
<b>C16:1 (n-7)</b>	1.3 ± 0.2	1.4 ± 0.2	0.1 ± 0.0 <sup>#</sup>	0.2 ± 0.0
<b>C18:0</b>	22.6 ± 0.4	22.8 ± 0.4	21.8 ± 2.3	21.6 ± 2.4
<b>C18:1 (n-9)</b>	15.9 ± 0.2	15.6 ± 0.3	21.7 ± 0.6 <sup>#</sup>	21.1 ± 1.1
<b>C18:1 (n-7)</b>	3.8 ± 0.4	4.0 ± 0.3	4.7 ± 1.3	5.0 ± 0.5
<b>C18:2 (n-6)</b>	0.9 ± 0.1	0.8 ± 0.1	2.8 ± 0.9 <sup>#</sup>	2.8 ± 0.8
<b>C18:3 (n-3)</b>	10.4 ± 0.5	10.5 ± 0.3	7.7 ± 0.9 <sup>#</sup>	7.4 ± 1.2
<b>C20:3 (n-6)</b>	2.4 ± 0.1	2.4 ± 0.1	3.0 ± 0.9	3.7 ± 2.0
<b>C20:4 (n-6)</b>	16.5 ± 2.0	16.0 ± 0.6	12.1 ± 1.7 <sup>#</sup>	11.5 ± 1.0
<b>C22:6 (n-3)</b>	0.8 ± 0.2	0.8 ± 0.2	2.5 ± 0.6 <sup>#</sup>	2.6 ± 0.6

**Table 7.2. Fatty acid composition of the total polar lipid fraction from cortex or midbrain of wild type and  $\gamma$ -synuclein<sup>-/-</sup> mice.** Data as means ± S.D (number of mice = 6-8, # p < 0.05 between midbrain and cortex in wild type animals) as a % of total fatty acids. Fatty acids are indicated with the number before colon showing the number of carbon atoms, the figure afterwards denoting the number of double bonds. The position of the first double bond is shown in brackets.

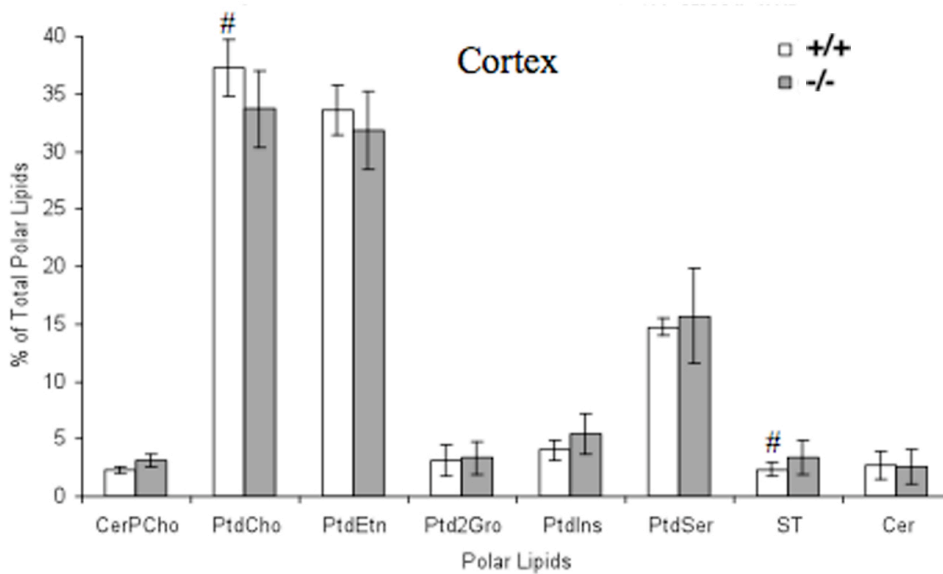
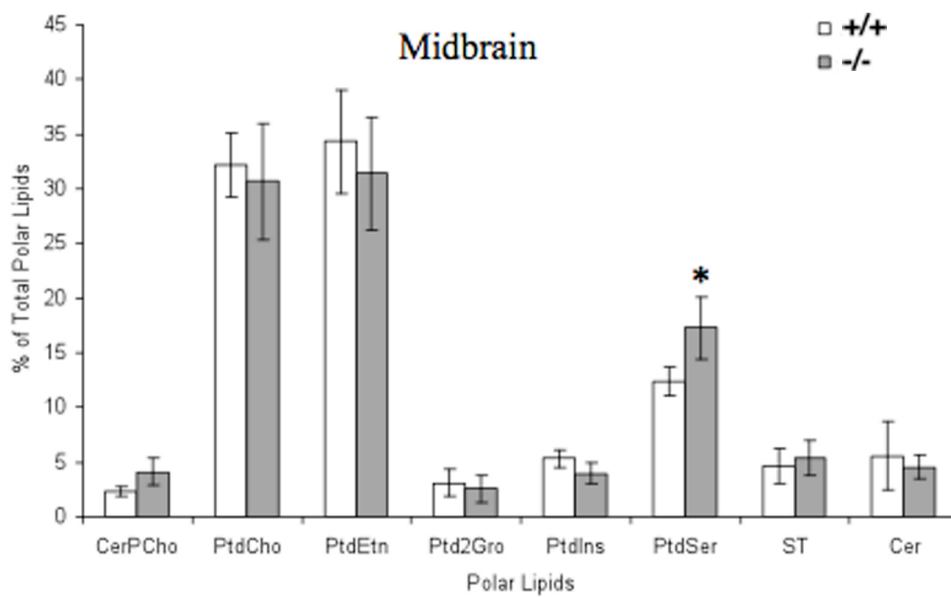


**Fig. 7.1. Midbrain and cortex polar lipid composition (% of total polar lipids) from wild type and  $\gamma$ -synuclein<sup>-/-</sup> mice.** Values represent means  $\pm$  SD (number of mice = 5, \* effect of  $\gamma$ -synuclein deficiency (-/-) when compared with wild type (+/+), # differences between midbrain (top panel) and cortex (bottom panel) in wild type animals,  $p < 0.05$  for both). CerPCho, sphingomyelin; PtdCho, phosphatidylcholine; PtdEtn, phosphatidylethanolamine; Ptd2Gro, cardiolipin; PtdIns, phosphatidylinositol; PtdSer, phosphatidylserine; ST, sulfatide; Cer, cerebroside.

### **7.2.3. Results: Alterations in fatty acid patterns of phosphatidylserine and ethanolamine phospholipids in cortex of $\gamma$ -synuclein<sup>-/-</sup> mice**

The fatty acid composition of PtdSer and PtdEtn, which in brain tissues represent two lipid classes significantly enriched with the n-3 polyunsaturated fatty acid (PUFA) DHA, are shown in Fig. 7.2 and 7.3, respectively. Total lipids were extracted from dissected cerebral cortex or midbrain samples with both PtdSer and PtdEtn separated from other lipid species by two-dimensional TLC and the fatty acid composition of each determined by gas chromatography. For PtdSer, the levels of both C18:0 and DHA were higher in cortex compared to midbrain while oleate was reduced (Fig. 7.2). Moreover, the level of DHA in PtdSer was significantly increased in the cortex of  $\gamma$ -synuclein<sup>-/-</sup> mice compared to wild type animals (30.0% and 25.8% of total fatty acids, respectively) with a concomitant decrease in the proportion of stearate (C18:0) (Fig. 7.2). PtdEtn contained both ARA and DHA as major fatty acids and, similar to PtdSer, the proportion of DHA was enhanced significantly in cortex tissue in  $\gamma$ -synuclein<sup>-/-</sup> mice as compared to control wild type mice (25.4% and 21.4% respectively, Fig. 7.3). The proportions of ARA were unaffected by  $\gamma$ -synuclein deficiency in PtdEtn from both cortex and midbrain tissues (Fig. 7.3). In addition to fatty acids from the diacyl form of PtdEtn, we also analysed the profile of dimethylacetal (DMA) derivatives that represent aliphatic chains from ether derivatives (mainly plasmalogens) of PtdEtn (Fig. 7.3). Four DMA were identified with a domination of C18:0-DMA, but no significant changes in the relative proportion of these compounds in cortex and midbrain were found between wild type and  $\gamma$ -synuclein<sup>-/-</sup> mice.

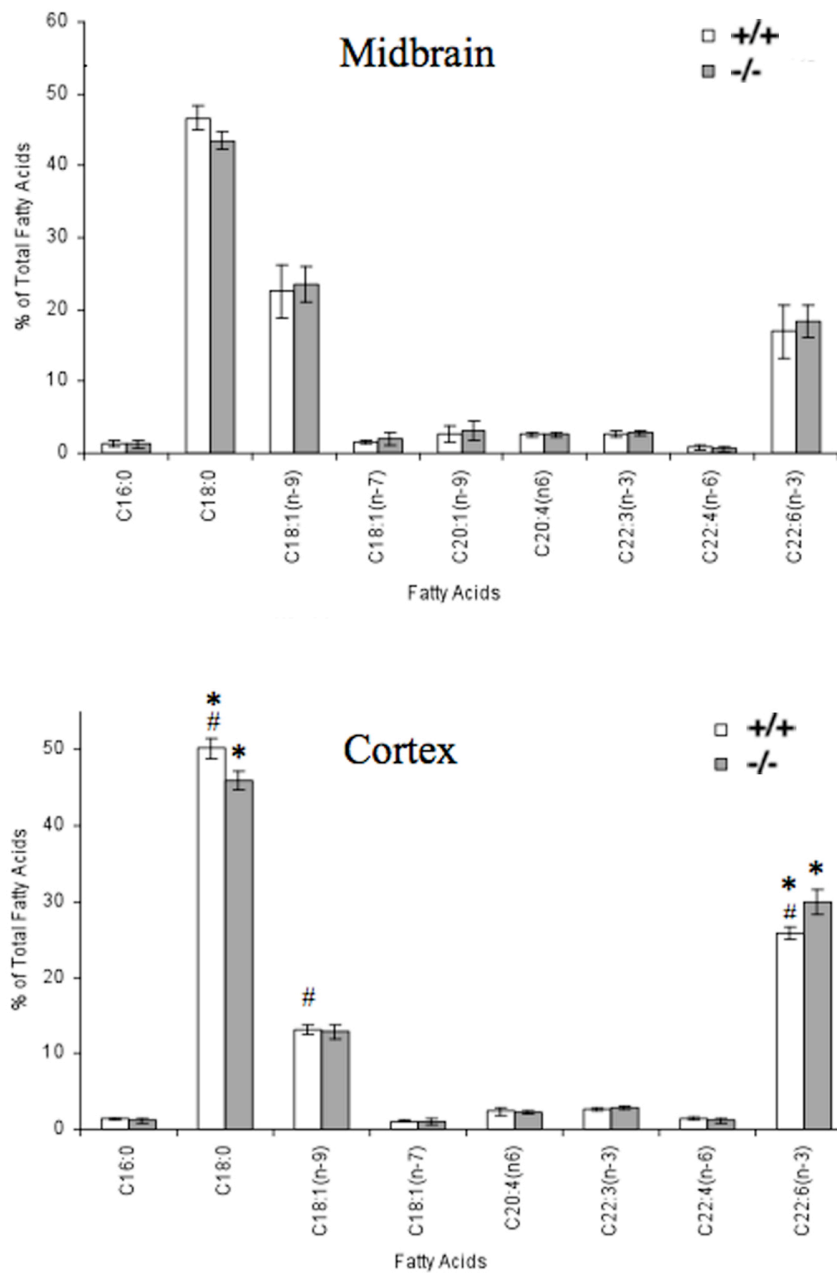


**Fig. 7.2. Fatty acid composition of phosphatidylserine from midbrain or cortex in wild type and  $\gamma$ -synuclein<sup>-/-</sup> mice.** Values represent means  $\pm$  SD (number of mice = 5, \* effect of  $\gamma$ -synuclein<sup>-/-</sup> when compared with wild type, # differences between midbrain (top panel) and cortex (bottom panel) in wild type animals,  $p < 0.05$  for both) as a % of total fatty acids. Fatty acids are indicated with the number before colon showing the number of carbon atoms, the figure afterwards denoting the number of double bonds. The position of the first double bond is shown in brackets. Only the major fatty acids ( $\geq 0.5\%$ ) are listed.

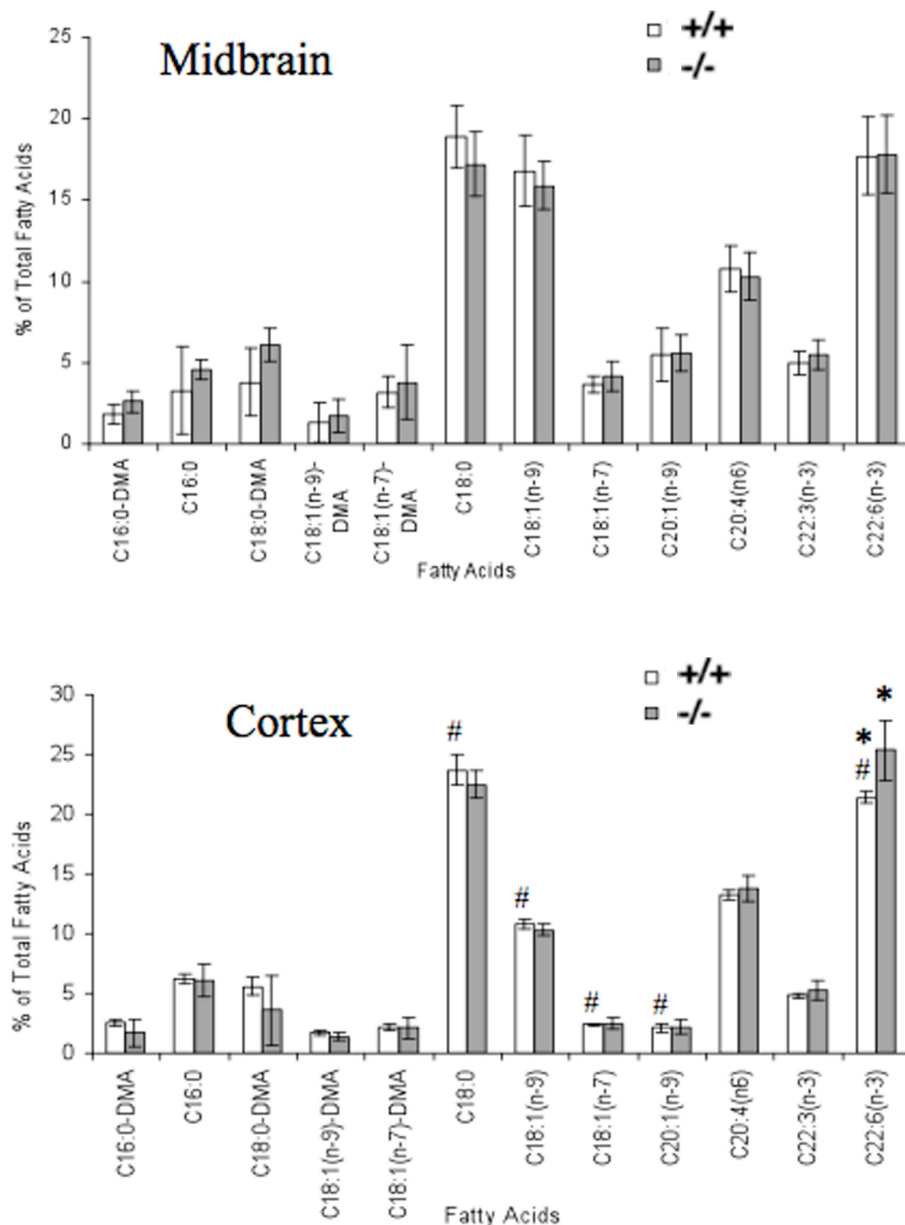


**Fig. 7.3. Fatty acid and dimethylacetal composition of ethanolamine phospholipids from midbrain and cortex of wild type and  $\gamma$ -synuclein<sup>-/-</sup> mice.** Values represent means  $\pm$  SD (number of mice = 5, \* effect of  $\gamma$ -synuclein<sup>-/-</sup> when compared with wild type, # differences between midbrain (top panel) and cortex (bottom panel) in wild type animals,  $p < 0.05$  for both) as a % of total fatty acids. Fatty acids are indicated with the number before colon showing the number of carbon atoms, the figure afterwards denoting the number of double bonds. The position of the first double bond is shown in brackets. Only the major fatty acids ( $\geq 0.5\%$ ) are listed.

#### **7.2.4. Results: Alterations in fatty acid patterns in various other major polar lipids in cortex and midbrain of $\gamma$ -synuclein<sup>-/-</sup> mice**

Table 7.3 below shows data on the fatty acid composition for other major polar lipids in cortex and midbrain from wild type and  $\gamma$ -synuclein<sup>-/-</sup> mice. These data (including Figures 7.2 and 7.3 above) show a fatty acid distribution typical of that for murine brain tissues. Fatty acid composition of these polar lipids were measured in the same way as for PtdSer and PtdEtn in section 7.2.3, with extraction of total lipids from cerebral cortex or midbrain tissue, separation of these individual polar lipids by two-dimensional TLC and the fatty acid composition for each polar lipid determined by gas chromatography. Phosphatidylcholine (PtdCho) in both cortex and midbrain is characterized by a domination of palmitate (approximately 48% and 40% in cortex and midbrain, respectively), stearate (14% and 16%) and oleate (21% and 24%) with much lower levels of the two major brain long-chain PUFAs, ARA and DHA (Table 7.3). In the cortex, the relative concentrations of ARA and DHA in PtdCho were approximately 6% and 3%, respectively. In the midbrain, about 4% of each of ARA and DHA was found in PtdCho. The levels of all above-mentioned fatty acids were significantly different between the two brain regions. In contrast, there were no significant differences in these parameters between wild type and  $\gamma$ -synuclein<sup>-/-</sup> mice.

Phosphatidylinositol (PtdIns) is enriched with two fatty acids, stearic (around 44% in both cortex and midbrain) and ARA (37% and 34% in cortex and midbrain, respectively). DHA is a minor component in PtdIns and its relative concentration was about 2% in cortex and 4% in midbrain, these being significantly different.  $\gamma$ -synuclein<sup>-/-</sup> resulted in an increased level of ARA in PtdIns in cortex tissue but did not affect the fatty acid profiles of this lipid in the midbrain (Table 7.3).

Oleic acid and ARA were the major acids found in brain diphosphatidylglycerol (Ptd<sub>2</sub>Gro, cardiolipin). In this lipid, another C18:1 isomer, *cis*-vaccenic acid, was also present in appreciable amounts especially in the midbrain (around 11% versus 7% in cortex). The relative concentration of ARA was higher in Ptd<sub>2</sub>Gro from the cortex than in Ptd<sub>2</sub>Gro from the midbrain (18% and 13%, respectively). In comparison to other polar lipids isolated from the brain, Ptd<sub>2</sub>Gro contains higher levels of C16 and C18 monoenic acids, namely C16:1n-7 (up to 5%), C18:1n-9 (up to 38%) and C18:1n-7 (up to 15%). The proportion of the latter was significantly higher in the

midbrain than in cortex at the expense of arachidonic acid (Table 7.3). No statistically significant changes were found when comparing Ptd<sub>2</sub>Gro fatty acid profiles in the cortex between wild type and  $\gamma$ -synuclein<sup>-/-</sup> animals, whereas in midbrain the proportion of C18:1n-7 was increased in  $\gamma$ -synuclein<sup>-/-</sup> compared to wild type mice (Table 7.3).

Sphingomyelin (CerPCho) from both cortex and midbrain contained stearic acid as its major fatty acid (up to 81% of total fatty acids in cortex, and up to 65% of that in midbrain). The presence of two very long chain acids, lignoceric (C24:0) and nervonic (C24:1n-6), is also characteristic for this lipid. Their levels were higher in midbrain than cortex. CerPCho fatty acids were unchanged as a response to  $\gamma$ -synuclein<sup>-/-</sup> in the cortex whereas in the midbrain a decreased percentage (~10%) of C18:0 was found.

Fatty acids from both sulfatides and cerebroside did not show any differences between cortex and midbrain.  $\gamma$ -synuclein<sup>-/-</sup> resulted in a decreased proportion of lignoceric acid in sulfatides and cerebroside in the cortex (Table 7.3). In the midbrain region, a reduced relative proportion of behenic acid (C22:0) was found in cerebroside in  $\gamma$ -synuclein<sup>-/-</sup> mice (Table 7.3).

Fatty acids (% of total)	Cortex		Midbrain	
	wild type	$\gamma$ -synuclein <sup>-/-</sup>	wild type	$\gamma$ -synuclein <sup>-/-</sup>
<b>Phosphatidylcholine</b>				
<b>C16:0</b>	48.0 ± 2.7	45.2 ± 1.9	39.2 ± 3.5 <sup>#</sup>	39.2 ± 2.6
<b>C16:1 (n-7)</b>	0.7 ± 0.1	0.8 ± 0.3	0.7 ± 0.2	0.9 ± 0.2
<b>C18:0</b>	3.7 ± 0.7	13.0 ± 0.7	16.5 ± 1.2 <sup>#</sup>	15.1 ± 1.6
<b>C18:1 (n-9)</b>	20.6 ± 0.8	20.9 ± 1.1	24.1 ± 1.6 <sup>#</sup>	23.9 ± 1.1
<b>C18:1 (n-7)</b>	5.1 ± 2.0	6.8 ± 0.9	7.2 ± 0.6	8.1 ± 1.6
<b>C20:1 (n-9)</b>	0.7 ± 0.1	0.7 ± 0.1	1.7 ± 0.5 <sup>#</sup>	1.6 ± 0.3
<b>C20:4 (n-6)</b>	5.7 ± 0.6	6.4 ± 0.5	3.9 ± 0.7 <sup>#</sup>	4.1 ± 0.6
<b>C22:6 (n-3)</b>	3.2 ± 0.5	3.8 ± 0.4	3.7 ± 0.6	4.3 ± 0.6
<b>Phosphatidylinositol</b>				
<b>C16:0</b>	8.2 ± 1.8	6.7 ± 1.9	7.3 ± 1.8	9.4 ± 2.1
<b>C18:0</b>	44.1 ± 3.2	40.7 ± 1.1	44.9 ± 3.2	40.7 ± 2.1
<b>C18:1 (n-9)</b>	5.1 ± 0.8	5.1 ± 0.6	5.5 ± 0.5	8.4 ± 2.4*
<b>C18:1 (n-7)</b>	2.2 ± 0.2	2.5 ± 0.4	2.5 ± 0.4	3.4 ± 0.7
<b>C20:4 (n-6)</b>	36.8 ± 3.5	41.8 ± 2.4*	33.5 ± 3.6	32.4 ± 1.1
<b>C22:6 (n-3)</b>	2.0 ± 0.8	2.2 ± 0.5	4.6 ± 1.7 <sup>#</sup>	4.2 ± 1.3

## Cardiolipin

---

<b>C16:0</b>	6.7 ± 2.2	6.1 ± 2.2	7.8 ± 1.3	8.5 ± 1.9
<b>C16:1 (n-7)</b>	5.3 ± 1.1	5.1 ± 1.1	4.1 ± 2.6	4.8 ± 1.6
<b>C18:0</b>	8.1 ± 3.4	8.2 ± 3.5	10.6 ± 3.3	6.8 ± 2.9
<b>C18:1 (n-9)</b>	38.1 ± 2.2	36.4 ± 2.2	36.8 ± 2.3	33.9 ± 3.2
<b>C18:1 (n-7)</b>	6.9 ± 0.7	5.8 ± 0.9	10.5 ± 2.3 <sup>#</sup>	15.4 ± 3.0*
<b>C18:2 (n-6)</b>	5.7 ± 2.1	4.8 ± 0.4	3.9 ± 0.6	4.2 ± 0.5
<b>C20:3 (n-6)</b>	1.9 ± 0.2	2.3 ± 0.4	1.7 ± 0.2	1.8 ± 0.2
<b>C20:4 (n-6)</b>	17.7 ± 2.3	19.4 ± 2.1	13.1 ± 2.2 <sup>#</sup>	13.4 ± 0.8
<b>C22:6 (n-3)</b>	9.4 ± 2.3	11.5 ± 3.3	10.4 ± 2.9	10.7 ± 1.4

---

## Sphingomyelin

---

<b>C16:0</b>	4.8 ± 2.1	5.2 ± 2.0	5.2 ± 2.3	6.9 ± 4.0
<b>C16:1 (n-7)</b>	0.8 ± 0.2	0.7 ± 0.4	1.2 ± 0.6	1.6 ± 0.6
<b>C18:0</b>	80.6 ± 3.4	77.8 ± 1.7	65.0 ± 8.4 <sup>#</sup>	55.1 ± 5.8*
<b>C18:1 (n-9)</b>	0.5 ± 0.2	1.2 ± 0.5	0.7 ± 0.3	1.7 ± 0.8
<b>C20:0</b>	2.3 ± 0.3	2.3 ± 0.3	2.8 ± 0.4	2.4 ± 0.2
<b>C22:0</b>	2.7 ± 0.5	2.4 ± 0.5	5.0 ± 2.1	4.6 ± 1.6
<b>C24:0</b>	2.1 ± 0.4	1.7 ± 0.4	4.5 ± 2.5	3.9 ± 1.0
<b>C24:1 (n-6)</b>	4.1 ± 2.1	7.3 ± 1.9	11.1 ± 5.7	19.9 ± 9.3

---

## Sulfatide

---

<b>C16:0</b>	6.9 ± 3.1	8.6 ± 1.8	7.9 ± 2.4	8.4 ± 2.4
<b>C16:1 (n-7)</b>	1.7 ± 0.2	1.8 ± 0.5	1.7 ± 1.0	1.6 ± 0.9
<b>C18:0</b>	20.7 ± 2.9	23.6 ± 2.4	19.0 ± 2.8	16.5 ± 3.5
<b>C18:1 (n-9)</b>	11.5 ± 1.7	13.2 ± 3.6	13.3 ± 1.4	14.1 ± 2.8
<b>C18:1 (n-7)</b>	1.4 ± 0.4	1.7 ± 0.4	2.2 ± 0.7	1.5 ± 0.9
<b>C20:0</b>	1.6 ± 0.2	1.5 ± 0.3	1.5 ± 0.4	1.3 ± 0.2
<b>C20:1 (n-9)</b>	1.6 ± 0.5	1.5 ± 0.7	2.2 ± 0.7	1.9 ± 0.6
<b>C20:4 (n-6)</b>	2.1 ± 1.1	2.3 ± 1.3	2.0 ± 0.5	2.2 ± 0.6
<b>C22:0</b>	6.6 ± 1.1	5.8 ± 0.8	6.0 ± 0.8	5.4 ± 0.8
<b>C24:0</b>	14.4 ± 2.0	11.5 ± 2.1*	12.9 ± 2.6	11.7 ± 1.2
<b>C24:1 (n-6)</b>	28.8 ± 4.9	27.7 ± 4.3	29.2 ± 3.7	34.5 ± 5.2

---

## Cerebroside

<b>C16:0</b>	3.1 ± 0.7	5.3 ± 2.7	3.7 ± 1.3	5.0 ± 2.5
<b>C16:1 (n-7)</b>	1.7 ± 0.2	1.7 ± 0.8	1.4 ± 0.7	0.8 ± 0.1
<b>C18:0</b>	11.4 ± 4.2	13.2 ± 4.4	12.1 ± 2.9	9.1 ± 3.0
<b>C18:1 (n-9)</b>	2.8 ± 1.1	4.6 ± 2.8	4.0 ± 0.7	7.0 ± 3.1
<b>C18:1 (n-7)</b>	0.4 ± 0.1	0.4 ± 0.2	0.8 ± 0.5	1.2 ± 0.5
<b>C20:0</b>	2.5 ± 0.1	2.0 ± 0.4	1.8 ± 0.5	1.6 ± 0.7
<b>C20:1 (n-9)</b>	0.4 ± 0.2	0.6 ± 0.3	0.8 ± 0.3	1.4 ± 0.5
<b>C20:4 (n-6)</b>	1.5 ± 0.9	2.3 ± 1.0	1.7 ± 1.0	2.2 ± 0.4
<b>C22:0</b>	12.0 ± 1.6	9.1 ± 1.7	10.2 ± 1.6	7.5 ± 0.8*
<b>C22:1</b>	1.9 ± 0.8	2.5 ± 0.2	2.0 ± 0.2	2.3 ± 0.3
<b>C24:0</b>	22.8 ± 4.0	15.7 ± 3.7*	21.4 ± 4.3	15.2 ± 2.8
<b>C24:1 (n-6)</b>	39.6 ± 6.5	42.4 ± 5.5	40.2 ± 6.3	46.9 ± 4.7

**Table 7.3. Fatty acid composition (% of total fatty acids) in individual polar lipid classes from cortex or midbrain of wild type and  $\gamma$ -synuclein<sup>-/-</sup> mice.** Data as means ± S.D (number of mice = 6-7). The asterisk (\*) indicates a significant effect of  $\gamma$ -synuclein<sup>-/-</sup> when compared with WT (p < 0.05). The hash (#) indicates significant differences between midbrain and cortex in WT animals (p < 0.05). Fatty acids are indicated with the number before colon showing the number of carbon atoms, the figure afterwards denoting the number of double bonds. The position of the first double bond is shown in brackets.

### 7.3. Summary of results and discussion

$\gamma$ -synuclein<sup>-/-</sup> mice were used to determine the effects of  $\gamma$ -synuclein<sup>-/-</sup> on lipid metabolism in the brain focusing on two different brain regions, the cerebral cortex and the midbrain. Using these mice, we found that the level of phosphatidylserine (PtdSer) was increased in the midbrain in response to loss of  $\gamma$ -synuclein whereas no changes in the relative proportions of membrane polar lipids were observed in the cerebral cortex of  $\gamma$ -synuclein<sup>-/-</sup> compared to wild type mice. In addition, higher levels of DHA were found in PtdSer and phosphatidylethanolamine (PtdEtn) from the cerebral cortex of  $\gamma$ -synuclein<sup>-/-</sup> mice. These findings show that  $\gamma$ -synuclein<sup>-/-</sup> leads to alterations in the lipid profile in specific brain tissues and suggest that this protein, like  $\alpha$ -synuclein, might affect neuronal function via modulation of lipid metabolism. We saw no effect of  $\gamma$ -synuclein<sup>-/-</sup> on the total polar lipid content and TAG accumulation in the cerebral cortex and midbrain, which contrasts to studies with  $\alpha$ -synuclein deficient mice where an increase in TAG content of the whole brain has previously been demonstrated (Barcelo-Coblijn et al., 2007).

Neither the mitochondria-specific phospholipid Ptd<sub>2</sub>Gro (found in both brain regions studied, making up 4% of the total polar lipids), nor the fatty acid profile of Ptd<sub>2</sub>Gro was affected by  $\gamma$ -synuclein<sup>-/-</sup>. This is in contrast to the findings reported for  $\alpha$ -synuclein deficient mice in which there was a reduction in total brain Ptd<sub>2</sub>Gro content with a strongly altered acyl chain composition, a mitochondrial lipid abnormality which may explain the electron transport chain impairment reported in the brain of Parkinson's disease patients (Ellis et al., 2005). Our data suggest that deficiency of  $\gamma$ -synuclein is unlikely to affect mitochondrial function in the nervous system by altering lipid composition.

Similar to  $\alpha$ -synuclein deficiency (Barcelo-Coblijn et al., 2007),  $\gamma$ -synuclein<sup>-/-</sup> did not change the level of ethanolamine phospholipids in the brain. The plasmenyl species of PtdEtn are important phospholipid components of most electro-active cellular membranes, such as cardiac sarcolemma and neuronal cell membranes. Between one-half and two thirds of the ethanolamine phospholipids in the whole brain are in plasmalogen form and 11-12% of myelin phospholipids are plasmalogens (Nagan and Zoeller, 2001). A deficiency of ethanolamine plasmalogens has been shown to be associated with aging and some degenerative diseases, especially those associated

with peroxisomal disorders (Dragonas et al., 2009; Farooqui et al., 2000; Farooqui et al., 1997). The absence of ethanolamine plasmalogen alterations is consistent with only mild alterations in normal neural function in both  $\alpha$ -synuclein and  $\gamma$ -synuclein<sup>-/-</sup> mice. However, further comparative studies of aging mice would be important, due to various effects of aging on their nervous systems (Al-Wandi et al., 2010).

Among the polar lipids studied, only the relative proportion of PtdSer was altered in  $\gamma$ -synuclein<sup>-/-</sup> as compared to wild type mice. This change was evident only in the midbrain region where expression of  $\gamma$ -synuclein is much higher than in the cerebral cortex (Ninkina et al., 2003). Although this increase was relatively minor in whole midbrain tissue, the changes in PtdSer content may be more pronounced in specific neuronal populations since  $\gamma$ -synuclein has been shown to be expressed only in a subset of midbrain neurons (Ninkina et al., 2003). Previously, increases in PtdSer have been noted in plasma membrane phospholipids from affected regions of Alzheimer's disease brains, where they may induce formation of amyloid fibers (Farooqui et al., 1997; Zhao et al., 2004). It is also of note that PtdSer has roles in apoptosis, in the regulation of many enzymes and in control of the channel function of the acetylcholine receptor (Farooqui et al., 2000; Mozzi et al., 2003; Sunshine and McNamee, 1992). Thus, alteration in PtdSer may have implications for neuronal cell functions. However, the changes we observed were not sufficient for triggering overt pathological alterations in the nervous system of  $\gamma$ -synuclein<sup>-/-</sup> mice (Ninkina et al., 2003; Robertson et al., 2004; Senior et al., 2008).

Three lipid classes in brain contain high levels of PUFA. Whereas PtdSer and PtdEtn are enriched in DHA, PtdIns contains substantial amounts of ARA. In comparison to the midbrain region, the cortex region was enriched in ARA but has lower levels of DHA (Table 7.2). These differences may be partly explained by higher content of PtdCho (see Fig 7.1), which possesses elevated levels of ARA, in the cerebral cortex (see Table 7.3). Interestingly, statistically significant changes were found in the relative amount of PtdSer in the midbrain region of  $\gamma$ -synuclein<sup>-/-</sup> mice and in the DHA content of both PtdSer and ethanolamine phospholipids in the cerebral cortex. Because only a limited number of cortical neurons normally express  $\gamma$ -synuclein, changes of DHA levels in these cells might be much more profound than those revealed by analysis of total cortex phospholipids. It is noteworthy that although  $\alpha$ -

synuclein null mutant mice have slightly decreased levels of DHA in whole brain PtdEtn and PtdSer, an increased uptake of this fatty acid into brain phospholipids has also been reported (Golovko et al., 2007). It is well known that DHA is essential to perinatal neurological development during which it increases in the CNS. The high demand for DHA in the brain is maintained either by dietary supply or by biosynthesis from  $\alpha$ -linolenate within the liver (Barcelo-Coblijn et al., 2007). Since no very long-chain PUFA were present in the diet, and no changes in the liver (data not shown) or plasma PUFA profiles (Table 7.1) were found in our study, we suggest that the differences in DHA levels likely relate to possible effects of  $\gamma$ -synuclein deficiency on DHA metabolism in the developing brain. Alternatively, complete absence of  $\gamma$ -synuclein might trigger systemic changes, including alterations in adipose and other tissues normally expressing this protein, that activate compensatory mechanisms during brain development. To address this question, a brain-specific, conditional knockout of  $\gamma$ -synuclein may be required.

There is a growing body of evidence regarding the importance of PUFA in brain function. Its deficiency is associated with cognitive decline during aging and with neurodegenerative diseases (Lukiw and Bazan, 2008). The beneficial neurophysiological role of DHA most probably relates to metabolites such as eicosanoids and other autacoids which are important as modulators of membrane microdomain composition, receptor signalling and gene expression (Kim, 2007). A recent study demonstrated a role for neuroprotectin D1 (NPD1) in the homeostatic regulation of brain cell survival and repair involving neurotrophic, anti-apoptotic and anti-inflammatory signalling in Alzheimer's disease (Lukiw and Bazan, 2008). Unfortunately, there is no information about the possible involvement of such DHA metabolites in Parkinson's disease, to which the synuclein family has been linked.  $\gamma$ -synuclein<sup>-/-</sup> mice, which exhibit higher levels of DHA accumulation in certain brain regions, may provide a useful model for future research in this area.

## **Chapter 8 - Final Discussion**

## 8. Final Discussion

### 8.1. A possible role for $\gamma$ -synuclein in white adipose tissue

In this study we made use of mice with a targeted deletion of the  $\gamma$ -synuclein gene in order to determine the molecular and cellular consequences of  $\gamma$ -synuclein<sup>-/-</sup> on lipid metabolism in adipose and brain tissues. Outside of the nervous system,  $\gamma$ -synuclein expression is restricted to very few cell types but is particularly high in white adipose tissue, suggesting that it plays an important role in the adipocyte. Our major finding in this study was that  $\gamma$ -synuclein is a novel regulator of adipocyte function *in vivo* that influences whole-body energy balance. Knockout of  $\gamma$ -synuclein, which is highly expressed in WAT, led to decreased weight gain in mice fed a high fat diet, and this was associated with increased energy expenditure and lipid oxidation. In addition, we observed increased basal and isoproterenol-stimulated lipolysis in isolated adipocytes from these mice, increased NEFA levels in adipose tissue and decreased adipocyte size *in vivo*. Together these data suggests that  $\gamma$ -synuclein loss may increase lipolysis in adipocytes and that this may lead to increased lipid oxidation in adipose, and potentially other tissues. In support of this hypothesis, we observed increased levels of ATGL, the key triglyceride lipase in WAT. It has previously been demonstrated that overexpression of ATGL specifically in adipose tissue, like  $\gamma$ -synuclein loss, leads to obesity resistance with increased energy expenditure and lipid oxidation, decreased adipocyte size and reduced hepatic steatosis following high fat diet feeding without affecting food intake (Ahmadian et al., 2009). The significant overlap between the phenotypes of adipose specific ATGL transgenic and  $\gamma$ -synuclein<sup>-/-</sup> mice suggests that increased ATGL expression has the potential to contribute to the decreased adiposity and improved metabolic health of mice lacking  $\gamma$ -synuclein. We did not observe altered levels of perilipin A, HSL nor changes in HSL phosphorylation in these mice suggesting a selective effect on ATGL rather than a general increase in components of the lipolytic pathway. It is notable that ATGL mRNA expression was not altered in WAT of null mutant mice suggesting that  $\gamma$ -synuclein loss may affect ATGL accumulation. The exact mechanism of this effect is a key question for future studies. However, it is clear that the increased lipolysis

observed in  $\gamma$ -synuclein<sup>-/-</sup> adipocytes could alone drive the obesity resistance and improved metabolic phenotype in these mice.

Since  $\gamma$ -synuclein expression is not exclusive to adipose tissue, it is possible that loss of  $\gamma$ -synuclein expression in other tissues contributes to some aspects of the phenotypes we observed. However, we have shown that specifically re-expressing  $\gamma$ -synuclein in the fat pads of null mutant mice reverses the observed decrease in adipocyte size. Critically, this reversal was only seen in those adipocytes re-expressing  $\gamma$ -synuclein and not in non-transduced cells in the same depot, indicating that this aspect of the *in vivo* phenotype is cell-autonomous. Despite this, we cannot exclude a role for either an effect of  $\gamma$ -synuclein<sup>-/-</sup> in the brain, or compensatory responses in non-adipose tissues to global  $\gamma$ -synuclein<sup>-/-</sup>, that could contribute to other aspects of the phenotype such as the increased energy expenditure or decreased hepatic steatosis. Thus far we have not observed any significant changes in the expression of genes, such as those regulating  $\beta$ -oxidation and lipid metabolism in the liver to suggest this. In addition, other studies, such as those targeting ATGL or perilipin A, imply that altering lipolysis selectively in adipose tissue is capable of profoundly influencing lipid accumulation and metabolism in other tissues and organs (Ahmadian et al., 2009; Martinez-Botas et al., 2000; Miyoshi et al., 2010).

An intriguing link between function of  $\alpha$ -synuclein in neuronal synapses and  $\gamma$ -synuclein in adipocytes might also explain how  $\gamma$ -synuclein affects lipolysis and the size of mature adipocytes in conditions of nutrient excess. In the presynaptic terminals  $\alpha$ -synuclein enhances neurotransmitter exocytosis by promoting the assembly of SNARE complexes that play a pivotal role in the synaptic vesicle docking and fusion pore formation at the plasma membrane, and this function becomes particularly important during periods of increased synaptic activity (Burre et al., 2010). Synaptic SNARE complexes comprise of a vSNARE protein VAMP-2/synaptobrevin and two tSNARE proteins, syntaxin-1 and SNAP-25 (summarised in (Rizo and Rosenmund, 2008; Sudhof and Rothman, 2009)). Their functional homologs, vSNARE protein VAMP-4 and tSNARE proteins syntaxin-5 and SNAP-23, form SNARE complexes in adipocytes. These complexes are involved in fusion between neutral TAG packaged within amphipathic lipoproteins and the lipid droplet phospholipid monolayer, the process underlying lipid accumulation in the adipocyte and consequent increase in its

size (Andersson et al., 2006; Bostrom et al., 2007; Bostrom et al., 2005; Olofsson et al., 2009). More broadly, recent screens of genes affecting lipid droplet formation, fusion and morphology in insect cells and yeast have revealed roles in these processes for several proteins involved in vesicle trafficking (Szymanski et al., 2007; Guo et al., 2008). We have demonstrated that in conditions of increased lipid supply, i.e. in HFD-fed mice, the lack of  $\gamma$ -synuclein substantially attenuates assembly of SNARE complexes in adipocytes. It is therefore possible that the decreased SNARE complex formation seen in  $\gamma$ -synuclein<sup>-/-</sup> adipocytes reduces TAG incorporation into the lipid droplet contributing to the decreased adipocyte size. Indeed, one possibility is that the increased lipolysis and WAT NEFA levels we observe may partly reflect the increased availability of TAG, which has not been appropriately incorporated into the core of the lipid droplet. This TAG is subsequently hydrolysed, with this process requiring compensatory increases in ATGL protein levels (summarised in Fig. 8.1). This could be particularly apparent in situations of increased turnover, for example when WAT is exposed to increased dietary lipids. Overall our data suggest that both  $\alpha$ -synuclein and  $\gamma$ -synuclein share the ability to potentiate SNARE-mediated fusion in physiological and/or environmental conditions requiring increased efficiency of cellular mechanisms that depend on this fusion, the former important for synaptic transmission in neuronal synapses and the latter important for lipid droplet maintenance and expansion in adipocytes.

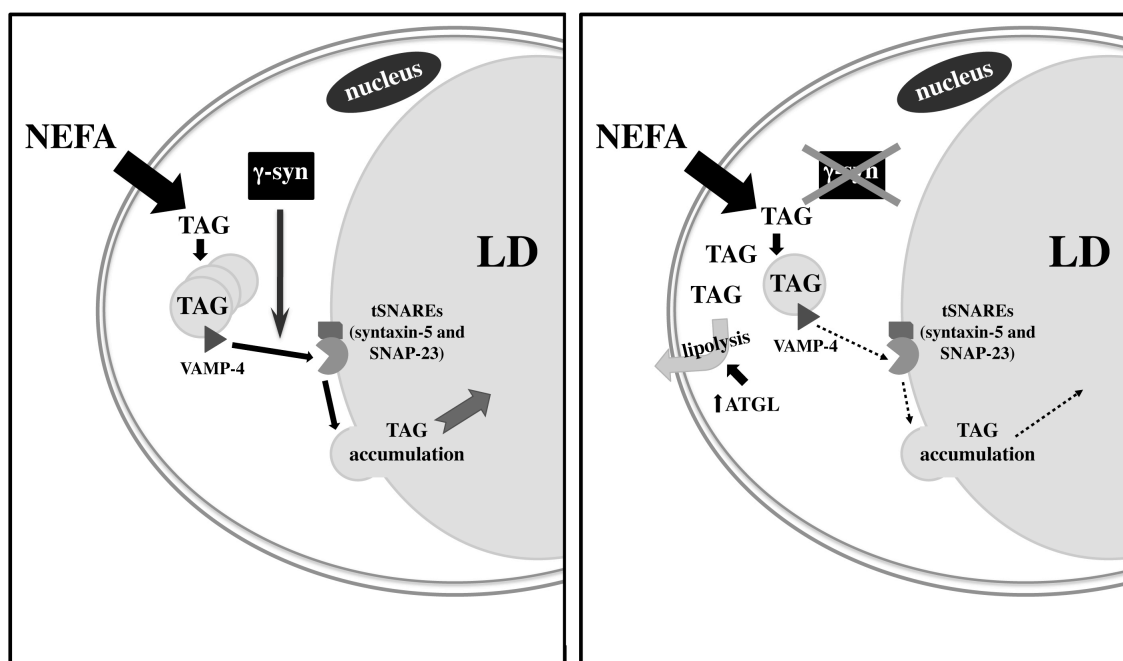


**Fig. 8.1. A proposed model for the role of  $\gamma$ -synuclein in white adipocytes in times of energy surplus.** When the NEFA supply to WAT is low (e.g. balanced or low fat diet) and the amount of newly synthesized TAG is limited, a basal level of SNARE complex assembly matches the demand for lipid droplet fusion. Therefore  $\gamma$ -synuclein has little effect on adipocyte physiology. In contrast, when adipocytes synthesize large quantities of TAG due to the increased supply of NEFA (e.g. in HFD-fed mice) the ability of  $\gamma$ -synuclein to potentiate SNARE-mediated fusion of lipid droplets becomes critical for the efficient accumulation of these TAG (left panel). In  $\gamma$ -synuclein<sup>-/-</sup> adipocytes (right panel) the un-potentiated rate of SNARE complex assembly holds up lipid droplet fusion creating a bottleneck. This leads to decreased availability of droplet coat components (e.g. PAT proteins perilipin, ADRP, TIP47) for sequestering large amounts of newly synthesizing TAGs, which as known from experiments with cells and animals deficient for these proteins, stimulates TAG hydrolysis that require compensatory increase of ATGL level.

In this study we also examined the ability of MEFs derived from  $\gamma$ -synuclein<sup>-/-</sup> mice to differentiate into adipocytes in culture. Our data suggested that  $\gamma$ -synuclein was not essential for adipocyte differentiation in this system as wild type and mutant MEFs differentiated into adipocytes with the same efficiency and kinetics as wild type MEFs. We interpret this to mean that the decreased adipose mass of  $\gamma$ -synuclein<sup>-/-</sup> mice was not due to a reduced capacity of adipose depots to expand when required. This is an important observation as human syndromes of lipodystrophy and mouse models of restricted adipose expandability demonstrate that merely constraining adipose mass leads to dyslipidaemia, insulin resistance and metabolic disease (Schweiger et al., 2009; Moitra et al., 1998). As the loss of  $\gamma$ -synuclein appears to selectively affect mature adipocytes without inhibiting their formation, it may prove a useful therapeutic target for improving obesity related metabolic disease.

$\gamma$ -synuclein appears to play an important role in adipocyte lipid metabolism, particularly in conditions of nutrient excess. Our study suggests that increased  $\gamma$ -synuclein expression could contribute to the development of obesity-related metabolic disease but also that inhibiting  $\gamma$ -synuclein expression or function may represent a novel potential therapeutic avenue for the treatment of this prevalent condition.

## **8.2. A possible role for $\gamma$ -synuclein in brain lipid homeostasis**

As well as the effects of  $\gamma$ -synuclein<sup>-/-</sup> on lipid metabolism in WAT, we have also identified changes in lipid handling in the CNS of mice lacking  $\gamma$ -synuclein. We found that the level of phosphatidylserine was increased in the midbrain region but not in the cerebral cortex of  $\gamma$ -synuclein<sup>-/-</sup> mice compared to wild type. In addition to this, higher levels of docosahexaenoic acid were found in phosphatidylserine and phosphatidylethanolamine from the cerebral cortex of  $\gamma$ -synuclein<sup>-/-</sup> mice. These alterations in lipid handling resulting from deficiency of  $\gamma$ -synuclein did not appear to cause overt pathological changes in the nervous system of  $\gamma$ -synuclein<sup>-/-</sup> mice (Ninkina et al., 2003; Robertson et al., 2004; Senior et al., 2008). However, it may be that under certain conditions, the modified lipid metabolism induced by  $\gamma$ -synuclein<sup>-/-</sup> will alter neuronal function.

### **8.3. Final comments**

$\gamma$ -synuclein is expressed at a high level in certain populations of neurons as well as white adipocytes, and we have shown that in both these cell types,  $\gamma$ -synuclein has the ability to modulate lipid handling. The closely related protein,  $\alpha$ -synuclein, has been heavily implicated in both lipid biochemistry and human neurodegeneration disease, a group of disorders where dysfunction of lipid homeostasis is known to play a role. There is currently no well-defined pathological role for  $\gamma$ -synuclein in human neurodegenerative conditions. We have shown that loss of  $\gamma$ -synuclein function in white adipocytes causes alterations in lipid handling, ultimately leading to changes in whole-body metabolic outcome, and so it is possible that  $\gamma$ -synuclein plays a role in the development of human obesity and related disorders. Indeed it is also feasible that the modulation of lipid metabolism in the brain by  $\gamma$ -synuclein might affect neuronal function in certain human neurodegenerative diseases.

## Bibliography

Abel, E.D., Peroni, O., Kim, J.K., Kim, Y.B., Boss, O., Hadro, E., Minnemann, T., Shulman, G.I., and Kahn, B.B. (2001). Adipose-selective targeting of the GLUT4 gene impairs insulin action in muscle and liver. *Nature* 409, 729-733.

Abeliovich, A., Schmitz, Y., Farinas, I., Choi-Lundberg, D., Ho, W.H., Castillo, P.E., Shinsky, N., Verdugo, J.M., Armanini, M., Ryan, A., Hynes, M., Phillips, H., Sulzer, D., and Rosenthal, A. (2000). Mice lacking alpha-synuclein display functional deficits in the nigrostriatal dopamine system. *Neuron* 25, 239-252.

Abumrad, N., Harmon, C., and Ibrahimi, A. (1998). Membrane transport of long-chain fatty acids: evidence for a facilitated process. *J Lipid Res* 39, 2309-2318.

Abumrad, N.A., el-Maghrabi, M.R., Amri, E.Z., Lopez, E., and Grimaldi, P.A. (1993). Cloning of a rat adipocyte membrane protein implicated in binding or transport of long-chain fatty acids that is induced during preadipocyte differentiation. Homology with human CD36. *J Biol Chem* 268, 17665-17668.

Adams, M., Montague, C.T., Prins, J.B., Holder, J.C., Smith, S.A., Sanders, L., Digby, J.E., Sewter, C.P., Lazar, M.A., Chatterjee, V.K., and O'Rahilly, S. (1997). Activators of peroxisome proliferator-activated receptor gamma have depot-specific effects on human preadipocyte differentiation. *J Clin Invest* 100, 3149-3153.

Ahmadian, M., Duncan, R.E., Varady, K.A., Frasson, D., Hellerstein, M.K., Birkenfeld, A.L., Samuel, V.T., Shulman, G.I., Wang, Y., Kang, C., and Sul, H.S. (2009). Adipose overexpression of desnutrin promotes fatty acid use and attenuates diet-induced obesity. *Diabetes* 58, 855-866.

Ahn, B.H., Rhim, H., Kim, S.Y., Sung, Y.M., Lee, M.Y., Choi, J.Y., Wolozin, B., Chang, J.S., Lee, Y.H., Kwon, T.K., Chung, K.C., Yoon, S.H., Hahn, S.J., Kim, M.S., Jo, Y.H., and Min, D.S. (2002). alpha-Synuclein interacts with phospholipase D isozymes and inhibits pervanadate-induced phospholipase D activation in human embryonic kidney-293 cells. *J Biol Chem* 277, 12334-12342.

Ahn, M., Kim, S., Kang, M., Ryu, Y., and Kim, T.D. (2006). Chaperone-like activities of alpha-synuclein: alpha-synuclein assists enzyme activities of esterases. *Biochem Biophys Res Commun* 346, 1142-1149.

Al-Wandi, A., Ninkina, N., Millership, S., Williamson, S.J., Jones, P.A., and Buchman, V.L. (2010). Absence of alpha-synuclein affects dopamine metabolism and synaptic markers in the striatum of aging mice. *Neurobiol Aging* 31, 796-804.

Amri, E.Z., Ailhaud, G., and Grimaldi, P.A. (1994). Fatty acids as signal transducing molecules: involvement in the differentiation of preadipose to adipose cells. *J Lipid Res* 35, 930-937.

Andersson, L., Bostrom, P., Ericson, J., Rutberg, M., Magnusson, B., Marchesan, D., Ruiz, M., Asp, L., Huang, P., Frohman, M.A., Boren, J., and Olofsson, S.O. (2006). PLD1 and ERK2 regulate cytosolic lipid droplet formation. *J Cell Sci* 119, 2246-2257.

Anthonsen, M.W., Ronnstrand, L., Wernstedt, C., Degerman, E., and Holm, C. (1998). Identification of novel phosphorylation sites in hormone-sensitive lipase that are phosphorylated in response to isoproterenol and govern activation properties in vitro. *J Biol Chem* 273, 215-221.

Arner, P., Hellstrom, L., Wahrenberg, H., and Bronnegard, M. (1990). Beta-adrenoceptor expression in human fat cells from different regions. *J Clin Invest* 86, 1595-1600.

Ashwell, M., Priest, P., Bondoux, M., Sowter, C., and McPherson, C.K. (1976). Human fat cell sizing--a quick, simple method. *J Lipid Res* 17, 190-192.

Assayag, K., Yakunin, E., Loeb, V., Selkoe, D.J., and Sharon, R. (2007). Polyunsaturated fatty acids induce alpha-synuclein-related pathogenic changes in neuronal cells. *Am J Pathol* 171, 2000-2011.

Avram, M.M., Avram, A.S., and James, W.D. (2007). Subcutaneous fat in normal and diseased states 3. Adipogenesis: from stem cell to fat cell. *J Am Acad Dermatol* 56, 472-492.

Baar, R.A., Dingfelder, C.S., Smith, L.A., Bernlohr, D.A., Wu, C., Lange, A.J., and Parks, E.J. (2005). Investigation of in vivo fatty acid metabolism in AFABP/aP2(-/-) mice. *Am J Physiol Endocrinol Metab* 288, E187-193.

Barcelo-Coblijn, G., Golovko, M.Y., Weinhofer, I., Berger, J., and Murphy, E.J. (2007). Brain neutral lipids mass is increased in alpha-synuclein gene-ablated mice. *J Neurochem* 101, 132-141.

Bastard, J.P., Jardel, C., Bruckert, E., Blondy, P., Capeau, J., Laville, M., Vidal, H., and Hainque, B. (2000). Elevated levels of interleukin 6 are reduced in serum and

subcutaneous adipose tissue of obese women after weight loss. *J Clin Endocrinol Metab* 85, 3338-3342.

Bezaire, V., Mairal, A., Anesia, R., Lefort, C., and Langin, D. (2009). Chronic TNF $\alpha$  and cAMP pre-treatment of human adipocytes alter HSL, ATGL and perilipin to regulate basal and stimulated lipolysis. *FEBS Lett* 583, 3045-3049.

Bickel, P.E., Tansey, J.T., and Welte, M.A. (2009). PAT proteins, an ancient family of lipid droplet proteins that regulate cellular lipid stores. *Biochim Biophys Acta* 1791, 419-440.

Biere, A.L., Wood, S.J., Wypych, J., Steavenson, S., Jiang, Y., Anafi, D., Jacobsen, F.W., Jarosinski, M.A., Wu, G.M., Louis, J.C., Martin, F., Narhi, L.O., and Citron, M. (2000). Parkinson's disease-associated alpha-synuclein is more fibrillogenic than beta- and gamma-synuclein and cannot cross-seed its homologs. *J Biol Chem* 275, 34574-34579.

Bjorntorp, P., and Furman, R.H. (1962). Lipolytic activity in rat epididymal fat pads. *Am J Physiol* 203, 316-322.

Bjorntorp, P., Karlsson, M., and Pettersson, P. (1982). Expansion of adipose tissue storage capacity at different ages in rats. *Metabolism* 31, 366-373.

Blaak, E.E., Van Baak, M.A., Kemerink, G.J., Pakbiers, M.T., Heidendal, G.A., and Saris, W.H. (1994). Beta-adrenergic stimulation of energy expenditure and forearm skeletal muscle metabolism in lean and obese men. *Am J Physiol* 267, E306-315.

Bolinder, J., Kager, L., Ostman, J., and Arner, P. (1983). Differences at the receptor and postreceptor levels between human omental and subcutaneous adipose tissue in the action of insulin on lipolysis. *Diabetes* 32, 117-123.

Bostrom, P., Andersson, L., Rutberg, M., Perman, J., Lidberg, U., Johansson, B.R., Fernandez-Rodriguez, J., Ericson, J., Nilsson, T., Boren, J., and Olofsson, S.O. (2007). SNARE proteins mediate fusion between cytosolic lipid droplets and are implicated in insulin sensitivity. *Nat Cell Biol* 9, 1286-1293.

Bostrom, P., Rutberg, M., Ericsson, J., Holmdahl, P., Andersson, L., Frohman, M.A., Boren, J., and Olofsson, S.O. (2005). Cytosolic lipid droplets increase in size by microtubule-dependent complex formation. *Arterioscler Thromb Vasc Biol* 25, 1945-1951.

- Bougnères, P., Stunff, C.L., Pecqueur, C., Pinglier, E., Adnot, P., and Ricquier, D. (1997). In vivo resistance of lipolysis to epinephrine. A new feature of childhood onset obesity. *J Clin Invest* 99, 2568-2573.
- Bradford, M.M. (1976). A rapid and sensitive method for the quantitation of microgram quantities of protein utilizing the principle of protein-dye binding. *Anal Biochem* 72, 248-254.
- Bradley, R.L., Mansfield, J.P., and Maratos-Flier, E. (2005). Neuropeptides, including neuropeptide Y and melanocortins, mediate lipolysis in murine adipocytes. *Obes Res* 13, 653-661.
- Brasaemle, D.L., Levin, D.M., Adler-Wailes, D.C., and Londos, C. (2000a). The lipolytic stimulation of 3T3-L1 adipocytes promotes the translocation of hormone-sensitive lipase to the surfaces of lipid storage droplets. *Biochim Biophys Acta* 1483, 251-262.
- Brasaemle, D.L., Rubin, B., Harten, I.A., Gruia-Gray, J., Kimmel, A.R., and Londos, C. (2000b). Perilipin A increases triacylglycerol storage by decreasing the rate of triacylglycerol hydrolysis. *J Biol Chem* 275, 38486-38493.
- Broersen, K., van den Brink, D., Fraser, G., Goedert, M., and Davletov, B. (2006). Alpha-synuclein adopts an alpha-helical conformation in the presence of polyunsaturated fatty acids to hinder micelle formation. *Biochemistry* 45, 15610-15616.
- Bruening, W., Giasson, B.I., Klein-Szanto, A.J., Lee, V.M., Trojanowski, J.Q., and Godwin, A.K. (2000). Synucleins are expressed in the majority of breast and ovarian carcinomas and in preneoplastic lesions of the ovary. *Cancer* 88, 2154-2163.
- Bryant, N.J., Govers, R., and James, D.E. (2002). Regulated transport of the glucose transporter GLUT4. *Nat Rev Mol Cell Biol* 3, 267-277.
- Buchman, V.L., Adu, J., Pinon, L.G., Ninkina, N.N., and Davies, A.M. (1998a). Persyn, a member of the synuclein family, influences neurofilament network integrity. *Nat Neurosci* 1, 101-103.
- Buchman, V.L., Hunter, H.J., Pinon, L.G., Thompson, J., Privalova, E.M., Ninkina, N.N., and Davies, A.M. (1998b). Persyn, a member of the synuclein family, has a distinct pattern of expression in the developing nervous system. *J Neurosci* 18, 9335-9341.

Buckingham, B.P., Inman, D.M., Lambert, W., Oglesby, E., Calkins, D.J., Steele, M.R., Vetter, M.L., Marsh-Armstrong, N., and Horner, P.J. (2008). Progressive ganglion cell degeneration precedes neuronal loss in a mouse model of glaucoma. *J Neurosci* 28, 2735-2744.

Burre, J., Sharma, M., Tsetsenis, T., Buchman, V., Etherton, M.R., and Sudhof, T.C. (2010). Alpha-synuclein promotes SNARE-complex assembly in vivo and in vitro. *Science* 329, 1663-1667.

Cabin, D.E., Shimazu, K., Murphy, D., Cole, N.B., Gottschalk, W., McIlwain, K.L., Orrison, B., Chen, A., Ellis, C.E., Paylor, R., Lu, B., and Nussbaum, R.L. (2002). Synaptic vesicle depletion correlates with attenuated synaptic responses to prolonged repetitive stimulation in mice lacking alpha-synuclein. *J Neurosci* 22, 8797-8807.

Cao, D., Maitra, A., Saavedra, J.A., Klimstra, D.S., Adsay, N.V., and Hruban, R.H. (2005). Expression of novel markers of pancreatic ductal adenocarcinoma in pancreatic nonductal neoplasms: additional evidence of different genetic pathways. *Mod Pathol* 18, 752-761.

Carlson, L.A. (1963). Studies on the effect of nicotinic acid on catecholamine stimulated lipolysis in adipose tissue in vitro. *Acta Med Scand* 173, 719-722.

Chandra, S., Fornai, F., Kwon, H.B., Yazdani, U., Atasoy, D., Liu, X., Hammer, R.E., Battaglia, G., German, D.C., Castillo, P.E., and Sudhof, T.C. (2004). Double-knockout mice for alpha- and beta-synucleins: effect on synaptic functions. *Proc Natl Acad Sci U S A* 101, 14966-14971.

Chartier-Harlin, M.C., Kachergus, J., Roumier, C., Mouroux, V., Douay, X., Lincoln, S., Levecque, C., Larvor, L., Andrieux, J., Hulihan, M., Waucquier, N., Defebvre, L., Amouyel, P., Farrer, M., and Destee, A. (2004). Alpha-synuclein locus duplication as a cause of familial Parkinson's disease. *Lancet* 364, 1167-1169.

Clifford, G.M., Londos, C., Kraemer, F.B., Vernon, R.G., and Yeaman, S.J. (2000). Translocation of hormone-sensitive lipase and perilipin upon lipolytic stimulation of rat adipocytes. *J Biol Chem* 275, 5011-5015.

Coe, N.R., Simpson, M.A., and Bernlohr, D.A. (1999). Targeted disruption of the adipocyte lipid-binding protein (aP2 protein) gene impairs fat cell lipolysis and increases cellular fatty acid levels. *J Lipid Res* 40, 967-972.

Cole, N.B., Murphy, D.D., Grider, T., Rueter, S., Brasaemle, D., and Nussbaum, R.L. (2002). Lipid droplet binding and oligomerization properties of the Parkinson's disease protein alpha-synuclein. *J Biol Chem* 277, 6344-6352.

Cone, R.D. (2005). Anatomy and regulation of the central melanocortin system. *Nat Neurosci* 8, 571-578.

Connacher, A.A., Bennet, W.M., Jung, R.T., Bier, D.M., Smith, C.C., Scrimgeour, C.M., and Rennie, M.J. (1991). Effect of adrenaline infusion on fatty acid and glucose turnover in lean and obese human subjects in the post-absorptive and fed states. *Clin Sci (Lond)* 81, 635-644.

Considine, R.V., Sinha, M.K., Heiman, M.L., Kriauciunas, A., Stephens, T.W., Nyce, M.R., Ohannesian, J.P., Marco, C.C., McKee, L.J., Bauer, T.L., and et al. (1996). Serum immunoreactive-leptin concentrations in normal-weight and obese humans. *N Engl J Med* 334, 292-295.

Contreras, J.A., Danielsson, B., Johansson, C., Osterlund, T., Langin, D., and Holm, C. (1998). Human hormone-sensitive lipase: expression and large-scale purification from a baculovirus/insect cell system. *Protein Expr Purif* 12, 93-99.

Conway, K.A., Harper, J.D., and Lansbury, P.T. (1998). Accelerated in vitro fibril formation by a mutant alpha-synuclein linked to early-onset Parkinson disease. *Nat Med* 4, 1318-1320.

Cookson, M.R., and van der Brug, M. (2008). Cell systems and the toxic mechanism(s) of alpha-synuclein. *Exp Neurol* 209, 5-11.

Dauer, W., Kholodilov, N., Vila, M., Trillat, A.C., Goodchild, R., Larsen, K.E., Staal, R., Tieu, K., Schmitz, Y., Yuan, C.A., Rocha, M., Jackson-Lewis, V., Hersch, S., Sulzer, D., Przedborski, S., Burke, R., and Hen, R. (2002). Resistance of alpha - synuclein null mice to the parkinsonian neurotoxin MPTP. *Proc Natl Acad Sci U S A* 99, 14524-14529.

Daval, M., Diot-Dupuy, F., Bazin, R., Hainault, I., Viollet, B., Vaulont, S., Hajdouch, E., Ferre, P., and Foufelle, F. (2005). Anti-lipolytic action of AMP-activated protein kinase in rodent adipocytes. *J Biol Chem* 280, 25250-25257.

Davidson, W.S., Jonas, A., Clayton, D.F., and George, J.M. (1998). Stabilization of alpha-synuclein secondary structure upon binding to synthetic membranes. *J Biol Chem* 273, 9443-9449.

De Franceschi, G., Frare, E., Pivato, M., Relini, A., Penco, A., Greggio, E., Bubacco, L., Fontana, A., and de Laureto, P.P. (2011). Structural and morphological characterization of aggregated species of alpha-synuclein induced by docosahexaenoic acid. *J Biol Chem* 286, 22262-22274.

Dev, K.K., Hofele, K., Barbieri, S., Buchman, V.L., and van der Putten, H. (2003). Part II: alpha-synuclein and its molecular pathophysiological role in neurodegenerative disease. *Neuropharmacology* 45, 14-44.

Dole, V.P. (1961). Effect of nucleic acid metabolites on lipolysis in adipose tissue. *J Biol Chem* 236, 3125-3130.

Dragonas, C., Bertsch, T., Sieber, C.C., and Brosche, T. (2009). Plasmalogens as a marker of elevated systemic oxidative stress in Parkinson's disease. *Clin Chem Lab Med* 47, 894-897.

Drolet, R.E., Behrouz, B., Lookingland, K.J., and Goudreau, J.L. (2004). Mice lacking alpha-synuclein have an attenuated loss of striatal dopamine following prolonged chronic MPTP administration. *Neurotoxicology* 25, 761-769.

Dusserre, E., Moulin, P., and Vidal, H. (2000). Differences in mRNA expression of the proteins secreted by the adipocytes in human subcutaneous and visceral adipose tissues. *Biochim Biophys Acta* 1500, 88-96.

Egan, J.J., Greenberg, A.S., Chang, M.K., Wek, S.A., Moos, M.C., Jr., and Londos, C. (1992). Mechanism of hormone-stimulated lipolysis in adipocytes: translocation of hormone-sensitive lipase to the lipid storage droplet. *Proc Natl Acad Sci U S A* 89, 8537-8541.

Elia, M., and Livesey, G. (1992). Energy expenditure and fuel selection in biological systems: the theory and practice of calculations based on indirect calorimetry and tracer methods. *World Rev Nutr Diet* 70, 68-131.

Eliezer, D., Kutluay, E., Bussell, R., Jr., and Browne, G. (2001). Conformational properties of alpha-synuclein in its free and lipid-associated states. *J Mol Biol* 307, 1061-1073.

Ellis, C.E., Murphy, E.J., Mitchell, D.C., Golovko, M.Y., Scaglia, F., Barcelo-Coblijn, G.C., and Nussbaum, R.L. (2005). Mitochondrial lipid abnormality and electron transport chain impairment in mice lacking alpha-synuclein. *Mol Cell Biol* 25, 10190-10201.

Engfeldt, P., Hellmer, J., Wahrenberg, H., and Arner, P. (1988). Effects of insulin on adrenoceptor binding and the rate of catecholamine-induced lipolysis in isolated human fat cells. *J Biol Chem* 263, 15553-15560.

Enoksson, S., Talbot, M., Rife, F., Tamborlane, W.V., Sherwin, R.S., and Caprio, S. (2000). Impaired in vivo stimulation of lipolysis in adipose tissue by selective beta2-adrenergic agonist in obese adolescent girls. *Diabetes* 49, 2149-2153.

Fan, Y., Limprasert, P., Murray, I.V., Smith, A.C., Lee, V.M., Trojanowski, J.Q., Sopher, B.L., and La Spada, A.R. (2006). Beta-synuclein modulates alpha-synuclein neurotoxicity by reducing alpha-synuclein protein expression. *Hum Mol Genet* 15, 3002-3011.

Farmer, S.R. (2006). Transcriptional control of adipocyte formation. *Cell Metab* 4, 263-273.

Farooqui, A.A., Horrocks, L.A., and Farooqui, T. (2000). Glycerophospholipids in brain: their metabolism, incorporation into membranes, functions, and involvement in neurological disorders. *Chem Phys Lipids* 106, 1-29.

Farooqui, A.A., Rapoport, S.I., and Horrocks, L.A. (1997). Membrane phospholipid alterations in Alzheimer's disease: deficiency of ethanolamine plasmalogens. *Neurochem Res* 22, 523-527.

Fink, A.L. (2006). The aggregation and fibrillation of alpha-synuclein. *Acc Chem Res* 39, 628-634.

Fisher, R.M., Eriksson, P., Hoffstedt, J., Hotamisligil, G.S., Thorne, A., Ryden, M., Hamsten, A., and Arner, P. (2001). Fatty acid binding protein expression in different adipose tissue depots from lean and obese individuals. *Diabetologia* 44, 1268-1273.

Flowers, J.M., Leigh, P.N., Davies, A.M., Ninkina, N.N., Buchman, V.L., Vaughan, J., Wood, N.W., and Powell, J.F. (1999). Mutations in the gene encoding human persyn are not associated with amyotrophic lateral sclerosis or familial Parkinson's disease. *Neurosci Lett* 274, 21-24.

Follenzi, A., Ailles, L.E., Bakovic, S., Geuna, M., and Naldini, L. (2000). Gene transfer by lentiviral vectors is limited by nuclear translocation and rescued by HIV-1 pol sequences. *Nat Genet* 25, 217-222.

Fontana, L., Eagon, J.C., Trujillo, M.E., Scherer, P.E., and Klein, S. (2007). Visceral fat adipokine secretion is associated with systemic inflammation in obese humans. *Diabetes* 56, 1010-1013.

Fornai, F., Schluter, O.M., Lenzi, P., Gesi, M., Ruffoli, R., Ferrucci, M., Lazzeri, G., Busceti, C.L., Pontarelli, F., Battaglia, G., Pellegrini, A., Nicoletti, F., Ruggieri, S., Paparelli, A., and Sudhof, T.C. (2005). Parkinson-like syndrome induced by continuous MPTP infusion: convergent roles of the ubiquitin-proteasome system and alpha-synuclein. *Proc Natl Acad Sci U S A* 102, 3413-3418.

Fortin, D.L., Troyer, M.D., Nakamura, K., Kubo, S., Anthony, M.D., and Edwards, R.H. (2004). Lipid rafts mediate the synaptic localization of alpha-synuclein. *J Neurosci* 24, 6715-6723.

Fox, C.S., Massaro, J.M., Hoffmann, U., Pou, K.M., Maurovich-Horvat, P., Liu, C.Y., Vasan, R.S., Murabito, J.M., Meigs, J.B., Cupples, L.A., D'Agostino, R.B., Sr., and O'Donnell, C.J. (2007). Abdominal visceral and subcutaneous adipose tissue compartments: association with metabolic risk factors in the Framingham Heart Study. *Circulation* 116, 39-48.

Frandsen, P.M., Madsen, L.B., Bendixen, C., and Larsen, K. (2009). Porcine gamma-synuclein: molecular cloning, expression analysis, chromosomal localization and functional expression. *Mol Biol Rep* 36, 971-979.

Fredrikson, G., Tornqvist, H., and Belfrage, P. (1986). Hormone-sensitive lipase and monoacylglycerol lipase are both required for complete degradation of adipocyte triacylglycerol. *Biochim Biophys Acta* 876, 288-293.

Fujishiro, M., Gotoh, Y., Katagiri, H., Sakoda, H., Ogihara, T., Anai, M., Onishi, Y., Ono, H., Abe, M., Shojima, N., Fukushima, Y., Kikuchi, M., Oka, Y., and Asano, T. (2003). Three mitogen-activated protein kinases inhibit insulin signaling by different mechanisms in 3T3-L1 adipocytes. *Mol Endocrinol* 17, 487-497.

Furuhashi, M., Fucho, R., Gorgun, C.Z., Tuncman, G., Cao, H., and Hotamisligil, G.S. (2008). Adipocyte/macrophage fatty acid-binding proteins contribute to metabolic deterioration through actions in both macrophages and adipocytes in mice. *J Clin Invest* 118, 2640-2650.

Galvin, J.E., Giasson, B., Hurtig, H.I., Lee, V.M., and Trojanowski, J.Q. (2000). Neurodegeneration with brain iron accumulation, type 1 is characterized by alpha-, beta-, and gamma-synuclein neuropathology. *Am J Pathol* 157, 361-368.

Galvin, J.E., Uryu, K., Lee, V.M., and Trojanowski, J.Q. (1999). Axon pathology in Parkinson's disease and Lewy body dementia hippocampus contains alpha-, beta-, and gamma-synuclein. *Proc Natl Acad Sci U S A* 96, 13450-13455.

Garton, A.J., Campbell, D.G., Cohen, P., and Yeaman, S.J. (1988). Primary structure of the site on bovine hormone-sensitive lipase phosphorylated by cyclic AMP-dependent protein kinase. *FEBS Lett* 229, 68-72.

Garton, A.J., and Yeaman, S.J. (1990). Identification and role of the basal phosphorylation site on hormone-sensitive lipase. *Eur J Biochem* 191, 245-250.

George, J.M., Jin, H., Woods, W.S., and Clayton, D.F. (1995). Characterization of a novel protein regulated during the critical period for song learning in the zebra finch. *Neuron* 15, 361-372.

Goedert, M., and Spillantini, M.G. (1998). Lewy body diseases and multiple system atrophy as alpha-synucleinopathies. *Mol Psychiatry* 3, 462-465.

Goldstein, B.J., and Scalia, R. (2004). Adiponectin: A novel adipokine linking adipocytes and vascular function. *J Clin Endocrinol Metab* 89, 2563-2568.

Golovko, M.Y., Barcelo-Coblijn, G., Castagnet, P.I., Austin, S., Combs, C.K., and Murphy, E.J. (2009). The role of alpha-synuclein in brain lipid metabolism: a downstream impact on brain inflammatory response. *Mol Cell Biochem* 326, 55-66.

Golovko, M.Y., Rosenberger, T.A., Faergeman, N.J., Feddersen, S., Cole, N.B., Pribill, I., Berger, J., Nussbaum, R.L., and Murphy, E.J. (2006). Acyl-CoA synthetase activity links wild-type but not mutant alpha-synuclein to brain arachidonate metabolism. *Biochemistry* 45, 6956-6966.

Golovko, M.Y., Rosenberger, T.A., Feddersen, S., Faergeman, N.J., and Murphy, E.J. (2007). Alpha-synuclein gene ablation increases docosahexaenoic acid incorporation and turnover in brain phospholipids. *J Neurochem* 101, 201-211.

Gorbatyuk, O.S., Li, S., Nha Nguyen, F., Manfredsson, F.P., Kondrikova, G., Sullivan, L.F., Meyers, C., Chen, W., Mandel, R.J., and Muzyczka, N. (2010). alpha-Synuclein expression in rat substantia nigra suppresses phospholipase D2 toxicity and nigral neurodegeneration. *Mol Ther* 18, 1758-1768.

Granneman, J.G., Moore, H.P., Granneman, R.L., Greenberg, A.S., Obin, M.S., and Zhu, Z. (2007). Analysis of lipolytic protein trafficking and interactions in adipocytes. *J Biol Chem* 282, 5726-5735.

Gray, S.L., Nora, E.D., Grosse, J., Manieri, M., Stoeger, T., Medina-Gomez, G., Burling, K., Wattler, S., Russ, A., Yeo, G.S., Chatterjee, V.K., O'Rahilly, S., Voshol, P.J., Cinti, S., and Vidal-Puig, A. (2006). Leptin deficiency unmasks the deleterious

effects of impaired peroxisome proliferator-activated receptor gamma function (P465L PPARgamma) in mice. *Diabetes* 55, 2669-2677.

Greenberg, A.S., Egan, J.J., Wek, S.A., Moos, M.C., Jr., Londos, C., and Kimmel, A.R. (1993). Isolation of cDNAs for perilipins A and B: sequence and expression of lipid droplet-associated proteins of adipocytes. *Proc Natl Acad Sci U S A* 90, 12035-12039.

Greenberg, A.S., Shen, W.J., Muliro, K., Patel, S., Souza, S.C., Roth, R.A., and Kraemer, F.B. (2001). Stimulation of lipolysis and hormone-sensitive lipase via the extracellular signal-regulated kinase pathway. *J Biol Chem* 276, 45456-45461.

Griffin, M.E., Marcucci, M.J., Cline, G.W., Bell, K., Barucci, N., Lee, D., Goodyear, L.J., Kraegen, E.W., White, M.F., and Shulman, G.I. (1999). Free fatty acid-induced insulin resistance is associated with activation of protein kinase C theta and alterations in the insulin signaling cascade. *Diabetes* 48, 1270-1274.

Griggio, M.A. (1988). Thermogenic mechanisms in cold-acclimated animals. *Braz J Med Biol Res* 21, 171-176.

Guo, J., Shou, C., Meng, L., Jiang, B., Dong, B., Yao, L., Xie, Y., Zhang, J., Chen, Y., Budman, D.R., and Shi, Y.E. (2007). Neuronal protein synuclein gamma predicts poor clinical outcome in breast cancer. *Int J Cancer* 121, 1296-1305.

Guo, Y., Walther, T.C., Rao, M., Stuurman, N., Goshima, G., Terayama, K., Wong, J.S., Vale, R.D., Walter, P., and Farese, R.V. (2008). Functional genomic screen reveals genes involved in lipid-droplet formation and utilization. *Nature* 453, 657-661.

Gupta, A., Godwin, A.K., Vanderveer, L., Lu, A., and Liu, J. (2003a). Hypomethylation of the synuclein gamma gene CpG island promotes its aberrant expression in breast carcinoma and ovarian carcinoma. *Cancer Res* 63, 664-673.

Gupta, A., Inaba, S., Wong, O.K., Fang, G., and Liu, J. (2003b). Breast cancer-specific gene 1 interacts with the mitotic checkpoint kinase BubR1. *Oncogene* 22, 7593-7599.

Haemmerle, G., Lass, A., Zimmermann, R., Gorkiewicz, G., Meyer, C., Rozman, J., Heldmaier, G., Maier, R., Theussl, C., Eder, S., Kratky, D., Wagner, E.F., Klingenspor, M., Hoefler, G., and Zechner, R. (2006). Defective lipolysis and altered energy metabolism in mice lacking adipose triglyceride lipase. *Science* 312, 734-737.

Haemmerle, G., Zimmermann, R., Strauss, J.G., Kratky, D., Riederer, M., Knipping, G., and Zechner, R. (2002). Hormone-sensitive lipase deficiency in mice changes the plasma lipid profile by affecting the tissue-specific expression pattern of lipoprotein lipase in adipose tissue and muscle. *J Biol Chem* 277, 12946-12952.

Hajer, G.R., van der Graaf, Y., Olijhoek, J.K., Edlinger, M., and Visseren, F.L. (2007). Low plasma levels of adiponectin are associated with low risk for future cardiovascular events in patients with clinical evident vascular disease. *Am Heart J* 154, 750 e751-757.

Hamilton, J.A., and Kamp, F. (1999). How are free fatty acids transported in membranes? Is it by proteins or by free diffusion through the lipids? *Diabetes* 48, 2255-2269.

Hammond, V.A., and Johnston, D.G. (1987). Substrate cycling between triglyceride and fatty acid in human adipocytes. *Metabolism* 36, 308-313.

Harada, K., Shen, W.J., Patel, S., Natu, V., Wang, J., Osuga, J., Ishibashi, S., and Kraemer, F.B. (2003). Resistance to high-fat diet-induced obesity and altered expression of adipose-specific genes in HSL-deficient mice. *Am J Physiol Endocrinol Metab* 285, E1182-1195.

Hashimoto, M., Rockenstein, E., Mante, M., Mallory, M., and Masliah, E. (2001). beta-Synuclein inhibits alpha-synuclein aggregation: a possible role as an anti-parkinsonian factor. *Neuron* 32, 213-223.

Hellmer, J., Marcus, C., Sonnenfeld, T., and Arner, P. (1992). Mechanisms for differences in lipolysis between human subcutaneous and omental fat cells. *J Clin Endocrinol Metab* 75, 15-20.

Hellstrom, L., Langin, D., Reynisdottir, S., Dauzats, M., and Arner, P. (1996). Adipocyte lipolysis in normal weight subjects with obesity among first-degree relatives. *Diabetologia* 39, 921-928.

Hibuse, T., Maeda, N., Funahashi, T., Yamamoto, K., Nagasawa, A., Mizunoya, W., Kishida, K., Inoue, K., Kuriyama, H., Nakamura, T., Fushiki, T., Kihara, S., and Shimomura, I. (2005). Aquaporin 7 deficiency is associated with development of obesity through activation of adipose glycerol kinase. *Proc Natl Acad Sci U S A* 102, 10993-10998.

- Hirsch, A.H., and Rosen, O.M. (1984). Lipolytic stimulation modulates the subcellular distribution of hormone-sensitive lipase in 3T3-L1 cells. *J Lipid Res* 25, 665-677.
- Hirsch, J., Fried, S.K., Edens, N.K., and Leibel, R.L. (1989). The fat cell. *Med Clin North Am* 73, 83-96.
- Hoffstedt, J., Arner, P., Schalling, M., Pedersen, N.L., Sengul, S., Ahlberg, S., Iliadou, A., and Lavebratt, C. (2001). A common hormone-sensitive lipase i6 gene polymorphism is associated with decreased human adipocyte lipolytic function. *Diabetes* 50, 2410-2413.
- Honor, R.C., Dhillon, G.S., and Londos, C. (1985). cAMP-dependent protein kinase and lipolysis in rat adipocytes. I. Cell preparation, manipulation, and predictability in behavior. *J Biol Chem* 260, 15122-15129.
- Horowitz, J.F., and Klein, S. (2000). Whole body and abdominal lipolytic sensitivity to epinephrine is suppressed in upper body obese women. *Am J Physiol Endocrinol Metab* 278, E1144-1152.
- Hu, F.B., Manson, J.E., Stampfer, M.J., Colditz, G., Liu, S., Solomon, C.G., and Willett, W.C. (2001). Diet, lifestyle, and the risk of type 2 diabetes mellitus in women. *N Engl J Med* 345, 790-797.
- Ibanez, P., Bonnet, A.M., Debarges, B., Lohmann, E., Tison, F., Pollak, P., Agid, Y., Durr, A., and Brice, A. (2004). Causal relation between alpha-synuclein gene duplication and familial Parkinson's disease. *Lancet* 364, 1169-1171.
- Illiano, G., and Cuatrecasas, P. (1972). Modulation of adenylate cyclase activity in liver and fat cell membranes by insulin. *Science* 175, 906-908.
- Inaba, S., Li, C., Shi, Y.E., Song, D.Q., Jiang, J.D., and Liu, J. (2005). Synuclein gamma inhibits the mitotic checkpoint function and promotes chromosomal instability of breast cancer cells. *Breast Cancer Res Treat* 94, 25-35.
- Indrigo, M., Papale, A., Orellana, D., and Brambilla, R. (2010). Lentiviral vectors to study the differential function of ERK1 and ERK2 MAP kinases. *Methods Mol Biol* 661, 205-220.
- Jahn, R., and Scheller, R.H. (2006). SNAREs--engines for membrane fusion. *Nat Rev Mol Cell Biol* 7, 631-643.
- Jakes, R., Spillantini, M.G., and Goedert, M. (1994). Identification of two distinct synucleins from human brain. *FEBS Lett* 345, 27-32.

- Jenco, J.M., Rawlingson, A., Daniels, B., and Morris, A.J. (1998). Regulation of phospholipase D2: selective inhibition of mammalian phospholipase D isoenzymes by alpha- and beta-synucleins. *Biochemistry* 37, 4901-4909.
- Jenkins, C.M., Mancuso, D.J., Yan, W., Sims, H.F., Gibson, B., and Gross, R.W. (2004). Identification, cloning, expression, and purification of three novel human calcium-independent phospholipase A2 family members possessing triacylglycerol lipase and acylglycerol transacylase activities. *J Biol Chem* 279, 48968-48975.
- Jenkins-Kruchten, A.E., Bennaars-Eiden, A., Ross, J.R., Shen, W.J., Kraemer, F.B., and Bernlohr, D.A. (2003). Fatty acid-binding protein-hormone-sensitive lipase interaction. Fatty acid dependence on binding. *J Biol Chem* 278, 47636-47643.
- Ji, H., Liu, Y.E., Jia, T., Wang, M., Liu, J., Xiao, G., Joseph, B.K., Rosen, C., and Shi, Y.E. (1997). Identification of a breast cancer-specific gene, BCSG1, by direct differential cDNA sequencing. *Cancer Res* 57, 759-764.
- Jo, E., McLaurin, J., Yip, C.M., St George-Hyslop, P., and Fraser, P.E. (2000). alpha-Synuclein membrane interactions and lipid specificity. *J Biol Chem* 275, 34328-34334.
- Jocken, J.W., Blaak, E.E., Schifflers, S., Arner, P., van Baak, M.A., and Saris, W.H. (2007a). Association of a beta-2 adrenoceptor (ADRB2) gene variant with a blunted in vivo lipolysis and fat oxidation. *Int J Obes (Lond)* 31, 813-819.
- Jocken, J.W., Langin, D., Smit, E., Saris, W.H., Valle, C., Hul, G.B., Holm, C., Arner, P., and Blaak, E.E. (2007b). Adipose triglyceride lipase and hormone-sensitive lipase protein expression is decreased in the obese insulin-resistant state. *J Clin Endocrinol Metab* 92, 2292-2299.
- Jovanovic, Z., Tung, Y.C., Lam, B.Y., O'Rahilly, S., and Yeo, G.S. (2010). Identification of the global transcriptomic response of the hypothalamic arcuate nucleus to fasting and leptin. *J Neuroendocrinol* 22, 915-925.
- Kadowaki, T., and Yamauchi, T. (2005). Adiponectin and adiponectin receptors. *Endocr Rev* 26, 439-451.
- Kampf, J.P., Parmley, D., and Kleinfeld, A.M. (2007). Free fatty acid transport across adipocytes is mediated by an unknown membrane protein pump. *Am J Physiol Endocrinol Metab* 293, E1207-1214.
- Karagiannides, I., Tchkonina, T., Dobson, D.E., Steppan, C.M., Cummins, P., Chan, G., Salvatori, K., Hadzopoulou-Cladaras, M., and Kirkland, J.L. (2001). Altered

expression of C/EBP family members results in decreased adipogenesis with aging. *Am J Physiol Regul Integr Comp Physiol* 280, R1772-1780.

Karpe, F., and Tan, G.D. (2005). Adipose tissue function in the insulin-resistance syndrome. *Biochem Soc Trans* 33, 1045-1048.

Karube, H., Sakamoto, M., Arawaka, S., Hara, S., Sato, H., Ren, C.H., Goto, S., Koyama, S., Wada, M., Kawanami, T., Kurita, K., and Kato, T. (2008). N-terminal region of alpha-synuclein is essential for the fatty acid-induced oligomerization of the molecules. *FEBS Lett* 582, 3693-3700.

Kershaw, E.E., Hamm, J.K., Verhagen, L.A., Peroni, O., Katic, M., and Flier, J.S. (2006). Adipose triglyceride lipase: function, regulation by insulin, and comparison with adiponutrin. *Diabetes* 55, 148-157.

Kim, H.Y. (2007). Novel metabolism of docosaehaenoic acid in neural cells. *J Biol Chem* 282, 18661-18665.

Kim, J.B., and Spiegelman, B.M. (1996). ADD1/SREBP1 promotes adipocyte differentiation and gene expression linked to fatty acid metabolism. *Genes Dev* 10, 1096-1107.

Kim, J.K., Fillmore, J.J., Sunshine, M.J., Albrecht, B., Higashimori, T., Kim, D.W., Liu, Z.X., Soos, T.J., Cline, G.W., O'Brien, W.R., Littman, D.R., and Shulman, G.I. (2004). PKC-theta knockout mice are protected from fat-induced insulin resistance. *J Clin Invest* 114, 823-827.

Kim, J.Y., Tillison, K., Lee, J.H., Rearick, D.A., and Smas, C.M. (2006). The adipose tissue triglyceride lipase ATGL/PNPLA2 is downregulated by insulin and TNF-alpha in 3T3-L1 adipocytes and is a target for transactivation by PPARgamma. *Am J Physiol Endocrinol Metab* 291, E115-127.

Kim, J.Y., van de Wall, E., Laplante, M., Azzara, A., Trujillo, M.E., Hofmann, S.M., Schraw, T., Durand, J.L., Li, H., Li, G., Jelicks, L.A., Mehler, M.F., Hui, D.Y., Deshaies, Y., Shulman, G.I., Schwartz, G.J., and Scherer, P.E. (2007). Obesity-associated improvements in metabolic profile through expansion of adipose tissue. *J Clin Invest* 117, 2621-2637.

Kitajka, K., Puskas, L.G., Zvara, A., Hackler, L., Jr., Barcelo-Coblijn, G., Yeo, Y.K., and Farkas, T. (2002). The role of n-3 polyunsaturated fatty acids in brain: modulation of rat brain gene expression by dietary n-3 fatty acids. *Proc Natl Acad Sci U S A* 99, 2619-2624.

Kraegen, E.W., Cooney, G.J., Ye, J.M., Thompson, A.L., and Furler, S.M. (2001). The role of lipids in the pathogenesis of muscle insulin resistance and beta cell failure in type II diabetes and obesity. *Exp Clin Endocrinol Diabetes* 109 Suppl 2, S189-201.

Kralisch, S., Klein, J., Lossner, U., Bluher, M., Paschke, R., Stumvoll, M., and Fasshauer, M. (2005). Isoproterenol, TNFalpha, and insulin downregulate adipose triglyceride lipase in 3T3-L1 adipocytes. *Mol Cell Endocrinol* 240, 43-49.

Kruger, R., Kuhn, W., Muller, T., Woitalla, D., Graeber, M., Kosel, S., Przuntek, H., Eppelen, J.T., Schols, L., and Riess, O. (1998). Ala30Pro mutation in the gene encoding alpha-synuclein in Parkinson's disease. *Nat Genet* 18, 106-108.

Kruger, R., Schols, L., Muller, T., Kuhn, W., Woitalla, D., Przuntek, H., Eppelen, J.T., and Riess, O. (2001). Evaluation of the gamma-synuclein gene in German Parkinson's disease patients. *Neurosci Lett* 310, 191-193.

Ktistakis, N.T., Brown, H.A., Sternweis, P.C., and Roth, M.G. (1995). Phospholipase D is present on Golgi-enriched membranes and its activation by ADP ribosylation factor is sensitive to brefeldin A. *Proc Natl Acad Sci U S A* 92, 4952-4956.

Kubo, S., Nemani, V.M., Chalkley, R.J., Anthony, M.D., Hattori, N., Mizuno, Y., Edwards, R.H., and Fortin, D.L. (2005). A combinatorial code for the interaction of alpha-synuclein with membranes. *J Biol Chem* 280, 31664-31672.

Kuhn, M., Haebig, K., Bonin, M., Ninkina, N., Buchman, V.L., Poths, S., and Riess, O. (2007). Whole genome expression analyses of single- and double-knock-out mice implicate partially overlapping functions of alpha- and gamma-synuclein. *Neurogenetics* 8, 71-81.

Lafontan, M. (2008). Advances in adipose tissue metabolism. *Int J Obes (Lond)* 32 Suppl 7, S39-51.

Lafontan, M., and Berlan, M. (1995). Fat cell alpha 2-adrenoceptors: the regulation of fat cell function and lipolysis. *Endocr Rev* 16, 716-738.

Lafontan, M., Moro, C., Sengenès, C., Galitzky, J., Crampes, F., and Berlan, M. (2005). An unsuspected metabolic role for atrial natriuretic peptides: the control of lipolysis, lipid mobilization, and systemic nonesterified fatty acids levels in humans. *Arterioscler Thromb Vasc Biol* 25, 2032-2042.

Lagathu, C., Bastard, J.P., Auclair, M., Maachi, M., Capeau, J., and Caron, M. (2003). Chronic interleukin-6 (IL-6) treatment increased IL-6 secretion and induced insulin

resistance in adipocyte: prevention by rosiglitazone. *Biochem Biophys Res Commun* 311, 372-379.

Langin, D., and Arner, P. (2006). Importance of TNF $\alpha$  and neutral lipases in human adipose tissue lipolysis. *Trends Endocrinol Metab* 17, 314-320.

Langin, D., Dicker, A., Tavernier, G., Hoffstedt, J., Mairal, A., Ryden, M., Arner, E., Sicard, A., Jenkins, C.M., Viguier, N., van Harmelen, V., Gross, R.W., Holm, C., and Arner, P. (2005). Adipocyte lipases and defect of lipolysis in human obesity. *Diabetes* 54, 3190-3197.

Langin, D., Lucas, S., and Lafontan, M. (2000). Millennium fat-cell lipolysis reveals unsuspected novel tracks. *Horm Metab Res* 32, 443-452.

Large, V., Hellstrom, L., Reynisdottir, S., Lonqvist, F., Eriksson, P., Lannfelt, L., and Arner, P. (1997). Human beta-2 adrenoceptor gene polymorphisms are highly frequent in obesity and associate with altered adipocyte beta-2 adrenoceptor function. *J Clin Invest* 100, 3005-3013.

Large, V., Reynisdottir, S., Langin, D., Fredby, K., Klannemark, M., Holm, C., and Arner, P. (1999). Decreased expression and function of adipocyte hormone-sensitive lipase in subcutaneous fat cells of obese subjects. *J Lipid Res* 40, 2059-2066.

Lass, A., Zimmermann, R., Haemmerle, G., Riederer, M., Schoiswohl, G., Schweiger, M., Kienesberger, P., Strauss, J.G., Gorkiewicz, G., and Zechner, R. (2006). Adipose triglyceride lipase-mediated lipolysis of cellular fat stores is activated by CGI-58 and defective in Chanarin-Dorfman Syndrome. *Cell Metab* 3, 309-319.

Lavedan, C., Buchholtz, S., Auburger, G., Albin, R.L., Athanassiadou, A., Blancato, J., Burguera, J.A., Ferrell, R.E., Kostic, V., Leroy, E., Leube, B., Mota-Vieira, L., Papapetropoulos, T., Pericak-Vance, M.A., Pinkus, J., Scott, W.K., Ulm, G., Vasconcelos, J., Vilchez, J.J., Nussbaum, R.L., and Polymeropoulos, M.H. (1998a). Absence of mutation in the beta- and gamma-synuclein genes in familial autosomal dominant Parkinson's disease. *DNA Res* 5, 401-402.

Lavedan, C., Leroy, E., Dehejia, A., Buchholtz, S., Dutra, A., Nussbaum, R.L., and Polymeropoulos, M.H. (1998b). Identification, localization and characterization of the human gamma-synuclein gene. *Hum Genet* 103, 106-112.

Lee, D., Paik, S.R., and Choi, K.Y. (2004). Beta-synuclein exhibits chaperone activity more efficiently than alpha-synuclein. *FEBS Lett* 576, 256-260.

Lee, F.J., Liu, F., Pristupa, Z.B., and Niznik, H.B. (2001). Direct binding and functional coupling of alpha-synuclein to the dopamine transporters accelerate dopamine-induced apoptosis. *FASEB J* 15, 916-926.

Li, J.Y., Henning Jensen, P., and Dahlstrom, A. (2002). Differential localization of alpha-, beta- and gamma-synucleins in the rat CNS. *Neuroscience* 113, 463-478.

Lincoln, S., Crook, R., Chartier-Harlin, M.C., Gwinn-Hardy, K., Baker, M., Mouroux, V., Richard, F., Becquet, E., Amouyel, P., Destee, A., Hardy, J., and Farrer, M. (1999a). No pathogenic mutations in the beta-synuclein gene in Parkinson's disease. *Neurosci Lett* 269, 107-109.

Lincoln, S., Gwinn-Hardy, K., Goudreau, J., Chartier-Harlin, M.C., Baker, M., Mouroux, V., Richard, F., Destee, A., Becquet, E., Amouyel, P., Lynch, T., Hardy, J., and Farrer, M. (1999b). No pathogenic mutations in the persyn gene in Parkinson's disease. *Neurosci Lett* 259, 65-66.

Lindsay, R.S., Funahashi, T., Hanson, R.L., Matsuzawa, Y., Tanaka, S., Tataranni, P.A., Knowler, W.C., and Krakoff, J. (2002). Adiponectin and development of type 2 diabetes in the Pima Indian population. *Lancet* 360, 57-58.

Liscovitch, M., Czarny, M., Fiucci, G., and Tang, X. (2000). Phospholipase D: molecular and cell biology of a novel gene family. *Biochem J* 345 Pt 3, 401-415.

Liu, H., Liu, W., Wu, Y., Zhou, Y., Xue, R., Luo, C., Wang, L., Zhao, W., Jiang, J.D., and Liu, J. (2005). Loss of epigenetic control of synuclein-gamma gene as a molecular indicator of metastasis in a wide range of human cancers. *Cancer Res* 65, 7635-7643.

Liu, H., Zhou, Y., Boggs, S.E., Belinsky, S.A., and Liu, J. (2007). Cigarette smoke induces demethylation of prometastatic oncogene synuclein-gamma in lung cancer cells by downregulation of DNMT3B. *Oncogene* 26, 5900-5910.

Livak, K.J., and Schmittgen, T.D. (2001). Analysis of relative gene expression data using real-time quantitative PCR and the 2(-Delta Delta C(T)) Method. *Methods* 25, 402-408.

Long, Y.C., and Zierath, J.R. (2006). AMP-activated protein kinase signaling in metabolic regulation. *J Clin Invest* 116, 1776-1783.

Lu, A., Gupta, A., Li, C., Ahlborn, T.E., Ma, Y., Shi, E.Y., and Liu, J. (2001). Molecular mechanisms for aberrant expression of the human breast cancer specific

gene 1 in breast cancer cells: control of transcription by DNA methylation and intronic sequences. *Oncogene* 20, 5173-5185.

Lukiw, W.J., and Bazan, N.G. (2008). Docosahexaenoic acid and the aging brain. *J Nutr* 138, 2510-2514.

Maroteaux, L., Campanelli, J.T., and Scheller, R.H. (1988). Synuclein: a neuron-specific protein localized to the nucleus and presynaptic nerve terminal. *J Neurosci* 8, 2804-2815.

Marsh, J.A., Singh, V.K., Jia, Z., and Forman-Kay, J.D. (2006). Sensitivity of secondary structure propensities to sequence differences between alpha- and gamma-synuclein: implications for fibrillation. *Protein Sci* 15, 2795-2804.

Martinez-Botas, J., Anderson, J.B., Tessier, D., Lapillonne, A., Chang, B.H., Quast, M.J., Gorenstein, D., Chen, K.H., and Chan, L. (2000). Absence of perilipin results in leanness and reverses obesity in *Lepr(db/db)* mice. *Nat Genet* 26, 474-479.

Matarese, V., and Bernlohr, D.A. (1988). Purification of murine adipocyte lipid-binding protein. Characterization as a fatty acid- and retinoic acid-binding protein. *J Biol Chem* 263, 14544-14551.

Mauriege, P., Despres, J.P., Prud'homme, D., Pouliot, M.C., Marcotte, M., Tremblay, A., and Bouchard, C. (1991). Regional variation in adipose tissue lipolysis in lean and obese men. *J Lipid Res* 32, 1625-1633.

Miyoshi, H., Perfield, J.W., 2nd, Obin, M.S., and Greenberg, A.S. (2008). Adipose triglyceride lipase regulates basal lipolysis and lipid droplet size in adipocytes. *J Cell Biochem* 105, 1430-1436.

Miyoshi, H., Perfield, J.W., 2nd, Souza, S.C., Shen, W.J., Zhang, H.H., Stancheva, Z.S., Kraemer, F.B., Obin, M.S., and Greenberg, A.S. (2007). Control of adipose triglyceride lipase action by serine 517 of perilipin A globally regulates protein kinase A-stimulated lipolysis in adipocytes. *J Biol Chem* 282, 996-1002.

Miyoshi, H., Souza, S.C., Endo, M., Sawada, T., Perfield, J.W., 2nd, Shimizu, C., Stancheva, Z., Nagai, S., Strissel, K.J., Yoshioka, N., Obin, M.S., Koike, T., and Greenberg, A.S. (2010). Perilipin overexpression in mice protects against diet-induced obesity. *J Lipid Res* 51, 975-982.

Miyoshi, H., Souza, S.C., Zhang, H.H., Strissel, K.J., Christoffolete, M.A., Kovsan, J., Rudich, A., Kraemer, F.B., Bianco, A.C., Obin, M.S., and Greenberg, A.S. (2006). Perilipin promotes hormone-sensitive lipase-mediated adipocyte lipolysis via

phosphorylation-dependent and -independent mechanisms. *J Biol Chem* 281, 15837-15844.

Moitra, J., Mason, M.M., Olive, M., Krylov, D., Gavrilova, O., Marcus-Samuels, B., Feigenbaum, L., Lee, E., Aoyama, T., Eckhaus, M., Reitman, M.L., and Vinson, C. (1998). Life without white fat: a transgenic mouse. *Genes Dev* 12, 3168-3181.

Mori, F., Hayashi, S., Yamagishi, S., Yoshimoto, M., Yagihashi, S., Takahashi, H., and Wakabayashi, K. (2002). Pick's disease: alpha- and beta-synuclein-immunoreactive Pick bodies in the dentate gyrus. *Acta Neuropathol* 104, 455-461.

Mottagui-Tabar, S., Ryden, M., Lofgren, P., Faulds, G., Hoffstedt, J., Brookes, A.J., Andersson, I., and Arner, P. (2003). Evidence for an important role of perilipin in the regulation of human adipocyte lipolysis. *Diabetologia* 46, 789-797.

Mozzi, R., Buratta, S., and Goracci, G. (2003). Metabolism and functions of phosphatidylserine in mammalian brain. *Neurochem Res* 28, 195-214.

Mukaetova-Ladinska, E.B., Milne, J., Andras, A., Abdel-All, Z., Cerejeira, J., Grealley, E., Robson, J., Jaros, E., Perry, R., McKeith, I.G., Brayne, C., Xuereb, J., Cleghorn, A., Doherty, J., McIntosh, G., and Milton, I. (2008). Alpha- and gamma-synuclein proteins are present in cerebrospinal fluid and are increased in aged subjects with neurodegenerative and vascular changes. *Dement Geriatr Cogn Disord* 26, 32-42.

Mulder, H., Sorhede-Winzell, M., Contreras, J.A., Fex, M., Strom, K., Ploug, T., Galbo, H., Arner, P., Lundberg, C., Sundler, F., Ahren, B., and Holm, C. (2003). Hormone-sensitive lipase null mice exhibit signs of impaired insulin sensitivity whereas insulin secretion is intact. *J Biol Chem* 278, 36380-36388.

Munzberg, H., and Myers, M.G., Jr. (2005). Molecular and anatomical determinants of central leptin resistance. *Nat Neurosci* 8, 566-570.

Myerowitz, R., Mizukami, H., Richardson, K.L., Finn, L.S., Tifft, C.J., and Proia, R.L. (2004). Global gene expression in a type 2 Gaucher disease brain. *Mol Genet Metab* 83, 288-296.

Nagan, N., and Zoeller, R.A. (2001). Plasmalogens: biosynthesis and functions. *Prog Lipid Res* 40, 199-229.

Newsholme, E.A. (1978). Substrate cycles: their metabolic, energetic and thermic consequences in man. *Biochem Soc Symp*, 183-205.

Nichols, G.A., and Gomez-Caminero, A. (2007). Weight changes following the initiation of new anti-hyperglycaemic therapies. *Diabetes Obes Metab* 9, 96-102.

Ninkina, N., Papachroni, K., Robertson, D.C., Schmidt, O., Delaney, L., O'Neill, F., Court, F., Rosenthal, A., Fleetwood-Walker, S.M., Davies, A.M., and Buchman, V.L. (2003). Neurons expressing the highest levels of gamma-synuclein are unaffected by targeted inactivation of the gene. *Mol Cell Biol* 23, 8233-8245.

Ninkina, N., Peters, O., Millership, S., Salem, H., van der Putten, H., and Buchman, V.L. (2009). Gamma-synucleinopathy: neurodegeneration associated with overexpression of the mouse protein. *Hum Mol Genet* 18, 1779-1794.

Ninkina, N.N., Alimova-Kost, M.V., Paterson, J.W., Delaney, L., Cohen, B.B., Imreh, S., Gnuchev, N.V., Davies, A.M., and Buchman, V.L. (1998). Organization, expression and polymorphism of the human persyn gene. *Hum Mol Genet* 7, 1417-1424.

Nishino, N., Tamori, Y., Tateya, S., Kawaguchi, T., Shibakusa, T., Mizunoya, W., Inoue, K., Kitazawa, R., Kitazawa, S., Matsuki, Y., Hiramatsu, R., Masubuchi, S., Omachi, A., Kimura, K., Saito, M., Amo, T., Ohta, S., Yamaguchi, T., Osumi, T., Cheng, J., Fujimoto, T., Nakao, H., Nakao, K., Aiba, A., Okamura, H., Fushiki, T., and Kasuga, M. (2008). FSP27 contributes to efficient energy storage in murine white adipocytes by promoting the formation of unilocular lipid droplets. *J Clin Invest* 118, 2808-2821.

Okuya, S., Tanabe, K., Tanizawa, Y., and Oka, Y. (2001). Leptin increases the viability of isolated rat pancreatic islets by suppressing apoptosis. *Endocrinology* 142, 4827-4830.

Olofsson, S.O., Bostrom, P., Andersson, L., Rutberg, M., Perman, J., and Boren, J. (2009). Lipid droplets as dynamic organelles connecting storage and efflux of lipids. *Biochim Biophys Acta* 1791, 448-458.

Olsson, H., Stralfors, P., and Belfrage, P. (1986). Phosphorylation of the basal site of hormone-sensitive lipase by glycogen synthase kinase-4. *FEBS Lett* 209, 175-180.

Oort, P.J., Knotts, T.A., Grino, M., Naour, N., Bastard, J.P., Clement, K., Ninkina, N., Buchman, V.L., Permana, P.A., Luo, X., Pan, G., Dunn, T.N., and Adams, S.H. (2008). Gamma-synuclein is an adipocyte-neuron gene coordinately expressed with leptin and increased in human obesity. *J Nutr* 138, 841-848.

Osuga, J., Ishibashi, S., Oka, T., Yagyu, H., Tozawa, R., Fujimoto, A., Shionoiri, F., Yahagi, N., Kraemer, F.B., Tsutsumi, O., and Yamada, N. (2000). Targeted disruption of hormone-sensitive lipase results in male sterility and adipocyte hypertrophy, but not in obesity. *Proc Natl Acad Sci U S A* 97, 787-792.

Otto, T.C., and Lane, M.D. (2005). Adipose development: from stem cell to adipocyte. *Crit Rev Biochem Mol Biol* 40, 229-242.

Pals, P., Lincoln, S., Manning, J., Heckman, M., Skipper, L., Hulihan, M., Van den Broeck, M., De Pooter, T., Cras, P., Crook, J., Van Broeckhoven, C., and Farrer, M.J. (2004). alpha-Synuclein promoter confers susceptibility to Parkinson's disease. *Ann Neurol* 56, 591-595.

Pan, Z.Z., Bruening, W., Giasson, B.I., Lee, V.M., and Godwin, A.K. (2002). Gamma-synuclein promotes cancer cell survival and inhibits stress- and chemotherapy drug-induced apoptosis by modulating MAPK pathways. *J Biol Chem* 277, 35050-35060.

Papachroni, K., Ninkina, N., Wanless, J., Kalofoutis, A.T., Gnucnev, N.V., and Buchman, V.L. (2005). Peripheral sensory neurons survive in the absence of alpha- and gamma-synucleins. *J Mol Neurosci* 25, 157-164.

Park, J.Y., and Lansbury, P.T., Jr. (2003). Beta-synuclein inhibits formation of alpha-synuclein protofibrils: a possible therapeutic strategy against Parkinson's disease. *Biochemistry* 42, 3696-3700.

Park, S.M., Jung, H.Y., Kim, T.D., Park, J.H., Yang, C.H., and Kim, J. (2002). Distinct roles of the N-terminal-binding domain and the C-terminal-solubilizing domain of alpha-synuclein, a molecular chaperone. *J Biol Chem* 277, 28512-28520.

Path, G., Bornstein, S.R., Gurniak, M., Chrousos, G.P., Scherbaum, W.A., and Hauner, H. (2001). Human breast adipocytes express interleukin-6 (IL-6) and its receptor system: increased IL-6 production by beta-adrenergic activation and effects of IL-6 on adipocyte function. *J Clin Endocrinol Metab* 86, 2281-2288.

Payton, J.E., Perrin, R.J., Woods, W.S., and George, J.M. (2004). Structural determinants of PLD2 inhibition by alpha-synuclein. *J Mol Biol* 337, 1001-1009.

Perez, R.G., Waymire, J.C., Lin, E., Liu, J.J., Guo, F., and Zigmond, M.J. (2002). A role for alpha-synuclein in the regulation of dopamine biosynthesis. *J Neurosci* 22, 3090-3099.

Perrin, R.J., Woods, W.S., Clayton, D.F., and George, J.M. (2000). Interaction of human alpha-Synuclein and Parkinson's disease variants with phospholipids. Structural analysis using site-directed mutagenesis. *J Biol Chem* 275, 34393-34398.

Perrin, R.J., Woods, W.S., Clayton, D.F., and George, J.M. (2001). Exposure to long chain polyunsaturated fatty acids triggers rapid multimerization of synucleins. *J Biol Chem* 276, 41958-41962.

Petersen, E.W., Carey, A.L., Sacchetti, M., Steinberg, G.R., Macaulay, S.L., Febbraio, M.A., and Pedersen, B.K. (2005). Acute IL-6 treatment increases fatty acid turnover in elderly humans in vivo and in tissue culture in vitro. *Am J Physiol Endocrinol Metab* 288, E155-162.

Poitout, V., Rouault, C., Guerre-Millo, M., and Reach, G. (1998). Does leptin regulate insulin secretion? *Diabetes Metab* 24, 321-326.

Polymeropoulos, M.H., Lavedan, C., Leroy, E., Ide, S.E., Dehejia, A., Dutra, A., Pike, B., Root, H., Rubenstein, J., Boyer, R., Stenroos, E.S., Chandrasekharappa, S., Athanassiadou, A., Papapetropoulos, T., Johnson, W.G., Lazzarini, A.M., Duvoisin, R.C., Di Iorio, G., Golbe, L.I., and Nussbaum, R.L. (1997). Mutation in the alpha-synuclein gene identified in families with Parkinson's disease. *Science* 276, 2045-2047.

Puri, V., Konda, S., Ranjit, S., Aouadi, M., Chawla, A., Chouinard, M., Chakladar, A., and Czech, M.P. (2007). Fat-specific protein 27, a novel lipid droplet protein that enhances triglyceride storage. *J Biol Chem* 282, 34213-34218.

Ramakrishnan, M., Jensen, P.H., and Marsh, D. (2003). Alpha-synuclein association with phosphatidylglycerol probed by lipid spin labels. *Biochemistry* 42, 12919-12926.

Rappley, I., Gitler, A.D., Selvy, P.E., LaVoie, M.J., Levy, B.D., Brown, H.A., Lindquist, S., and Selkoe, D.J. (2009). Evidence that alpha-synuclein does not inhibit phospholipase D. *Biochemistry* 48, 1077-1083.

Reynisdottir, S., Dauzats, M., Thorne, A., and Langin, D. (1997). Comparison of hormone-sensitive lipase activity in visceral and subcutaneous human adipose tissue. *J Clin Endocrinol Metab* 82, 4162-4166.

Reynisdottir, S., Wahrenberg, H., Carlstrom, K., Rossner, S., and Arner, P. (1994). Catecholamine resistance in fat cells of women with upper-body obesity due to decreased expression of beta 2-adrenoceptors. *Diabetologia* 37, 428-435.

Rhodes, C.J. (2005). Type 2 diabetes-a matter of beta-cell life and death? *Science* 307, 380-384.

Rizack, M.A. (1964). Activation of an Epinephrine-Sensitive Lipolytic Activity from Adipose Tissue by Adenosine 3',5'-Phosphate. *J Biol Chem* 239, 392-395.

Rizo, J., and Rosenmund, C. (2008). Synaptic vesicle fusion. *Nat Struct Mol Biol* 15, 665-674.

Robertson, D.C., Schmidt, O., Ninkina, N., Jones, P.A., Sharkey, J., and Buchman, V.L. (2004). Developmental loss and resistance to MPTP toxicity of dopaminergic neurones in substantia nigra pars compacta of gamma-synuclein, alpha-synuclein and double alpha/gamma-synuclein null mutant mice. *J Neurochem* 89, 1126-1136.

Rockenstein, E., Hansen, L.A., Mallory, M., Trojanowski, J.Q., Galasko, D., and Masliah, E. (2001). Altered expression of the synuclein family mRNA in Lewy body and Alzheimer's disease. *Brain Res* 914, 48-56.

Rodbell, M. (1964). Metabolism of Isolated Fat Cells. I. Effects of Hormones on Glucose Metabolism and Lipolysis. *J Biol Chem* 239, 375-380.

Rosen, E.D., and Spiegelman, B.M. (2006). Adipocytes as regulators of energy balance and glucose homeostasis. *Nature* 444, 847-853.

Rothwell, N.J., and Stock, M.J. (1979). A role for brown adipose tissue in diet-induced thermogenesis. *Nature* 281, 31-35.

Rotter, V., Nagaev, I., and Smith, U. (2003). Interleukin-6 (IL-6) induces insulin resistance in 3T3-L1 adipocytes and is, like IL-8 and tumor necrosis factor-alpha, overexpressed in human fat cells from insulin-resistant subjects. *J Biol Chem* 278, 45777-45784.

Rousset, S., Alves-Guerra, M.C., Mozo, J., Miroux, B., Cassard-Doulcier, A.M., Bouillaud, F., and Ricquier, D. (2004). The biology of mitochondrial uncoupling proteins. *Diabetes* 53 Suppl 1, S130-135.

Ruiperez, V., Darios, F., and Davletov, B. (2010). Alpha-synuclein, lipids and Parkinson's disease. *Prog Lipid Res* 49, 420-428.

Ryden, M., Dicker, A., van Harmelen, V., Hauner, H., Brunnberg, M., Perbeck, L., Lonqvist, F., and Arner, P. (2002). Mapping of early signaling events in tumor necrosis factor-alpha-mediated lipolysis in human fat cells. *J Biol Chem* 277, 1085-1091.

Ryden, M., Jocken, J., van Harmelen, V., Dicker, A., Hoffstedt, J., Wren, M., Blomqvist, L., Mairal, A., Langin, D., Blaak, E., and Arner, P. (2007). Comparative studies of the role of hormone-sensitive lipase and adipose triglyceride lipase in human fat cell lipolysis. *Am J Physiol Endocrinol Metab* 292, E1847-1855.

Sacco, M.G., Gribaldo, L., Barbieri, O., Turchi, G., Zucchi, I., Collotta, A., Bagnasco, L., Barone, D., Montagna, C., Villa, A., Marafante, E., and Vezzoni, P. (1998). Establishment and characterization of a new mammary adenocarcinoma cell line derived from MMTV neu transgenic mice. *Breast Cancer Res Treat* 47, 171-180.

Saha, A.R., Ninkina, N.N., Hanger, D.P., Anderton, B.H., Davies, A.M., and Buchman, V.L. (2000). Induction of neuronal death by alpha-synuclein. *Eur J Neurosci* 12, 3073-3077.

Saladin, R., De Vos, P., Guerre-Millo, M., Leturque, A., Girard, J., Staels, B., and Auwerx, J. (1995). Transient increase in obese gene expression after food intake or insulin administration. *Nature* 377, 527-529.

Santomauro, A.T., Boden, G., Silva, M.E., Rocha, D.M., Santos, R.F., Ursich, M.J., Strassmann, P.G., and Wajchenberg, B.L. (1999). Overnight lowering of free fatty acids with Acipimox improves insulin resistance and glucose tolerance in obese diabetic and nondiabetic subjects. *Diabetes* 48, 1836-1841.

Schaffer, J.E., and Lodish, H.F. (1994). Expression cloning and characterization of a novel adipocyte long chain fatty acid transport protein. *Cell* 79, 427-436.

Scheja, L., Makowski, L., Uysal, K.T., Wiesbrock, S.M., Shimshek, D.R., Meyers, D.S., Morgan, M., Parker, R.A., and Hotamisligil, G.S. (1999). Altered insulin secretion associated with reduced lipolytic efficiency in *aP2*<sup>-/-</sup> mice. *Diabetes* 48, 1987-1994.

Schluter, O.M., Fornai, F., Alessandri, M.G., Takamori, S., Geppert, M., Jahn, R., and Sudhof, T.C. (2003). Role of alpha-synuclein in 1-methyl-4-phenyl-1,2,3,6-tetrahydropyridine-induced parkinsonism in mice. *Neuroscience* 118, 985-1002.

Schwartz, M.W., Woods, S.C., Porte, D., Jr., Seeley, R.J., and Baskin, D.G. (2000). Central nervous system control of food intake. *Nature* 404, 661-671.

Schweiger, M., Lass, A., Zimmermann, R., Eichmann, T.O., and Zechner, R. (2009). Neutral lipid storage disease: genetic disorders caused by mutations in adipose triglyceride lipase/PNPLA2 or CGI-58/ABHD5. *Am J Physiol Endocrinol Metab* 297, E289-296.

Scow, R.O., and Blanchette-Mackie, E.J. (1985). Why fatty acids flow in cell membranes. *Prog Lipid Res* 24, 197-241.

Sengenès, C., Berlan, M., De Glisezinski, I., Lafontan, M., and Galitzky, J. (2000). Natriuretic peptides: a new lipolytic pathway in human adipocytes. *FASEB J* 14, 1345-1351.

Sengenès, C., Bouloumie, A., Hauner, H., Berlan, M., Busse, R., Lafontan, M., and Galitzky, J. (2003). Involvement of a cGMP-dependent pathway in the natriuretic peptide-mediated hormone-sensitive lipase phosphorylation in human adipocytes. *J Biol Chem* 278, 48617-48626.

Sengenès, C., Zakaroff-Girard, A., Moulin, A., Berlan, M., Bouloumie, A., Lafontan, M., and Galitzky, J. (2002). Natriuretic peptide-dependent lipolysis in fat cells is a primate specificity. *Am J Physiol Regul Integr Comp Physiol* 283, R257-265.

Senior, S.L., Ninkina, N., Deacon, R., Bannerman, D., Buchman, V.L., Cragg, S.J., and Wade-Martins, R. (2008). Increased striatal dopamine release and hyperdopaminergic-like behaviour in mice lacking both alpha-synuclein and gamma-synuclein. *Eur J Neurosci* 27, 947-957.

Serpell, L.C., Berriman, J., Jakes, R., Goedert, M., and Crowther, R.A. (2000). Fiber diffraction of synthetic alpha-synuclein filaments shows amyloid-like cross-beta conformation. *Proc Natl Acad Sci U S A* 97, 4897-4902.

Sharon, R., Bar-Joseph, I., Frosch, M.P., Walsh, D.M., Hamilton, J.A., and Selkoe, D.J. (2003a). The formation of highly soluble oligomers of alpha-synuclein is regulated by fatty acids and enhanced in Parkinson's disease. *Neuron* 37, 583-595.

Sharon, R., Bar-Joseph, I., Mirick, G.E., Serhan, C.N., and Selkoe, D.J. (2003b). Altered fatty acid composition of dopaminergic neurons expressing alpha-synuclein and human brains with alpha-synucleinopathies. *J Biol Chem* 278, 49874-49881.

Sharon, R., Goldberg, M.S., Bar-Josef, I., Betensky, R.A., Shen, J., and Selkoe, D.J. (2001). alpha-Synuclein occurs in lipid-rich high molecular weight complexes, binds fatty acids, and shows homology to the fatty acid-binding proteins. *Proc Natl Acad Sci U S A* 98, 9110-9115.

Shen, W.J., Patel, S., Miyoshi, H., Greenberg, A.S., and Kraemer, F.B. (2009). Functional interaction of hormone-sensitive lipase and perilipin in lipolysis. *J Lipid Res* 50, 2306-2313.

Shen, W.J., Patel, S., Natsu, V., and Kraemer, F.B. (1998). Mutational analysis of structural features of rat hormone-sensitive lipase. *Biochemistry* 37, 8973-8979.

Shen, W.J., Sridhar, K., Bernlohr, D.A., and Kraemer, F.B. (1999). Interaction of rat hormone-sensitive lipase with adipocyte lipid-binding protein. *Proc Natl Acad Sci U S A* 96, 5528-5532.

Shimabukuro, M., Wang, M.Y., Zhou, Y.T., Newgard, C.B., and Unger, R.H. (1998). Protection against lipoapoptosis of beta cells through leptin-dependent maintenance of Bcl-2 expression. *Proc Natl Acad Sci U S A* 95, 9558-9561.

Shvadchak, V.V., Falomir-Lockhart, L.J., Yushchenko, D.A., and Jovin, T.M. (2011). Specificity and kinetics of alpha-synuclein binding to model membranes determined with fluorescent excited state intramolecular proton transfer (ESIPT) probe. *J Biol Chem* 286, 13023-13032.

Singleton, A., Gwinn-Hardy, K., Sharabi, Y., Li, S.T., Holmes, C., Dendi, R., Hardy, J., Crawley, A., and Goldstein, D.S. (2004). Association between cardiac denervation and parkinsonism caused by alpha-synuclein gene triplication. *Brain* 127, 768-772.

Soper, J.H., Kehm, V., Burd, C.G., Bankaitis, V.A., and Lee, V.M. (2011). Aggregation of alpha-synuclein in *S. cerevisiae* is associated with defects in endosomal trafficking and phospholipid biosynthesis. *J Mol Neurosci* 43, 391-405.

Soto, I., Oglesby, E., Buckingham, B.P., Son, J.L., Roberson, E.D., Steele, M.R., Inman, D.M., Vetter, M.L., Horner, P.J., and Marsh-Armstrong, N. (2008). Retinal ganglion cells downregulate gene expression and lose their axons within the optic nerve head in a mouse glaucoma model. *J Neurosci* 28, 548-561.

Soukas, A., Socci, N.D., Saatkamp, B.D., Novelli, S., and Friedman, J.M. (2001). Distinct transcriptional profiles of adipogenesis in vivo and in vitro. *J Biol Chem* 276, 34167-34174.

Souza, J.M., Giasson, B.I., Lee, V.M., and Ischiropoulos, H. (2000). Chaperone-like activity of synucleins. *FEBS Lett* 474, 116-119.

Souza, S.C., Muliro, K.V., Liscum, L., Lien, P., Yamamoto, M.T., Schaffer, J.E., Dallal, G.E., Wang, X., Kraemer, F.B., Obin, M., and Greenberg, A.S. (2002). Modulation of hormone-sensitive lipase and protein kinase A-mediated lipolysis by perilipin A in an adenoviral reconstituted system. *J Biol Chem* 277, 8267-8272.

Souza, S.C., Palmer, H.J., Kang, Y.H., Yamamoto, M.T., Muliro, K.V., Paulson, K.E., and Greenberg, A.S. (2003). TNF-alpha induction of lipolysis is mediated

through activation of the extracellular signal related kinase pathway in 3T3-L1 adipocytes. *J Cell Biochem* 89, 1077-1086.

Spillantini, M.G., Crowther, R.A., Jakes, R., Cairns, N.J., Lansbury, P.L., and Goedert, M. (1998a). Filamentous alpha-synuclein inclusions link multiple system atrophy with Parkinson's disease and dementia with Lewy bodies. *Neurosci Lett* 251, 205-208.

Spillantini, M.G., Crowther, R.A., Jakes, R., Hasegawa, M., and Goedert, M. (1998b). alpha-Synuclein in filamentous inclusions of Lewy bodies from Parkinson's disease and dementia with lewy bodies. *Proc Natl Acad Sci U S A* 95, 6469-6473.

Spillantini, M.G., Divane, A., and Goedert, M. (1995). Assignment of human alpha-synuclein (SNCA) and beta-synuclein (SNCB) genes to chromosomes 4q21 and 5q35. *Genomics* 27, 379-381.

Spillantini, M.G., and Goedert, M. (2000). The alpha-synucleinopathies: Parkinson's disease, dementia with Lewy bodies, and multiple system atrophy. *Ann N Y Acad Sci* 920, 16-27.

Spillantini, M.G., Schmidt, M.L., Lee, V.M., Trojanowski, J.Q., Jakes, R., and Goedert, M. (1997). Alpha-synuclein in Lewy bodies. *Nature* 388, 839-840.

Stich, V., De Glisezinski, I., Crampes, F., Hejnova, J., Cottet-Emard, J.M., Galitzky, J., Lafontan, M., Riviere, D., and Berlan, M. (2000). Activation of alpha(2)-adrenergic receptors impairs exercise-induced lipolysis in SCAT of obese subjects. *Am J Physiol Regul Integr Comp Physiol* 279, R499-504.

Stich, V., de Glisezinski, I., Crampes, F., Suljkovicova, H., Galitzky, J., Riviere, D., Hejnova, J., Lafontan, M., and Berlan, M. (1999). Activation of antilipolytic alpha(2)-adrenergic receptors by epinephrine during exercise in human adipose tissue. *Am J Physiol* 277, R1076-1083.

Stralfors, P., Bjorgell, P., and Belfrage, P. (1984). Hormonal regulation of hormone-sensitive lipase in intact adipocytes: identification of phosphorylated sites and effects on the phosphorylation by lipolytic hormones and insulin. *Proc Natl Acad Sci U S A* 81, 3317-3321.

Stralfors, P., and Honnor, R.C. (1989). Insulin-induced dephosphorylation of hormone-sensitive lipase. Correlation with lipolysis and cAMP-dependent protein kinase activity. *Eur J Biochem* 182, 379-385.

Su, C.L., Sztalryd, C., Contreras, J.A., Holm, C., Kimmel, A.R., and Londos, C. (2003). Mutational analysis of the hormone-sensitive lipase translocation reaction in adipocytes. *J Biol Chem* 278, 43615-43619.

Subramanian, V., Rothenberg, A., Gomez, C., Cohen, A.W., Garcia, A., Bhattacharyya, S., Shapiro, L., Dolios, G., Wang, R., Lisanti, M.P., and Brasaemle, D.L. (2004). Perilipin A mediates the reversible binding of CGI-58 to lipid droplets in 3T3-L1 adipocytes. *J Biol Chem* 279, 42062-42071.

Sudhof, T.C., and Rothman, J.E. (2009). Membrane fusion: grappling with SNARE and SM proteins. *Science* 323, 474-477.

Suganami, T., Mieda, T., Itoh, M., Shimoda, Y., Kamei, Y., and Ogawa, Y. (2007). Attenuation of obesity-induced adipose tissue inflammation in C3H/HeJ mice carrying a Toll-like receptor 4 mutation. *Biochem Biophys Res Commun* 354, 45-49.

Suganami, T., Nishida, J., and Ogawa, Y. (2005). A paracrine loop between adipocytes and macrophages aggravates inflammatory changes: role of free fatty acids and tumor necrosis factor alpha. *Arterioscler Thromb Vasc Biol* 25, 2062-2068.

Sumida, M., Sekiya, K., Okuda, H., Tanaka, Y., and Shiosaka, T. (1990). Inhibitory effect of tumor necrosis factor on gene expression of hormone sensitive lipase in 3T3-L1 adipocytes. *J Biochem* 107, 1-2.

Sung, Y.H., and Eliezer, D. (2006). Secondary structure and dynamics of micelle bound beta- and gamma-synuclein. *Protein Sci* 15, 1162-1174.

Sung, Y.H., and Eliezer, D. (2007). Residual structure, backbone dynamics, and interactions within the synuclein family. *J Mol Biol* 372, 689-707.

Sunshine, C., and McNamee, M.G. (1992). Lipid modulation of nicotinic acetylcholine receptor function: the role of neutral and negatively charged lipids. *Biochim Biophys Acta* 1108, 240-246.

Surgucheva, I., McMahan, B., Ahmed, F., Tomarev, S., Wax, M.B., and Surguchov, A. (2002). Synucleins in glaucoma: implication of gamma-synuclein in glaucomatous alterations in the optic nerve. *J Neurosci Res* 68, 97-106.

Sztalryd, C., Xu, G., Dorward, H., Tansey, J.T., Contreras, J.A., Kimmel, A.R., and Londos, C. (2003). Perilipin A is essential for the translocation of hormone-sensitive lipase during lipolytic activation. *J Cell Biol* 161, 1093-1103.

Szymanski, K.M., Binns, D., Bartz, R., Grishin, N.V., Li, W.P., Agarwal, A.K., Garg, A., Anderson, R.G., and Goodman, J.M. (2007). The lipodystrophy protein seipin is

found at endoplasmic reticulum lipid droplet junctions and is important for droplet morphology. *Proc Natl Acad Sci U S A* 104, 20890-20895.

Tansey, J.T., Huml, A.M., Vogt, R., Davis, K.E., Jones, J.M., Fraser, K.A., Brasaemle, D.L., Kimmel, A.R., and Londos, C. (2003). Functional studies on native and mutated forms of perilipins. A role in protein kinase A-mediated lipolysis of triacylglycerols. *J Biol Chem* 278, 8401-8406.

Tansey, J.T., Sztalryd, C., Gruia-Gray, J., Roush, D.L., Zee, J.V., Gavrilova, O., Reitman, M.L., Deng, C.X., Li, C., Kimmel, A.R., and Londos, C. (2001). Perilipin ablation results in a lean mouse with aberrant adipocyte lipolysis, enhanced leptin production, and resistance to diet-induced obesity. *Proc Natl Acad Sci U S A* 98, 6494-6499.

Tremblay, F., and Marette, A. (2001). Amino acid and insulin signaling via the mTOR/p70 S6 kinase pathway. A negative feedback mechanism leading to insulin resistance in skeletal muscle cells. *J Biol Chem* 276, 38052-38060.

Trigatti, B.L., Anderson, R.G., and Gerber, G.E. (1999). Identification of caveolin-1 as a fatty acid binding protein. *Biochem Biophys Res Commun* 255, 34-39.

Trujillo, M.E., and Scherer, P.E. (2006). Adipose tissue-derived factors: impact on health and disease. *Endocr Rev* 27, 762-778.

Tsai, M.H., Yu, C.L., Wei, F.S., and Stacey, D.W. (1989). The effect of GTPase activating protein upon ras is inhibited by mitogenically responsive lipids. *Science* 243, 522-526.

Tu, P.H., Galvin, J.E., Baba, M., Giasson, B., Tomita, T., Leight, S., Nakajo, S., Iwatsubo, T., Trojanowski, J.Q., and Lee, V.M. (1998). Glial cytoplasmic inclusions in white matter oligodendrocytes of multiple system atrophy brains contain insoluble alpha-synuclein. *Ann Neurol* 44, 415-422.

Tung, Y.C., Ma, M., Piper, S., Coll, A., O'Rahilly, S., and Yeo, G.S. (2008). Novel leptin-regulated genes revealed by transcriptional profiling of the hypothalamic paraventricular nucleus. *J Neurosci* 28, 12419-12426.

Ueda, K., Fukushima, H., Masliah, E., Xia, Y., Iwai, A., Yoshimoto, M., Otero, D.A., Kondo, J., Ihara, Y., and Saitoh, T. (1993). Molecular cloning of cDNA encoding an unrecognized component of amyloid in Alzheimer disease. *Proc Natl Acad Sci U S A* 90, 11282-11286.

Um, S.H., Frigerio, F., Watanabe, M., Picard, F., Joaquin, M., Sticker, M., Fumagalli, S., Allegrini, P.R., Kozma, S.C., Auwerx, J., and Thomas, G. (2004). Absence of S6K1 protects against age- and diet-induced obesity while enhancing insulin sensitivity. *Nature* 431, 200-205.

Uversky, V.N. (2007). Neuropathology, biochemistry, and biophysics of alpha-synuclein aggregation. *J Neurochem* 103, 17-37.

Uversky, V.N., Li, J., Souillac, P., Millett, I.S., Doniach, S., Jakes, R., Goedert, M., and Fink, A.L. (2002). Biophysical properties of the synucleins and their propensities to fibrillate: inhibition of alpha-synuclein assembly by beta- and gamma-synucleins. *J Biol Chem* 277, 11970-11978.

Valet, P., Berlan, M., Beauville, M., Crampes, F., Montastruc, J.L., and Lafontan, M. (1990). Neuropeptide Y and peptide YY inhibit lipolysis in human and dog fat cells through a pertussis toxin-sensitive G protein. *J Clin Invest* 85, 291-295.

Van Heek, M., Compton, D.S., France, C.F., Tedesco, R.P., Fawzi, A.B., Graziano, M.P., Sybertz, E.J., Strader, C.D., and Davis, H.R., Jr. (1997). Diet-induced obese mice develop peripheral, but not central, resistance to leptin. *J Clin Invest* 99, 385-390.

Vaughan, M. (1962). The production and release of glycerol by adipose tissue incubated in vitro. *J Biol Chem* 237, 3354-3358.

Vazquez-Vela, M.E., Torres, N., and Tovar, A.R. (2008). White adipose tissue as endocrine organ and its role in obesity. *Arch Med Res* 39, 715-728.

Venda, L.L., Cragg, S.J., Buchman, V.L., and Wade-Martins, R. (2010). alpha-Synuclein and dopamine at the crossroads of Parkinson's disease. *Trends Neurosci* 33, 559-568.

Vidal-Puig, A., Jimenez-Linan, M., Lowell, B.B., Hamann, A., Hu, E., Spiegelman, B., Flier, J.S., and Moller, D.E. (1996). Regulation of PPAR gamma gene expression by nutrition and obesity in rodents. *J Clin Invest* 97, 2553-2561.

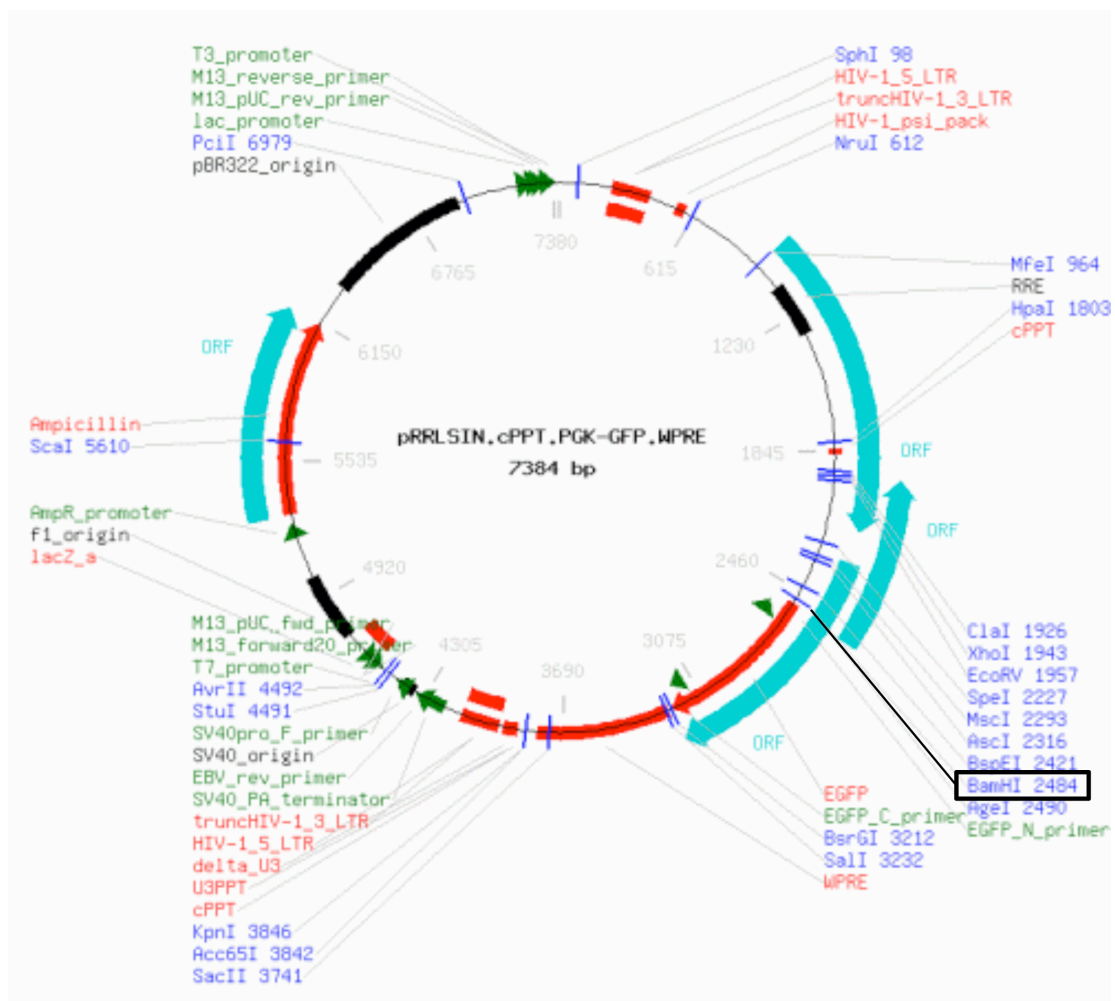
Villena, J.A., Roy, S., Sarkadi-Nagy, E., Kim, K.H., and Sul, H.S. (2004). Desnutrin, an adipocyte gene encoding a novel patatin domain-containing protein, is induced by fasting and glucocorticoids: ectopic expression of desnutrin increases triglyceride hydrolysis. *J Biol Chem* 279, 47066-47075.

- Volles, M.J., and Lansbury, P.T., Jr. (2003). Zeroing in on the pathogenic form of alpha-synuclein and its mechanism of neurotoxicity in Parkinson's disease. *Biochemistry* 42, 7871-7878.
- Vozarova, B., Weyer, C., Hanson, K., Tataranni, P.A., Bogardus, C., and Pratley, R.E. (2001). Circulating interleukin-6 in relation to adiposity, insulin action, and insulin secretion. *Obes Res* 9, 414-417.
- Wang, Y.L., Takeda, A., Osaka, H., Hara, Y., Furuta, A., Setsuie, R., Sun, Y.J., Kwon, J., Sato, Y., Sakurai, M., Noda, M., Yoshikawa, Y., and Wada, K. (2004). Accumulation of beta- and gamma-synucleins in the ubiquitin carboxyl-terminal hydrolase L1-deficient gad mouse. *Brain Res* 1019, 1-9.
- Webber, J., Taylor, J., Greathead, H., Dawson, J., Buttery, P.J., and Macdonald, I.A. (1994). A comparison of the thermogenic, metabolic and haemodynamic responses to infused adrenaline in lean and obese subjects. *Int J Obes Relat Metab Disord* 18, 717-724.
- Weisberg, S.P., McCann, D., Desai, M., Rosenbaum, M., Leibel, R.L., and Ferrante, A.W., Jr. (2003). Obesity is associated with macrophage accumulation in adipose tissue. *J Clin Invest* 112, 1796-1808.
- Wolins, N.E., Quaynor, B.K., Skinner, J.R., Schoenfish, M.J., Tzekov, A., and Bickel, P.E. (2005). S3-12, Adipophilin, and TIP47 package lipid in adipocytes. *J Biol Chem* 280, 19146-19155.
- Wu, X., Hoffstedt, J., Deeb, W., Singh, R., Sedkova, N., Zilbering, A., Zhu, L., Park, P.K., Arner, P., and Goldstein, B.J. (2001). Depot-specific variation in protein-tyrosine phosphatase activities in human omental and subcutaneous adipose tissue: a potential contribution to differential insulin sensitivity. *J Clin Endocrinol Metab* 86, 5973-5980.
- Yu, C., Chen, Y., Cline, G.W., Zhang, D., Zong, H., Wang, Y., Bergeron, R., Kim, J.K., Cushman, S.W., Cooney, G.J., Atcheson, B., White, M.F., Kraegen, E.W., and Shulman, G.I. (2002). Mechanism by which fatty acids inhibit insulin activation of insulin receptor substrate-1 (IRS-1)-associated phosphatidylinositol 3-kinase activity in muscle. *J Biol Chem* 277, 50230-50236.
- Zarranz, J.J., Alegre, J., Gomez-Esteban, J.C., Lezcano, E., Ros, R., Ampuero, I., Vidal, L., Hoenicka, J., Rodriguez, O., Atares, B., Llorens, V., Gomez Tortosa, E., del

- Ser, T., Munoz, D.G., and de Yebenes, J.G. (2004). The new mutation, E46K, of alpha-synuclein causes Parkinson and Lewy body dementia. *Ann Neurol* 55, 164-173.
- Zhang, H.H., Halbleib, M., Ahmad, F., Manganiello, V.C., and Greenberg, A.S. (2002). Tumor necrosis factor-alpha stimulates lipolysis in differentiated human adipocytes through activation of extracellular signal-related kinase and elevation of intracellular cAMP. *Diabetes* 51, 2929-2935.
- Zhang, Y., Proenca, R., Maffei, M., Barone, M., Leopold, L., and Friedman, J.M. (1994). Positional cloning of the mouse obese gene and its human homologue. *Nature* 372, 425-432.
- Zhao, H., Tuominen, E.K., and Kinnunen, P.K. (2004). Formation of amyloid fibers triggered by phosphatidylserine-containing membranes. *Biochemistry* 43, 10302-10307.
- Zhao, Y.F., Feng, D.D., and Chen, C. (2006). Contribution of adipocyte-derived factors to beta-cell dysfunction in diabetes. *Int J Biochem Cell Biol* 38, 804-819.
- Zierath, J.R., Livingston, J.N., Thorne, A., Bolinder, J., Reynisdottir, S., Lonqvist, F., and Arner, P. (1998). Regional difference in insulin inhibition of non-esterified fatty acid release from human adipocytes: relation to insulin receptor phosphorylation and intracellular signalling through the insulin receptor substrate-1 pathway. *Diabetologia* 41, 1343-1354.
- Zimmermann, R., Strauss, J.G., Haemmerle, G., Schoiswohl, G., Birner-Gruenberger, R., Riederer, M., Lass, A., Neuberger, G., Eisenhaber, F., Hermetter, A., and Zechner, R. (2004). Fat mobilization in adipose tissue is promoted by adipose triglyceride lipase. *Science* 306, 1383-1386.

## Appendix

**Appendix 1. Map of the pRRLsin.cPPT.hPGK-eGFP lentiviral expression vector (Follenzi et al., 2000).** The coding region of human  $\gamma$ -synuclein was inserted into the unique BamHI site downstream of a human phosphoglycerate kinase-1 (PGK) promoter.



**Appendix 2. Quantification of  $\gamma$ -synuclein protein abundance in epididymal WAT of mice fed HFD or on calorific restriction.**

**HFD feeding**

<b>Diet</b>	<b>11 week LFD</b>	<b>11 week HFD</b>
<b><math>\gamma</math>-synuclein</b>		
<b>(% of LFD)</b>	<b>100 <math>\pm</math> 16</b>	<b>299 <math>\pm</math> 20*</b>

**Calorific restriction**

<b>Diet</b>	<b>HFD control</b>	<b>36 hour LFD</b>	<b>1 week LFD</b>	<b>36 hour fast</b>
<b><math>\gamma</math>-synuclein</b>				
<b>(% of HFD control)</b>	<b>100 <math>\pm</math> 19</b>	<b>88 <math>\pm</math> 12</b>	<b>22 <math>\pm</math> 9*</b>	<b>26 <math>\pm</math> 11*</b>

(LFD low fat diet, HFD high fat diet, \*  $p < 0.05$ , Mann-Whitney U-test, n=4).

**Appendix 3. Raw weights of major WAT depots from wild type and  $\gamma$ -synuclein<sup>-/-</sup> mice fed a LFD or HFD for 11 weeks.**

<b>Genotype</b>	<b>+/+</b>	<b>-/-</b>	<b>+/+</b>	<b>-/-</b>
<b>Diet</b>	<b>11 week LFD</b>		<b>11 week HFD</b>	
<b>ED WAT (g)</b>	<b>0.58 ± 0.09</b>	<b>0.52 ± 0.06</b>	<b>2.07 ± 0.11</b>	<b>1.40 ± 0.14**</b>
<b>SC WAT (g)</b>	<b>0.32 ± 0.05</b>	<b>0.31 ± 0.03</b>	<b>1.16 ± 0.07</b>	<b>0.72 ± 0.05**</b>
<b>RP WAT (g)</b>	<b>0.12 ± 0.03</b>	<b>0.11 ± 0.02</b>	<b>0.52 ± 0.02</b>	<b>0.37 ± 0.03**</b>

(n=12-14, +/+ wild type, -/-  $\gamma$ -synuclein<sup>-/-</sup>, ED epididymal, SC subcutaneous, RP retroperitoneal, LFD low fat diet, HFD high fat diet, \*\* p < 0.01, Mann-Whitney U-test, n=12-14).

**Appendix 4. Western blot quantification of protein marker expression in epididymal WAT.**

<b>Genotype</b>	<b>+/+</b>	<b>-/-</b>	<b>+/+</b>	<b>-/-</b>
<b>Diet</b>	<b>11 week LFD</b>		<b>11 week HFD</b>	
<b>% of +/+ LFD</b>				
<b>HSL</b>	<b>100 ± 5.0</b>	<b>94.2 ± 13.4</b>	<b>93.7 ± 9.7</b>	<b>108.5 ± 9.0</b>
<b>perilipin A</b>	<b>100 ± 6.7</b>	<b>112.1 ± 17.7</b>	<b>75.9 ± 14.3</b>	<b>84.7 ± 12.4</b>
<b>ATGL</b>	<b>100 ± 7.8</b>	<b>108.5 ± 13.5</b>	<b>82.2 ± 7.2</b>	<b>144.4 ± 14.5**</b>

(+/+ wild type, -/-  $\gamma$ -synuclein<sup>-/-</sup>, LFD low fat diet, HFD high fat diet, HSL hormone-sensitive lipase, ATGL adipose triglyceride lipase, \*\* p < 0.01, Mann-Whitney U-test, n=6).

## **Appendix 5. Publication list.**

**Millership, S.**, Ninkina, N., Guschina, I., Norton, J., Brambilla, R., Oort, P., Adams, S., Voshol, P., Rochford, J.J., and Buchman, V.L. Increased lipolysis and altered lipid homeostasis protect gamma-synuclein null mutant mice from diet-induced obesity. Submitted to **Cell Metabolism**.

Peters, O., **Millership, S.**, Shelkovernikova, T., Keeling, L., Hann, A., Ninkina, N., and Buchman, V.L. Gamma-synuclein transgenic mice recapitulate pathological features of amyotrophic lateral sclerosis. Submitted to **PNAS**.

**Millership, S.**, Anwar, S., Peters, O., Ninkina, N., Doig, N., Connor-Robson, N., Threlfell, S., Kooner, G., Deacon, R.M., Bannerman, D.M., Bolam, J.P., Chandra, S.S., Cragg, S.J., Wade-Martins, R., and Buchman, V.L. (2011). Functional Alterations to the Nigrostriatal System in Mice Lacking All Three Members of the Synuclein Family. **J Neurosci** 31, 7264-7274.

Shelkovernikova, T.A., Ustyugov, A.A., **Millership, S.**, Peters, O., Anichtchik, O., Spillantini, M.G., Buchman, V.L., Bachurin, S.O., and Ninkina, N.N. (2010). Dimebon does not ameliorate pathological changes caused by expression of truncated (1-120) human alpha-synuclein in dopaminergic neurons of transgenic mice. **Neurodegener Dis** 8, 430-437.

Guschina, I., **Millership, S.**, O'Donnell, V., Ninkina, N., Harwood, J., and Buchman, V. (2010). Lipid classes and fatty acid patterns are altered in the brain of gamma-synuclein null mutant mice. **Lipids** 46, 121-130.

Al-Wandi, A., Ninkina, N., **Millership, S.**, Williamson, S.J., Jones, P.A., and Buchman, V.L. (2010). Absence of alpha-synuclein affects dopamine metabolism and synaptic markers in the striatum of aging mice. **Neurobiol Aging** 31, 796-804.

Ninkina, N., Peters, O., **Millership, S.**, Salem, H., van der Putten, H., and Buchman, V.L. (2009). Gamma-synucleinopathy: neurodegeneration associated with overexpression of the mouse protein. **Hum Mol Genet** 18, 1779-1794.